



U31: Vehicle Stability and Dynamics Electronic Stability Control Final Report

This project was funded by the NTRCI University Transportation Center under a grant from the U.S. Department of Transportation Research and Innovative Technology Administration (#DTRT-06-G-0043)

The contents of this report reflect the views of the authors, who are responsible for the facts and the accuracy of the information presented herein. This document is disseminated under the sponsorship of the Department of Transportation University Transportation Centers Program, in the interest of information exchange. The U.S. Government assumes no liability for the contents or use thereof.

Doug Pape
Michael Arant
Wayne Brock
Damon Delorenzis
Tim LaClair
Alvin Lim
Joseph Petrolino
Anthony Spezia

September 2011

Technical Report Documentation Page

1. Report No.		2. Government Accession No.		3. Recipient's Catalog No.	
4. Title and Subtitle U31: Vehicle Stability and Dynamics: Electronic Stability Control				5. Report Date September 2011	
				6. Performing Organization Code	
7. Author(s) Doug Pape, Michael Arant, Wayne Brock, Damon Delorenzis, Tim LaClair Alvin Lim, Joseph Petrolino, Anthony Spezia				8. Performing Organization Report No. NTRCI-50-2011-022	
9. Performing Organization Name and Address National Transportation Research Center, Inc. University Transportation Center 9125 Cross Park Drive Suite 150 Knoxville, TN 37923				10. Work Unit No. (TRAIS)	
				11. Contract or Grant No. RITA Grant – DTRT-06G-0043	
12. Sponsoring Agency Name and Address U.S. Department of Transportation Research and Innovative Technology Administration 1200 New Jersey Avenue, SE Washington, DC 20590				13. Type of Report and Period Covered DRAFT Final Report January – September 2011	
				14. Sponsoring Agency Code	
15. Supplementary Notes					
16. Abstract					
<p>A team led by NTRCI is working to improve the roll and yaw stability of heavy duty combination trucks through developing stability algorithms, assembling demonstration hardware, and investigating robust wireless communication.</p> <p>Modern electronic stability control (ESC) products automatically slow a vehicle rounding a corner too quickly or apply individual brakes when necessary to improve the steering characteristics of a vehicle. Air brake systems in North America provide no electronic communication between a tractor and semitrailer, limiting the degree to which control systems can be optimized. Prior research has demonstrated stability improvements where dynamic measurements and control commands are communicated between units of a vehicle.</p> <p>Three related activities were undertaken: (1) Develop an algorithm for the optimum yaw and roll control of a combination vehicle. Vehicle state parameters needed to control the vehicle and the proper brake response were determined. An integrated stability control for the tractor and semitrailer requires communication between the two units. Dynamic models were used to assess the algorithm. (2) Implement the ESC algorithm in the laboratory. Hardware components suitable for the harsh environment for measurement, sensor-to-controller communication, and semitrailer-to-tractor communication and brake actuation were specified and assembled as a working system. The goal was to collect the needed vehicle state information, transmit the information to the ESC system, and then actuate the brakes in response to controller commands. (3) Develop a wireless network with the data rate and reliability necessary to communicate dynamic signals for a vehicle stability control system. Adaptive connectivity-aware, multi-hop routing was selected because it can perform in the harsh environment where packet collisions and fading often will exist. The protocol is to give high priority to urgent messages.</p>					
17. Key Words Electronic stability control; vehicle dynamics; rollover; jackknife; commercial vehicle; brakes; antilock; safety; crash, wireless			18. Distribution Statement No restrictions		
19. Security Classif. (of this report) Unclassified		20. Security Classif. (of this page) Unclassified		21. No. of Pages 196	22. Price

This Page Intentionally Left Blank.

Table of Contents

LIST OF ABBREVIATIONS	XI
UNITS OF MEASUREMENT	XIII
EXECUTIVE SUMMARY	XV
BACKGROUND	XV
BRIEF OVERVIEW.....	XV
CONCLUSION	XVI
FUTURE PROGRAM EFFORTS	XVI
CHAPTER 1 – INTRODUCTION AND BACKGROUND	1
1.1 BACKGROUND	1
1.2 PROJECT TEAM	1
1.2.1 CU-ICAR.....	1
1.2.2 Auburn University.....	1
1.2.3 ORNL.....	2
1.2.4 Battelle.....	2
1.2.5 Bendix	2
1.2.6 National Instruments	2
1.2.7 Volvo.....	2
1.2.8 NTRCI	2
1.3 PROJECT DESCRIPTION.....	2
1.4 PROJECT SCHEDULE.....	3
CHAPTER 2 – LITERATURE REVIEW	5
2.1 INTRODUCTION TO COMMERCIAL VEHICLE AIR BRAKES	5
2.1.1 Historical Perspective	5
2.1.2 Design of Modern Commercial Vehicle Air Brakes	8
2.1.3 The Future of Commercial Vehicle Air Brake Systems.....	17
2.2 COMMERCIAL VEHICLE STABILITY	19
2.2.1 Roll Stability	19
2.2.2 Yaw Stability	20
2.3 PRIOR COMMERCIAL VEHICLE STABILITY SYSTEMS	25
2.3.1 Roll Stability Systems.....	25
2.3.2 Correcting Yaw Instability	26
2.3.3 Combined Roll and Yaw Stability.....	28
2.3.4 Current Roll and Yaw Stability Systems	30
2.3.5 Multiple Unit Stability	31
2.4 SENSORS AND VEHICLE OBSERVABILITY.....	34
2.4.1 Measuring Vehicle Parameters	34
2.4.2 Estimating Vehicle States	35
2.4.3 Communication Networks	41
2.5 WIRELESS VEHICLE COMMUNICATION PROTOCOLS AND PERFORMANCE	41
CHAPTER 3 – STABILITY CONTROL OF A TRACTOR AND SEMITRAILER	45
3.1 CONTROLLER DEVELOPMENT OVERVIEW	45
3.1.1 TruckSim®	46
3.1.2 LabVIEW	47
3.1.3 Commercial Vehicle Brake System.....	49
3.1.4 Stability Control Overview.....	50

Table of Contents (Continued)

3.2	TRACTOR TRAILER STABILITY	51
3.2.1	Vehicle Degrees of Freedom	52
3.2.2	States and Vehicle Parameter Measurement.....	53
3.2.3	Control Tier Approach.....	53
3.3	BRAKE ACTUATION AND BRAKE CONTROL	58
3.3.1	Modeling ABS.....	58
3.3.2	Full Air Brake Simulation	60
3.3.3	Electronically Controlled Braking Systems	63
3.3.4	Stopping Performance	64
3.4	RESULTS OF SIMULATING THE ESC ALGORITHMS IN LABVIEW AND TRUCKSIM®	69
3.4.1	Maneuver Test Speeds.....	69
3.4.2	Vehicle Configurations and Maneuvers	70
3.4.3	Loaded Vehicle on an Exit Ramp.....	72
3.4.4	Unloaded Vehicle on an Exit Ramp	78
3.4.5	Loaded Vehicle in a Lane Change.....	83
3.4.6	Unloaded Vehicle in a Lane Change	88
3.5	CRITICAL CONTROL ISSUES.....	93
3.5.1	Brake Response Time	93
3.5.2	Proportioning of Drive and Trailer Brakes	93
3.5.3	Pulsing of Trailer Brakes to Manage Swing-out.....	95
3.6	CONCLUSIONS.....	97
3.6.1	Relative Effectiveness of Air and ECBS in Braking.....	98
3.6.2	Tuning the Electronic Stability Controller.....	98
3.6.3	Future work.....	98
3.6.4	Discussion on Extension to Multi-Trailer Vehicles	99
CHAPTER 4 – SENSORS AND PROTOCOLS		101
4.1	TEST AND DEMONSTRATION PLAN	102
4.1.1	Braking System	102
4.1.2	Sensors	103
4.1.3	Communication Networks	103
4.1.4	Functional Testing.....	104
4.2	VEHICLE SYSTEM HARDWARE	104
4.2.1	Braking System	105
4.2.2	Pneumatic Controls.....	107
4.2.3	Electrical Components.....	109
4.2.4	Sensors	110
4.2.5	Networks	111
4.3	DEVELOPMENT CONTROLLER HARDWARE.....	113
4.3.1	Control System Configurations	114
4.3.2	Control System Electrical Hardware	117
4.4	CONTROL SYSTEM DEVELOPMENT SOFTWARE.....	120
4.4.1	Control System Software	120
4.4.2	Data Sets and Parameters	121
4.5	PHYSICAL IMPLEMENTATION	127
4.5.1	System-Under-Test Hardware	127
4.5.2	Controllers	130

Table of Contents (Continued)

4.6	RESULTS AND APPLICATIONS.....	133
4.6.1	Truck Brake Systems.....	133
4.6.2	Development Control System Hardware and Software.....	133
4.6.3	Generalizations to Longer Combination Vehicles	134
CHAPTER 5 – FEASIBILITY OF INTRA-VEHICLE WIRELESS COMMUNICATION.....		135
5.1	BENEFITS OF WIRELESS ELECTRONIC STABILITY CONTROL.....	135
5.2	CHALLENGING PROBLEMS OF INTRA-VEHICLE WIRELESS COMMUNICATION.....	135
5.3	SUMMARY OF WIRELESS COMMUNICATION PROTOCOLS.....	136
5.3.1	IEEE 802.11a/b/g/n (Wi-Fi)	136
5.3.2	DSRC (IEEE 802.11p)	137
5.3.3	WiMAX.....	138
5.3.4	Other Wireless Communication Protocols	138
5.4	IMPROVING RELIABILITY AND THROUGHPUT IN WIRELESS VEHICLE NETWORKS	138
5.4.1	Secure and Robust Framework for Wireless Intra-Vehicle Networks.....	139
5.4.2	Fast Recovery Transmission Rate Adaptation Method.....	140
5.4.3	Reliable and High-Connectivity Multi-hop Communication Protocol	140
5.4.4	Efficient Broadcast Protocol	140
5.5	IMPLEMENTATION OF WIRELESS INTRA-VEHICLE NETWORKS.....	141
5.5.1	Requirements for Wireless Communication in Vehicle Electronic Stability Control	141
5.5.2	Wireless Hardware Configuration of Wireless Vehicle Electronic Stability Control	143
5.5.3	Networking Protocols for Transmission of Sensor and Actuator Control Data.....	143
5.5.4	Implementation of Fast Recovery Rate Adaptation Method	144
5.5.5	Implementation of Multi-Hop Communication Protocol	144
5.5.6	Implementation of Efficient Broadcast Protocol	145
5.6	EXPERIMENTAL RESULTS AND ANALYSIS OF WIRELESS INTRA-VEHICLE NETWORKS	146
5.6.1	Experimental Setups for Studying Performance of Wireless Intra-vehicle Communication.....	146
5.6.2	Results of Antenna Polarization Mismatch in Wireless Intra-vehicle Communication.....	149
5.6.3	Results of Spatial Multiplexing Malfunction (SMM)	151
5.6.4	Results of Space-Time Block Code (STBC) and the Number of Streams.....	152
5.6.5	Results of Optimal Antenna Alignments.....	154
5.6.6	Results of Throughput Performance of Fast Recovery Rate Adaptation (FRRA) Algorithm.....	155
5.6.7	Results of Performance of Multi-Hop Wireless Protocol	157
5.6.8	Results of Performance of Efficient Broadcast Protocol.....	159
5.7	CONCLUSIONS.....	160
5.7.1	Satisfying the Requirements for Intra-Vehicle Wireless Communication.....	160
5.7.2	Selection of Wireless Communication Protocols	161
5.7.3	Future Work.....	161
CHAPTER 6 – CONCLUSIONS AND RECOMMENDATIONS		163
6.1	STABILITY CONTROL ALGORITHM.....	163
6.2	HARDWARE BENCH TEST SYSTEM DEMONSTRATION	163
6.3	WIRELESS INTRA-VEHICLE COMMUNICATION.....	164
CHAPTER 7 – REFERENCES.....		165

List of Figures

Figure 1-1.	Chart. Schedule of tasks.....	3
Figure 2-1.	Drawing. Widdifield & Button friction buffer brake.....	6
Figure 2-2.	Drawing. Westinghouse straight air brake.....	6
Figure 2-3.	Photo. The first truck in 1896 produced by Daimler Motoren Gesellschaft.....	7
Figure 2-4.	Photo. 1898 Winton semi-truck carrying a new Winton motor car.	7
Figure 2-5.	Drawing. Drum-style air brake.....	8
Figure 2-6.	Drawing. Wedge brake design.....	9
Figure 2-7.	Drawing. S-cam brake design.....	9
Figure 2-8.	Photo. Cross-section of an air brake air chamber with spring brake.....	10
Figure 2-9.	Drawing. Air chamber with parking brake applied.	11
Figure 2-10.	Drawing. Air chamber with parking brake released.	11
Figure 2-11.	Drawing. Air chamber with service bake applied.....	12
Figure 2-12.	Drawing. Automatic slack adjuster.....	13
Figure 2-13.	Drawing. Brake pedal treadle valve.	14
Figure 2-14.	Diagram. Bendix air brake system diagram for tractor.....	15
Figure 2-15.	Diagram. Bendix ATR6 traction relay valve and antilock traction control assembly.....	16
Figure 2-16.	Drawing. Bendix antilock brake modulator valve.....	17
Figure 2-17.	Diagram. Overturning moment (Arant 2010).....	19
Figure 2-18.	Equation. Load transfer across an axle during cornering.....	19
Figure 2-19.	Histogram. Commercial vehicle accident type (Kharrazi and Thomson 2008a).....	20
Figure 2-20.	Histogram. Yaw instability accident type (Kharrazi and Thomson 2008a).	21
Figure 2-21.	Diagram. Passenger car yaw instability (Tekin and Unlusoy 2010).....	22
Figure 2-22.	Equation. Understeer gradient, due to tire stiffness and mass distribution.	22
Figure 2-23.	Equation. The purely geometric turning equation is modified by the understeer term.....	23
Figure 2-24.	Graph. Constant radius understeer results (El-Gindy 1995).....	23
Figure 2-25.	Equation. Ratio of the articulation angle to steer angle.....	24
Figure 2-26.	Equation. Critical speed for a tractor.....	24
Figure 2-27.	Equation. Critical speed for a trailer.....	24
Figure 2-28.	Equation. The lateral acceleration depends on the forward velocity and the turn radius.	25
Figure 2-29.	Diagram. Tractor and trailer yaw control (Andersky and Conklin 2008).....	26
Figure 2-30.	Diagram. Tractor trailer understeer and oversteer corrections (Goodarzi et al. 2009).....	26
Figure 2-31.	Diagram. Articulated vehicle stability control illustration (Freightliner LLC 2007).....	27
Figure 2-32.	Diagram. Example yaw controller (Zhou et al. 2008).....	27
Figure 2-33.	Diagram. Oversteer correction (Nantais 2006).....	28
Figure 2-34.	Diagram. Yaw and roll stability regimes (MacAdam 1982).....	29
Figure 2-35.	Graph. Combined yaw and roll controller for a car (Yoon et al. 2009).....	30
Figure 2-36.	Diagram. Yaw and roll controller (Chen and Peng 1999).	30
Figure 2-37.	Graph. RAMS rearward amplification (MacAdam et al. 2000).....	32
Figure 2-38.	Diagram. RAMS control illustration (MacAdam et al. 2000).....	32
Figure 2-39.	Diagram. RAMS diagonal brake illustration (MacAdam et al. 2000).....	33
Figure 2-40.	Graph. RAMS roll suppression (MacAdam et al. 2000).	33

List of Figures (Continued)

Figure 2-41.	Equation. Side slip angle.	36
Figure 2-42.	Equation. State space formulation of vehicle side slip from tire behavior.	37
Figure 2-43.	Equation. Kinematic formulation side slip.	37
Figure 2-44.	Equation. Side slip or “Crab angle” of a vehicle from measurable yaw angles.	37
Figure 2-45.	Graph. Side slip error from GPS measurement (Daily and Bevely 2004).	38
Figure 2-46.	Drawing. Bendix wheel speed sensor installation.	40
Figure 3-1.	Animation still. TruckSim® vehicle animation (Mechanical Simulation Corporation 2009a).	46
Figure 3-2.	Screen shot. TruckSim® interface (Mechanical Simulation Corporation 2009a).	47
Figure 3-3.	Screen shot. LabVIEW front panel.	48
Figure 3-4.	Block diagram. LabVIEW block diagram.	48
Figure 3-5.	Sketch. Tractor brake system (Andersky and Conklin 2008).	49
Figure 3-6.	Diagram. Stability control algorithm. (This figure appears truncated because it is part of the LabView block diagram.)	51
Figure 3-7.	Equation. A vehicle traveling forward has a lateral velocity that is the product of the forward velocity and the side slip.	52
Figure 3-8.	Plot. Fifth wheel roll moment (Arant et al. 2009).	53
Figure 3-9.	Equation. Side slip.	53
Figure 3-10.	Equation. Tractor yaw control estimator.	55
Figure 3-11.	Block diagram. Tractor yaw controller (Limroth 2009a).	55
Figure 3-12.	Sketch. Tractor yaw control brake response (Andersky and Conklin 2008).	55
Figure 3-13.	Diagram. Trailer yaw control.	57
Figure 3-14.	Equation. Roll restoring moment.	58
Figure 3-15.	Equation. Overturning moment.	58
Figure 3-16.	Diagram. Tractor and trailer roll control.	58
Figure 3-17.	Diagram. ABS controller.	59
Figure 3-18.	Diagram. Axle transport delay.	60
Figure 3-19.	Diagram. Brake demand to TruckSim®.	60
Figure 3-20.	Diagram. Brake transport delay to axle modulator.	61
Figure 3-21.	Plot. Measured wheel pulses (Choi and Cho 2001, 57-72).	62
Figure 3-22.	Plots. Measured brake performance ($\mu = 0.75$) (Kienhöfer, Miller, and Cebon 2008, 571-583).	63
Figure 3-23.	Sketch. Electronic control brake system diagram (Palkovics and Fries 2001, 227-89).	64
Figure 3-24.	Plot. Tractor full stop ($\mu = 0.75$).	65
Figure 3-25.	Plot. Trailer full stop ($\mu = 0.75$).	65
Figure 3-26.	Plot. Tractor slip control ($\mu = 0.75$).	65
Figure 3-27.	Plot. Trailer slip control ($\mu = 0.75$).	65
Figure 3-28.	Plot. FMVSS 121 dry straight line stop.	66
Figure 3-29.	Plot. Straight line braking ($\mu = 0.75$) (Unit 1, the tractor, and Unit 2, the tank semitrailer, have the same speed in both cases, so their plots are coincident.)	68
Figure 3-30.	Plot. Drive axle brake pressure ($\mu = 0.75$).	69
Figure 3-31.	Plot. Trailer axle brake pressure ($\mu = 0.75$).	69
Figure 3-32.	Plot. Drive axle slip ratio ($\mu = 0.75$).	69
Figure 3-33.	Plot. Trailer axle slip ratio ($\mu = 0.75$).	69

List of Figures (Continued)

Figure 3-34. Animation still. Unloaded vehicle.....	71
Figure 3-35. Animation still. Loaded vehicle.....	71
Figure 3-36. Diagram. Lane change cones.....	72
Figure 3-37. Animation still. Exit ramp – loaded vehicle – roll illustration ($\mu = 0.85$).....	73
Figure 3-38. Animation still. Exit ramp – loaded vehicle – brake vectors ($\mu = 0.85$).....	73
Figure 3-39. Animation still. Exit ramp, loaded vehicle – ESC articulation control ($\mu = 0.25$).....	74
Figure 3-40. Plots. Exit ramp – loaded vehicle – roll and tracking errors.....	75
Figure 3-41. Plots. Exit ramp – loaded vehicle – brake pressures.....	77
Figure 3-42. Plot. Exit ramp – loaded vehicle – trailer side slip ($\mu = 0.25$).....	78
Figure 3-43. Animation still. Exit ramp – unloaded vehicle – yaw illustration ($\mu = 0.5$).....	79
Figure 3-44. Plots. Exit ramp – unloaded vehicle – tracking error and steering demand.....	80
Figure 3-45. Plots. Exit ramp – unloaded vehicle – brake pressures.....	82
Figure 3-46. Plot. Exit ramp – unloaded vehicle – trailer side slip ($\mu = 0.25$).....	83
Figure 3-47. Animation still. Lane change – loaded vehicle – roll illustration ($\mu = 0.85$).....	84
Figure 3-48. Plots. Lane change – loaded vehicle – roll and tracking errors.....	85
Figure 3-49. Plot. Lane change – loaded vehicle – vehicle speed ($\mu = 0.85$).....	86
Figure 3-50. Plot. Lane change – loaded vehicle – brake pressures.....	87
Figure 3-51. Animation still. Lane change – unloaded vehicle – yaw illustration ($\mu = 0.85$).....	88
Figure 3-52. Plots. Lane change – unloaded vehicle – tracking error and steering demand.....	89
Figure 3-53. Plots. Lane change – unloaded vehicle – brake pressure.....	90
Figure 3-54. Plots. Lane change – unloaded vehicle – side slip angles.....	92
Figure 3-55. Diagram. Drive axle brake limiter.....	93
Figure 3-56. Animation Still. Jackknife at the drive axle, induced by braking.....	94
Figure 3-57. Plot. Exit ramp – loaded vehicle – drive axle brake pressure ($\mu = 0.5$).....	95
Figure 3-58. Plot. Exit ramp – loaded vehicle – tractor side slip ($\mu = 0.5$).....	95
Figure 3-59. Plot. Exit ramp – loaded vehicle – trailer brake pressure – side slip control illustration ($\mu = 0.5$).....	96
Figure 3-60. Plot. Exit ramp – loaded vehicle – trailer wheel speed – side slip control wheel speed ($\mu = 0.5$).....	96
Figure 3-61. Plot. Exit ramp – loaded vehicle – trailer side slip – side slip control wheel speed ($\mu = 0.5$).....	97
Figure 3-62. Plot. Exit ramp – loaded vehicle – trailer roll – side slip control wheel speed ($\mu = 0.5$).....	97
Figure 4-1. Diagram. The hardware bench test system.....	102
Figure 4-2. Diagram. Simplified schematic of a typical air brake system.....	106
Figure 4-3. Diagram. Hardware system-under-test, brake system functional layout.....	107
Figure 4-4. Diagram. Brake system pneumatic functional layout.....	108
Figure 4-5. Diagram. Brake system electrical functional layout.....	109
Figure 4-6. Diagram. Brake system network functional layout – single CPU controller.....	112
Figure 4-7. Diagram. Brake system network functional layout – dual CPU controller.....	113
Figure 4-8. Diagram. Development controller configuration – single CPU controller.....	116
Figure 4-9. Diagram. Development controller configuration – dual CPU controller.....	117
Figure 4-10. Diagram. Control system electrical schematic.....	119
Figure 4-11. Screen shot. NI-XNET database editor.....	122

List of Figures (Continued)

Figure 4-12.	Screen shot. NI-XNET, Setting CAN signal properties.....	123
Figure 4-13.	Screen shot. CAN port configuration.....	124
Figure 4-14.	Diagram. CAN frame capture implemented in a LabVIEW® program.....	124
Figure 4-15.	Screen shot. NI-DAQ I/O terminal assignments.....	125
Figure 4-16.	Screen shot. NI MAX connection diagram.....	126
Figure 4-17.	Screen shot. NI MAX data plot and calibration.	126
Figure 4-18.	Photo. Hardware bench test system.....	127
Figure 4-19.	Photo. Speed sensor array around the tone ring.	128
Figure 4-20.	Photo. Air cylinder, traction relay valve, ABS modulator, treadle valve.	129
Figure 4-21.	Photo. Layout of test stand assembly.	130
Figure 4-22.	Photo. Development controller for trailer (left) and tractor (right).....	131
Figure 4-23.	Photo. PXI chassis for trailer (top) and tractor (bottom).....	132
Figure 5-1.	Diagram. Network architecture.	145
Figure 5-2.	Photo. NCAT test track at Auburn University.....	147
Figure 5-3.	Photo. Wireless controller and antennas attached to the third trailer.....	147
Figure 5-4.	Diagram. Three antenna alignment configurations for STBC and streams tests.....	148
Figure 5-5.	Diagram. Three antenna alignment configurations for optimal antenna alignment tests.....	149
Figure 5-6.	Plot. Results of wireless intra-vehicle networks with tractor-trailer stationary in NCAT garage.....	150
Figure 5-7.	Plot. Results of wireless intra-vehicle networks with tractor-trailer running at NCAT test track.	151
Figure 5-8.	Plot. Results of throughput and packet loss with spatial multiplexing malfunction.....	152
Figure 5-9.	Plot. Results of tests on effects of STBC and number of streams.	153
Figure 5-10.	Plot. Results of tests on optimal antenna alignments.	155
Figure 5-11.	Plot. Results of stationary tests of fixed rate, ath9k, and FRRA algorithms.....	156
Figure 5-12.	Plot. Results of mobile tests of fixed rate, ath9k, and FRRA algorithms.	156
Figure 5-13.	Plot. Results of throughput tests of multi-hop packet forwarding.....	157
Figure 5-14.	Plot. Results of throughput tests for different distances in each hop.	158
Figure 5-15.	Plot. Results of throughput tests for different number of hops over the same distances.	158
Figure 5-16.	Plot. Throughput for broadcast with aggregation and traditional broadcast.....	159
Figure 5-17.	Plot. Delivery ratio for efficient broadcast with aggregation and traditional broadcast.....	160

List of Tables

Table 2-1.	Test standards for air brake systems.....	18
Table 3-1.	Full vehicle stopping distance (meters) from 97 km/h (60 mph).....	67
Table 3-2.	Full vehicle stopping distance (meters) from 150 km/h (93 mph).....	67
Table 3-3.	Vehicle speeds at the threshold of stability (km/h) – lane change maneuver.	70
Table 3-4.	Vehicle speeds at the threshold of stability (km/h) – exit ramp maneuver.....	70
Table 3-5.	Simulation permutation parameters.	71
Table 4-1.	Sensor requirements and specifications.	103
Table 4-2.	CAN frame properties for system-under-test.....	122
Table 4-3.	CAN signal properties for system-under-test.....	123
Table 5-1.	Selection of methods for overcoming wireless channel degradation.	139
Table 5-2.	Maximum throughput rate achieved at different distances in the multi-hop experiments.....	159

List of Abbreviations

Abbreviation	Definition
A/D	Analog/digital
ABS	Antilock braking system
A-BUS	Automobile Bitserielle Universal-Schnittstelle
AC	Alternating current
ACVS	Advanced commercial vehicle systems
ADC	Analog-to-digital converter
AHS	Automated highway systems
AP	Access point
ATC	Automatic traction control
Auburn	Auburn University
AWG	American Wire Gauge
a_y	Lateral acceleration
Battelle	Battelle Memorial Institute
Bendix	Bendix Commercial Vehicle Systems, LLC
CAN	Controller area network
CG	Center of gravity
CN	Cluster head node
CPU	Central processing unit
CTS	Clear to Send
CU-ICAR	Clemson University International Center for Automotive Research
CVISN	Commercial Vehicle Information Systems and Networks
CVSA	Commercial Vehicle Safety Alliance
D2B	Domestic Digital Data Bus
DAQ	Data acquisition
DFS	Dynamic frequency selection
DLC	Data Link Connector
DOT	U.S. Department of Transportation
DSRC	Dedicated short-range communication
ECBS	Electronically controlled braking system
ECU	Electronic Control Unit
EMC	Electromagnetic compatibility
ESC	Electronic stability control. In this report, ESC is used as a generic term for any electronic system that automatically applies brakes on the tractor or semitrailer to enhance the stability of the vehicle in any way.
FCC	Federal Communications Commission
FHWA	Federal Highway Administration
FMCSA	Federal Motor Carrier Safety Administration
FMVSS	Federal Motor Vehicle Safety Standard
FRRA	Fast Recovery Rate Adaptation
GPIB	General Purpose Interface Bus
GPS	Global positioning system
GVW(R)	Gross vehicle weight (rating)

List of Abbreviations (Continued)

Abbreviation	Definition
IDB-C	ITS (Intelligent Transportation System) Data Bus-C
IEEE	Institute of Electrical and Electronic Engineers
IMU	Inertial Measurement Unit
IP	Internet protocol
ISO	International Organization for Standards
K&C	Kinematics and compliance test
KWP	Keyword Protocol
LabVIEW®	Laboratory Virtual Instrumentation Engineering Workbench
LBT	LBT, Inc.
LCV	Longer combination vehicle
LIN	Local Interconnect Network
MAC	Media access control
MAX	Measurement & Automation Explorer
MCS	Modulation (and) Coding Scheme
Michelin	Michelin Americas Research Company
MID	Message Identification (Character)
MIMO	Multiple-input, multiple-output
MOST	Media Oriented System Transport
MRR	Multi-rate retry
NCAT	National Center for Asphalt Technology
NHTSA	National Highway Traffic Safety Administration
NI	National Instruments
NTPd	Network Time Protocol daemon
NTRCI	National Transportation Research Center, Inc.
OBD	On-board diagnostics
OE	Original equipment
OEM	Original equipment manufacturer
ORNL	Oak Ridge National Laboratory
PHY	Physical (layer)
QR/QRV	Quick release/QR valve
RAMS	Rearward Amplification Suppression (system)
RITA	Research and Innovative Technology Administration (USDOT)
RTS	Request to Send
SAE	Society of Automotive Engineers
SMM	Spatial Multiplexing Malfunction
SNR	Signal to noise ratio
STBC	Space-Time Block Code
STP	Shielded twisted pair
TCP	Transmission Control Protocol
TCS	Traction Control System
TDM	Time Division Multiplexing
TDMA	Time Division Multiple Access
TMC	Technology and Maintenance Council (American Trucking Associations)

List of Abbreviations (Continued)

Abbreviation	Definition
UDP	User Datagram Protocol
UNECE	United Nations Economic Commission for Europe
UTP	Unshielded twisted pair
VAN	Vehicle Area Network
VME	VERSAmodule Eurocard
Volvo	Volvo Trucks North America
WABCO	Westinghouse Air Brake Company (Wabtec)
WAVE	Wireless access in vehicular environments
WLAN	Wireless local area network
WPA	Wi-Fi Protected Access
WPAN	Wireless personal area network

Units of Measurement

Unit	Meaning
kg	kilogram
km/h	kilometer per hour
kPa	kilopascal
m	meter
m/s	meter per second
m/s^2	meter per second squared
mm	millimeter
N•m	Newton-meter
s	second

The Page Intentionally Left Blank.

Executive Summary

The purpose of this project was to explore ways to improve the roll and yaw stability of combination heavy duty commercial trucks. The three-pronged approach included developing stability algorithms, assembling demonstration hardware, and investigating robust wireless communication between individual units of the vehicle. The project aimed to establish building blocks for an integrated electronic stability control (ESC) system to help a driver maintain control of a tractor-semitrailer combination vehicle. The significance of the project is the potential for improving the safety and productivity of commercial vehicle operations through reductions in truck-related crashes, injuries, and fatalities. The project was sponsored by the National Transportation Research Center, Inc., through a grant from the U.S. Department of Transportation's Research and Innovative Technology Administration.

Background

Modern ESC products automatically slow a vehicle rounding a corner too quickly or apply individual brakes when necessary to improve the steering characteristics of a vehicle. Air brake systems in North America provide no electronic communication between a tractor and semitrailer, limiting the degree to which control systems can be optimized. Prior research has demonstrated stability improvements where dynamic measurements and control commands are communicated between units of a vehicle. This project was needed to develop a control algorithm, demonstrate the necessary hardware, and document the feasibility of an intra-vehicle wireless network to provide communications without changing the standard equipment connections between a tractor and semitrailer.

Brief Overview

To define a new algorithm for ESC, researchers first determined which vehicle states need to be measured for controlling the vehicle. They developed an algorithm to calculate the proper brake response to specific conditions. An integrated stability control for the tractor and semitrailer will require communication between the two units. Dynamic models were used to optimize the competing stability needs of yaw and roll.

Equipment to test this and other ESC algorithms was implemented in the laboratory. Hardware components suitable for the harsh environment for measurement, sensor-to-controller communication, semitrailer-to-tractor communication, and brake actuation were specified and assembled as a working system. The goal was to demonstrate collection of the needed vehicle state information, transmit the information to the ESC system, and then actuate the brakes in response to controller commands.

A wireless network was developed to support whole-vehicle ESC. Communicating dynamic signals requires a high data rate with high reliability. The rate adaptation algorithm distinguished channel fading from data packet collisions. The network's adaptive multi-hop

routing was aware of the connectivity of its wireless links. Adaptability was necessary to avoid packet collisions and tolerate fading in the harsh vehicle environment. Experiments on an actual vehicle demonstrated that the protocol can reliably transmit high-priority, urgent messages.

Research included an extensive literature review of air brake and braking control evolution and technology back to the 1860s, a description of the structure and system processes involved in commercial vehicle air brake systems, a discussion of the physics and mechanics of truck stability, and a description of existing wireless communication protocols for vehicles. Simulation models were used to supplement laboratory-scale bench testing and track testing.

Conclusion

An algorithm for improving the stability of a multi-unit, heavy-duty combination vehicle has been developed and demonstrated in simulations. The ESC system reflected in this algorithm can manage more than one unit symbiotically. The algorithm accounts for both roll and yaw instabilities, and it acts in a way that can manage a developing instability in one mode without diminishing the stability of other modes. Time-domain simulations have shown its effectiveness in transient and steady-state maneuvers. The algorithm works on a range of surface frictions, though some maneuvers on extremely slippery (e.g., snow) surfaces are only minimally improved.

The hardware bench test system for a complete tractor-semitrailer brake system and control unit was built and exercised. The system has the flexibility to implement different architectures within the controller. The sensing and decision-making processors can be a single, centralized unit, or they can be a pair on the tractor and semitrailer. Functional and performance test protocols for the equipment have been written.

Wi-Fi has been demonstrated on a three-semitrailer combination unit in motion in a test track environment. A throughput rate in excess of what is necessary for the control algorithms has been experimentally confirmed. When the vehicle is stationary, the throughput rate is limited only by the wireless equipment itself. Nearly 100 Mbps was achieved. Vibration of the vehicle while in motion limited the reliable throughput rate to 40 Mbps.

Future Program Efforts

Though the stability algorithm was implemented in a simulation, its inputs were limited to quantities that can be measured in practice in an actual vehicle. This established the bandwidth needed to implement the measurement and control system, providing guidance to the subsequent tasks.

The algorithm uses a tiered approach—it calculates the stability margin for the tractor and trailers and for roll and yaw in sequence. The simulations have shown this approach to be effective, but a more robust approach is possible. If a single, integrated set of the equations of motion for the entire vehicle were developed, then the stability could be expressed in state space.

That is, the stability threshold could be expressed in a compact mathematical formula rather than as a sequence of tests. This would allow the control interventions to be optimized, automatically balancing any conflicting needs.

One next step is to execute the functional and performance test protocols developed for the ECS equipment. The equipment is available to serve this purpose in future research, experimenting with the performance of different sensors and actuators, control algorithms, and electronics architectures.

Work should continue to reduce the cost and improve the reliability of intra-vehicle communication. Dedicated hardware could be made to cost less money when manufactured in quantities and to use less power. Research in algorithms and protocols has proven the reliability needed for a system that supports safety functions.

This Page Intentionally Left Blank.

Chapter 1 – Introduction and Background

A team led by the National Transportation Research Center, Inc., (NTRCI) worked to improve the roll and yaw stability of combination heavy duty trucks by developing stability algorithms, assembling demonstration hardware, and investigating robust wireless communication.

The team beginning this work completed a series of projects for NTRCI on heavy vehicle stability. The team explored the roll stability of a van semitrailer (Knee et al. 2005), a flatbed semitrailer (Pape et al. 2008), and a tank semitrailer (Arant et al. 2009 and LaClair et al. 2010). A project running concurrently gathered data on the behavior of a triple trailer combination vehicle in normal maneuvers (Pape et al. 2011).

1.1 Background

Modern electronic stability control (ESC) products automatically slow a vehicle rounding a corner too quickly or apply individual brakes when necessary to improve the steering characteristics of a vehicle. Air brake systems in North America provide no electronic communication between a tractor and semitrailer, limiting the degree to which control systems can be optimized. Prior research has demonstrated stability improvements when dynamic measurements and control commands are communicated between units of a vehicle. The purpose of this project was to establish building blocks for an integrated system to help a driver maintain control of a combination unit vehicle. Those building blocks are a control algorithm, a demonstration of the necessary hardware, and an intra-vehicle wireless network to provide communications without changing the standard equipment connections between a tractor and semitrailer.

1.2 Project Team

Two academic institutions, Clemson University International Center of Automotive Research (CU-ICAR) and Auburn University National Center for Asphalt Technology (NCAT), had leading roles in the technical work of this project. Two research institutions, Battelle and Oak Ridge National Laboratory (ORNL), supported particular aspects of the technical work. Three commercial companies, National Instruments, Volvo, and Bendix Commercial Vehicle Systems, LLC, donated equipment for the project and provided valuable advice. More complete descriptions of each organization and its role follow.

1.2.1 CU-ICAR

CU-ICAR had the lead role in developing algorithms for vehicle stability and in designing and building the working demonstration model.

1.2.2 Auburn University

Auburn University had primary responsibility for the investigation of wireless communication between units of a combination vehicle.

1.2.3 ORNL

ORNL contributed expertise to the working demonstration of sensors and protocols.

1.2.4 Battelle

Battelle provided technical expertise to the background of air brakes and contributed to the management task. Battelle had primary responsibility for assembling and editing the final report, using contributions by other team members.

1.2.5 Bendix

Bendix donated the braking system components for the hardware bench test system, which included the Bendix ABS-6 actuation, sensing, and control hardware. Bendix also participated in several technical discussions, bringing their extensive vehicle stability experience to the team.

1.2.6 National Instruments

National Instruments contributed products and expertise to the project. The company donated hardware and software for designing, building, and testing the controller. Staff gave advice in controller hardware-in-the-loop system development methods.

1.2.7 Volvo

Volvo contributed a tractor electrical harness, including the connections for the ABS-6 system, and technical support.

1.2.8 NTRCI

NTRCI staff played an active role in managing the project and coordinating the activities of the numerous contractor teams.

1.3 Project Description

The first of three integrated activities was to develop an algorithm for the optimum yaw and roll control of a combination vehicle. The study determined which vehicle state parameters are needed to control the vehicle and the proper brake response to specific conditions. An integrated stability control for the tractor and semitrailer will require communication between the two units. Dynamic models were used to optimize the competing stability needs of yaw and roll.

Closely tied to the first activity was the laboratory implementation of a braking system. Hardware components suitable for the harsh environment for measurement, sensor-to-controller communication, semitrailer-to-tractor communication, and brake actuation were specified and assembled to a working system. The goal was to demonstrate collecting the needed vehicle state information, transmitting the information to the ESC system, and then actuating the brakes in response to controller commands.

The third and final activity was to develop a wireless network for supporting a vehicle stability control system. Communicating these dynamic signals requires a high data rate with high reliability. The rate adaptation algorithm distinguished channel fading from data packet collisions. The network’s adaptive multi-hop routing was aware of the connectivity of its wireless links. Adaptivity was necessary to avoid packet collisions and tolerate fading in the harsh vehicle environment. The protocol demonstrated how to transmit high priority urgent messages reliably.

1.4 Project Schedule

This project was conducted in the first nine months of calendar 2011. The three main technical tasks ran in parallel through July 31, 2001. Figure 1-1 is the project schedule. The tasks are identified and their lead organizations are named below the figure.

Tasks	Month of the Project								
	01/11	02/11	03/11	04/11	05/11	06/11	07/11	08/11	09/11
1									
2									
3									
4									
5									

Figure 1-1. Chart. Schedule of tasks.

- Task 1: Program Management (NTRCI Lead)
- Task 2: Control Strategies (CU-ICAR Lead)
- Task 3: Sensors and Protocols (CU-ICAR Lead)
- Task 4: Wireless Investigation (Auburn Lead)
- Task 5: Reporting (Battelle Lead).

This Page Intentionally Left Blank.

Chapter 2 – Literature Review

Over the last 60 years, the heavy truck industry has matured into a very efficient and effective goods transportation enterprise. As is the case with most industries, the initial developments in the heavy trucking industry dealt primarily with operational limitations (payload limitations, human limitations, etc.) and equipment cost. Later developments were mostly focused on improving efficiencies and ergonomics (allowing the human to be more productive). In keeping with usual technology development trends, the last two decades have demonstrated a move toward improving vehicle safety in addition to improving operational efficiency. This interest in safety has also been increasing due to rising injury and disability costs as well as governmental regulations and mandates.

Examples of recent safety-related activities include the regulation requiring antilock brakes (ABS) on all tractors and trailers made after March 1, 1997 (NHTSA 2009) as well as the reduction of maximum stopping distances 96 km/h (60 mph) for class 8 vehicles from 102 m (335 ft) to 76 m (250 ft) in 2011 (NHTSA 2009).

Based in part on the results of ESC in reducing passenger car accident rates, injuries, and deaths, there is now interest by the U.S. government in ESC systems for commercial vehicles as well (NHTSA 2011). Additionally, other markets (Europe) have already begun the transition to ESC for commercial vehicles, increasing the probability that similar legislation will be forthcoming in the U.S. Thus there is now significant interest within the commercial vehicle industry for evaluation of ESC capabilities, costs, benefits, and limitations. It is with these facts in mind that the current research on commercial vehicle stability is being conducted.

2.1 Introduction to Commercial Vehicle Air Brakes

The air brakes currently used in commercial vehicles are the result of over 150 years of adaptation and development. Brake systems for heavy trucks continue to evolve and adapt to increasingly stringent safety and efficiency requirements.

2.1.1 Historical Perspective

The development of modern braking systems for heavy commercial vehicles is an example of emerging technology, combining elements of entrepreneurship, political expediency, and the growth of industrialization.

The first practical air brakes appeared in the 1860s, following several patents by George Westinghouse covering the technologies we are familiar with today (Figures 2-1 and 2-2). These include the use of compressed air to actuate the brakes (Synnestvedt 1895), implemented with control valves and gladhands (Westinghouse 1869), followed by the introduction of auxiliary reservoirs (Westinghouse 1872b) and fail-safe design (Westinghouse 1872a). In 1871, a train accident that killed 24 people occurred in Revere, Massachusetts, capturing public attention and prodding managers of eastern railways to adopt air brakes (Rodengen 1999).

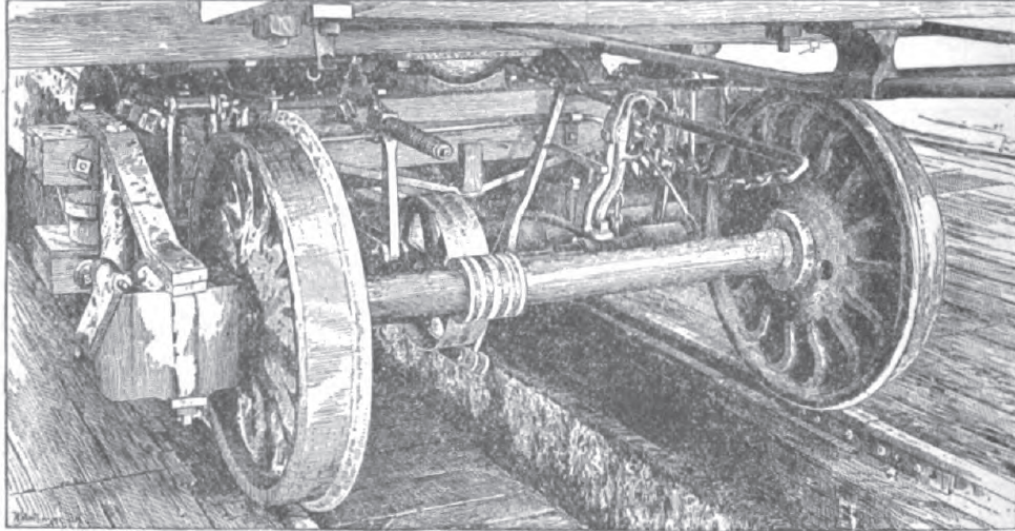


Figure 2-1. Drawing. Widdifield & Button friction buffer brake.

Source: (Master-Car Builders Association 1887)

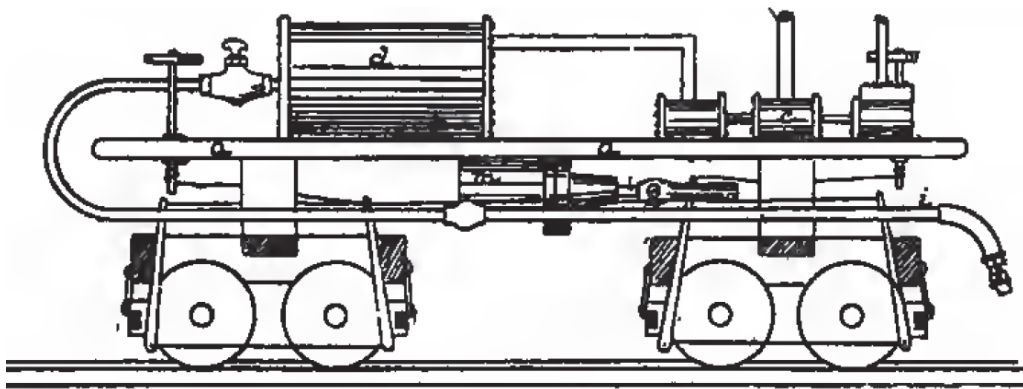


Figure 2-2. Drawing. Westinghouse straight air brake.

Source: (Synnestvedt 1895)

Westinghouse's developments formed the basis for the founding of Westinghouse Air Brake Company (Wabtec Corporation 2008), later shortened to WABCO. The company's technology became widely accepted and its use was institutionalized by the adoption in 1893 of the Federal Railroad Safety Appliances Act, mandating the use of air brakes on all trains in the U.S. by 1900.

The first truck was produced by Gottlieb Daimler in 1896 (Figure 2-3), with a 1500-kg payload (Mercedes Benz UK 2011). The first truck produced in the U.S. (Figure 2-4) was the product of the Winton Motor Carriage Company in 1898 (Stapleton 1997; Holdgreve 1999). The first truck produced by the longest surviving truck company in the U.S., Mack Trucks, was produced in 1900 (Mack Trucks LLC 2011). Mack also produced rail cars and locomotives. Winton began production of diesel engines in 1912, and in 1930 Winton's company was bought by General Motors, later to form part of Electro-Motive Division, which became the world's largest

producer of locomotives in the world (Electro-Motive Diesel 2011; Brazeau 2011). The technical link between the rail car and the heavy truck was close, and developments in technology similarly affected both.



Figure 2-3. Photo. The first truck in 1896 produced by Daimler Motoren Gesellschaft.

Source: (Mercedes Benz UK 2011)

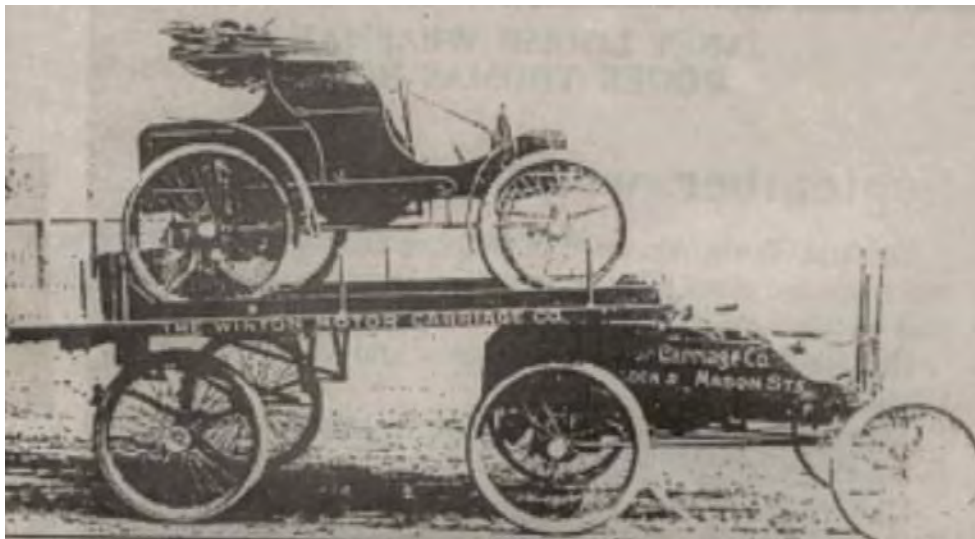


Figure 2-4. Photo. 1898 Winton semi-truck carrying a new Winton motor car.

Source: (Holdgreve 1999)

As the use of heavy trucks expanded, air brakes were adopted on these vehicles from the railroads. By 1949, air brakes became the standard for all heavy trucks, tractor-trailers, buses, fire trucks, and off-highway construction vehicles (Honeywell International 2011).

2.1.2 Design of Modern Commercial Vehicle Air Brakes

The basic form of the commercial vehicle air brake has changed little since 1949. Historically and today most commercial vehicles in use in the U.S. use drum brakes in which a pair of brake pads press against the inside of a brake drum to apply a braking effect, dissipating the vehicle's kinetic energy as heat generated by friction between the surfaces of the brake pad and the brake drum (See Figure 2-5).

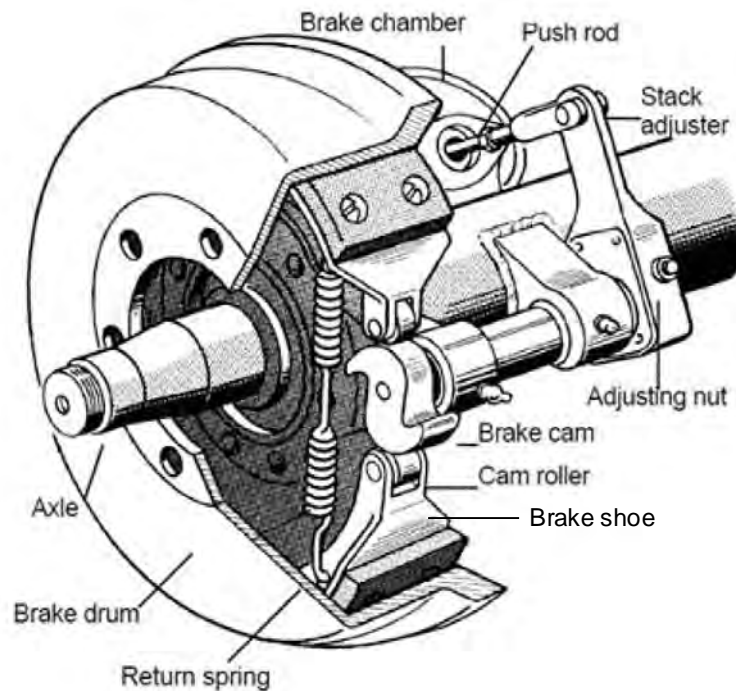


Figure 2-5. Drawing. Drum-style air brake.

Source: (South Carolina Department of Transportation 2011, 5-3)

Different methods of applying force to move the brake shoe and the attached brake pad or block against the brake drum have been used. The most common methods are the wedge design and the S-cam design. In the wedge design, the brake shoe is actuated by the motion of a wedge (See Figure 2-6). Outside of military vehicles and heavy construction vehicles, this design is no longer common in North America due to the higher air pressures required and greater sensitivity to changes in friction leading to compatibility issues when mixing wedge braked tractors with S-cam braked trailers. Further, wedge brakes are difficult to inspect and exhibit higher hysteresis than the S-cam design.

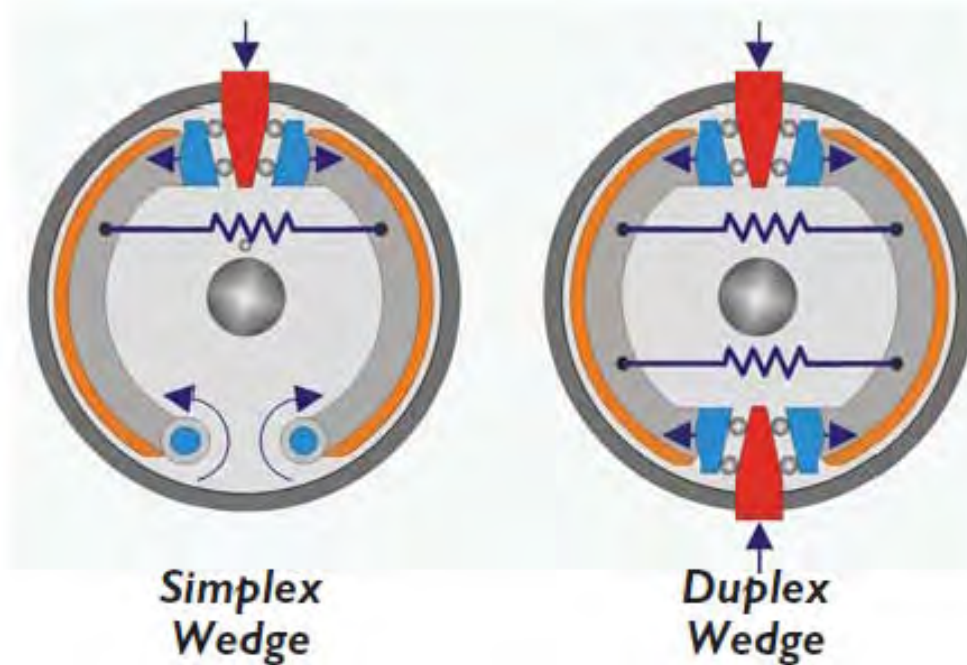


Figure 2-6. Drawing. Wedge brake design.

Source: (Bendix Spicer Foundation Brake LLC 2011b)

In the S-cam design, the brake shoe is actuated through the motion of an S-shaped lever, which acts on both brake shoes together (See Figure 2-7). This is the most commonly found type of brake design, used on approximately 95% of Class 5-8 air-braked vehicles in North America (Bendix Spicer Foundation Brake LLC 2011b).

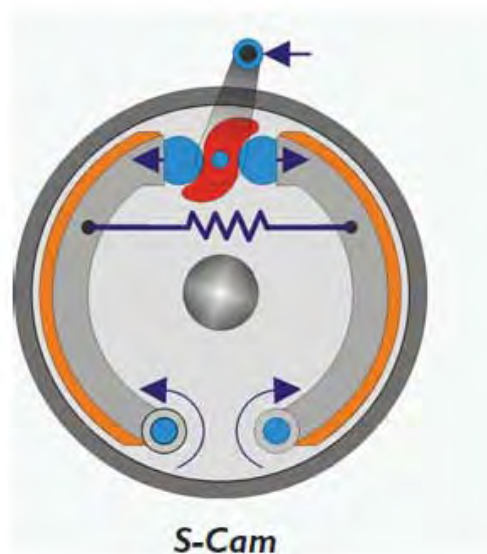


Figure 2-7. Drawing. S-cam brake design.

Source: (Bendix Spicer Foundation Brake LLC 2011b)

The control of the brake shoe actuation on an air brake is accomplished by a brake chamber, which converts an air pressure differential into a force applied on the brake shoe. Early designs of this brake chamber were direct acting, also referred to as the straight air brake design (see the early work of George Westinghouse, Figure 2-2). In this design the air pressure is applied directly to the diaphragm of the brake chamber, which moves in response to apply force to the brake shoe. When no air pressure is applied, the brake shoe is not moved and no braking action exists. In the case of an accidental loss of air pressure from a system failure, braking action is lost. For this reason, the so-called automatic air brake was developed, which provided for fail-safe operation in the case of an accidental pressure loss. This latter system is used in all air brake applications in modern times.

Brake Air Chamber

In modern air brake systems, the brake shoe is actuated by an air cylinder called an air chamber (See Figure 2-8). The air chamber is typically mounted at the wheel, and actuates the S-cam through the action of a pushrod.

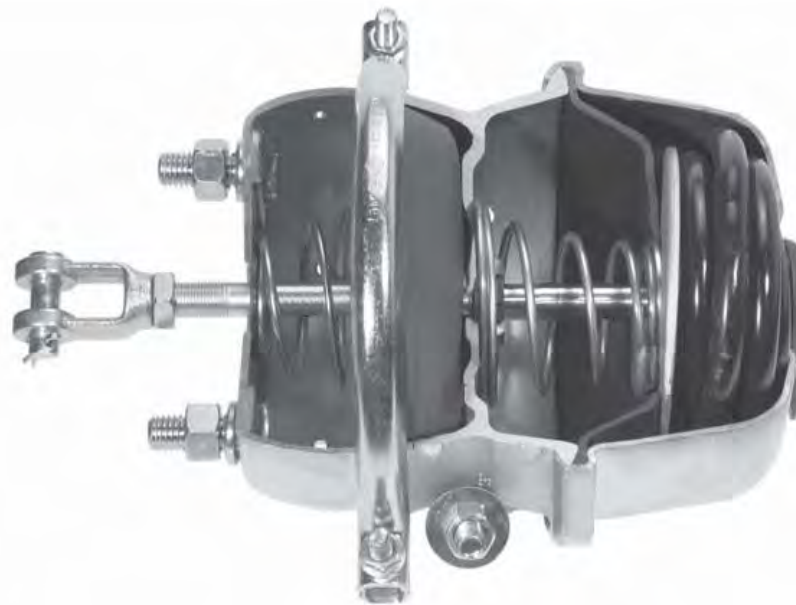


Figure 2-8. Photo. Cross-section of an air brake air chamber with spring brake.

Source: (Bendix Commercial Vehicle Systems LLC 2008a)

The air chamber with the fail-safe spring brake feature contains two separate pressure chambers. These are 1) the spring brake chamber and 2) the service brake chamber (See Figure 2-9). When the vehicle is parked and the parking brake is applied, both the spring brake chamber and the service brake chamber are de-pressurized. The parking brake is applied by the force of the parking brake spring acting on the diaphragm, which extends the pushrod.

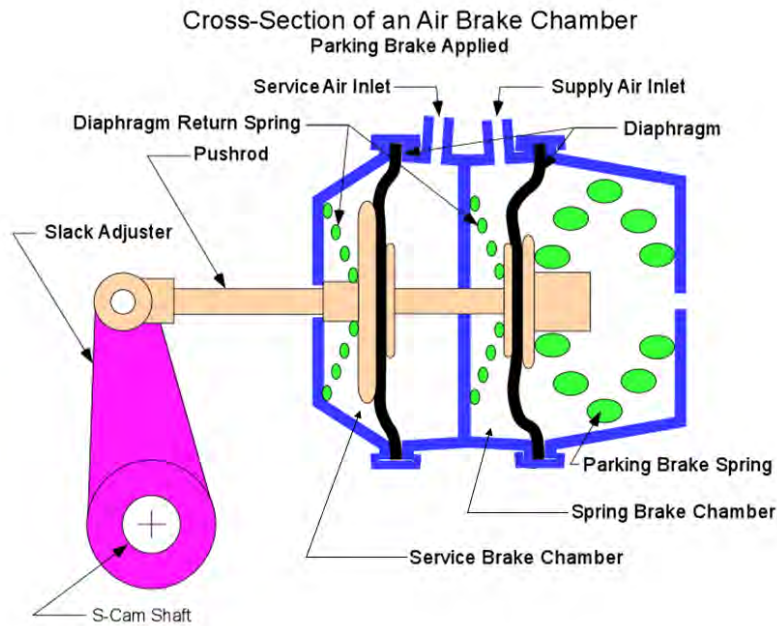


Figure 2-9. Drawing. Air chamber with parking brake applied.

When the driver releases the parking brake, supply air pressure is applied to the spring brake chamber, counteracting the force of the parking brake spring. The pressure of the supply air acts on the spring brake chamber diaphragm to push the parking brake spring back, releasing the parking brakes (See Figure 2-10).

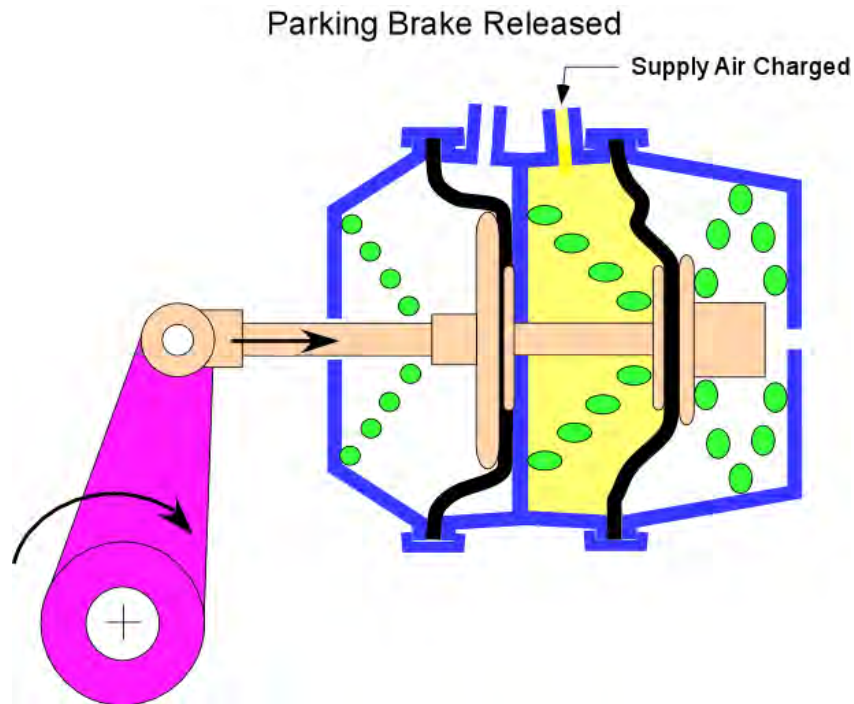


Figure 2-10. Drawing. Air chamber with parking brake released.

When the driver applies the service brake, service air pressure is applied to the service brake chamber. The pressure of the service air acts on the service brake chamber diaphragm to actuate the pushrod and apply force to the slack adjuster, which in turn rotates the S-cam shaft, resulting in the spreading of the shoes and contact between the pads and drum. (See Figure 2-7.)

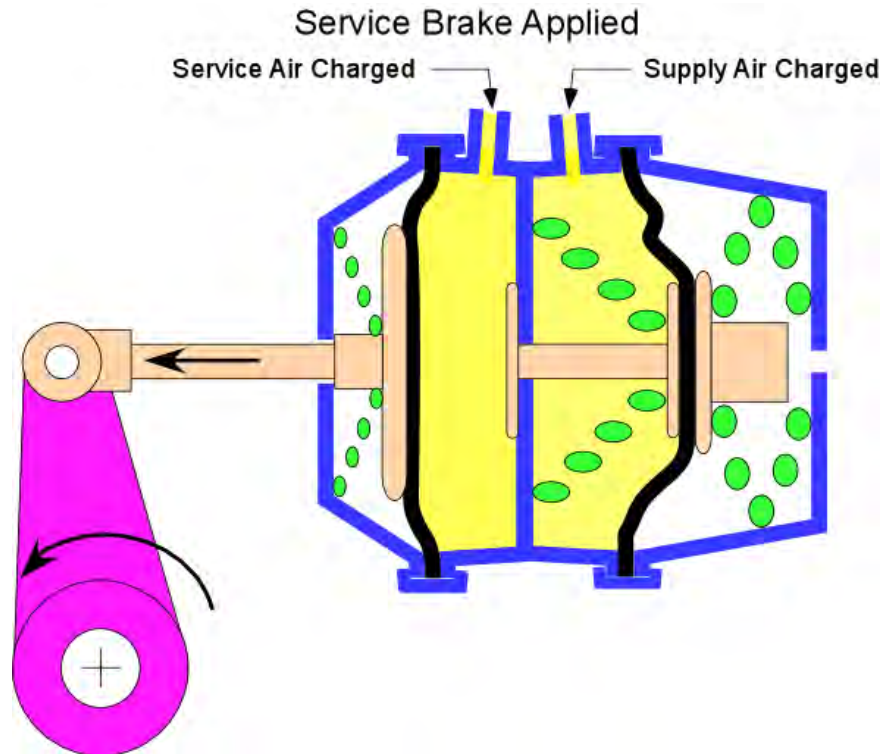


Figure 2-11. Drawing. Air chamber with service brake applied.

If the brake system air pressure is lost, pressure in both chambers of the air chamber falls and the parking brake is automatically engaged by the mechanical action of the parking brake spring.

Automatic Slack Adjuster

In the course of regular use, the typical brake pad and drum material will wear away, so that the distance of movement of the brake pad from its resting position to the position of contact with the brake drum will increase over time. If the brake pad wears without adjustment to compensate, the brake may become ineffective. The distance between rest and contact positions may become so great that the effective stroke of the air chamber pushrod cannot accommodate the increase. To mitigate this condition, the slack adjuster keeps the brake in constant adjustment by advancing the S-cam forward as the friction material wears (See Figure 2-12). In the early days, checking and adjustment of 'manual' slack adjusters was a part of every professional driver's daily routine. Air brakes do not provide the pedal 'feel' of hydraulic brakes, so drivers often are not aware of brake system problems until failure occurs in an emergency situation (Seiff 1994).



Figure 2-12. Drawing. Automatic slack adjuster.

Source: (Bendix Spicer Foundation Brake LLC 2011b)

Braking system maintenance has been an ongoing concern for commercial vehicle operators and regulators. According to the Commercial Vehicle Safety Alliance (CVSA), out of adjustment air brakes and brake system defects constitute the major defect areas resulting in commercial vehicles being placed out of service during roadside safety inspections (CVSA 2011). Fatalities involving the crash of a commercial vehicle make up 1 out of every 8 traffic deaths (NHTSA/DOT 2004). In one study, brake defects were found in 56% of tractor-trailer crashes (Stein 1989, 469). Of all large truck crashes, 29% involve brake failure, brake adjustment or other brake issues, according to the Large Truck Crash Causation Study (Hedlund and Blower 2011). All of these facts motivated the requirement in 1995 to equip all air-brake systems in commercial vehicles with automatic brake adjusters, commonly referred to as automatic slack adjusters, or simply as autoslacks.

Treadle Valve

The driver's brake signal for the application of the service brake is generated by a brake-pedal-actuated air valve, often referred to as a treadle valve (See Figure 2-13). The treadle valve operates both primary and secondary brake circuits, where the tractor drive axles are typically controlled by the primary circuit, and the tractor steer axle and trailer axle are typically controlled by the secondary circuit.

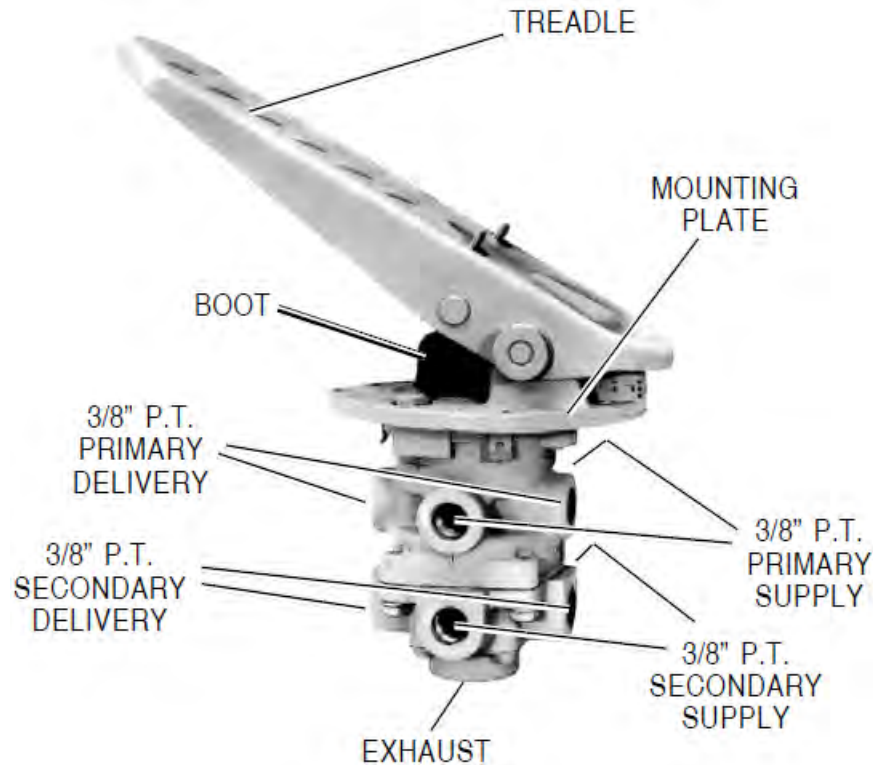


Figure 2-13. Drawing. Brake pedal treadle valve.

Source: (Bendix Commercial Vehicle Systems LLC 2007)

A schematic showing a typical air brake system pneumatic layout for a tractor is shown in Figure 2-14. Other valves between the treadle valve and the individual air chambers provide ABS or traction control. For axles located farther away from the treadle valve, a relay valve (sometimes called a distribution valve) is used to allow the large volume of air required to actuate the brakes to be stored in reservoirs close to the brake chambers, thus permitting a small air volume control signal to be delivered from the treadle valve, and reduce the delay in fully actuating the brakes.

The air volume required for supply and control is an important consideration, since movement of the air volume to actuate the brakes is a source of lag in their operation. It has been estimated that this lag is on the order of 400 to 600 milliseconds for a trailer axle to respond to a brake command (Murphy, Limpert, and Segel 1971; Winkler et al. 1976; Yanakiev, Eyre, and Kanellakopoulos 1997; Dunn 2003). For a multi-trailer combination vehicle these control signal transport delays are yet longer, so brake delay on the most rearward vehicle units can exceed 1 second. Efforts to control the stability of such vehicles with automatic controllers are limited by the control signal transport delay and the slow response of the brake mechanism itself. The cycle time of ABS implementations on air brakes can be on the order of 750 milliseconds (Kienhöfer, Miller, and Cebon 2008, 571).

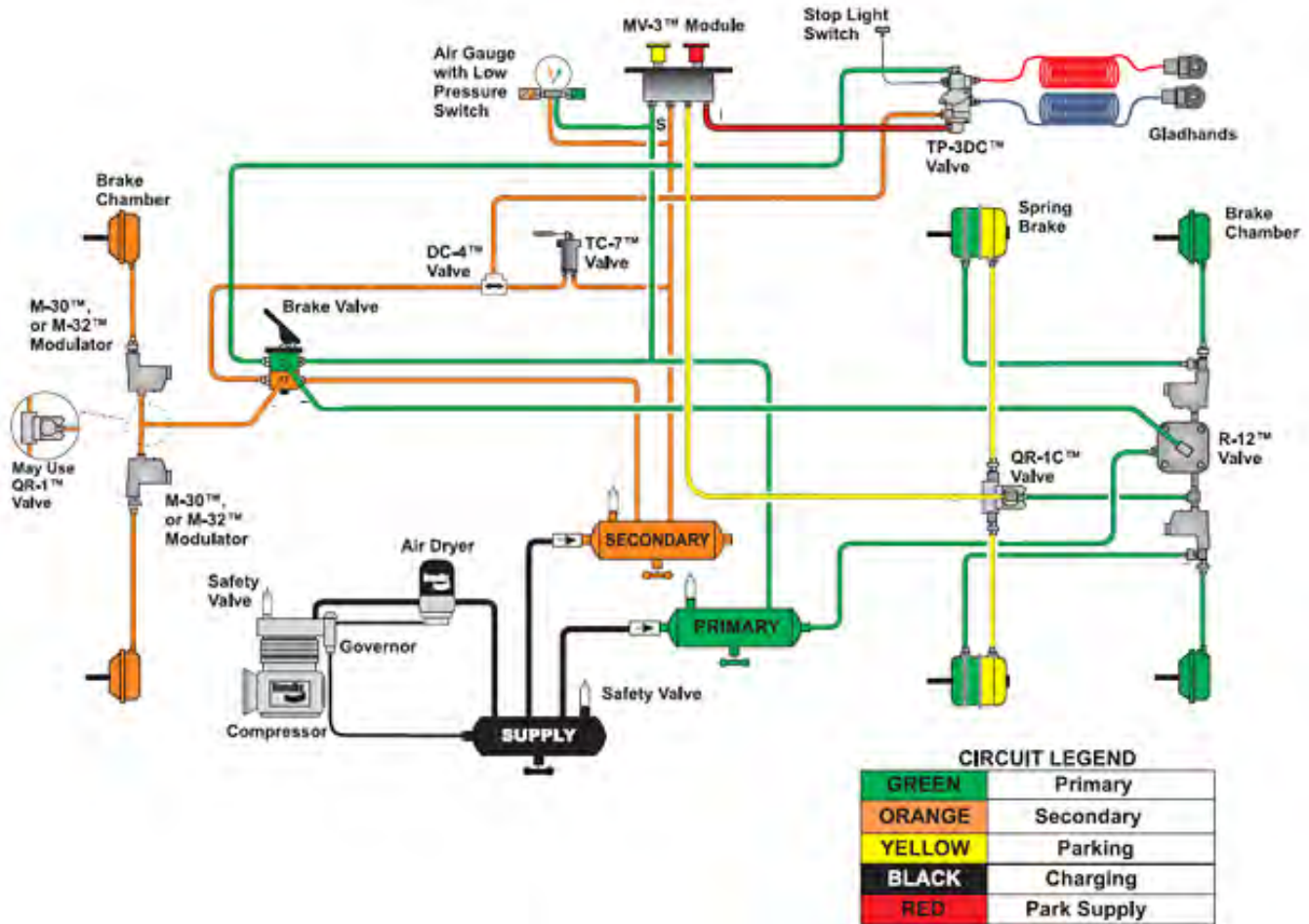


Figure 2-14. Diagram. Bendix air brake system diagram for tractor.

Source: (Bendix Commercial Vehicle Systems LLC 2004a)

Quick Release Valve

A characteristic of an air brake in general is that the level of hysteresis in such a brake is relatively high. In order to reduce the amount of hysteresis, the quick release (QR) valve was developed. The function of the quick release valve is to reduce the time needed to exhaust the air from the air chamber. It is typically mounted close to the chambers it serves (Bendix Commercial Vehicle Systems LLC 2004a). The quick release valves are shown in the schematic of Figure 2-14 as “QR-1 Valve” and “QR-1C Valve” and are often integrally combined with the relay valve.

Relay Valve

The air chambers on the trailer axles are located far away from the treadle valve controlling their action. This distance is more than 10 m, and in the case of triple trailer combinations can exceed 25 m. To reduce hysteresis and lag, the air chambers controlling the brakes on a remote axle are themselves controlled by a relay valve. When the driver applies the brakes, air travels through

the delivery (i.e., the control) line to the relay valve and moves an internal piston. This closes the exhaust and opens the delivery of air to the air brake chambers, thus actuating the brakes. The primary benefit of using a relay valve is it reduces the volume of air needed to control the brake, thereby making the actuation more responsive. The brake force is adjustable and when released the relay valve exhausts to atmosphere. Relay valves are generally mounted close to the chambers they serve and are available in both remote and reservoir mount designs. Relay valves are also typically used on the rear axle brakes on tractors. Relay valves are also used on axles of trailers. The relay valve is shown in the schematic of Figure 2-14 as “R-12 Valve.”

Traction Control Valve

Some tractors come with a traction control feature, which applies the brakes to prevent drive tires from spinning on slippery surfaces. To permit an electronic signal to apply the brake, a solenoid is added to open the delivery of air to the air brake chambers under an electrical signal. The valve may be incorporated into the relay valve or it may be separate. In normal operation, this valve performs the standard relay function, and the traction relay valve is normally mounted near the service brakes it serves, as is the standard relay valve. (Bendix Commercial Vehicle Systems LLC 2008b). See Figure 2-15. A valve of this type is used on axles other than the drive axles to support ESC systems and other systems where an electronic controller applies the brakes.

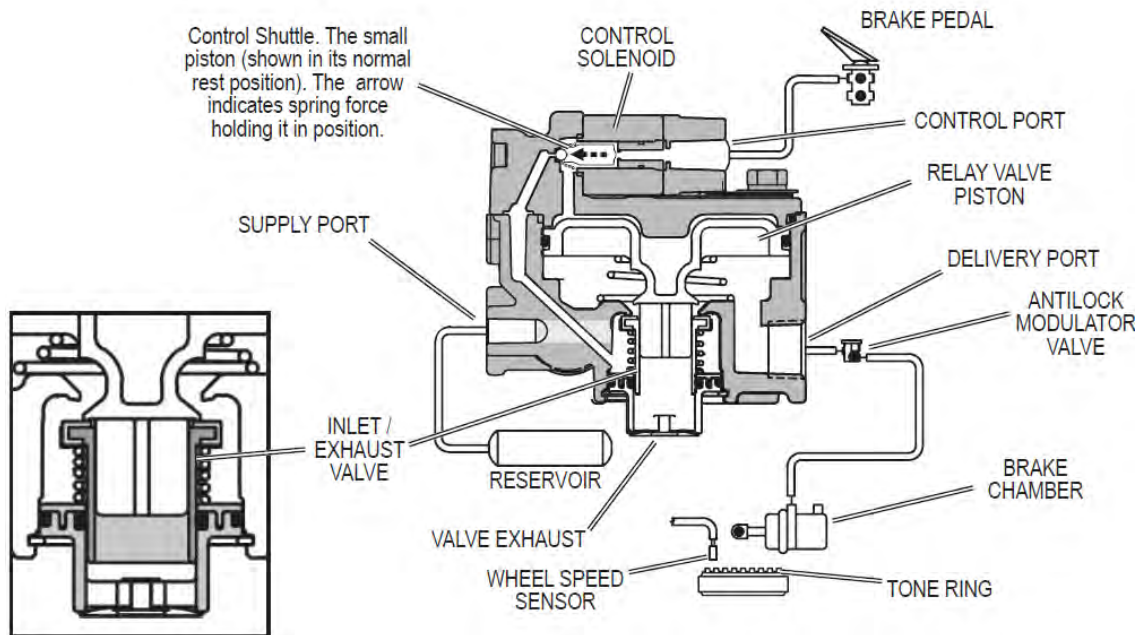


Figure 2-15. Diagram. Bendix ATR6 traction relay valve and antilock traction control assembly.

Source: (Bendix Commercial Vehicle Systems LLC 2004a)

Antilock Brake Modulator Valve (ABS)

The antilock braking system (ABS), intermittently releases the braking force when necessary to prevent the wheel from locking. A modulator valve between the quick release or relay valve and

the air chamber has a solenoid controlled by the ABS controller. When the valve is shut, pressure is able to build up again. (Bendix Commercial Vehicle Systems LLC 2004a). The modulator valve is shown in the schematic of Figure 2-14 as “M-30 or M-32 Modulator” and a section view of this valve is shown in Figure 2-16.

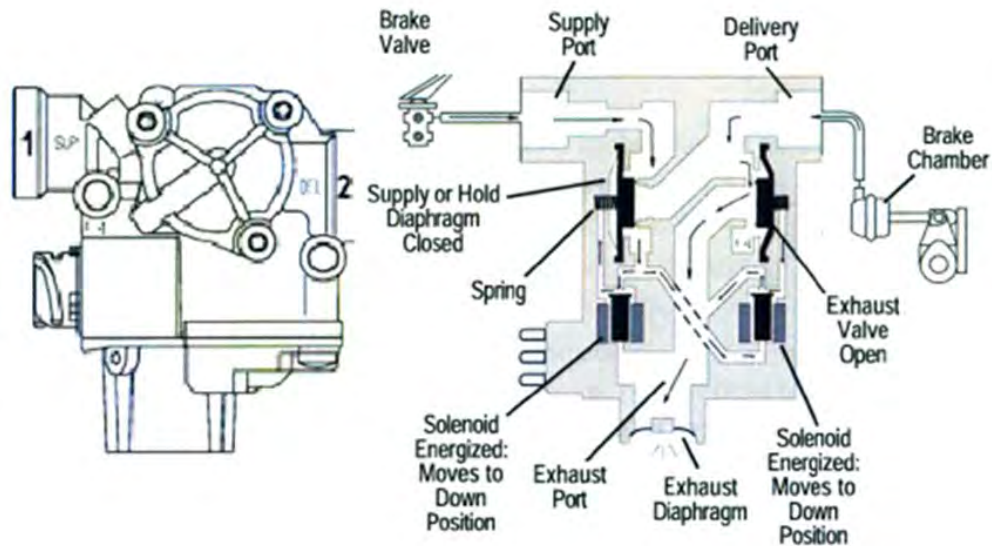


Figure 2-16. Drawing. Bendix antilock brake modulator valve.

Source: (Bendix Commercial Vehicle Systems LLC 2004b)(Bendix Commercial Vehicle Systems LLC 2004a)

2.1.3 The Future of Commercial Vehicle Air Brake Systems

In recent years, issues of traffic congestion, fuel availability and cost, and driver availability have prompted analysts and policy makers to search for ways to increase the efficiency of freight hauling. One way to accomplish this is to increase the capacity of commercial vehicles (Woodroffe et al. 2009a). Furthermore, the Federal Motor Carrier Safety Administration (FMCSA) continues in its mission to improve commercial vehicle safety, in order to reduce the rate of accidents and injury due to crashes of heavy trucks. Both of these efforts promote the improvement of the effectiveness and efficiency of braking systems on heavy duty trucks. To this end, several developments in air brake systems are occurring now or are on the horizon.

The first of these is a recent change to Federal Motor Vehicle Safety Standards (FMVSS) requiring a reduction in stopping distance for heavy trucks. In 2009, the National Highway Traffic Safety Administration (NHTSA) mandated this reduction by a series of updates to FMVSS No. 121 (NHTSA 2010). These updates reduce the required stopping distance of tractors traveling at 60 miles per hour from 355 feet to 250 feet, a reduction of 30 percent. The transition to the new stopping distance requirement will be completed in two phases from 2011 to 2013, with standard 6x4 tractors built on or after August 1, 2011, required to meet the new standard. It addresses approximately 70 percent of all new heavy tractors built (Bendix Spicer

Foundation Brake LLC 2011b). All other tractors, including severe service 6x4 units, built before August 2013 may continue to meet the old standard.

Although many manufacturers and suppliers thought the reduction in stopping distance could be achieved only through adoption of more expensive disc brakes on commercial vehicles, it seems that most manufacturers have been able to meet the standard through brake system hysteresis reductions and by larger drums called enhanced drum brakes (Bendix Spicer Foundation Brake LLC 2011c, 2; Brothers 2009). Nevertheless, all the major brake suppliers to the industry offer a line of disc brakes (Bendix Spicer Foundation Brake LLC 2011a; Haldex Commercial Vehicle Systems 2011; Meritor WABCO 2011).

The next change in air brake systems is a movement to adopt ESC in heavy trucks. ESC has been shown to be very effective at reducing the rate of accidents in passenger cars (Dang 2004; Lieberman et al. 2003; Aga and Okada A. 2003). ESC shows promise of being similarly effective in reducing the incidence of accidents of heavy vehicles (Barickman et al. 2009; Woodrooffe et al. 2009b). In Europe, the adoption of ESC in commercial vehicles has been pushed by the adoption of ECE R13 (2008). In 2007, the United Nations Economic Commission for Europe (UNECE) amended Regulation 13, requiring new trucks to be equipped with ESC starting in 2010 (Wurster et al. 2010).

This change required several major modifications to regulations and current design standards, including the adoption of an Electronically Controlled Braking System (ECBS). ECBS keeps the compressed air as the source of braking force, but the brake control is an electronic signal, i.e., the driver's electronically measured brake demand is transmitted to the brake control valve, in turn connected to the air supply reservoirs with the brake chambers.

Relevant Test Standards

Air brake systems are specified in part by standards governing their testing and evaluation. Table 2-1 presents a partial list of such standards, from the Society of Automobile Engineers International (SAE).

Table 2-1. Test standards for air brake systems.

SAE Standard No.	Standard Title
J294	Service Brake Structural Integrity Test Procedure-Vehicles Over 4500 kg (10,000 lb) GVWR (gross vehicle weight rating)
J1505	Brake Force Distribution Test Procedure-Trucks and Buses
J1854	Brake Force Distribution Performance Guide-Truck and Bus
J1859	Test Procedures for Determining Air Brake Valve Input-Output Characteristics
J1911	Test Procedure for Air Reservoir Capacity--Highway Type Vehicles
J2115	Air Brake Performance and Wear Test Code Commercial Vehicle Inertia Dynamometer
J2318	Air Brake Actuator Test Performance Requirements - Truck and Bus

2.2 Commercial Vehicle Stability

This section presents basic principles and background information on roll and yaw stability understeer/oversteer phenomena are also discussed, as are the physics and dynamics of articulated vehicles.

2.2.1 Roll Stability

The only way that a vehicle can remain upright during a handling maneuver is for the vehicle to transfer vertical load from one wheel to the other generating a moment counter to the overturning moment (Figure 2-17, Figure 2-18). The vehicle's and suspension's compliances have been neglected in this simplified analysis. This simplifying assumption is made for reasons:

- Calculating chassis roll requires more precise information on the vehicle (suspension stiffness, roll center, etc.) than needed to assess rigid chassis behavior
- Calculating chassis roll requires additional computational time when the goal is to have a fast estimator of roll potential.
- If the vehicle is kept well below its roll threshold, the effect of the assumption is minimal.

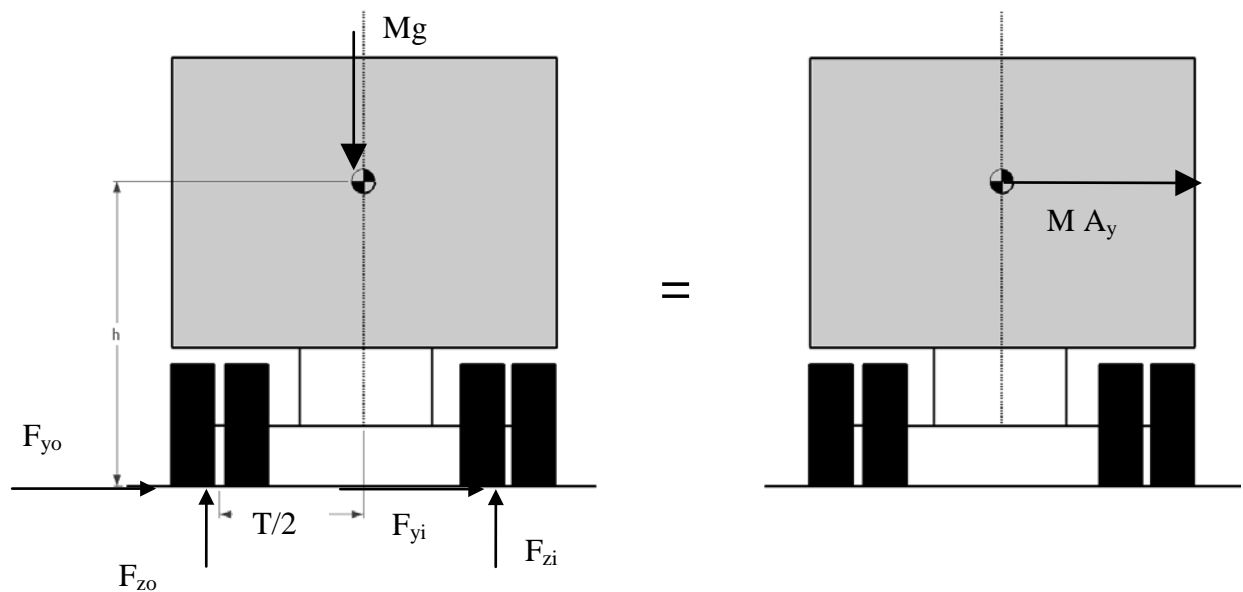


Figure 2-17. Diagram. Overturning moment (Arant 2010).

$$F_{zo} \cdot \frac{T}{2} - F_{zi} \cdot \frac{T}{2} = M A_y h_{cg}$$

Figure 2-18. Equation. Load transfer across an axle during cornering.

The vertical load will transfer from the tires on the inside of the curve to the tires on the outside of the curve. Load transfer continues until the vertical load on the inner wheel reaches zero. At this point the vehicle is said to be at its stability limit even though it will not actually roll over until the center of gravity (CG) location passes outside the outer tires or the roll inertia of the vehicle becomes greater than the stabilizing moment generated by the mass and half the track width. (Another possible outcome is yaw divergence—the tires cannot provide sufficient lateral force to maintain the curve and the vehicle slides off the road.)

The objective of any roll warning or roll mitigating controller is to anticipate roll instability and to intervene before instability is reached. If instability is detected, the controller will need to either reduce the lateral acceleration induced overturning moment or increase the potential restoring moment. However, as both corrective options are relatively slow to implement, the stability system will need to predict the roll state of the vehicle several seconds into the future.

2.2.2 Yaw Stability

While roll stability is generally considered the bigger issue in commercial vehicle safety (Figure 2-19), yaw instability is still a significant safety issue (Kharrazi and Thomson 2008a). Further, the types of maneuvers which result in yaw instability are more diverse than the maneuvers which generate roll instability (Figure 2-20) (Kharrazi and Thomson 2008a). Thus any attempt to manage yaw instability will have to manage a much larger set of driving situations as compared to roll instability.

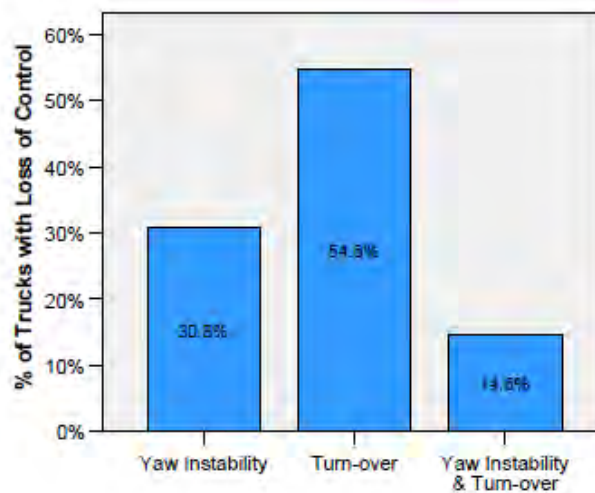


Figure 2-19. Histogram. Commercial vehicle accident type (Kharrazi and Thomson 2008a).

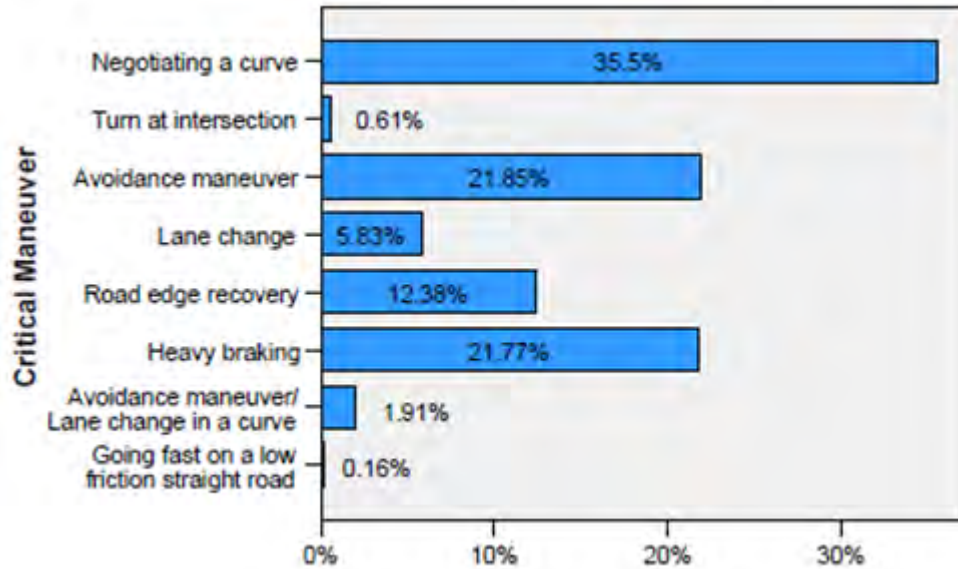


Figure 2-20. Histogram. Yaw instability accident type (Kharrazi and Thomson 2008a).

Yaw instability is also a more complex control problem than roll instability. While roll instability is primarily related to excessive lateral acceleration, yaw instability is a function of lateral acceleration and vehicle speed where instability can be observed in common commercial vehicles at lateral accelerations as low as 0.1 (Ma and Peng 1999). Yaw instability can also be triggered by the vehicle’s control system through poor activation of brakes. In particular, a jackknife event can be triggered if the trailer brakes do not match the drive axle brakes in deceleration (Ma and Peng 1999). This probably leads to an underrepresentation of yaw instability accidents in the crash data analysis because drivers occasionally willingly choose to be involved in a rear-end collision through less-than-full brake activation rather than risk a jackknife (Palkovics and Fries 2001).

Understeer and Oversteer

Yaw instability for a passenger car is manifested as either understeer or oversteer indicating which axle is saturating (Figure 2-21). In the case of understeer, the vehicle has reached the limit of lateral force potential at the front axle and the vehicle slides off the road. In the case of oversteer, the rear axle has reached the limit of lateral force potential and the vehicle spins. All passenger car yaw stability systems place priority on avoiding oversteer accidents, as these are the most dangerous.

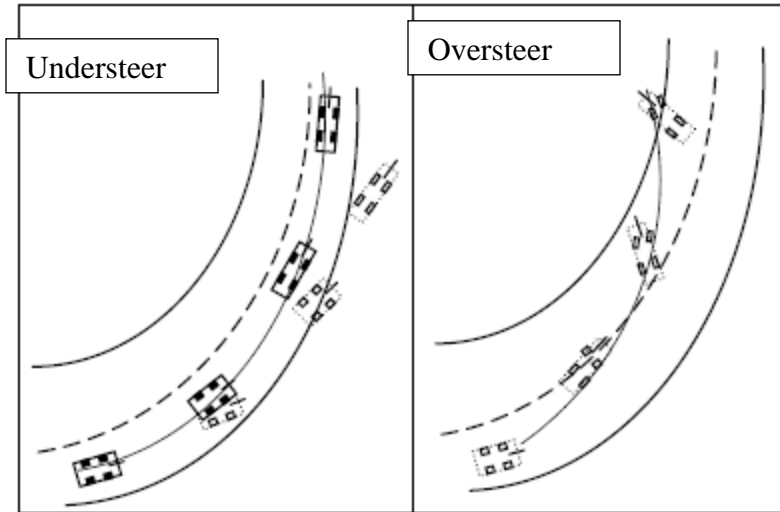


Figure 2-21. Diagram. Passenger car yaw instability (Tekin and Unlusoy 2010).

This steering behavior of the vehicle is often quantified as the understeer gradient, which is a measure of the amount of understeer present in the vehicle per g of lateral acceleration (Figure 2-22). It is usually denoted as degrees of road wheel steer per g of lateral acceleration.

$$K_{us} = \frac{M_f \cdot g}{C_{\alpha f}} - \frac{M_r \cdot g}{C_{\alpha r}}$$

Figure 2-22. Equation. Understeer gradient, due to tire stiffness and mass distribution.

Here, M_f and M_r are the mass carried by each axle and $C_{\alpha f}$ and $C_{\alpha r}$ are lateral forces generated by the tires on an axle per degree of slip. (Figure 2-22 is the component of understeer gradient attributable to the relative mass distribution and tire cornering stiffness between the front and rear of a vehicle. This is typically the largest contributor to understeer, but roll steer and many lesser effects contribute as well.) A positive gradient means that the vehicle is stable and understeering as the front axle has a lower ratio of lateral force to normal force. This means that as lateral acceleration builds (through an increase in speed or a decrease in turning radius), the driver has to input an increasing amount of steering to keep the desired path (Figure 2-23). Here δ is the road wheel steer angle (in radians), L is the vehicle wheelbase, R is the turn radius, and g is gravity. The first term in the equation's left hand side, the ratio of the wheelbase to the turn radius, represents the purely geometric or Ackerman steering relation. The second term on the left hand side of the equation in Figure 2-23 is the understeer term, which adds to (or subtracts from) the steer angle necessary to maintain a radius.

$$\delta = \frac{L}{R} + K_{us} \cdot \frac{V^2}{R \cdot g}$$

Figure 2-23. Equation. The purely geometric turning equation is modified by the understeer term.

In cases where K_{us} is negative, the steering input goes down with increasing lateral acceleration (and may even become a negative steering input). This leads to an unstable vehicle that is difficult or even impossible to control. Therefore all stability systems act to make sure that K_{us} is always positive (though short negative spikes are occasionally used to induce vehicle yawing in emergency maneuvers).

Understeer and Oversteer for Articulated Vehicles

In commercial vehicles, yaw instability is more complicated as each unit of the vehicle can become unstable in yaw. Moreover, unlike single unit vehicles, the understeer gradient changes with speed and lateral acceleration. Thus the models are good for fixed lateral accelerations and need to be updated as the vehicle's lateral acceleration changes (Yu et al. 2008), (Zhou et al. 2008). For illustration, Figure 2-24 shows a typical tractor response where the vehicle is initially understeering but transitions to oversteer. This is a typical loaded tractor and trailer behavior response.

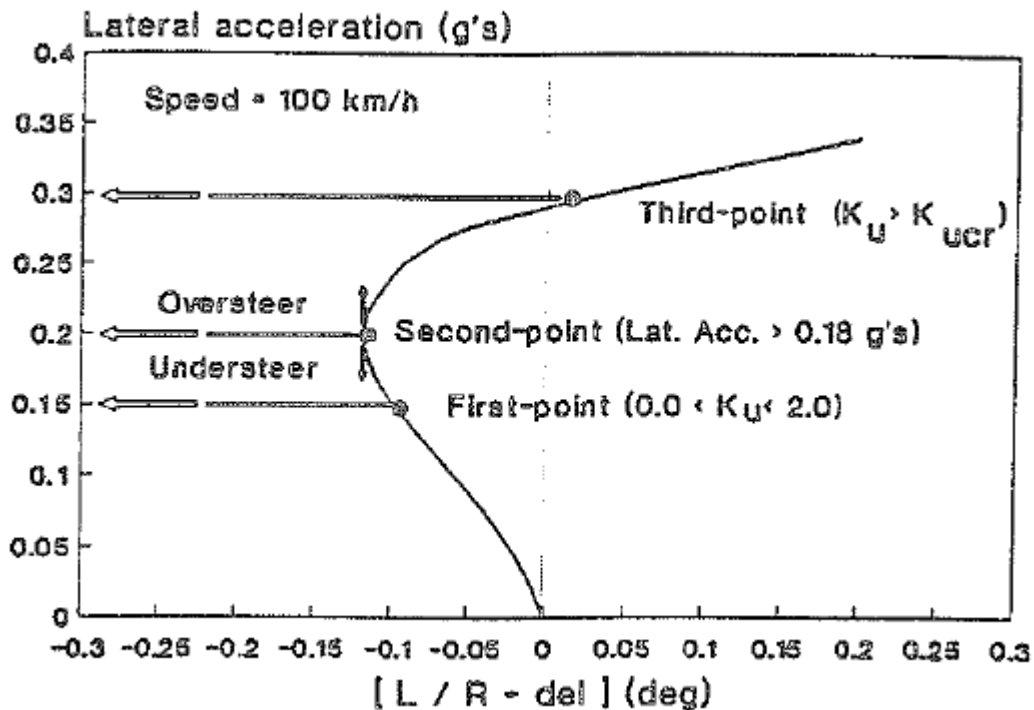


Figure 2-24. Graph. Constant radius understeer results (El-Gindy 1995).

As each unit of a tractor and trailer can be understeering or oversteering, there are four stability combinations for a typical tractor and semitrailer combination relating the behavior of the tractor and the trailer through the articulation of the vehicle (Figure 2-27). Here Γ is the articulation angle, δ is the road wheel steering angle, L_{tractor} is the tractor wheel base, L_{trailer} is the trailer wheel base, Ku_{tractor} is the tractor understeer gradient at the given conditions, Ku_{trailer} is the trailer understeer gradient at the given conditions, V is the vehicle speed, and g is gravity.

$$\frac{\Gamma}{\delta} = \frac{\frac{L_{\text{trailer}}}{L_{\text{tractor}}} + Ku_{\text{trailer}} \cdot \left(\frac{V}{\sqrt{L_{\text{tractor}} \cdot g}} \right)^2}{1 + Ku_{\text{tractor}} \cdot \left(\frac{V}{\sqrt{L_{\text{tractor}} \cdot g}} \right)^2}$$

Figure 2-25. Equation. Ratio of the articulation angle to steer angle.

$$V_{\text{crit}_{\text{tractor}}} = \sqrt{\frac{L_{\text{tractor}} \cdot g}{|Ku_{\text{tractor}}|}}$$

Figure 2-26. Equation. Critical speed for a tractor.

$$V_{\text{crit}_{\text{trailer}}} = \sqrt{\frac{L_{\text{trailer}} \cdot g}{|Ku_{\text{trailer}}|}}$$

Figure 2-27. Equation. Critical speed for a trailer.

- Tractor and trailer both understeer. Articulation angle gain (increase in articulation relative to steering input increase) will approach the ratio of the understeer gradients as speed increases (Figure 2-25). Vehicle is stable.
- Tractor understeer and trailer oversteer. As Ku_{trailer} is negative, the articulation gain is initially positive but becomes negative and the trailer swings out. This is an unstable arrangement at speed. However, at low speeds, the articulation gain is positive making the vehicle drivable.
- Tractor oversteer and trailer understeer. As speed increases toward the critical speed, the articulation gain approaches infinity. This results in the tractor yawing too much, which is a jackknife. The system is unstable at elevated speed.

- Tractor and trailer both oversteer. Response depends on ratio of understeer gradients to the ratio of the wheelbases. If the ratio of the understeer gradients is greater or less than the ratio of the wheelbases, the articulation gain will drive to either negative or positive infinity. This results in a jackknife or a swing out (excessive trailer yaw), though the difference will be hard to tell from the driving perspective. The vehicle is unstable at elevated speed.

Longer combination vehicles (LCVs) have even more complicated stability interactions in yaw making them difficult to analyze analytically. The above material on tractor and trailer understeer and oversteer interactions was drawn from course notes published by the University of Michigan (Winkler and Ervin 2006).

2.3 *Prior Commercial Vehicle Stability Systems*

The underlying equations and mechanics of past roll stability systems, yaw stability correction, and combinations of the two are presented in contrast to currently available roll and yaw stability systems in commercial vehicles.

2.3.1 *Roll Stability Systems*

Roll stability systems have been available since the early part of this century. A lateral accelerometer senses when the vehicle is approaching an assumed rollover threshold, and applies the brakes to slow the vehicle and reduce the cornering force.

To understand the relationship, it is easiest to start with the observation that the lateral acceleration the vehicle sees is a product of the vehicle's speed and the path radius, as in Figure 2-28.

$$A_y = \frac{V^2}{R}$$

Figure 2-28. Equation. The lateral acceleration depends on the forward velocity and the turn radius.

So to reduce the lateral acceleration, the vehicle's speed must decrease or the path radius must increase. By applying an understeer moment to the vehicle, the ESC system does both of these tasks (reduce speed and increase path radius) as the vehicle's yaw rate reduces and the path swings wide of the driver's intent. The only problems are that this is a relatively slow process and the driver usually attempts to override the path deviation through increased steering demand. Thus the system needs to intervene before rollover is imminent.

In the case of a tractor and trailer, there is an additional action that the ESC system can take to reduce rollover potential. As the trailer is always attached behind the tractor's longitudinal CG location, braking the trailer wheels will impart an understeering moment to the tractor

(Figure 2-29). The trailer brakes are also capable of removing significant kinetic energy from the vehicle, thereby reducing the vehicle's speed.

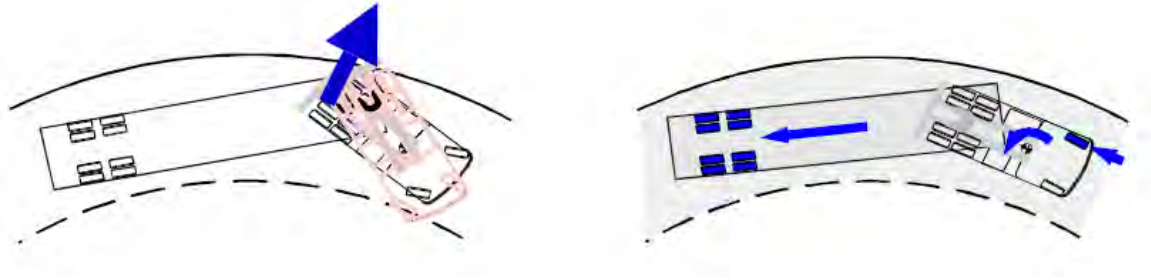


Figure 2-29. Diagram. Tractor and trailer yaw control (Andersky and Conklin 2008).

However, if the tractor is understeering, then the only solution is to brake the inside rear tractor wheels, much like would be done for a passenger car (Figure 2-30).

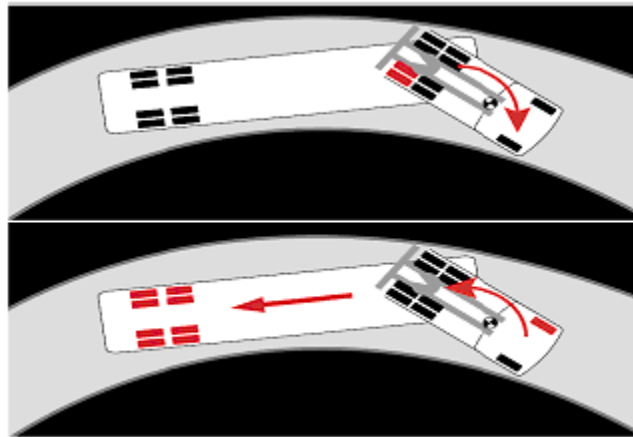


Figure 2-30. Diagram. Tractor trailer understeer and oversteer corrections (Goodarzi et al. 2009).

2.3.2 Correcting Yaw Instability

Generally, the yaw instabilities of the tractor are more significant as the tractor's mass moment of inertia is much smaller than the inertia of the longer trailer. Thus tractor instabilities happen much more quickly than trailer instabilities. An illustration of how the tractor and trailer will interact with and without stability is shown below in Figure 2-31.

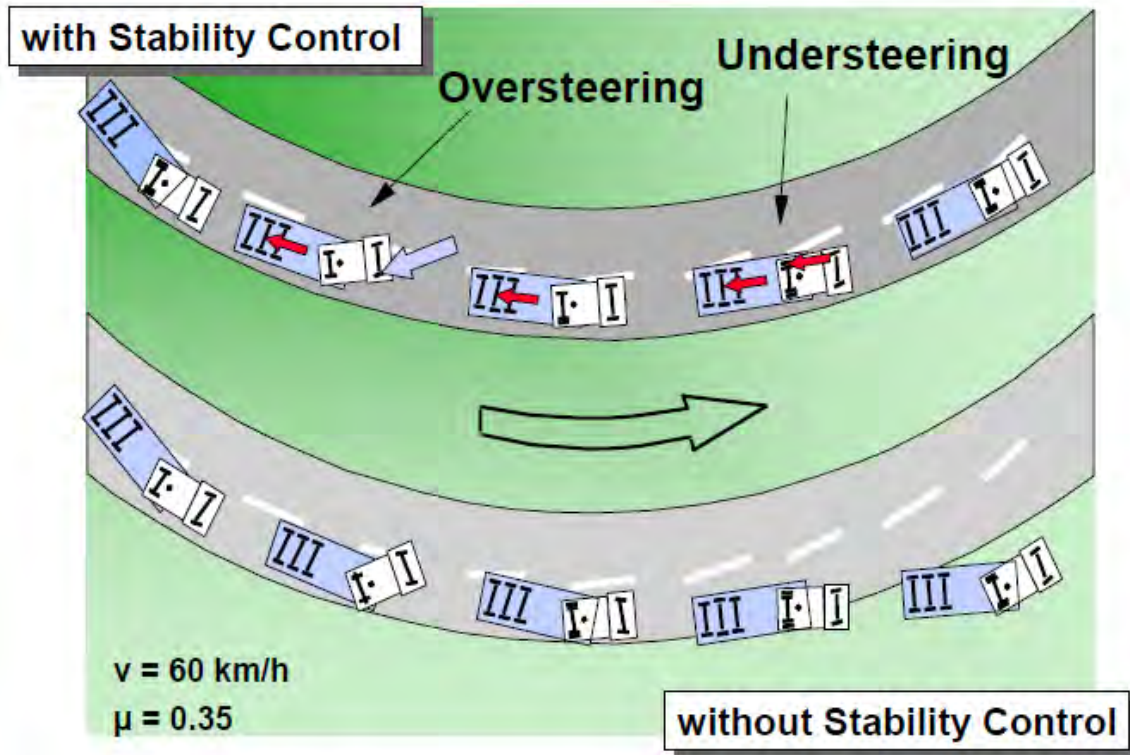


Figure 2-31. Diagram. Articulated vehicle stability control illustration (Freightliner LLC 2007).

The goal of the stability system is to evaluate each unit of the vehicle to determine the desired vehicle response based on steering inputs and a simple model of the vehicle's dynamic behavior. The desired behavior model can be implemented as a set of state equations (state space model) or a set of transfer functions (Ghoneim et al. 2000). The ideal output of the controller is a neutral steering vehicle (Zhou et al. 2008), as that is how the driver intuitively expects the vehicle to behave. An example controller is shown in Figure 2-32.

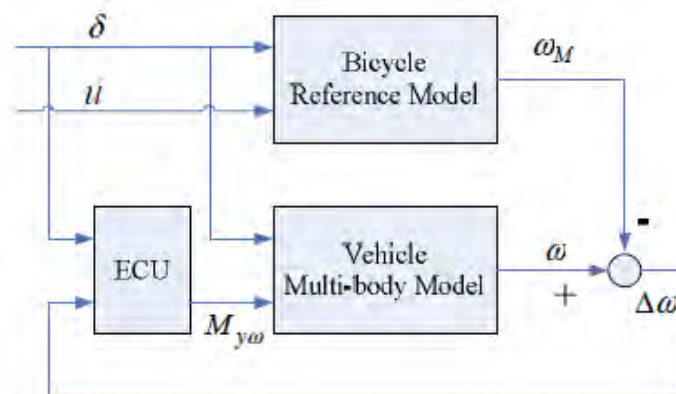


Figure 2-32. Diagram. Example yaw controller (Zhou et al. 2008).

As brakes are being used, it is not surprising that the vehicle's speed reduces somewhat when the system engages. However, Manning and Crolla found that despite the effect on speed control, brake based systems do offer the best compromise between controllability and driver intent (Manning and Crolla 2007). Further Nantais found that while brake based systems do result in the development of understeer, the effects are small enough and slow enough for the driver to compensate as needed (Nantais 2006).

Brake based stability controls work by generating yaw moments as shown in Figure 2-33. Here the oversteering of the vehicle is being corrected by introducing a moment counter to the vehicle's rotation.

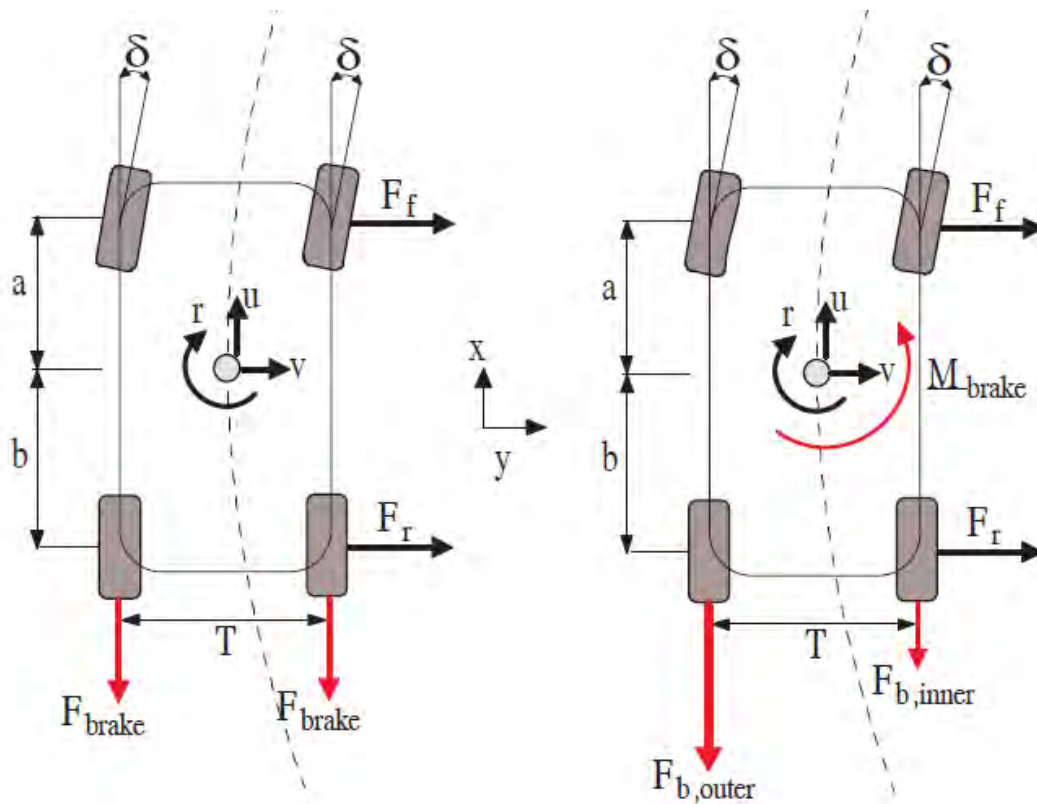


Figure 2-33. Diagram. Oversteer correction (Nantais 2006).

2.3.3 Combined Roll and Yaw Stability

The major difficulty in developing a controller to manage both yaw and roll stability is that the stability demands for yaw and roll may conflict (Zhou et al. 2008). For example, if a vehicle is understeering and rolling over, the yaw controller will indicate that more yaw rate is needed to correct the understeer. But increased yaw rate means increased lateral acceleration, which exacerbates the roll stability problem. Thus a priority or hierarchal control algorithm is needed to manage the inevitable trade-offs (Yoon et al. 2007).

This is not a hypothetical problem, as shown in Figure 2-19, where 14% of fatal truck accidents involved both yaw and roll instability (Kharrazi 2008b). Further, MacAdam noted that in some cases it is not possible to decouple the yaw and roll stability requirements for a commercial truck, particularly when the CG is relatively high (MacAdam 1982). Finally, large tire slip angles, which provide quick yaw corrections, also produce large lateral accelerations, which reduce roll stability (MacAdam 1982).

To visualize this interaction of yaw and roll, the reader is pointed to Figure 2-34, where the overlap of yaw and roll stability is clearly observable. Note that a significant portion of the stability map indicates both yaw and roll stability risks. However, there have been successful controllers built to manage both yaw and roll stability with some providing improved overall stability with both yaw and roll control enabled (Figure 2-35) (Chan 2010; Yoon et al. 2009). An example of such a controller is shown in Figure 2-36 (Chen and Peng 1999).

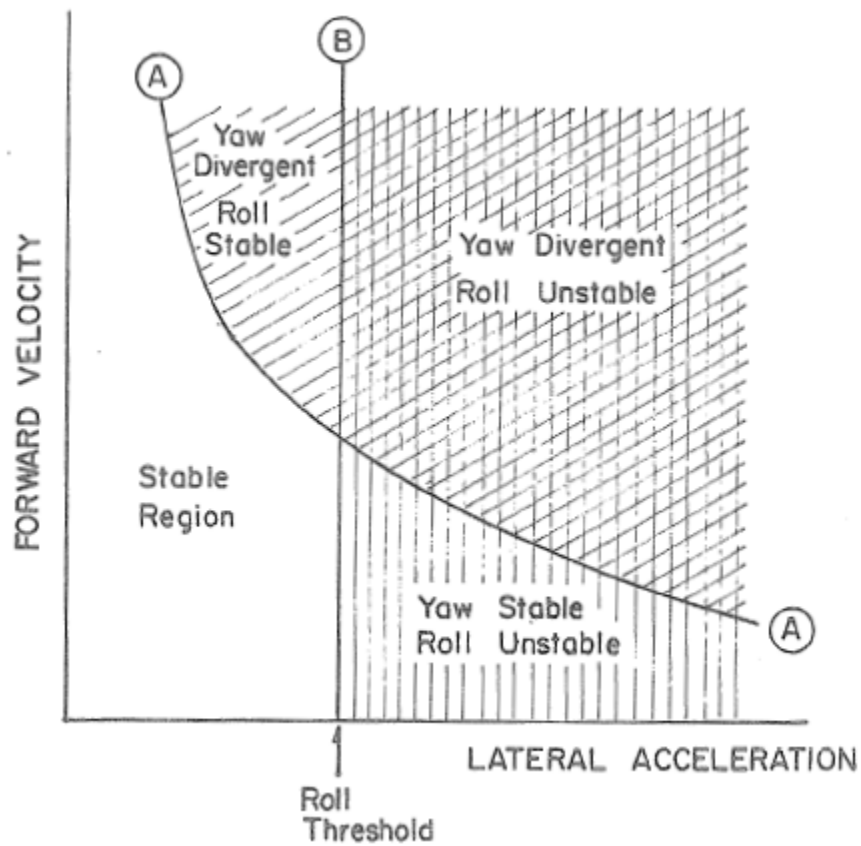


Figure 2-34. Diagram. Yaw and roll stability regimes (MacAdam 1982).

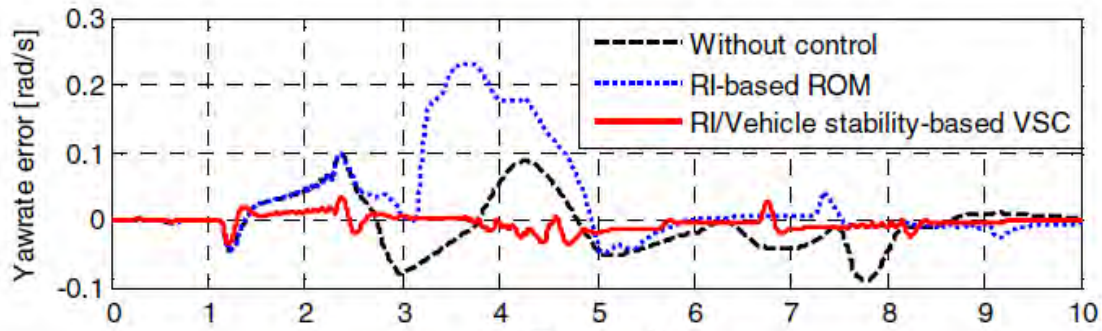


Figure 2-35. Graph. Combined yaw and roll controller for a car (Yoon et al. 2009).

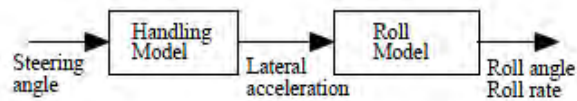


Figure 2-36. Diagram. Yaw and roll controller (Chen and Peng 1999).

To underscore the interaction of yaw and roll stability, the following excerpt on coupled yaw and roll from Bendix Commercial Vehicle Systems LLC, is presented (Andersky and Conklin 2008).

By helping a vehicle maintain directional stability during both oversteer and understeer situations, the driver's intended path continues to be followed, and loss-of-control situations are minimized. (Many rollovers are) the outcome of loss-of-control situations that begin when the driver maneuvers to avoid a situation – which, in turn, initiates directional instability – leading to the eventual lateral acceleration event culminating in the rollover.

Similarly, Woodrooffe and Blower (2010) noted that adding ESC improved roll stability and concluded that the added roll benefit came from the yaw controller activating before the roll controller, producing a restorative response before the activation of the roll controller. Clearly there are solutions where the competing goals of yaw and roll control can be achieved, but the controller approach must be rather sophisticated.

2.3.4 Current Roll and Yaw Stability Systems

Systems to manage heavy truck stability are available on the market today. All of the major brake control systems manufacturers offer a roll stability, or a combined yaw and roll stability, product. However, the stability control systems available in North America operate only within a single unit of a vehicle. There is no communication of vehicle dynamic states between units. Systems on a tractor that activate the trailer brakes must do so without knowledge of whether the trailer is equipped with ABS. (Although ABS has been mandated for trailers since 1997, the life of trailers can be decades, so many unequipped trailers remain on the road. The ABS status signal is communicated through the electrical connection between the tractor and semitrailer. A control system on the tractor cannot rely on this signal, however, because it could be pulling a

two-trailer combination with one unequipped trailer.) Trailer systems cannot activate the tractor brakes.

Generally most tractor systems are full ESC systems with yaw and roll stability. The systems can estimate some trailer behavior (yaw) based on the difference between the ideal (modeled tractor dynamic behavior) and the actual behavior as the trailer acts on the tractor. These systems can also anticipate a roll problem for the trailer from measured lateral accelerations at the tractor, though they have no measurements of the trailer's behavior.

Currently available trailer-only systems address only rollover. Yaw instability calculations would require either the articulation angle or the target yaw rate, neither of which is available to the trailer. When tractor and trailer ESC systems are paired, the result is a more stable vehicle system (Arant et al. 2009), but further improvements could be made if information were shared about the dynamic state of each unit.

2.3.5 Multiple Unit Stability

The control problem for ensuring stability increases in complexity and scope with the number of units in the vehicle. In fact, for multiple unit vehicles, closed form solutions defining the vehicle's stability may not be possible. Therefore, different approaches to evaluating and managing stability are needed.

Perhaps the two biggest issues facing a multiple unit controller are state measurement/control actuation delays and system interactions where improving the stability of one unit may negatively affect the stability of an adjacent unit. To understand the data communication issue, it helps to realize that an LCV can be over 110 feet from end to end. This is a significant transport distance, and the time for a pneumatic actuation command to travel this distance is considerable.

The only sequence of major studies on the stability control of LCVs (doubles and triples) is the Rearward Amplification Suppression system (RAMS) (MacAdam et al. 2000). The authors successfully demonstrated that precisely timed, momentary brake applications can limit the excessive motions of multi-unit vehicle and prevent rollover (Figure 2-37). Systems with and without communication between vehicle units were tested.

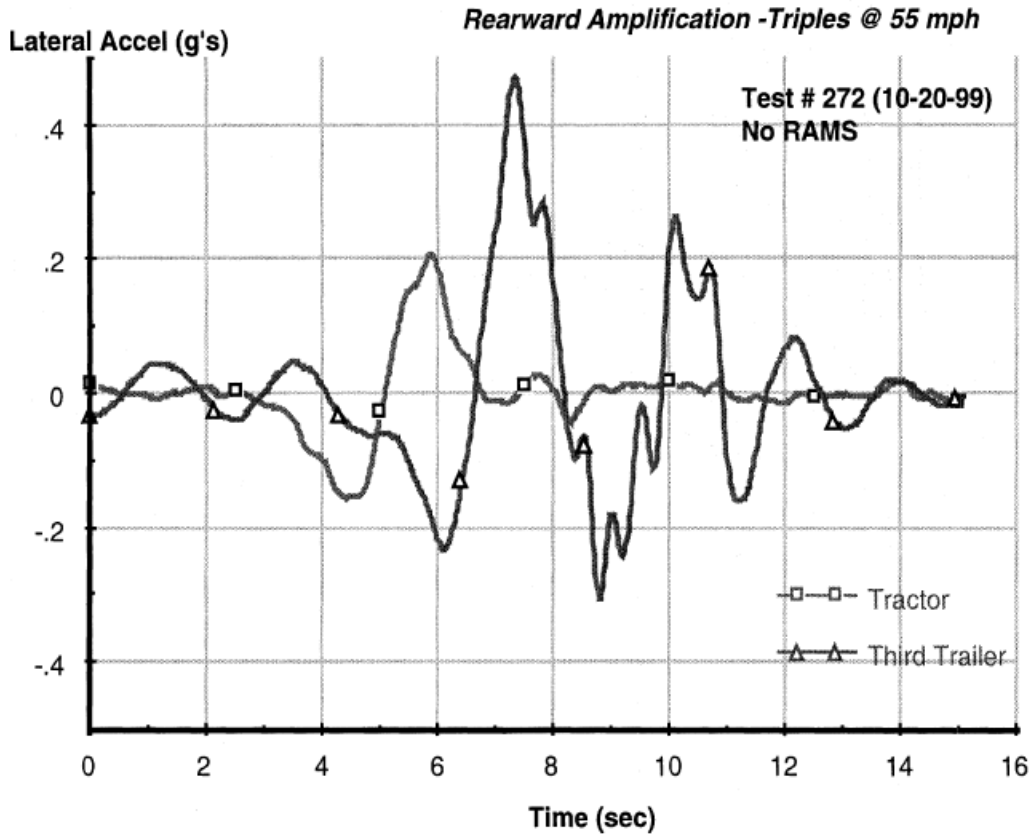


Figure 2-37. Graph. RAMS rearward amplification (MacAdam et al. 2000).

The control response used diagonal braking to produce countering yaw moments on each trailer suppressing the build-up of lateral acceleration (Figure 2-38, Figure 2-39).

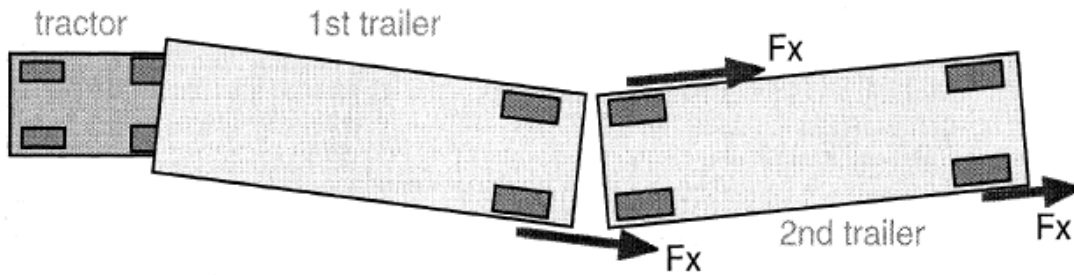


Figure 2-38. Diagram. RAMS control illustration (MacAdam et al. 2000).

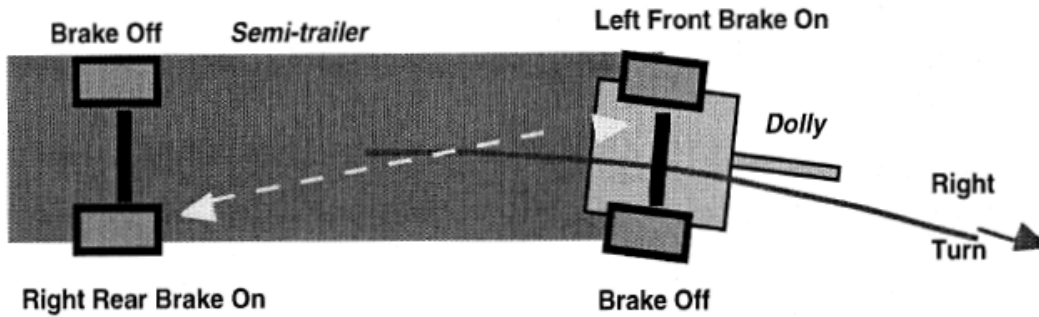


Figure 2-39. Diagram. RAMS diagonal brake illustration (MacAdam et al. 2000).

The results were quite encouraging even though there was no communication between the trailers and each system was reacting to the yaw rate and lateral accelerations seen at that unit (Figure 2-40).

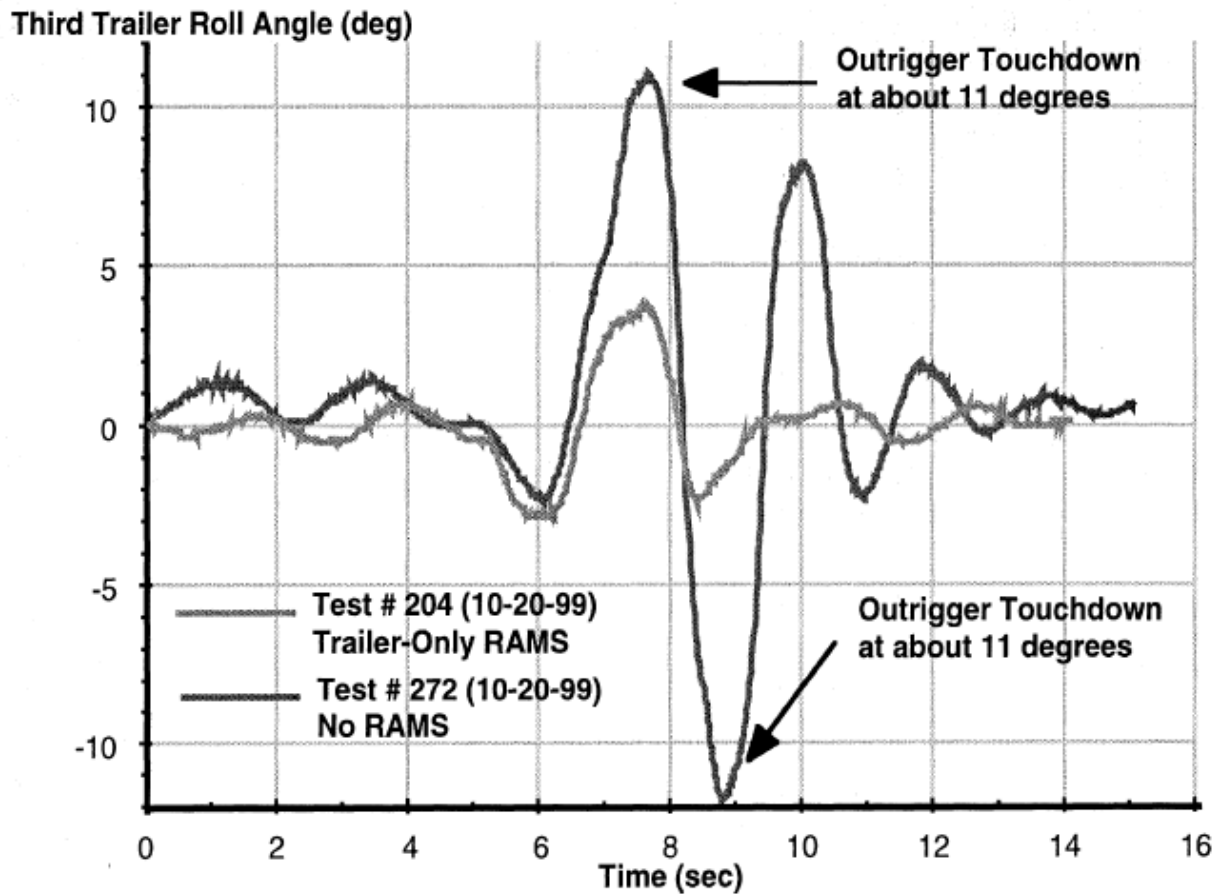


Figure 2-40. Graph. RAMS roll suppression (MacAdam et al. 2000).

2.4 Sensors and Vehicle Observability

Once a vehicle model has been developed and a controller constructed, the simulation or validation process will need information on the vehicle it is attempting to control. The two types of data needed by the controller are vehicle parameter data (mass, length, tire properties, etc.) and vehicle states (lateral acceleration, side slip, yaw rate, etc.). The problem is that, with few exceptions, the needed information is variable with time. Thus methods to determine both the parameters and states are needed.

2.4.1 Measuring Vehicle Parameters

A common practice when modeling passenger cars is to assume that the vehicle parameters are known, because vehicle mass changes little (Park et al. 2008). But this assumption is most definitely not true when dealing with commercial vehicles used to haul freight (Du and Zhang 2008; Wang and Hsieh 2009; Chen and Shieh 2011). These parameters are not only difficult to obtain, but vital for accurate stability control (Andersky and Conklin 2008; Brown et al. 2009). Therefore methods to evaluate the vehicle's parameters are needed.

Estimating Mass

Traditionally, one of the more difficult parameters to measure has been vehicle mass and mass distribution. Usually mass has been measured through monitoring acceleration when the engine power is known (Nantais 2006; Huh et al. 2007; Limroth 2009a) or through observed lateral accelerations and assumed tire cornering stiffness (Limroth 2009a; Limroth 2009b; Limroth et al. 2009). However, these methods become more complicated when the tractor can swap trailers (or the trailer swap tractors) as knowing the tire performance of all vehicle units and the engine performance from the trailer's perspective is difficult.

A second problem commonly encountered in estimating mass is accounting for road grade and road crown. Road grade results in a loss of gain of acceleration as potential energy is converted into kinetic energy. It also results in errors to the measured longitudinal acceleration. Meanwhile road crown results in errors to the measured lateral acceleration, which will negatively affect the mass estimate. While these effects can be accounted for by using other sensors (global positioning system, or GPS, yaw rate, etc.) the corrections usually require Kalman style filters, which means a time averaging approach.

Many tractors and trailers produced today are equipped with air suspensions, because air offers a superior ride and load leveling capabilities. Products are available to measure the load on axles using this pressure. Their output is displayed for the driver or loader; they are not yet integrated with stability controllers.

Measuring Tire Properties

A tire is a complicated structure that cannot be linearized in the modeling. That leaves a difficult problem in how to determine the tire properties for the given operational environment (load, road condition) (Cheng and Cebon 2011). The solution is to recognize that the shape of a tire's lateral and longitudinal force curves does not change that significantly between surface conditions and load conditions. Thus what is needed is to use the known mass and the measured lateral acceleration to determine the tractive potential of the tire or the effective ground coefficient of friction. With that known, reasonable estimates of the tire force can be obtained given the load, torque, and the slip angle.

Several techniques exist to measure the tire's performance, which account for measurement bias and error. Typical methods employ time based averaging of kinematic models or Kalman filters with secondary data sources such as GPS.

Measuring Unit Inertia

As the load on a commercial vehicle changes, the vehicle's inertial properties will change as well. With the mass known, the vehicle's inertia can be approximated sufficiently for stability control. In yaw, the inertia can be estimated by monitoring the yaw rate and lateral acceleration (Limroth 2009a). As the CG height of a heavy duty truck cannot be easily identified, the roll inertia cannot be directly calculated. Thus the roll inertia of the vehicle can be defined only in terms of the lateral acceleration. However, the stability model needs to know the relationship between lateral acceleration and roll rate/roll angle, so this method will meet the modeling needs.

2.4.2 Estimating Vehicle States

The identification of vehicle states can be generally broken into two categories: States that are directly observable, and states that are not directly observable. Directly observable states are ones for which sensors exist and are cost-effective to implement. Non-observable states are ones that are impractical to measure on the vehicle. Each of the major states to be measured is discussed below along with its observability.

In general the following variables need to be measured or calculated to analyze or control the dynamics of a vehicle:

- Steering-wheel (hand wheel) angle
- Lateral acceleration
- Yaw velocity
- Longitudinal velocity.

The following variables may be additionally measured or calculated:

- Roll angle
- Sideslip angle or lateral velocity
- Steering-wheel (hand wheel) torque
- Brake system pressure.

In order to measure or calculate the above variables, sensors are used to acquire the necessary data. The sensors may measure the variable directly or indirectly. The types of sensors in common use today are discussed below.

Lateral Acceleration

As accelerometers are relatively inexpensive, obtaining a direct measurement of the vehicle's lateral acceleration is possible. Road crown can introduce bias into the measurement. Lateral acceleration measurements can be compensated using GPS data or by comparing the measured results against physical model based observers or estimation using kinematic model based observers (Limroth 2009a).

Roll Rate

Angular rate sensors are also relatively inexpensive; thus measuring the roll rate is possible. However, the roll rate sensor can be noisy, so integrating the signal to produce a roll angle can be problematic (Cheli et al. 2007). To correct for this, the roll rate can be compared to the observed or modeled lateral acceleration, because the roll rate should be zero for a constant lateral acceleration. Depending on the quality of the measured signal, a corrective model, such as a Kalman filter, may be needed.

Lateral Velocity and Side Slip

Lateral velocity and side slip angle are often used interchangeably as the two are related kinematically (Figure 2-41) where β is the side slip angle, V_y is the lateral velocity, and V_x is the longitudinal velocity.

$$\beta = \tan^{-1}\left(\frac{V_y}{V_x}\right)$$

Figure 2-41. Equation. Side slip angle.

While direct sensing of lateral velocity using cameras or GPS units has been demonstrated, these approaches generally suffer from low data throughput and are prohibitively expensive to implement (Limroth 2009a). Therefore, estimation methods are usually employed in practice.

As the side slip is the result of the non-linear responses of all tires, it is particularly sensitive to errors in tire estimations (Best et al. 2000; Kim 2010). Typical approaches use state space estimators based on physical models of the vehicle (such as the equation in Figure 2-42) or kinematic models (such as the equation in Figure 2-43) (Limroth 2009a).

$$\begin{bmatrix} \dot{v}_y \\ \dot{r} \end{bmatrix} = \begin{bmatrix} -\frac{C_1 + C_2}{mv_x} & \frac{-aC_1 + bC_2}{mv_x} - v_x \\ -\frac{aC_1 + bC_2}{Jv_x} & -\frac{a^2C_1 + b^2C_2}{Jv_x} \end{bmatrix} \begin{bmatrix} v_y \\ r \end{bmatrix} + \begin{bmatrix} \frac{C_1}{m} \\ \frac{aC_1}{J} \end{bmatrix} \delta$$

Figure 2-42. Equation. State space formulation of vehicle side slip from tire behavior.

$$A_y = \dot{V}_y + V_x \cdot r$$

Figure 2-43. Equation. Kinematic formulation side slip.

The kinematic model has the advantage that it is accurate in the non-linear vehicle domain (no linearized terms) and it is easier and faster to solve, but it is subject to sensor bias errors (Cheli et al. 2007). The state space model simplifies the response and is less sensitive to sensor bias, though it does need regular corrections to the tire cornering stiffness. Thus a combination of techniques is generally employed.

The last method for evaluating side slip is from GPS data. Here the vehicle's velocity vector is measured using GPS and compared to the gyro measurement (Figure 2-44). As the GPS velocity error increases at lower speed (Doppler shift), the error is highest for low speed maneuvers (Figure 2-45).

$$\beta = \psi_{Gyro} - \psi_{GPS}$$

Figure 2-44. Equation. Side slip or "Crab angle" of a vehicle from measurable yaw angles.

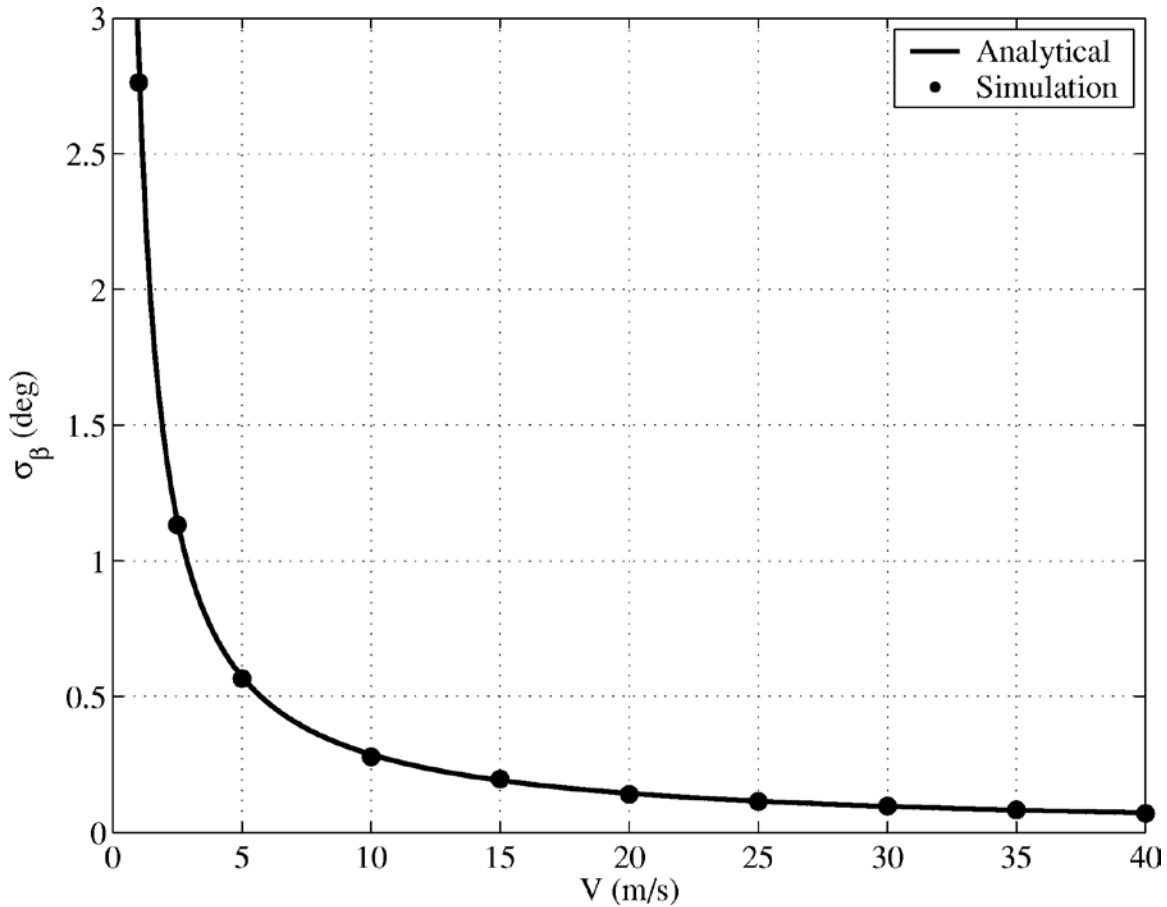


Figure 2-45. Graph. Side slip error from GPS measurement (Daily and Bevely 2004).

Yaw Rate Sensor (yaw rate or acceleration)

A yaw rate sensor, also sometimes called a gyro, is a device that measures angular velocity around a reference axis. Yaw rate sensors use the Coriolis effect, wherein a test mass is forced to vibrate normally at its resonant frequency. The vibration provides the mass with a linear velocity component. When the mass is rotated, the Coriolis force causes the vibration motion of the mass to be coupled to another vibration mode or plane of the mass. The magnitude of this secondary vibration is proportional to the angular rate of turn (Watson Industries Inc. 2010). Yaw rate sensors can be based on piezoelectric or micromechanical technology. In the micromechanical type, the Coriolis acceleration is measured by a micromechanical capacitive acceleration sensor. As with the capacitive accelerometers discussed earlier, yaw rate sensors using micromechanical technology can typically have a frequency response down to 0 Hz (DC), and are for this reason preferred for vehicle dynamic measurements. As with accelerometers, yaw rate sensors can vary in price from several thousand dollars for a research-quality unit to a few dollars for a production unit purchased in large quantities.

Inertial Measurement Unit (IMU)

An Inertial Measurement Unit (IMU) is an electronic device that measures a vehicle's velocity, orientation, and acceleration using a combination of accelerometers and gyros. IMUs have the advantage of being easy to mount and are easier to work with than the individual components. However, because they generate velocity and position from integration of acceleration and are using dead-reckoning, they suffer from accumulated error. Typically this condition is resolved by providing sensor fusion with complementary technology, which can reduce or eliminate the error bias. One example of this would be the elimination of roll angle error by resetting roll angle to zero when the vehicle is stopped on level ground. Another example would be the provision of GPS data to determine vehicle speed.

Because the cost of GPS devices has fallen considerably in recent years, some IMUs are now equipped with GPS capability (Racelogic 2010); however, these units still remain too expensive for use in production vehicles.

The cost of an accelerometer/gyro-based IMU can range from several thousand dollars for a research-quality unit to a few hundred dollars each for a high-quantity purchase.

Wheel Speed

Measurement of vehicle speed is not as trivial as it might first appear. The most effective way to measure the speed of a moving vehicle is to observe the vehicle from a position that is fixed with respect to a point of reference. This is the concept behind the use of GPS measurements. The use of GPS as the primary source of speed information for a vehicle is, however, not practical, since the use of GPS is subject to signal availability, and dropouts can present problems for vehicle dynamic control systems (Racelogic 2009).

However, sensing the vehicle speed by using a sensor on the vehicle is also problematic. Microwave and optical sensors are effective but not economical. Sensors that use the rotation of a vehicle component, such as a driveshaft or a wheel, rely on a known translation between the measured rotation and the vehicle speed. Even here, errors can result from a variety of sources, including 1) tire inflation pressure variation, 2) tire wear, 3) tire slip, and 4) tire diameter differences from factory fitment.

In modern vehicles speed sensing is usually done with the aid of a wheel speed sensor, which is a device that measures the rotational velocity of the wheel on a vehicle. Typically, a wheel speed sensor will be installed on each wheel, but cost considerations may limit the installation to the wheels of one axle of a tandem pair on a vehicle with tandem axles, with the assumption that the wheel speeds associated with the other axle will not be very different.

Wheel speed sensors have been designed using Hall Effect and magnetoresistive technology. Because magnetoresistive technology provides greater resolution (Gonzalez 2009), it is almost universally used for wheel speed sensors today.

The wheel speed sensor assembly consists of a speed sensor and an exciter ring (also called a tone wheel) (See Figure 2-46). The exciter ring is a steel ring with equally spaced teeth around its diameter. The sensor's magnet and pole piece form a magnetic field. As an exciter tooth passes by, the magnetic field is altered and an alternating current (AC) voltage is generated in the sensor coil. The number of AC cycles per revolution of the wheel depends on the number of teeth in the exciter ring. The frequency of AC cycles is directly proportional to the wheel speed. AC voltage is also proportional to speed, but also varies with the gap between the sensor tip and the exciter ring tooth (Bendix Commercial Vehicle Systems LLC 2004c).

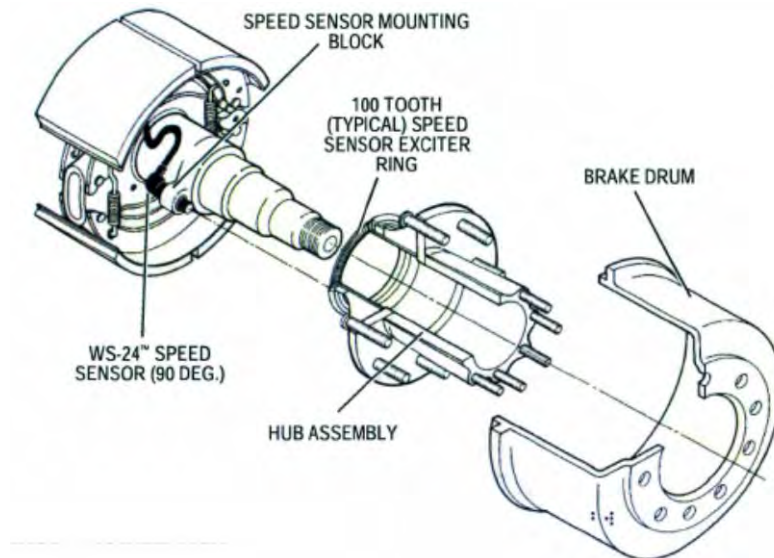


Figure 2-46. Drawing. Bendix wheel speed sensor installation.

Source: (Bendix Commercial Vehicle Systems LLC 2004c) (Bendix Commercial Vehicle Systems LLC 2004a)

Hand Wheel Angle Sensor

A variety of steering wheel (hand wheel) angle sensors are in use. The sensor itself is typically of a design that matches the algorithm used to collect data from the sensor, as there are a number of technical issues regarding the measurement of steering wheel angle that do not have commonly agreed solutions (Tseng et al. 1999). Examples of these problems are:

- Adjustment of steering wheel position center (i.e., zero position) to accommodate build variations of the vehicle, steering system misalignment, or tire variations such as conicity
- Adjustment of the steering wheel position center to accommodate dynamic variations due to road crown or vehicle loading
- Compensation for compliances in the steering system, both as designed and from wear
- Provision of steering wheel angle measurement range beyond 360 degrees of rotation.

Solutions to these problems can be implemented in hardware or software, and the specific form of the steering wheel angle sensor then follows suit. In order to provide a durable steering wheel angle sensor, many manufacturers design a sensor with an optical sensing element that receives a light signal passing through a toothed wheel (Hamamatsu Photonics Japan 2011). These sensors may have some computation done within the sensor assembly itself to provide solutions to steering center or range of angle measurement problems. Typically the dynamic adjustments are made by a remotely located processor that has access to other vehicle data.

Steering wheel angle sensors of various types can be purchased for less than \$100 although as noted above, each application might require additional expense beyond the purchase price to get a data-acquisition-ready setup.

2.4.3 Communication Networks

As previously discussed, the concept of a vehicle network for coordinating the vehicle dynamic performance of a combination vehicle goes back to the infancy of railroads. A network in this context means an intra-vehicle system of data and control information. Vehicle-external networks have also received their share of research interest, with applications in automated highway systems (AHS), advanced commercial vehicle systems (ACVS) and commercial vehicle fleet telematics to name but a few. The interested reader is referred to the work done in this area by the Federal Motor Carrier Safety Administration (FMCSA) in its Commercial Vehicle Information Systems and Networks (CVISN) effort (FMCSA 2011). For this discussion, the focus will be limited to the intra-vehicle network with the purpose of vehicle dynamic analysis and control.

Networks on commercial vehicles, as with sensing devices, have followed general industry trends in computing and networking technologies, and have served as the basis for networked control systems such as ABS and stability control.

There are several networking technologies currently developed or in development for in-vehicle use (Dominguez et al. 2007). Bosch developed the Controller Area Network (CAN) protocol, Volkswagen implemented the Automobile Bitserielle Universal-Schnittstelle (A-BUS), Renault and the PSA Group developed the Vehicle Area Network (VAN) protocol, BMW developed the M-BUS and Honda developed the Data Link Connector (DLC). The majority of these automobile manufacturers have in time adopted for general purpose communication the CAN standard (Dominguez et al. 2007; Etschberger 2001; Robert Bosch GmbH 1991; ISO 1992; ISO 1994). Other in-vehicle networking technologies are in common use as well (Davis 2011).

2.5 Wireless Vehicle Communication Protocols and Performance

Complete details of IEEE 802.11n technology are discussed in Paul and Ogunfunmi (2008) where the evolution of the IEEE 802.11n amendment is described following the discussion on the previous generation wireless local area network (WLAN) devices (IEEE 802.11a/b/g). The

key technique in IEEE 802.11n is the multiple-input, multiple-output (MIMO) technology which forms the foundation of high performance by transmitting and receiving data from multiple antennas. To understand the performance of MIMO, Paul and Ogunfunmi (2009) investigate IEEE 802.11n physical (PHY) layer, and Medvedev et al. (2006) discuss the complexity of various MIMO receiver structures for IEEE 802.11n WLANs. Moreover, the performance and enhancement of the media access control (MAC) layer of IEEE 802.11n are investigated in Abraham et al. (2005), Wang and Wei (2009), and Xiao (2005).

All the above-mentioned papers are either based on mathematical analysis or simulations, so the evaluation results cannot be used directly on analyzing the reliability of actual IEEE 802.11n networks. On the other hand, Fiehe et al. (2010) studied the performance of IEEE 802.11n using extensive measurement campaigns carried out in both interference-controlled and typical office environments. They discovered that in a typical office environment significant performance improvement can be expected in IEEE 802.11n but theoretically achievable bit rates cannot be reached. So far, there is no work about the empirical study of applying IEEE 802.11n in an outdoor environment, such as vehicular networks.

As discussed in Stallings (2004), the WiFi technology including IEEE 802.11a/b/g/n is originally designed for indoor use. Due to dynamic communication environments of outdoor WiFi networks, as described by Paul et al. (2011), it is difficult to achieve reliable performances. Particularly, Jarupan and Ekici (2011) discover the complexity and instability of communications in outdoor vehicular networks. To address these issues, much work has been done on applying WiFi technology to vehicular networks such as Bychkovsky et al. (2006), Mahajan et al. (2007), Eriksson et al. (2008), and Balasubramanian et al. (2008). Bychkovsky et al. (2006) conducted a measurement study with over 290 drive hours over a few cars under typical driving conditions, and they concluded that WiFi networks cannot provide reliable networking for vehicular network but can support only some delay-tolerant applications. The high mobility of vehicles led Mahajan et al. (2007) to investigate the connection times between vehicles and roadside access points. They concluded that regular periods of disconnection occur as vehicles move through areas poorly covered by the access points (APs). In the Cabernet project, Eriksson et al. (2008) studied how to deliver vehicular content using WiFi, and they concluded that only non-interactive vehicular applications can be supported by WiFi. In other words, it is impossible to use existing AP infrastructures to build reliable vehicular networks. To address this issue, Balasubramanian et al. (2008) proposed a new network access method called ViFi which uses a decentralized and lightweight probabilistic algorithm for coordination between participating base stations to minimize disruptions and support interactive applications for vehicles. Most previous work of WiFi vehicular networks focused on vehicle-to-infrastructure communications where vehicles are considered the wireless clients connecting to roadside APs to achieve network access. There is only limited work that studies vehicle-to-vehicle communications. For example, Jerbi et al. (2007) confirm the feasibility of using ad hoc networks to extend the

transmission range of the infrastructure and reduce the connection time for moving cars in vehicular networks.

In summary, most experimental studies on applying WiFi (IEEE 802.11a/b/g) technology to vehicular networks focused on building fast connections between cars and roadside APs to achieve vehicle-to-infrastructure communications. On the other hand, performance evaluations of IEEE 802.11n are conducted either on MAC or PHY layers for indoor environments. The studies from this project are the first to empirically investigate the network reliability of inter-vehicle and intra-vehicle communications in IEEE 802.11n based vehicular networks.

This Page Intentionally Left Blank.

Chapter 3 – Stability Control of a Tractor and Semitrailer

Recent work by NTRCI (Arant et al. 2009) resulted in the development of a validated functional vehicle model of a Volvo VT 830 tractor and an LBT fuel tank trailer (LaClair et al. 2010). The functional model was developed in TruckSim[®], a vehicle dynamics application developed by Mechanical Simulation Corporation (2009b). The data for the model was generated using Michelin's kinematics and compliance test facility in Greenville SC (Pape et al. 2008), (Arant et al. 2009).

The work presented here deals with the development of a complete integrated ESC system for a tractor and trailer as well as the evaluation of the potential benefits of such a system. As a validated vehicle model was available, the ESC development used the model of the Volvo VT 830 and LBT tank trailer as the reference vehicle; however, the results are applicable to any tractor and trailer vehicle. To assess the ESC system's capabilities, a simulated vehicle was subjected to different steering inputs in loaded and unloaded configurations on a range of road surfaces. The results indicate that improvements in stability are possible but determining the correct ESC system response is not always easy.

Four main tasks need to be addressed in the development of an ESC controller. The first task is to develop a simplified mathematical model of the vehicle to use as a reference vehicle. The second task is to develop the yaw control and roll control strategies. The third task is to identify the parameters to be measured. The fourth task is to convert the model in to a state space form or transfer function form for quick analysis so that the model can be used to control the actual vehicle.

An overarching constraint is for the model to be efficient. The controller must use the vehicle model in real time, so the model must be significantly faster than the actual vehicle to give the controller time to evaluate the reference model and then act on the conclusions drawn from the results of the reference model. How fast the model needs to be is not universally agreed upon; however, Chen recommends that the model be 60 times faster than real-time (Chen 1999).

3.1 Controller Development Overview

The ESC development process can be effectively divided into two parts. The first is the development of the vehicle in TruckSim[®] and the second is the development of the controller in LabVIEW. The TruckSim[®] model acts as a surrogate for an actual vehicle and on-track testing (which would be costly) while LabVIEW, described further in Section 3.1.2, is a flexible development environment in which the vehicle's controller was developed. In simpler terms, TruckSim[®] is the vehicle and LabVIEW is the language in which the ESC algorithm managing the truck's brakes was developed. TruckSim[®] and LabVIEW were selected because National Instruments (makers of LabVIEW) also makes real time hardware applications that can be used to implement the ESC controllers developed here on actual vehicles in the future.

3.1.1 TruckSim[®]

TruckSim[®] is a vehicle modeling software application that simulates the vehicle's dynamic behavior to various inputs (Figure 3-1). It is a functional model: the vehicle components are not modeled as structural bodies deforming under loads and moments, but rather the vehicle component responses to forces and displacements (transfer functions) are determined from look-up tables and the component responses are summed to determine the vehicle's behavior. This type of model does not require as much detailed information on the construction of the vehicle but rather relies on the measured responses of the actual vehicle acquired through controlled testing.

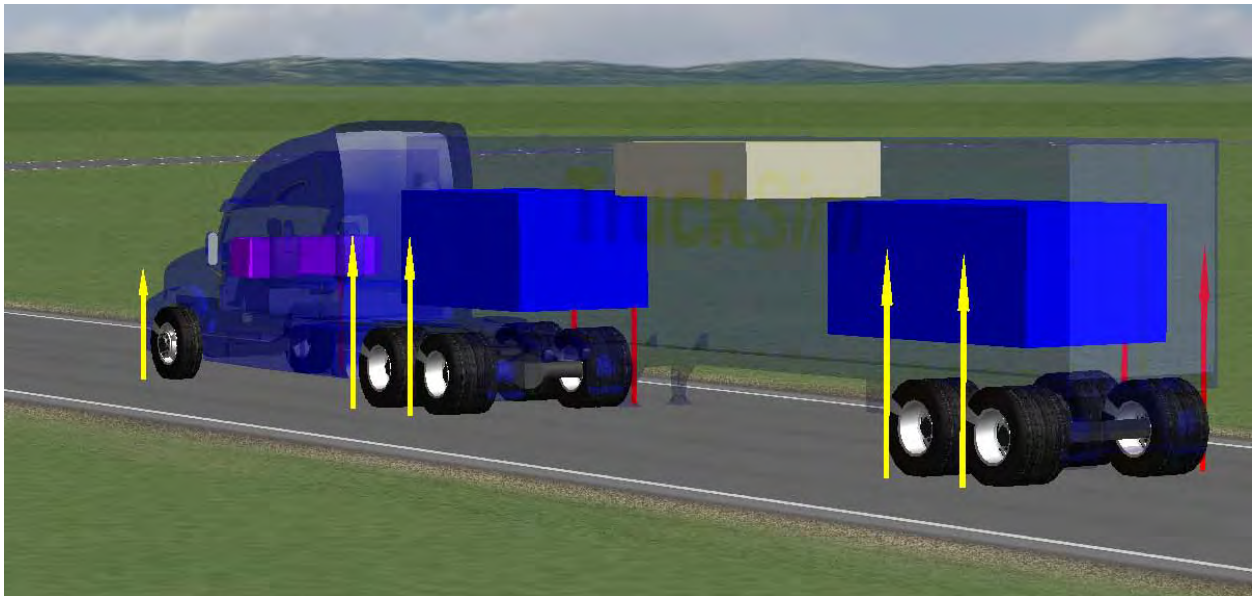


Figure 3-1. Animation still. TruckSim[®] vehicle animation (Mechanical Simulation Corporation 2009a).

The TruckSim[®] user interface (Figure 3-2) has the vehicle parameters in the (upper left and the driving scenario or procedure below the vehicle's configuration. The road surface condition is documented under miscellaneous data. The application manages the interface between TruckSim[®] and the controller (LabVIEW in this case) through the control menu (center top). Through changes in each of these inputs, the different vehicle configurations were evaluated with multiple controllers on multiple road circuits.

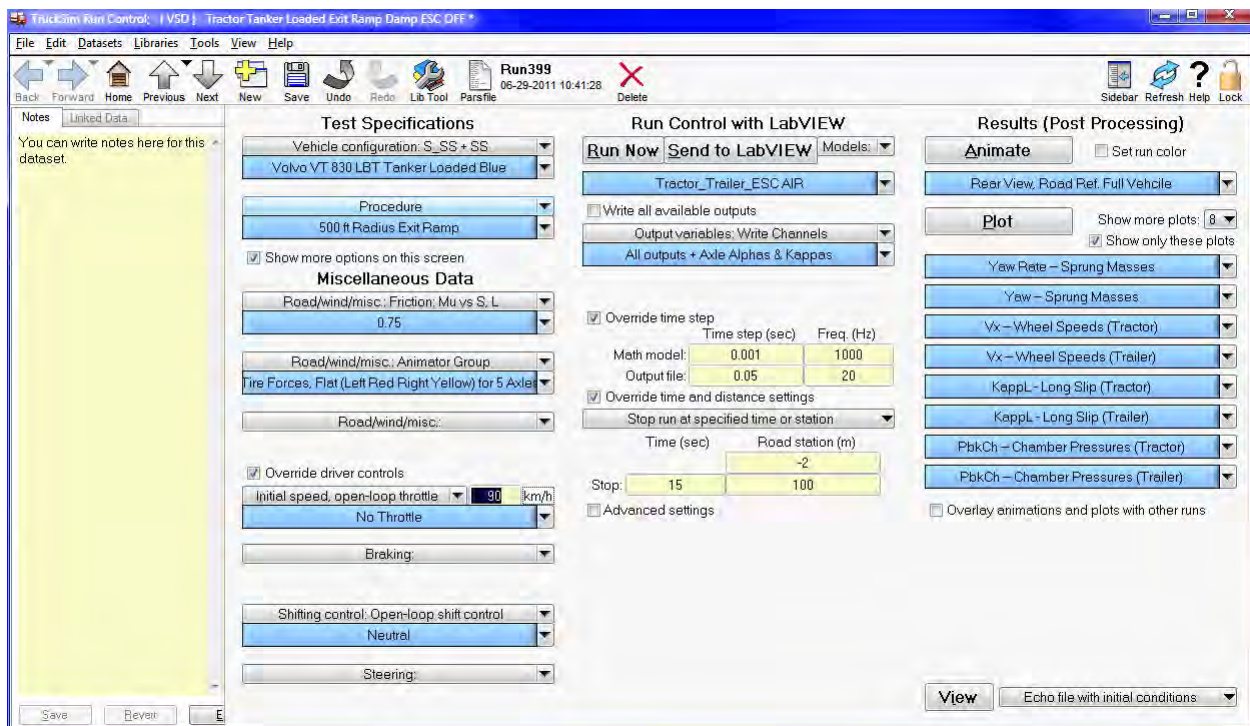


Figure 3-2. Screen shot. TruckSim® interface (Mechanical Simulation Corporation 2009a).

Data communication from TruckSim® to LabVIEW is defined by two tables in TruckSim® (an input and an output list). In this case, the vehicle's wheel speeds, steering demand, yaw rates, etc. are passed to LabVIEW and the wheel brake pressures (second table not displayed) are returned. At each simulation time step, TruckSim® passes the vehicle state parameters to LabVIEW, which then evaluates the vehicle's stability and provides TruckSim® with appropriate brake pressures for each wheel position. All stability responses are brake based. Active steering and active suspension are not employed in this controller design.

As it is beyond the scope of this report to describe how TruckSim® operates, the reader is advised to refer to the TruckSim® reference for further details (Mechanical Simulation Corporation 2009b).

3.1.2 LabVIEW

LabVIEW is a graphical programming language that can be used to interface with hardware or other applications. In this instance, it interfaces with TruckSim® and acts as the brake controller for the simulated vehicle. The LabVIEW application has two components: The first is a front panel that contains the user control inputs (Figure 3-3), and the latter is a block diagram or program logic structure (Figure 3-4). Note the two car icons in Figure 3-4, which manage the data transfer between LabVIEW and TruckSim®.

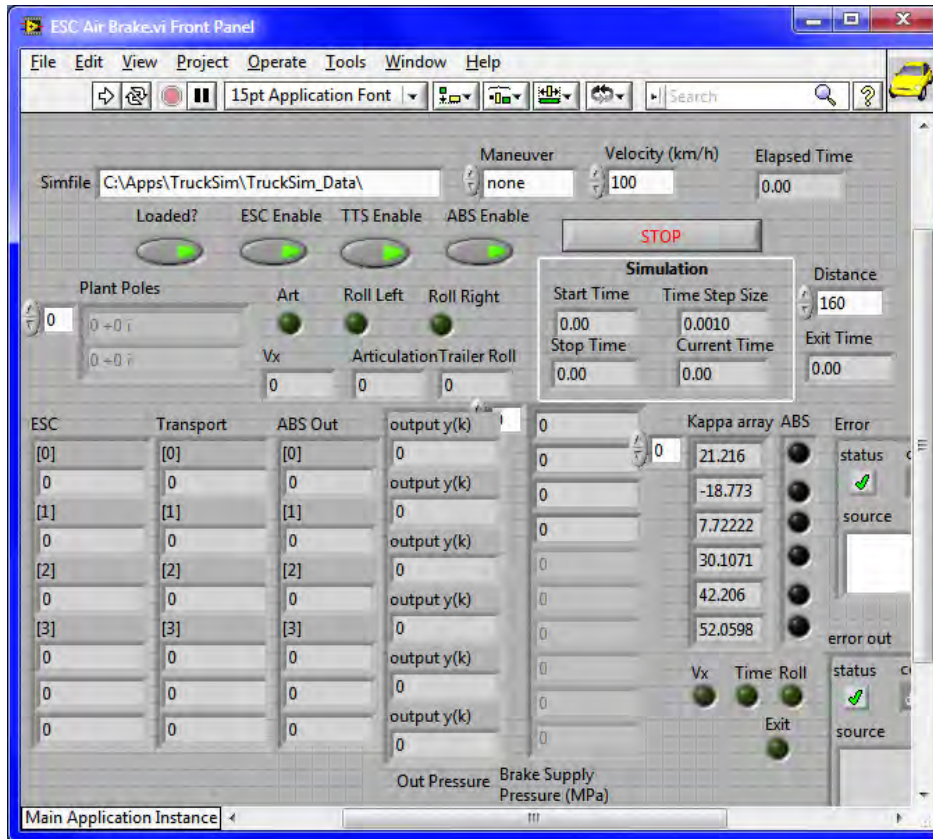


Figure 3-3. Screen shot. LabVIEW front panel.

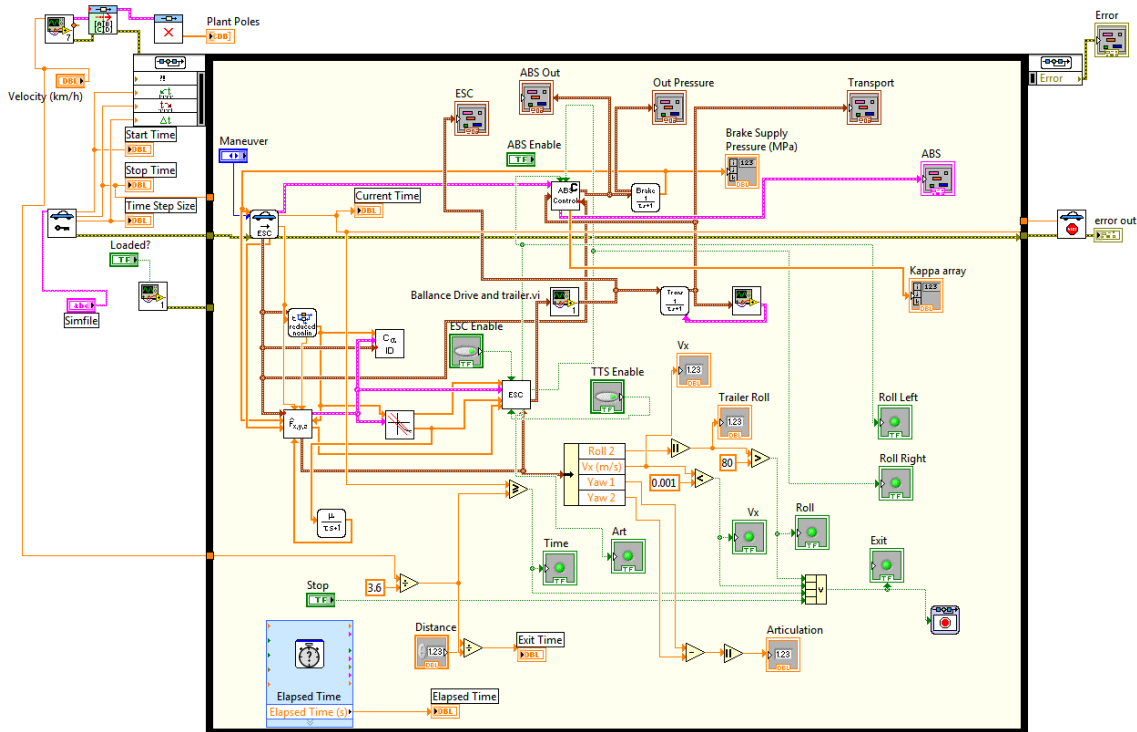


Figure 3-4. Block diagram. LabVIEW block diagram.

Figure 3-4 shows that LabVIEW evaluates the vehicle's dynamic state and determines what brake response is needed at each time step in the simulation. The LabVIEW algorithm uses a combination of ideal vehicle behavior predictions (simplified linear reference vehicle) and vehicle stability assessments, such as roll and side slip estimations, to define the appropriate control response.

3.1.3 Commercial Vehicle Brake System

As the stability system uses the vehicle's brakes to maintain stability, a discussion on commercial vehicle brake operation is in order. For U.S. vehicles, the brakes are controlled pneumatically, as shown in Figure 3-5. The brake pedal allows air pressure to travel to the axle relay valves, which then actuate air pressure chambers on each wheel, engaging and disengaging the brakes. To reduce the flow volume demand through the brake pedal, the brake command pressure is not the air source for actuating the brakes. That is accomplished by the modulators using a pressurized air supply at air reservoirs mounted near the brake sets on each axle. Each axle or axle group has its own modulator, which manages left and right braking.

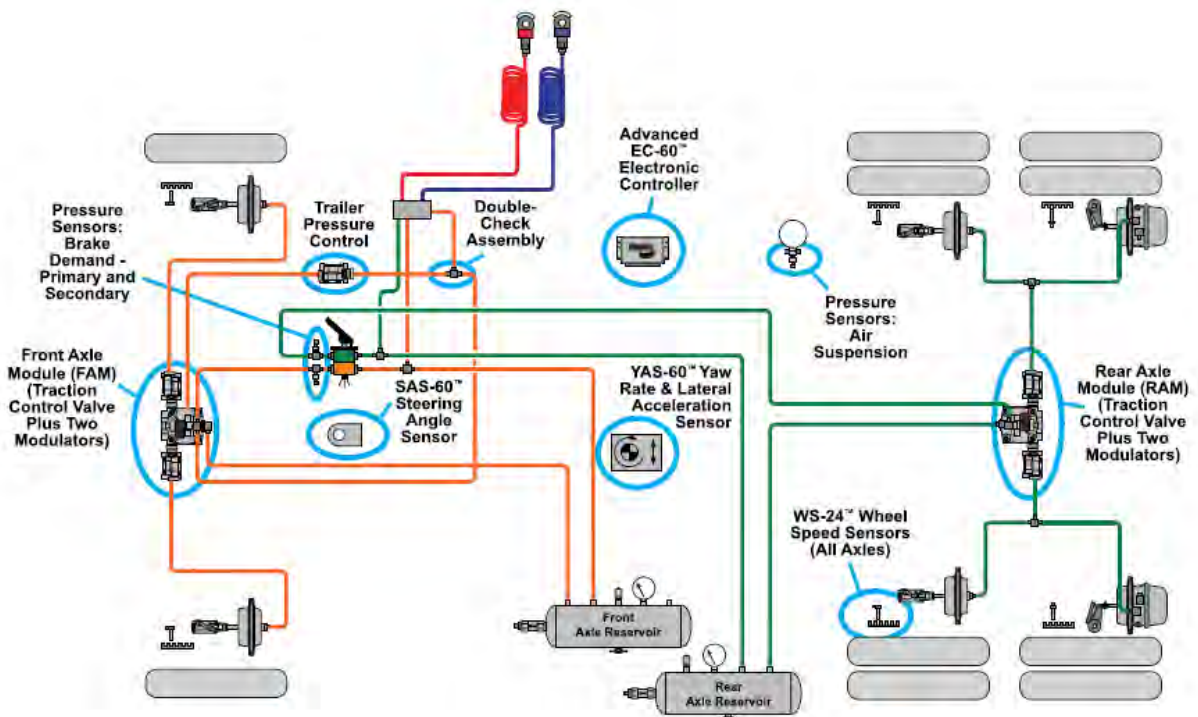


Figure 3-5. Sketch. Tractor brake system (Andersky and Conklin 2008).

The trailer brakes are usually managed in a similar method to the drive axles with an air command being sent via the blue glad-hand connector (top) and a pressurized tank filled via air from the red glad-hand connector (top).

When an electronic stability system is added, the time delay for the air to reach the modulators on the tractor (steer and drive axles) can be reduced through an electrical connection to the

modulators. However, the modulators still have a time delay as they respond pneumatically to the electronic brake command. However, the only communication to the trailer on current North American equipment is via a pneumatic command.

3.1.4 Stability Control Overview

Current North American commercial vehicle brake systems do not communicate vehicle state information or brake demand information between the tractor and trailer. The tractor ESC system can activate the trailer brakes but without any feedback on brake performance. As a result, current ESC systems cannot manage the entire vehicle's stability but only the stability of the tractor or a trailer to which they are mounted. The system developed here presumes that communication of vehicle state and brake management is possible enabling a full vehicle stability system.

The stability control algorithm developed in this research (Figure 3-5) can be divided into six major functional groups:

1. TruckSim[®] interface where data is passed between LabVIEW and TruckSim[®]. On an actual vehicle, this section would be replaced with input data from sensors and command signals to brake actuators.
2. Estimation of road friction and tire cornering stiffness (the three icons in the lower left).
3. Stability control algorithm (labeled ESC).
4. Brake transport delay $\left(\frac{1}{\tau_{S+1}}\right)$ to the axles.
5. Antilock brake function.
6. Transport delay in actuating the brakes $\left(\frac{1}{\tau_{S+1}}\right)$.

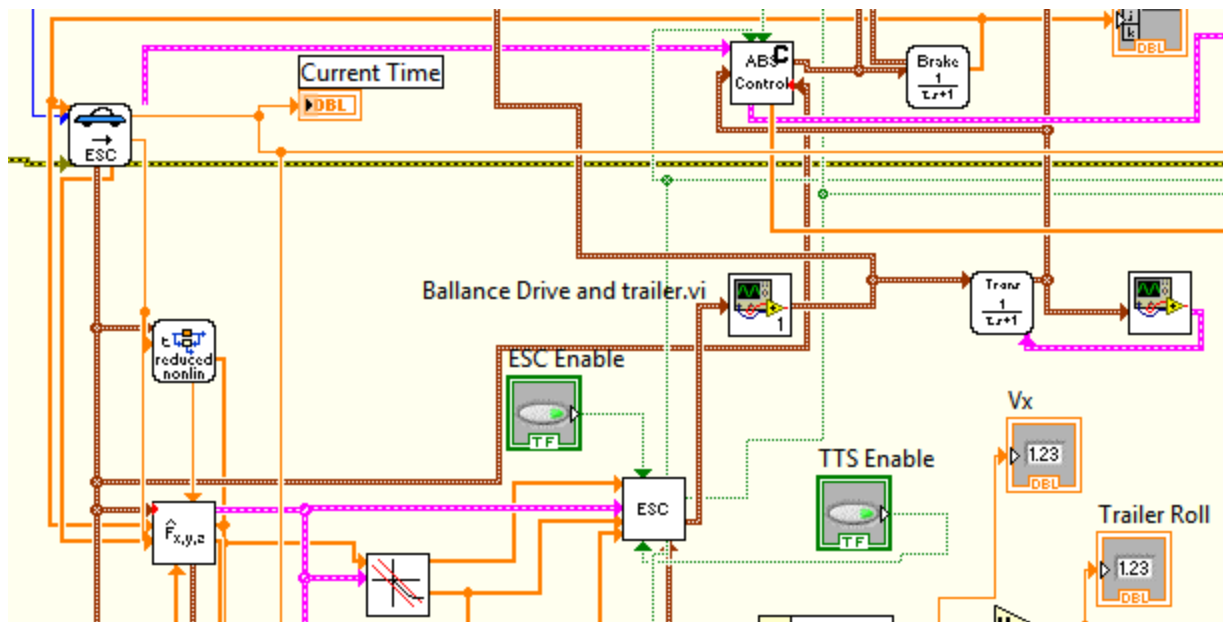


Figure 3-6. Diagram. Stability control algorithm.
 (This figure appears truncated because it is part of the LabView block diagram.)

Of particular importance in this analysis are the two transport delays, as trucks use a compressible medium (air) for brake command and actuation. Even in the case of ESC activation, which is communicated by electrical signal for the tractor, there is still a transport delay as the electrical signal is converted to a pneumatic actuation by the brake controller. And all commands to the trailer are communicated by pneumatic means regardless of command source (driver or ESC). For more information on the brake command process, please refer to Section 2.1.2.

The stability controller implemented here is a complete vehicle controller, meaning that the controller can sense the dynamic behavior of both the tractor and trailer and can control the tractor and trailer as a system. While this type of communication is not currently available on North American tractors and semitrailers, such communication could be introduced through the addition of a second electrical connector. Further, both pneumatic and electrical brake controls were evaluated to assess the benefit of reducing the signal delays. The research here is partly intended to provide justification for expanding ESC capabilities through enhancing vehicle communication capabilities and implementing electronically controlled braking.

3.2 Tractor Trailer Stability

As noted in Section 3.1.4, the majority of commercial ESC systems are tractor only systems. While trailer stability systems do exist, their use is much more limited and they tend to be roll control only with no provision for jackknife or trailer swing-out control. To produce a complete vehicle controller, the vehicle system needed to be re-assessed to determine what performance metrics needed to be monitored and what unit coupling interactions were present.

3.2.1 Vehicle Degrees of Freedom

Typical single unit vehicle control strategies that account for roll as well as yaw stability manage three vehicle states: Yaw rate, lateral velocity (or side slip), and roll rate (Du and Zhang 2008, 163-174), (Liebemann et al. 2004), (Bedner et al. 2007), (Yoon et al. 2009). Side slip and lateral velocity are related and can be interchanged easily as shown in the equation in Figure 3-7. Here v is the vehicle's lateral velocity, U is the forward velocity, and β is the side slip. (Small angle assumptions are being made). When solving combined roll and yaw systems, the roll rate is introduced as a variable to convert the second order roll equation into two first order equations for a total of four first order state equations.

$$v = \beta \cdot U$$

Figure 3-7. Equation. A vehicle traveling forward has a lateral velocity that is the product of the forward velocity and the side slip.

When linearizing the vehicle's equations of motion, the vehicle's forward velocity is usually assumed to be constant, or at least constant over a time step. Vehicle pitch is typically ignored, resulting in the assumption that there is no longitudinal load transfer. Aerodynamic and other secondary inputs are also ignored. While these assumptions do affect the accuracy of the model, the resulting errors are usually not significant enough to render the model unacceptable as a vehicle estimator. As computational time (model simplicity) is paramount, the errors are generally accepted.

When expanding the model to account for one or more trailers, the assumption is made that the forward speed of the trailer(s) is the same as the tractor since the trailer(s) follow the tractor. Pitch of the trailer(s) is also generally ignored (Sampson and Cebon 1998), (Sampson 2000), (Tianjun et al. 2007), (Tianjun and Liyong 2009, 508-11). The trailer(s) connections are modeled using constraint equations enforcing the same displacements on both vehicle units at the connection point.

For the work presented here, the vehicle unit side slip angles were used instead of lateral velocity. This selection has no effect on the modeling quality; the choice was based on the fact that the equations are simpler when using side slip. The simpler equations are likely faster, but the computational advantage has not been measured.

The kingpin connection was assumed to be rigid in the longitudinal and lateral directions, have no resistance to articulation, and have a non-linear roll stiffness as shown in Figure 3-8. As neither the tractor nor trailer models captured pitch, there was no pitch motion in the fifth wheel.

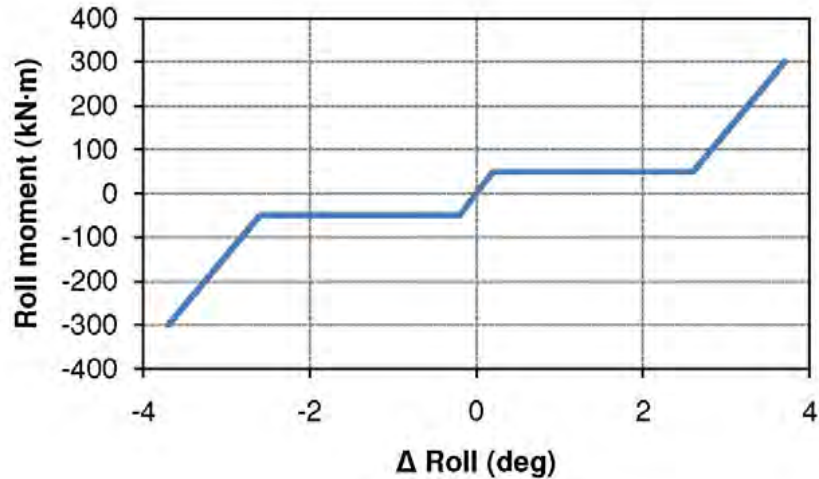


Figure 3-8. Plot. Fifth wheel roll moment (Arant et al. 2009).

3.2.2 States and Vehicle Parameter Measurement

The vehicle parameters used in the stability analysis were the tractor and trailer yaw rates, lateral accelerations, side slips, roll rates, and roll angles. Of these, yaw rate, roll rate, and lateral acceleration are easy to measure directly. Side slip and roll angle are not.

Side slip is the relationship between the vehicle unit's lateral and forward velocity (equation in Figure 3-9). However, lateral velocity is difficult to measure. Fortunately, there has been a significant amount of research on this subject with good side slip estimators being developed using yaw rate, lateral acceleration, and Kalman filtering of GPS data (Best, Gordon, and Dixon 2000, 57-75), (Gao et al. 2010, 217-234), (Anderson and Bevely 2010, 1413-1438), (Tin Leung et al. 2011, 29-58). Since this is already a well-researched problem with known solutions, the modeling here simply used the known side slip angle from the TruckSim[®] model.

$$\beta = \frac{V_y}{V_x} \approx \frac{V_y}{V}$$

Figure 3-9. Equation. Side slip.

For roll angle, Kalman filters have also been developed that work with roll rate and lateral acceleration (Kamnik, Boettiger, and Hunt 2003, 985-997), (Yu, Güvenç, and Özgüner 2008, 451-470). Rather than spend research time on redeveloping roll angle estimators, the decision was made to simply use the TruckSim[®] roll angle and document how to calculate the roll angle for future implementation when testing actual vehicles.

3.2.3 Control Tier Approach

The approach was to develop stability checks for the individual units and then evaluate each stability criterion in succession. This stability assessment procedure has been used by several

other researchers (Chen and Peng 1999), (Zhou, Guo, and Zhang 2008), (Yoon et al. 2010, 1247-1268). The only significant consequence of this change in stability assessment approach was the probability that the algorithm would take longer to evaluate (four stability checks instead of one) and that trade-offs between different stability requirements would be a little harder to achieve.

Implementing the stability system in LabVIEW was accomplished by implementing each stability criterion successively such that later controllers could pre-empt brake demands by earlier controllers. The controller order is designed to ensure that the more dangerous stability risks are managed even at the expense of lesser stability risks. The precedence of the stability risks is a combination of resulting crash severity and system controllability. More severe accidents or stability limitations that occur quickly are higher in priority. The order of the controllers was as follows:

- Tractor yaw control
- Trailer yaw control
- Jackknife or swing-out (programmed as a subset of trailer yaw control)
- Tractor and trailer roll control.

In some cases, communication of stability needs identified by one controller was passed to subsequent controllers to improve overall performance.

Finally, the resulting controller used a combination of reference controller and margin controller techniques. Tractor yaw control was managed by referencing the actual vehicle's response to the modeled vehicle's behavior. Errors between the actual vehicle's behavior and the modeled vehicle's behavior were used to develop corrective brake responses. For other stability criteria, such as roll control, the actual response of the vehicle was evaluated against a stability threshold margin, and the controller activated the brakes when the vehicle exceeded the acceptable margin of safety.

Tractor Yaw Control

The tractor yaw controller is the simplest of the controllers. The basic model is the well documented two-axle yaw controller, where the actual vehicle's states are compared to predicted states from a simple linear model of the vehicle (Figure 3-10) (Ghoneim et al. 2000, 124-144), (Ko and Lee 2002, 181-192), (Antonov, Fehn, and Kugi 2008, 780-801), (Limroth 2009a).

$$\begin{bmatrix} \dot{v}_y \\ \dot{r} \end{bmatrix} = \begin{bmatrix} \frac{C_1 + C_2}{mv_x} & \frac{-aC_1 + bC_2}{mv_x} - v_x \\ \frac{-aC_1 + bC_2}{Jv_x} & \frac{-a^2C_1 + b^2C_2}{Jv_x} \end{bmatrix} \begin{bmatrix} v_y \\ r \end{bmatrix} + \begin{bmatrix} \frac{C_1}{m} \\ \frac{aC_1}{J} \end{bmatrix} \delta$$

Figure 3-10. Equation. Tractor yaw control estimator.

Errors between the observed vehicle and the modeled vehicle (Figure 3-11) were used to define the appropriate yaw moment correction needed, which was then implemented through differential braking of the wheels.

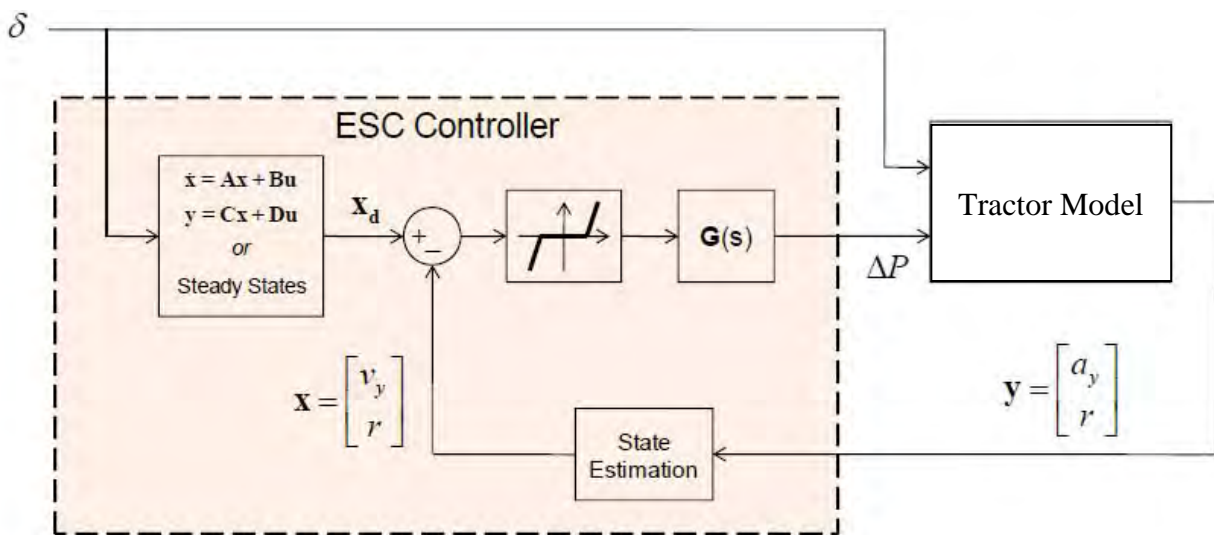


Figure 3-11. Block diagram. Tractor yaw controller (Limroth 2009a).

The tractor yaw controller equations shown compare the measured tractor's dynamic response to the predicted vehicle's response where the predicted response is based on the simplified linear model of the tractor. Brake corrections are made to align the actual vehicle's response to the model vehicle's response.



Figure 3-12. Sketch. Tractor yaw control brake response (Andersky and Conklin 2008).

For understeer cases, the controller would brake the inside rear drive axles to introduce a yaw moment. For oversteer cases such as shown in Figure 3-12, the outer front wheel is braked to introduce a moment counter to the yaw direction. The trailer brakes are activated, because the kingpin is always behind the tractor's CG location, so that trailer brakes always act to reduce tractor yaw.

Tractor yaw control is first in the series of controllers, as tractor yaw was deemed to be the least serious of the stability threats. The driver can sense this instability more readily than other instabilities and can directly affect the instability through a change in steering. This does not mean that tractor yaw stability is not a serious safety issue, but that the remaining stability issues either result in more serious accidents or are more difficult to manage and need to take priority. Drivers generally agree that it is better to slide off the road than to roll over or to have the trailer swing out and get tripped on a barrier or soft soil.

Trailer Yaw Control

Trailer yaw control has two goals. It must prevent both (a) trailer yaw divergence from the tractor, i.e., jackknife and swing-out, and (b) yaw divergence of the entire vehicle, where the tractor and trailer rotate essentially as a single unit with little articulation angle. The latter case may seem somewhat unlikely, but it can occur if the roll correction results in prolonged heavy braking of the drive and trailer axles such that the rear of the tractor and the trailer lose lateral stability. Typically, roll control overrides yaw control unless the risk of entire vehicle yaw instability is present, in which case trailer yaw control takes precedence.

The block diagram for the trailer yaw controller is Figure 3-13. The yaw controller approach was quite simple with the instability threat being defined as the current articulation angle and the articulation rate multiplied by a constant determined from the vehicle's inertia. This instability threat was measured against the restoring potential of the vehicle braking moments. Jackknife or yaw instability risk was mitigated by releasing the tractor drive axle brakes and activating the trailer brakes for a jackknife or releasing tractor and trailer brakes for a swing-out.

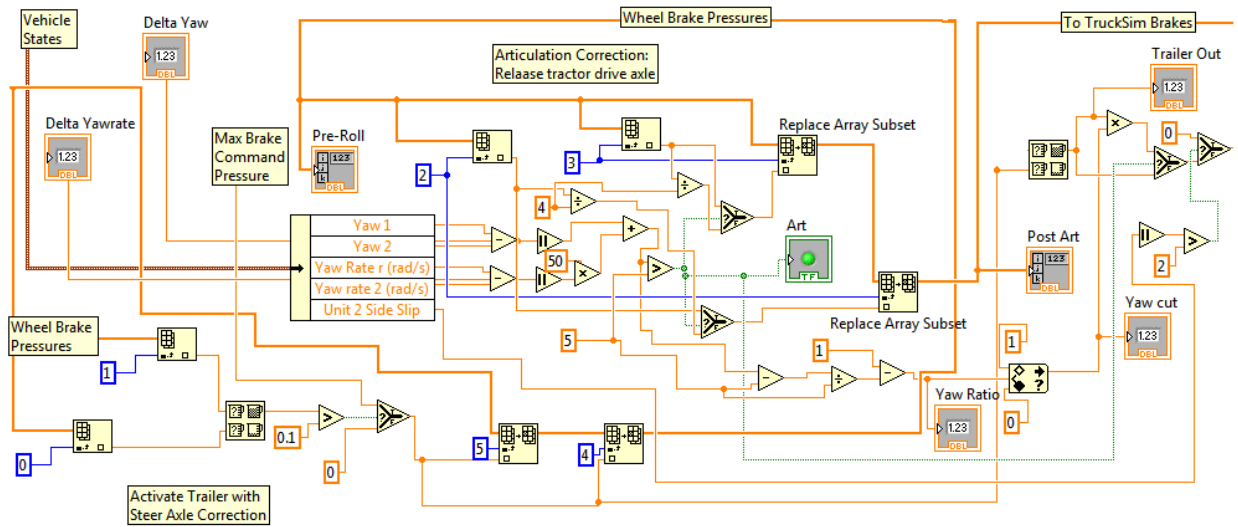


Figure 3-13. Diagram. Trailer yaw control.

For a jackknife, releasing the drive axles' brakes allows the tractor to use the drive axles' traction to regain yaw control and drive out of the tractor spin, while the trailer brakes act to reduce the tractor's yaw as well. For a swing-out, the tractor brakes are released to increase the speed of the tractor and allow the tractor to correct yaw divergence. The trailer brakes are also released so that the trailer tires can generate a larger lateral force (in place of a longitudinal brake force) such that the trailer swings back behind the tractor.

In some cases the tractor can experience yaw divergence (spin out) while the trailer is swinging outward. The result is that there is not a significant change in articulation even though the vehicle is experiencing yaw instability. To test for this type of instability, the side slip of the trailer is monitored. If the trailer begins to exhibit yaw instability, the trailer brakes are released to allow the trailer to re-establish yaw stability. As this type of yaw instability has been observed to lead to rollovers in the analysis, this is the top priority stability response, though it is a relatively rare occurrence.

Tractor and trailer Roll Control

The model assessed the rollover risk by comparing the restorative moment potential (Figure 3-14) against the overturning moment (Figure 3-15). When the overturning moment reached 50% of the restoring moment, the trailer brakes were engaged. To prevent the roll response from shocking the vehicle with pulses of full brake pressure, the brake response of the ESC system was inversely proportional to the stability margin. At 50% of stability margin the brakes began engaging and increased to 100% when the stability margin was reduced to 0% (Figure 3-16).

$$M_{restore} = \frac{M * g * t}{2}$$

Figure 3-14. Equation. Roll restoring moment.

$$M_{Overrtturn} = M * g * \phi + M * Ay * h + \frac{I_{zz} * \dot{\phi}^2}{2}$$

Figure 3-15. Equation. Overturning moment.

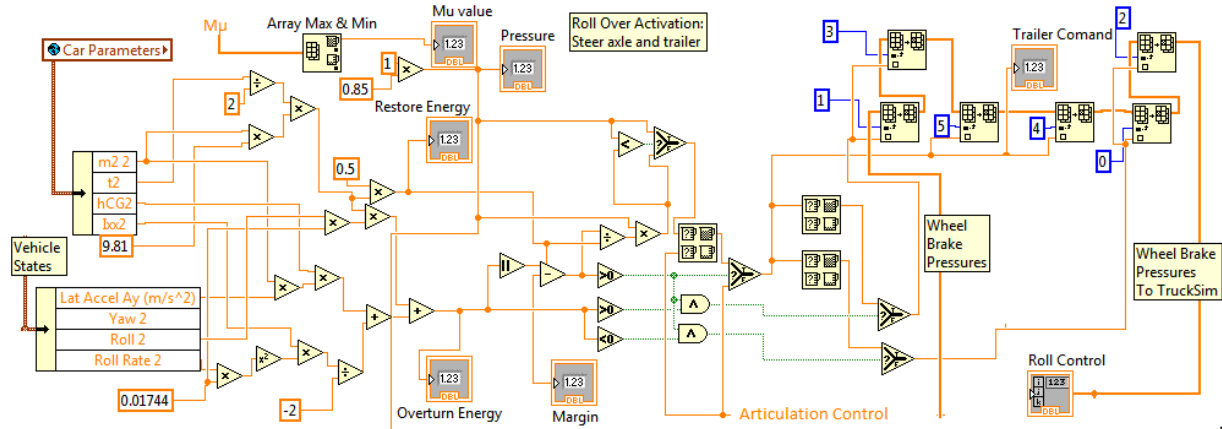


Figure 3-16. Diagram. Tractor and trailer roll control.

The roll controller engaged the outside steer tire to reduce the tractor yaw rate and thus the tractor and trailer lateral acceleration. It also engaged the trailer brakes to both reduce the tractor’s yaw rate and to slow the vehicle. The outside drive axles were also engaged, but any subsequent observation of increased tractor side slip would release the tractor brakes to prevent a jackknife.

3.3 Brake Actuation and Brake Control

As discussed in Section 3.1.3, commercial vehicles use pneumatic brakes as opposed to the hydraulic brakes used in most passenger vehicles. As air is a compressible medium, there are delays between when the brake command is given and the brake actuation. The simulation of the brake and ESC systems must account for these transport delays. But before understanding how the ESC system manages these delays, it helps to understand how the ABS brake function works, because the ESC system controls the brakes through the ABS.

3.3.1 Modeling ABS

When a brake command is given, be that from the driver or the ESC system, the response is an air pressure change in the hose connecting the relay valve and the brake chamber at the wheel. In line between the wheel and the relay valve is the ABS modulator, which releases pressure as needed to manage wheel lock-up, as explained at the end of Section 2.1.2. In the simulation, the

ABS system is modeled as a simple on/off switch that allows brake pressure to be applied to the brake chamber or dumps the brake pressure.

While the schematic of the controller is quite complicated (Figure 3-17), the function is simple. The controller allows the command pressure to pass through the system until the wheel slip reaches 50%, at which point the output pressure is cut (no brake pressure) until the wheel speed recovers to 90% of the vehicle's speed. At this time the controller allows the pressure to pass through again. Thus the controller attempts to maintain the wheel speed between 90% and 50% (10% slip to 50% slip). The 50% to 90% range is significantly larger than what is typical for a passenger car due to the media being compressible and the resulting brake response transient delays.

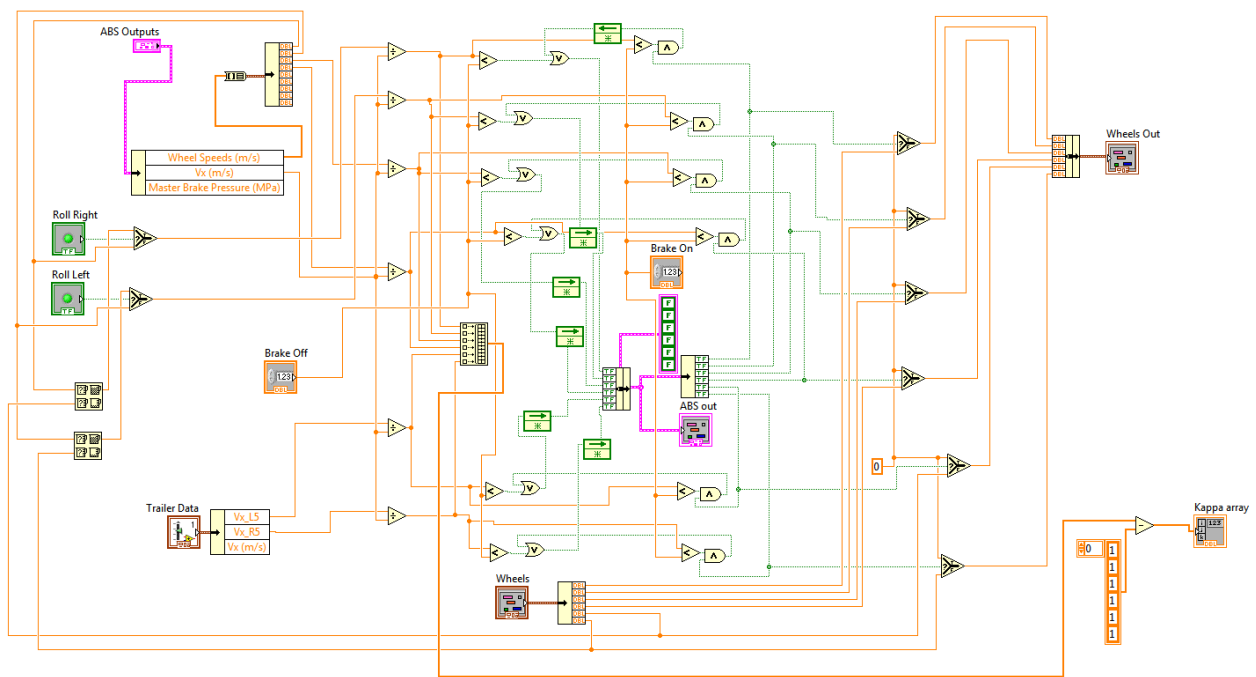


Figure 3-17. Diagram. ABS controller.

Once the brake demand leaves the ABS controller, it passes through a transport delay, which models the time delay of the air brake chambers (Figure 3-18) where the air pressure overcomes the restoring spring load within the brake chamber, rotates the S-cam, and activates the brakes. See Section 2.1.2 for details on the brake chamber operation. The output of the transport delay is then the input to TruckSim[®] and controls the brakes in the simulation (Figure 3-19).

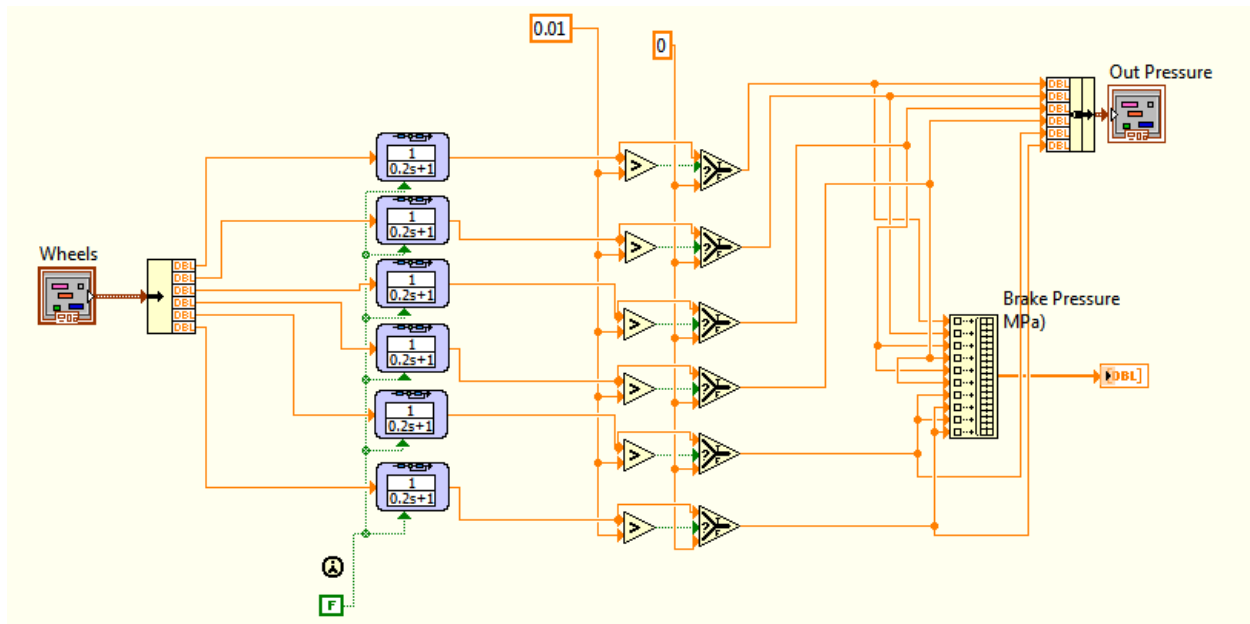


Figure 3-18. Diagram. Axle transport delay.

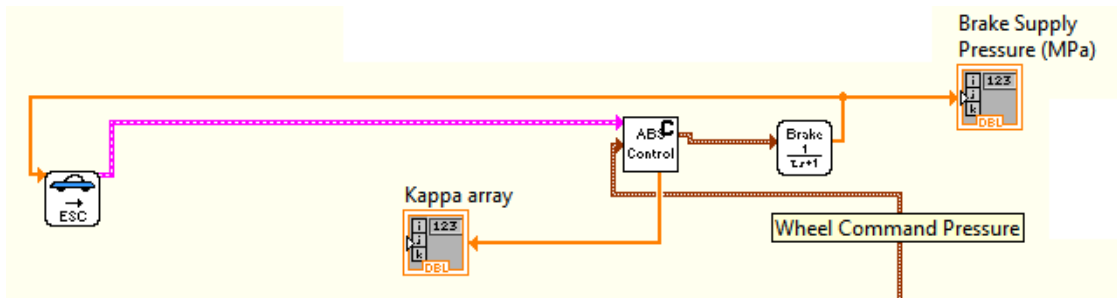


Figure 3-19. Diagram. Brake demand to TruckSim®.

3.3.2 Full Air Brake Simulation

Once the driver or an ESC system mounted on a tractor determines that a brake response is needed, a command is issued to the brake modulator on the appropriate axle. For steer and drive axles, this can be an electric signal from the ESC or pneumatic signal from the driver input. For the trailer axles, the command is pneumatic as there currently are no electrical brake command mechanisms between the tractor and trailer. To simulate the brake system, the modeled brake command passes through a first order time delay to simulate the actual vehicle's signal delay to the given axle with the trailer having a significantly longer delay than the drive axles (Figure 3-20). The signal transport delays values are drawn from published research journals (Dunn 2003), (Kienhöfer, Miller, and Cebon 2008, 571-583), (Bayan et al. 2009), (NHTSA 2010) and are realistic delays for a commercial brake system.

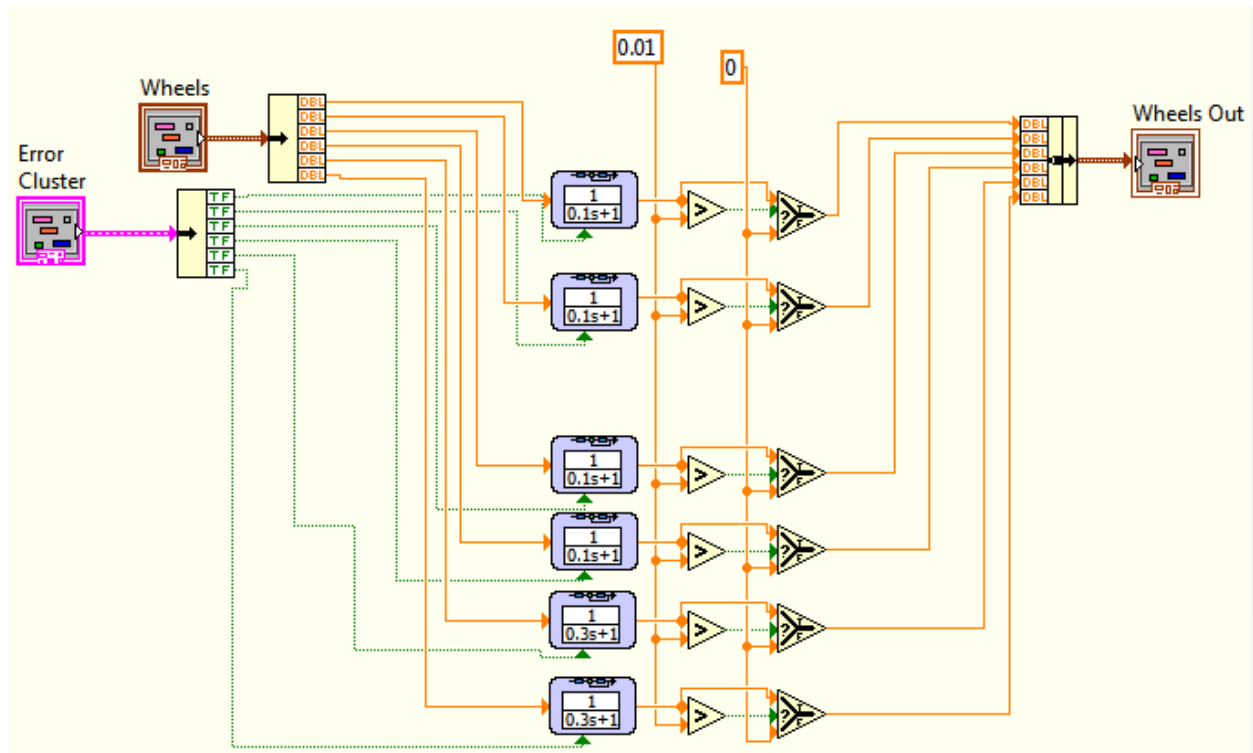


Figure 3-20. Diagram. Brake transport delay to axle modulator.

Both the transport delays and the ABS slip range were tuned to reproduce wheel performances seen in commercial vehicles (Choi and Cho 2001, 57-72), (Kienhöfer, Miller, and Cebon 2008, 571-583). The two criteria used were wheel cycle time (ABS engage to ABS disengage time) and wheel lock and unlock rates. Due to the signal delays, commercial vehicle brake systems generally have slow cycle times (on the order of 1 to 2 Hz, as shown in Figure 3-21) compared to hydraulic (passenger car) systems, which are usually 20 to 30 Hz on average.

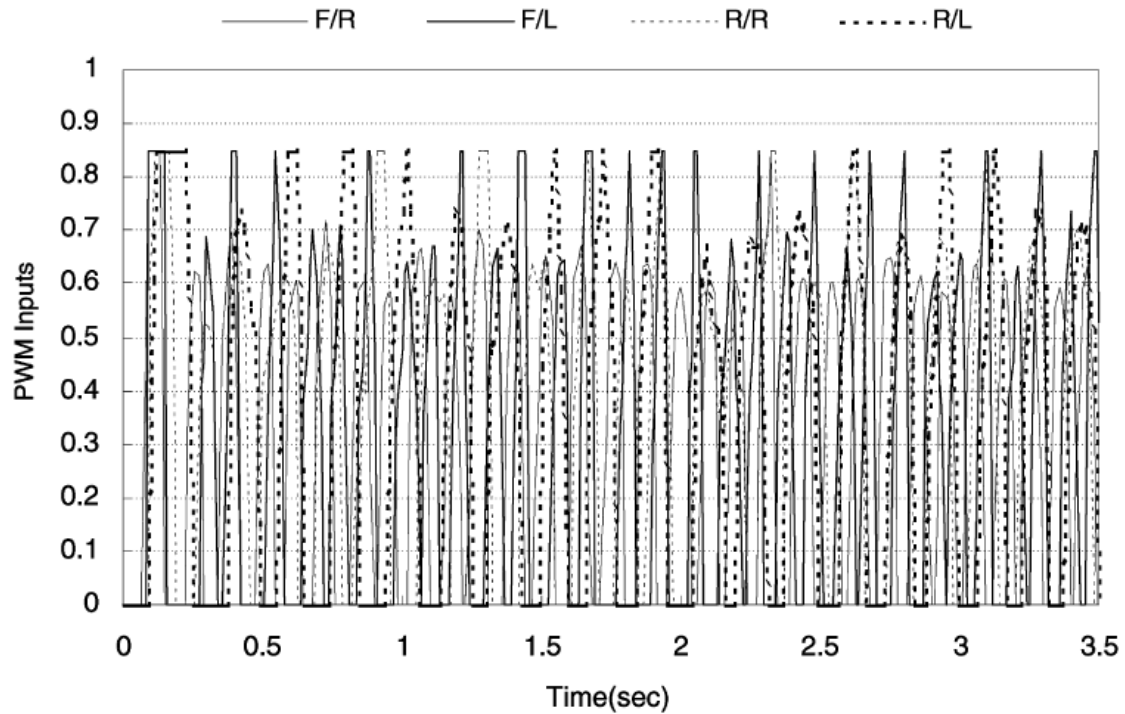


Figure 3-21. Plot. Measured wheel pulses (Choi and Cho 2001, 57-72).

In addition to having slower cycle times, commercial vehicle systems often cannot respond fast enough to prevent wheel lock at lower speeds. For example, Kienhoffer and Miller measured the wheel speeds and air chamber pressures for a typical commercial brake system and showed that on a damp ($\mu = 0.75$) surface, the wheels exhibited the anticipated lock-slip-lock behavior (Figure 3-22).

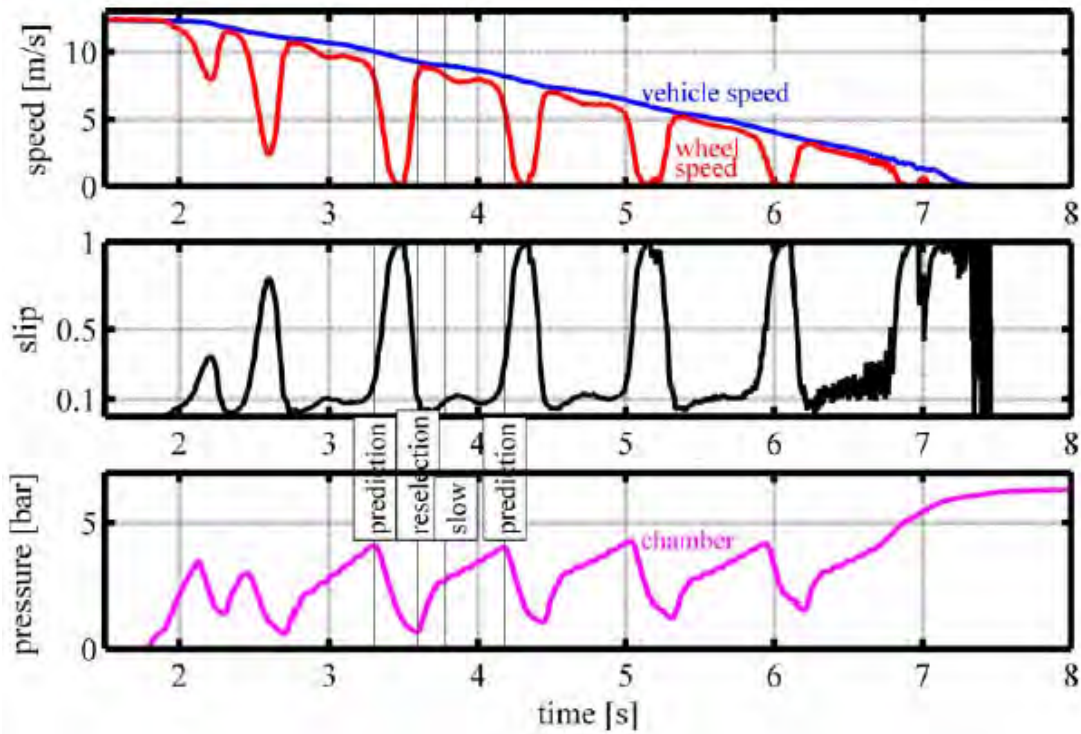


Figure 3-22. Plots. Measured brake performance ($\mu = 0.75$) (Kienhöfer, Miller, and Cebon 2008, 571-583).

3.3.3 Electronically Controlled Braking Systems

ECBS can dramatically reduce the signal delays in commercial vehicles by replacing the pneumatic signal with an electric signal (Figure 3-23). The actual braking is still pneumatic, but the brake actuator is at the brake chamber, eliminating the signal delays from the command (treadle valve) to the modulator and then from the modulator to the brake chamber.

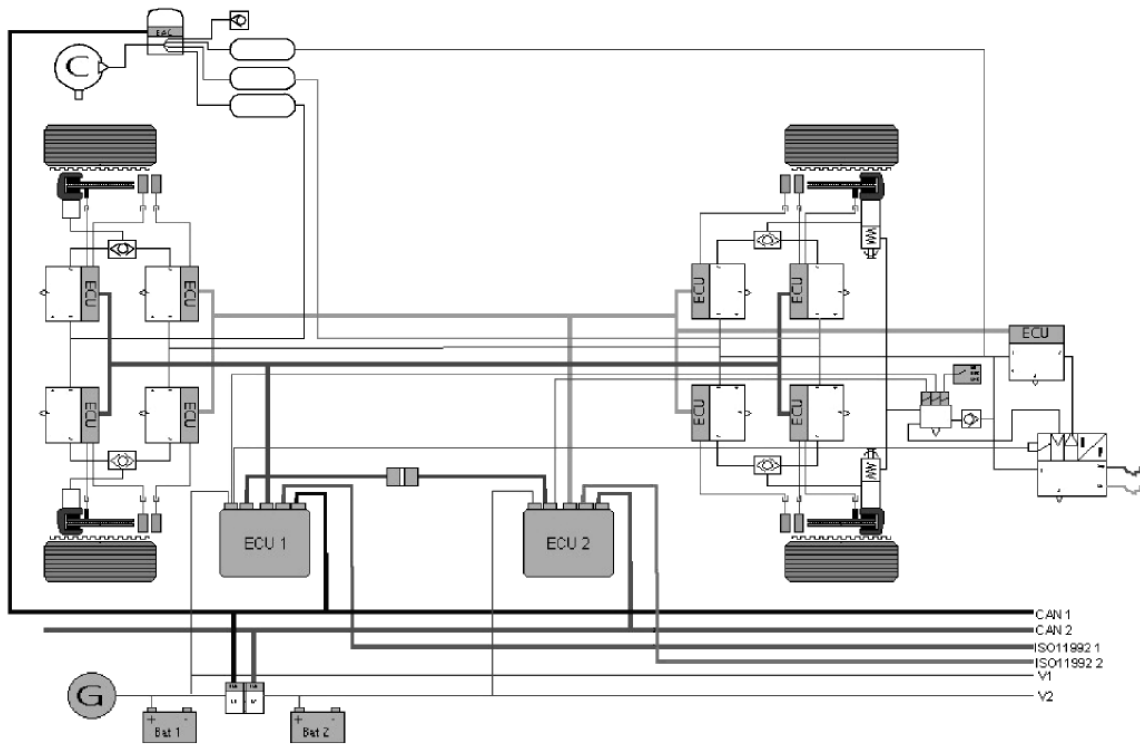


Figure 3-23. Sketch. Electronic control brake system diagram (Palkovics and Fries 2001, 227-89).

While ECBS has become common in Europe, it is not in use in the US as most experts interpret FMVSS 121 (the US federal regulations on commercial vehicle brake systems) as not permitting ECBS (NHTSA 2009), (Palkovics and Fries 2001, 227-89). In Europe, ECE R13 (2008), which is the European counterpart of FMVSS 121, was modified to permit ECBS as part of a mandate to include ESC on all commercial vehicles (Wurster, Ortlechner, and Schick 2010).

3.3.4 Stopping Performance

The first task in evaluating the pneumatic brake system model was to determine if the model produced the same wheel modulation as seen in actual vehicles (Figure 3-22). The brake model produced similar wheel control performance with the ABS cycle time being a little less than 1 Hz for both the tractor (Figure 3-24) and trailer (Figure 3-25). The ABS controller also demonstrated the anticipated wheel slip pattern for the tractor (Figure 3-26) and trailer (Figure 3-27), with the slip ratio κ cycling between 10 and 50 percent. The model also reproduced the full wheel lock behavior below speeds of 35 km/hour on a damp ($\mu = 0.75$) surface road (Figure 3-22). As it is most undesirable to have the steer wheels lock in braking (loss of lateral control), the steer wheels have a peak pressure of 0.75 MPa (108 psi) versus the drive and trailer axles at 0.85 MPa (120 psi). The brakes on the steer axle are also smaller than the drive and trailer axles. Thus the steer axles did not show the same lock-unlock cycle as their braking moment was lower.

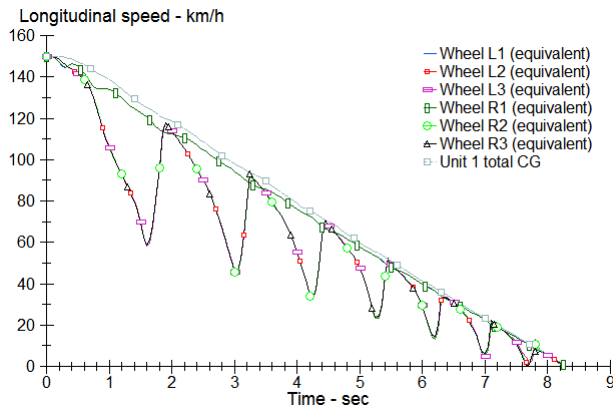


Figure 3-24. Plot. Tractor full stop ($\mu = 0.75$).

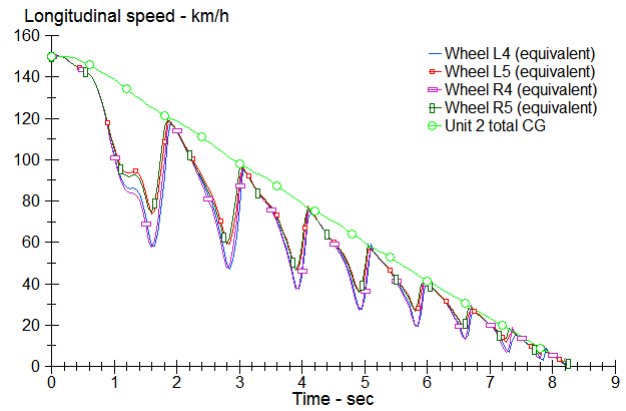


Figure 3-25. Plot. Trailer full stop ($\mu = 0.75$).

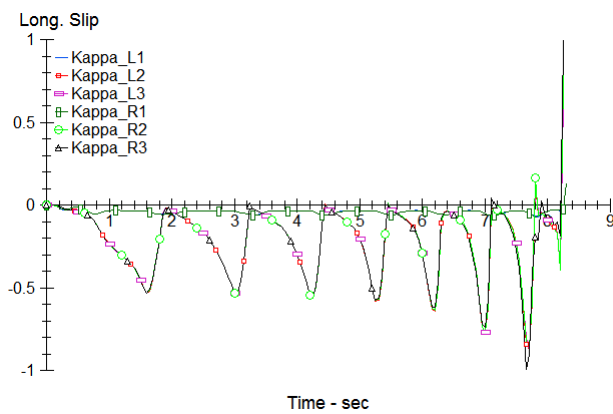


Figure 3-26. Plot. Tractor slip control ($\mu = 0.75$).

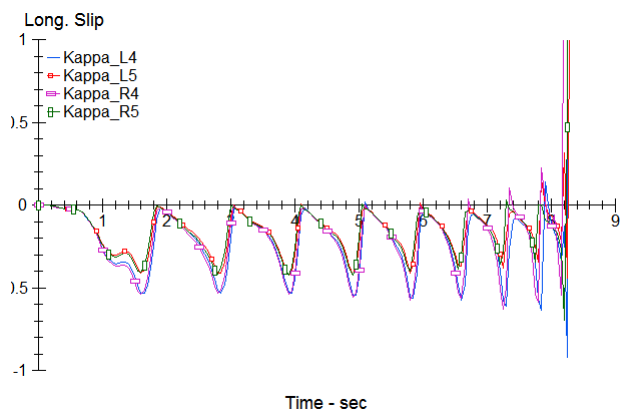


Figure 3-27. Plot. Trailer slip control ($\mu = 0.75$).

Note: Figure legends for the simulation results are defined as follows:

- Unit 1 – Tractor
- Unit 2 – Trailer
- L1 – Left steer axle
- R1 – Right steer axle
- L2 – Left forward drive axle
- R2 – Right forward drive axle
- L3 – Left rear drive axle
- R3 – Right rear drive axle
- L4 – Left forward trailer axle

- R4 – Right forward trailer axle
- L5 – Left rear trailer axle
- R5 – Right rear trailer axle.

To check the performance of the pneumatic brake system against relevant standards, the FMVSS 121 dry brake test requirement that the loaded vehicle stop from 97 km/h (60 mph) in 250 ft (76.2 m) was simulated (Figure 3-28). The simulated vehicle beat the requirement by 8.5 m (28 ft, which is a reasonable performance).

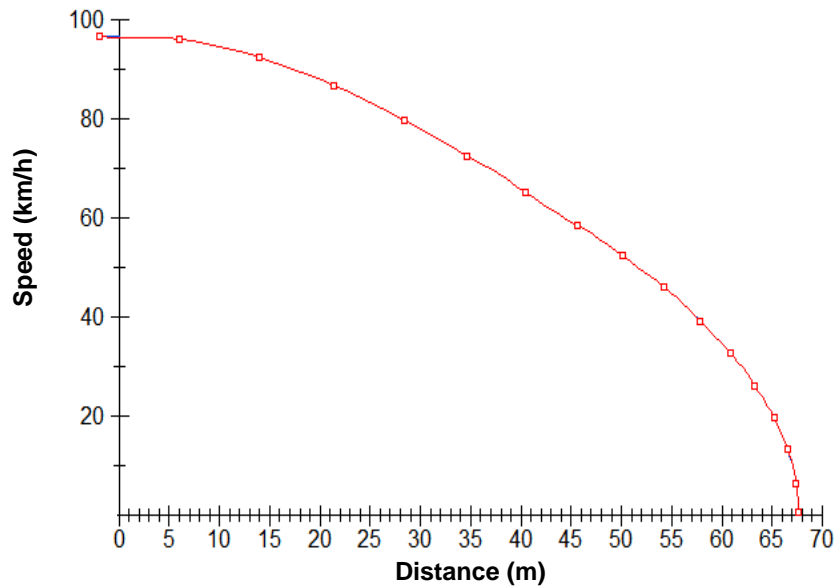


Figure 3-28. Plot. FMVSS 121 dry straight line stop.

To demonstrate the performance of the commercial vehicle brake system and to document the potential stopping improvements of ECBS, several straight line braking runs were evaluated on multiple road surfaces. To test the system's response over the full usage range of the vehicle, tests were conducted from 97 km/h (60 mph) and from 150 km/h (93 mph) test. The higher speed was not intended to be an actual operational condition; the simulation was a test at the extreme limits of the vehicle to show the effects under any conceivable speed. The results, shown in Table 3-1 and Table 3-2, indicate that ECBS has the potential to reduce stopping distances between 6% and 29% depending on the load and road conditions. Cases where there was a need for increased brake pressure modulation showed greater potential for the ECBS system (snow traction was so low that neither system ever reached peak operating pressure). The ECBS model used in this analysis was the same brake model as the air system but with the transport delays reduced as appropriate.

Table 3-1. Full vehicle stopping distance (meters) from 97 km/h (60 mph).

Road Surface	Loaded Vehicle Pneumatically Controlled Brakes	Loaded Vehicle Electronically Controlled Brakes	Unloaded Vehicle Pneumatically Controlled Brakes	Unloaded Vehicle Electronically Controlled Brakes
Dry ($\mu = 0.85$)	67.7	59.2	64.6	53.8
Damp ($\mu = 0.75$)	76.7	65.4	70.9	57.2
Wet ($\mu = 0.5$)	134.1	93.5	110.4	83.5
Snow ($\mu = 0.25$)	298.3	257.5	234.8	212.3

Table 3-2. Full vehicle stopping distance (meters) from 150 km/h (93 mph).

Road Surface	Loaded Vehicle Pneumatically Controlled Brakes	Loaded Vehicle Electronically Controlled Brakes	Unloaded Vehicle Pneumatically Controlled Brakes	Unloaded Vehicle Electronically Controlled Brakes
Dry ($\mu = 0.85$)	154.6	144.6	145.3	127.0
Damp ($\mu = 0.75$)	175.6	158.3	159.2	134.8
Wet ($\mu = 0.5$)	305.6	219.5	248.5	191.7
Snow ($\mu = 0.25$)	677.8	597.1	520.9	472.1

There are two primary reasons for the reduced stopping distance of the ECBS system (Figure 3-29). The first is that the electronic control brake system can supply pressure to the wheels much more quickly (Figure 3-30, Figure 3-31) as the transport time is much smaller. This removes the delay in deceleration seen in Figure 3-29 for the conventional ABS (or EBS) system (red and denoted by rectangles) where the vehicle travels approximately 10 meters before brake force builds sufficiently to slow the vehicle.

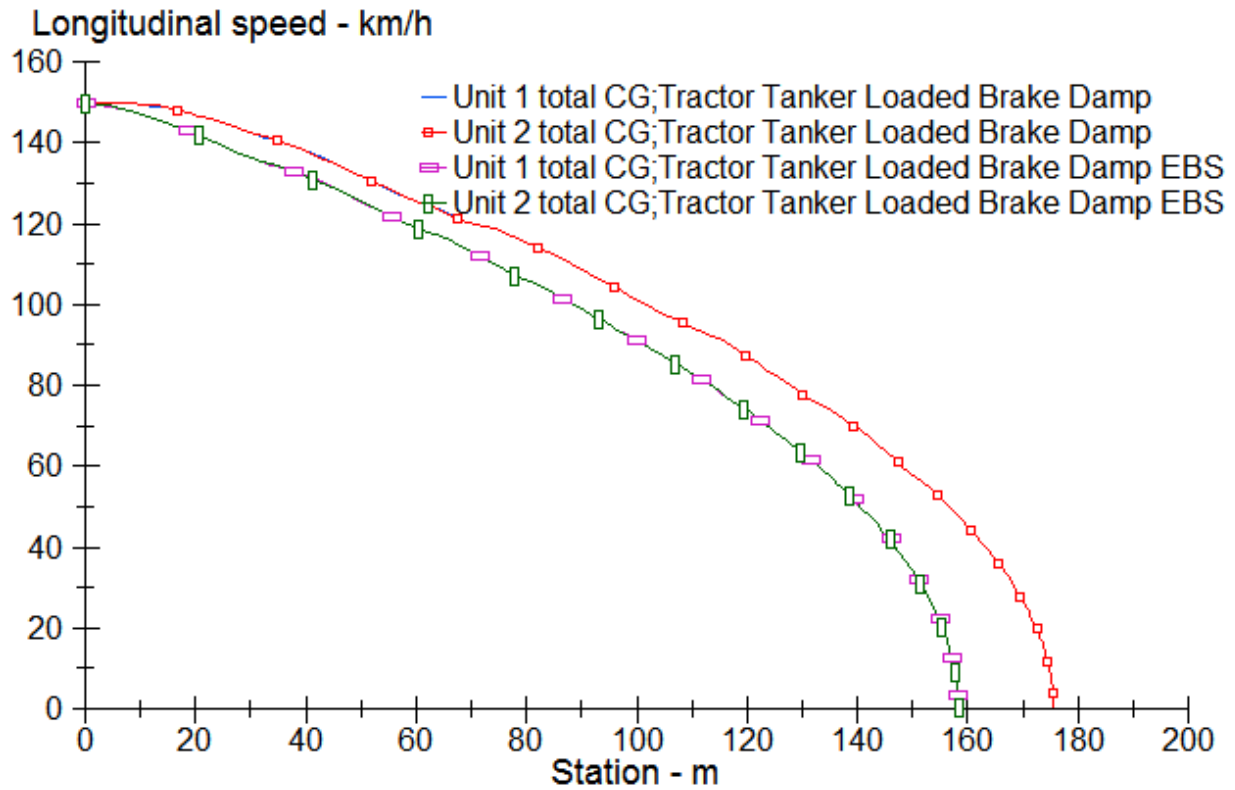


Figure 3-29. Plot. Straight line braking ($\mu = 0.75$) (Unit 1, the tractor, and Unit 2, the tank semitrailer, have the same speed in both cases, so their plots are coincident.)

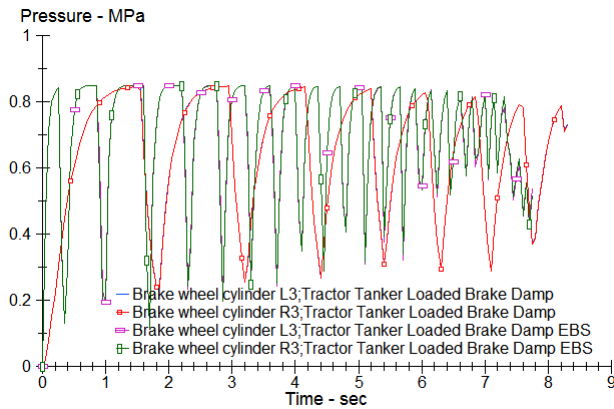


Figure 3-30. Plot. Drive axle brake pressure ($\mu = 0.75$).

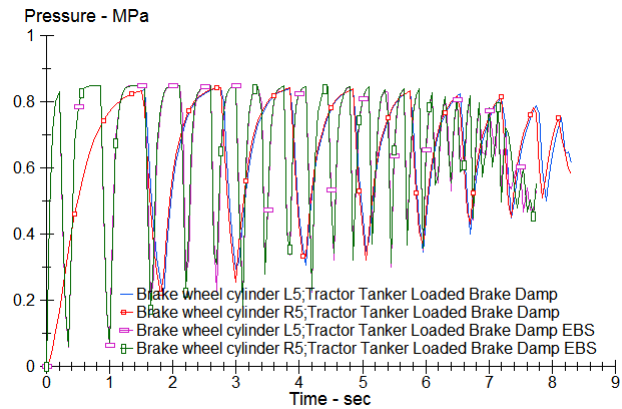


Figure 3-31. Plot. Trailer axle brake pressure ($\mu = 0.75$).

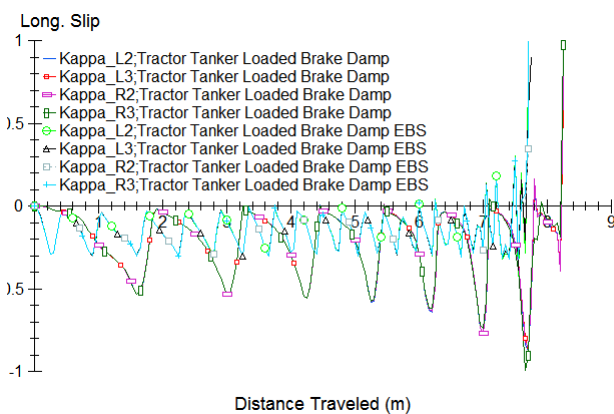


Figure 3-32. Plot. Drive axle slip ratio ($\mu = 0.75$).

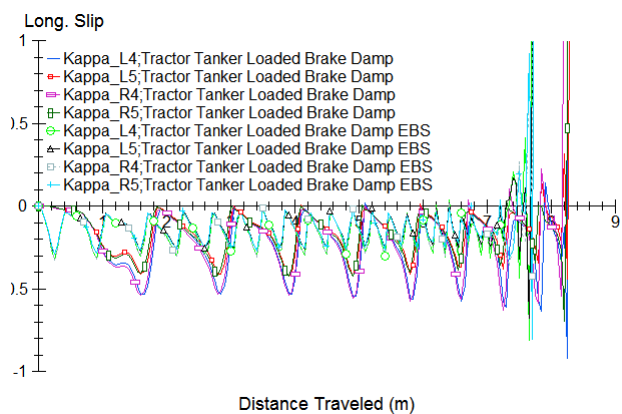


Figure 3-33. Plot. Trailer axle slip ratio ($\mu = 0.75$).

The second advantage of the ECBS system is that it can cycle much more quickly and maintain a tighter control on wheel slip (Figure 3-32, Figure 3-33), which keeps the tire operating in its peak tractive zone. This results in higher braking forces and higher decelerations.

3.4 Results of Simulating the ESC Algorithms in LabVIEW and TruckSim[®]

The evaluation of the ESC systems (pneumatic and ECBS) was divided into four operational regions based on vehicle load and maneuver. In almost all cases, the ESC system improved vehicle performance and the ESC plus ECBS system produced even better vehicle performance. In the analysis cases below, the blue vehicle represents the baseline tractor and semitrailer (no ESC), the red vehicle was equipped with the ESC system and pneumatic brakes, and the purple vehicle was equipped with ESC and ECBS.

3.4.1 Maneuver Test Speeds

The maneuvers modeled and presented here were intended to show the behavior of the vehicle with and without stability control. As the vehicle needed to be at its stability limit to demonstrate the performance of the ESC systems, the vehicle speed was adjusted for each load

case and maneuver. For the reader’s reference, Table 3-3 and Table 3-4 document the test speeds for each of the stability evaluations.

Table 3-3. Vehicle speeds at the threshold of stability (km/h) – lane change maneuver.

	Loaded	Unloaded
Dry ($\mu = 0.85$)	93	120
Damp ($\mu = 0.75$)	90	120
Wet ($\mu = 0.5$)	90	100
Snow ($\mu = 0.25$)	60	80

Table 3-4. Vehicle speeds at the threshold of stability (km/h) – exit ramp maneuver.

	Loaded	Unloaded
Dry ($\mu = 0.85$)	89	120
Damp ($\mu = 0.75$)	90	110
Wet ($\mu = 0.5$)	85	95
Snow ($\mu = 0.25$)	70	80

Note that as the road surface traction increases, the unloaded vehicle’s speed increases significantly. This is in line with the observation that the vehicle was severely traction limited in snow where yaw stability was the major risk.

3.4.2 Vehicle Configurations and Maneuvers

To evaluate the performance of the stability system, a tractor and semi-trailer was evaluated on multiple road surfaces in empty (Figure 3-34) and fully loaded (Figure 3-35) configurations. The payload consisted of a front mass (8,300 kg), a center mass (1,900 kg), and a rear mass (11,150 kg). The fully loaded vehicle weighed out at the US DOT limit of 80,000 lb. for a five-axle commercial vehicle. Note: TruckSim[®] did not have a tank truck animation, so a van trailer graphic is used here.



Figure 3-34. Animation still. Unloaded vehicle.



Figure 3-35. Animation still. Loaded vehicle.

The maneuvers simulated were a lane change to model transient behavior and an exit ramp to model steady state behavior. While the exit ramp is not a true steady state maneuver (there is a transient component entering the maneuver), it is about as close to a real steady state maneuver as the vehicle is likely to see. This is because the driver generally increases the steering to a set value at the initiation of the turn and then makes only minor adjustment to maintain a constant turning radius. The test cases were a permutation of the following three parameter sets (Table 3-5) for a total of 16 driving simulation cases plus an additional 8 straight line braking simulations.

Table 3-5. Simulation permutation parameters.

Road: mu = 0.25 – Snow mu = 0.5 – Wet mu = 0.75 – Damp mu = 0.85 – Dry	Vehicle Condition: 80,000 lb. GVW – Loaded 30,500 lb. – Empty	Maneuver: Double Lane Change Exit Ramp Straight Line Brake
------------------------------------------------------------------------------------	---------------------------------------------------------------------	---------------------------------------------------------------------

The exit ramp was a simple turn with a constant radius of 152 m (500 ft) with a straight segment approach. There was no spiral; the driver preview model blended the segments together. The road had no superelevation (bank) or grade. The lane change was a 4 meter wide path with a 3.5 meter offset after 70 meters and a return after 150 meters. The gate spacing was 30 meters on each side (Figure 3-36).

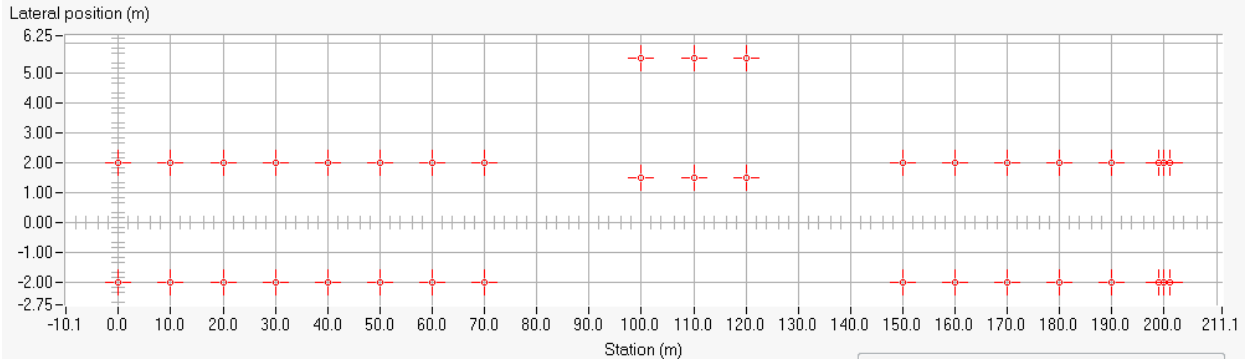


Figure 3-36. Diagram. Lane change cones.

In all figures and plots, the vehicle stability designations are as follows:

- Blue: No stability control
- Red: ESC system using conventional air brake system
- Purple: ESC with ECBS.

3.4.3 Loaded Vehicle on an Exit Ramp

As exit ramps expose the vehicle to sustained lateral accelerations, this maneuver primarily tests the roll stability of the vehicle (Figure 3-37) though lateral stability was also of concern for the lower friction road surface cases. The tractor is stable in roll, so only the trailer's roll angles are presented here.

Figure 3-38 illustrates how effective the ESC systems were at mitigating rollover. When a risk of rollover was detected (see Section 3.2.3), the tractor brakes were selectively actuated to generate a yaw moment counter to the turning direction. The trailer brakes were activated as well though the inner trailer brakes contributed very little as they were lightly loaded. The effect was to slow the vehicle and to increase the vehicle's path radius, both of which lowered the lateral acceleration and thus overturning moment. However, braking the drive axles did introduce a risk of jackknife, particularly on low friction (low μ) surfaces, and required close monitoring. The arrows in Figure 3-38 represent the resulting tire forces (vertical, lateral, and longitudinal) and are proportional to the force magnitude.



Figure 3-37. Animation still. Exit ramp – loaded vehicle – roll illustration ($\mu = 0.85$).

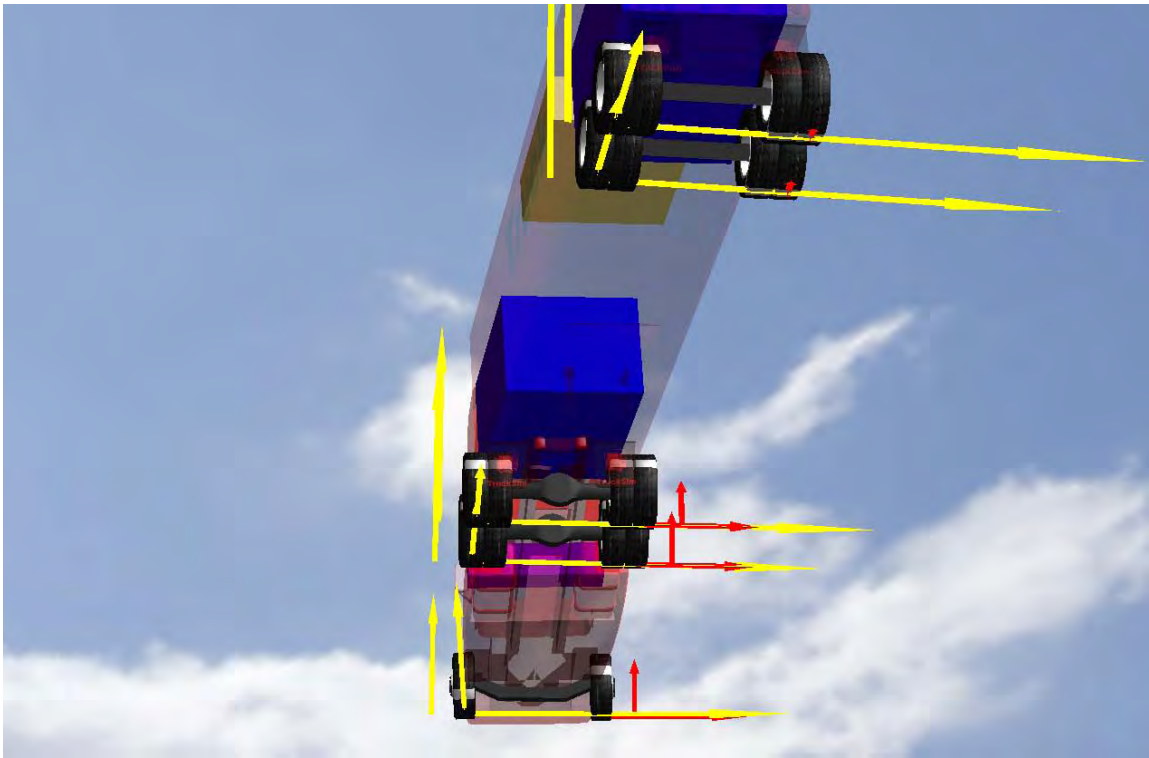


Figure 3-38. Animation still. Exit ramp – loaded vehicle – brake vectors ($\mu = 0.85$).

In addition to reducing rollover on high mu surfaces, the ESC system also acted to control jackknife behavior on low friction surfaces (Figure 3-39). This was done by releasing the tractor drive axle brakes and applying the trailer brakes so that the trailer re-aligned itself behind the tractor.

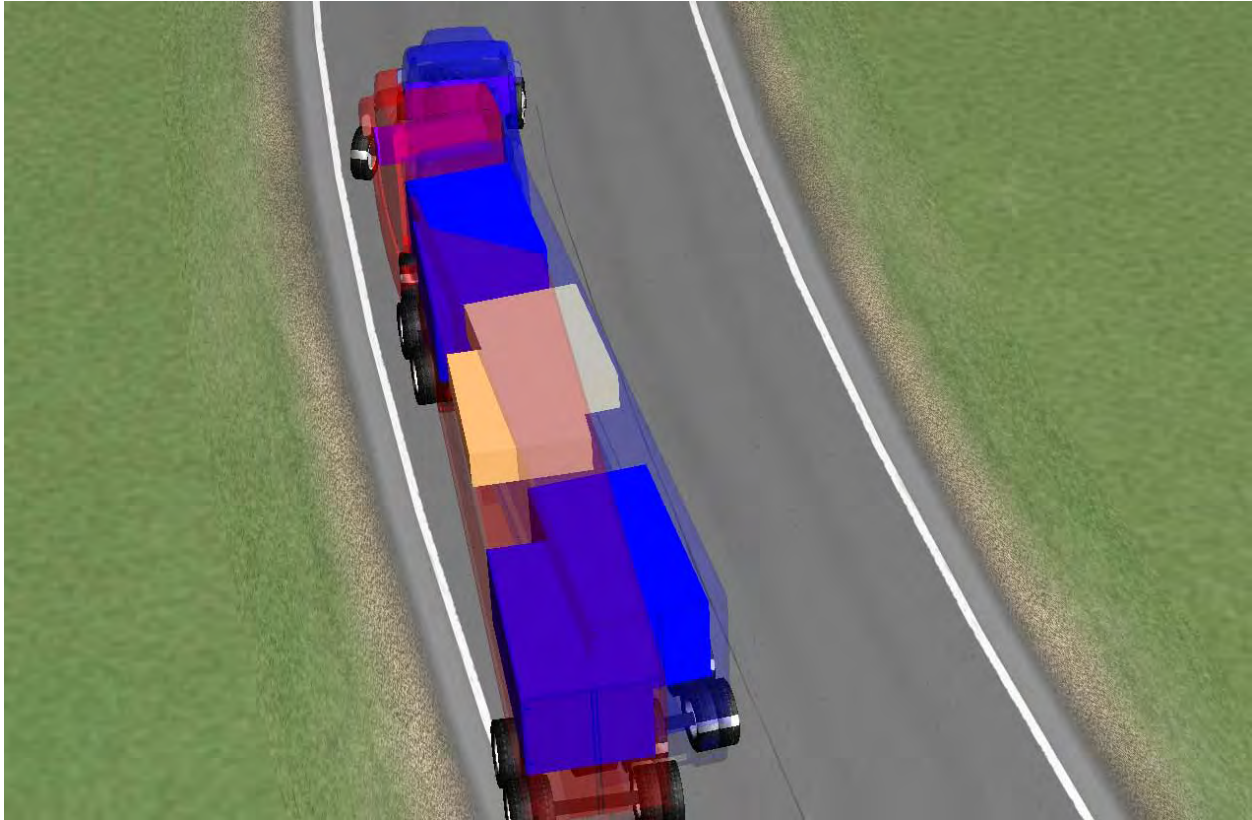


Figure 3-39. Animation still. Exit ramp, loaded vehicle – ESC articulation control ($\mu = 0.25$).

Figure 3-40 shows the response of the vehicle with both ESC systems and without an ESC system on multiple road surfaces. The results were generally as expected with the ECBS ESC system outperforming the pneumatic ESC system and both ESC systems demonstrating stability improvements over the non-ESC vehicle.

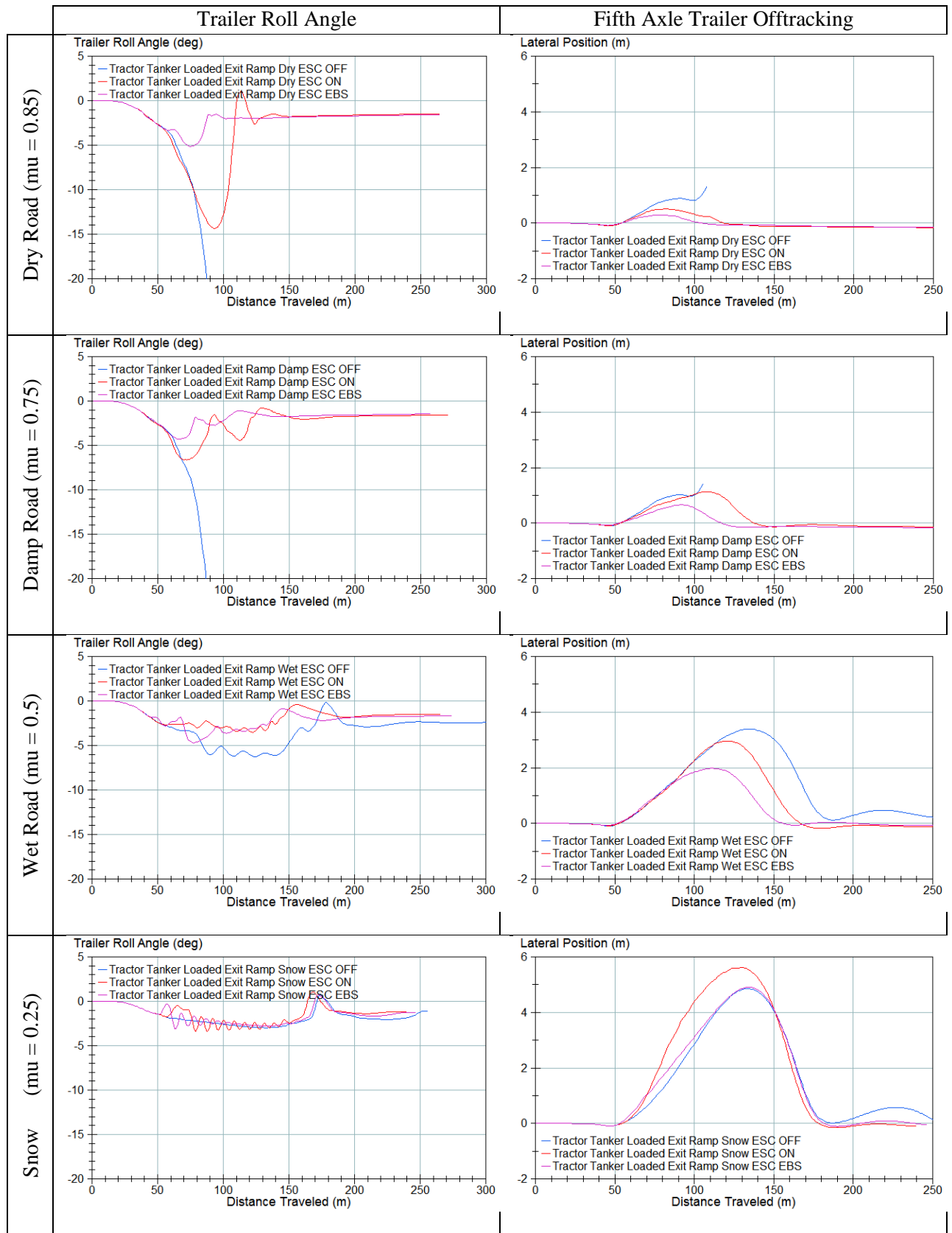


Figure 3-40. Plots. Exit ramp – loaded vehicle – roll and tracking errors.

All stability margin calculations were determined by increasing the maneuver speed of the ESC simulation until the resulting vehicle performance reproduced the performance seen with the nominal (no ESC) vehicle. The criteria for grading performance were the maximum path error during a maneuver segment, speed at wheel lift, or maximum articulation angle. The stability margin represents the increased entrance speed that the system can offer over the base vehicle for a given stability limit.

For the dry road ($\mu = 0.85$), the ESC system was able to provide a 6% rollover margin and the ESC + ECBS system provided a 12% stability margin. The advantage of the ECBS was that the brakes were activated much more quickly and aggressively (Figure 3-41). The faster acting ECBS brake system more quickly slowed the vehicle to a speed safe for the curve; thus the vehicle brakes could be released sooner allowing the tires to generate lateral forces sooner, which helped to limit path deviation.

For low friction surfaces, such as the wet road case, the air based ESC system provided a 2% offtracking margin and the ECBS based ESC system provided a 5% margin based on rear trailer path deviation. The ECBS based system was able to provide a better stability margin as it could actuate the brakes quickly to slow and modify the tractor's heading and then release quickly so that the tires could develop lateral forces needed to control the lateral slide of the trailer.

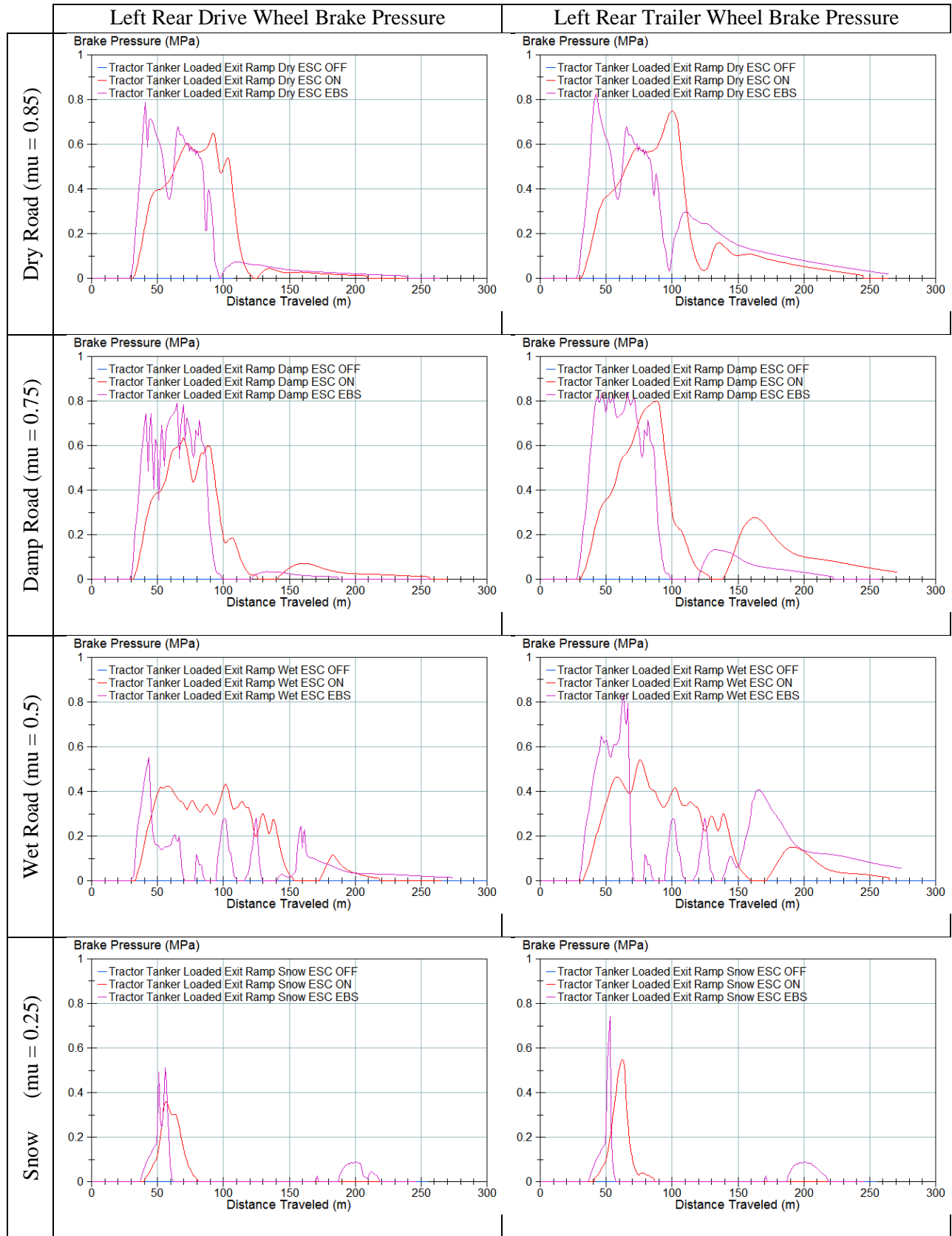


Figure 3-41. Plots. Exit ramp – loaded vehicle – brake pressures.

The snow was the only surface condition where the ESC systems had difficulty improving stability of the loaded vehicle on the ramp. In this case, there was so little traction that any braking forces resulted in a loss of lateral traction. For the ECBS system, the brakes could be pulsed fast enough to prevent the development of large trailer slip angles early in the maneuver. However, the amount of traction available was so low that any braking resulted in a loss of lateral force. The transport delays in the pneumatic ESC system resulted in longer brake durations, which resulted in longer periods of reduced lateral force and subsequently larger sustained trailer side slip angles (Figure 3-42).

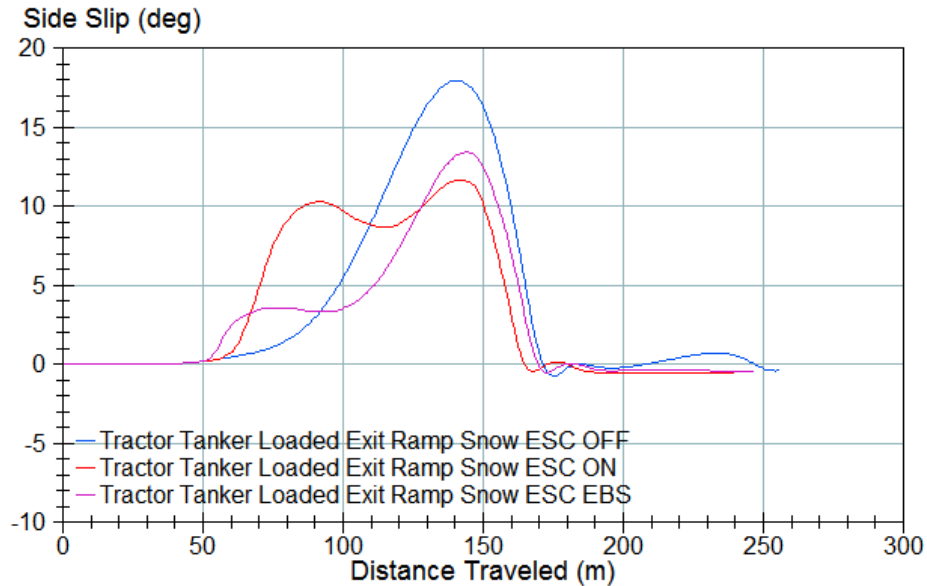


Figure 3-42. Plot. Exit ramp – loaded vehicle – trailer side slip ($\mu = 0.25$).

3.4.4 Unloaded Vehicle on an Exit Ramp

While the loaded vehicle on the exit ramp is predominantly a test of rollover control, the unloaded vehicle on the exit ramp is generally more demanding on yaw control, particularly for low friction cases. The controller objective was to mitigate both intra-vehicle instability (jackknife or swing-out) and total vehicle stability such as off tracking (as shown in the example in Figure 3-43). As drivers are typically much more concerned about jackknife or swing-out accidents, the ESC system was tuned to prevent these at the cost of path following deviations.

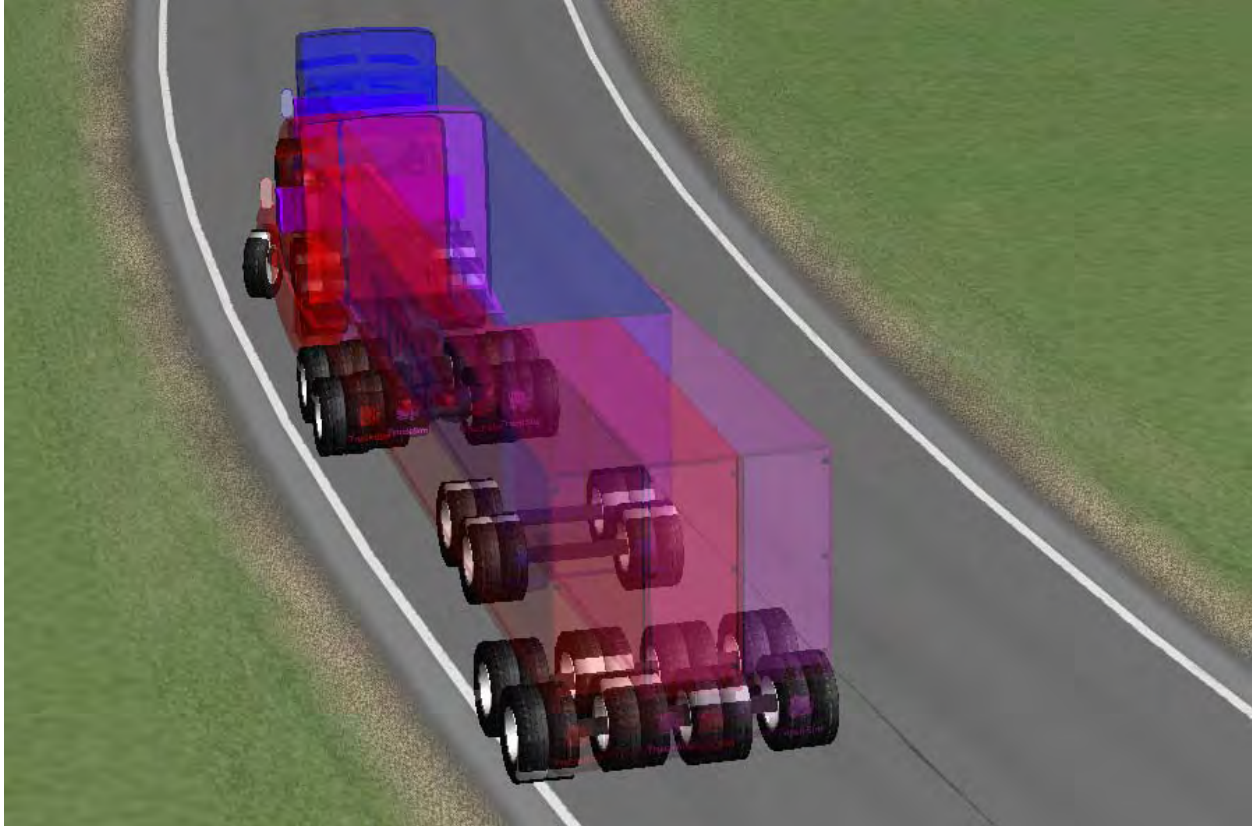


Figure 3-43. Animation still. Exit ramp – unloaded vehicle – yaw illustration ($\mu = 0.5$).

With an unloaded vehicle, there was little risk of a rollover. However, the relatively high CG of the empty tank truck did produce enough trailer roll to activate the ESC system in roll for the dry ($\mu = 0.85$) and damp ($\mu = 0.75$) cases. This caused a confounding activation of the left drive axle and trailer brakes (Figure 3-45), which resulted in the pneumatic ESC system having a relatively large tracking error (Figure 3-44). However, the pneumatic ESC system's performance was still better than the base vehicle's performance.

For the low friction cases ($\mu = 0.5, 0.25$), the pneumatic brake system produced significant path tracking errors (Figure 3-44) as the brakes engaged and remained engaged for long periods of time (Figure 3-45). With the brakes engaged, the lateral traction potential was limited and the trailer tracking error increased. The offtracking errors were not seen in the ECBS and ESC system, as the ECBS could cycle the brakes quickly enough to allow the trailer axles to generate lateral force and mitigate loss of lateral tracking.

Figure 3-44 also contains the driver steering demand during the maneuver. This was included to show how the driver tried to maintain vehicle path as the ESC systems managed yaw instability. Here it was noted that the ESC plus ECBS system resulted in lower driver corrections and the vehicle's stability was better than the pneumatic ESC system. The faster brake actuation (Figure 3-45) produced smaller path deviations, which meant that the driver needed a smaller steering correction. Thus the ECBS makes the vehicle safer and easier to drive.

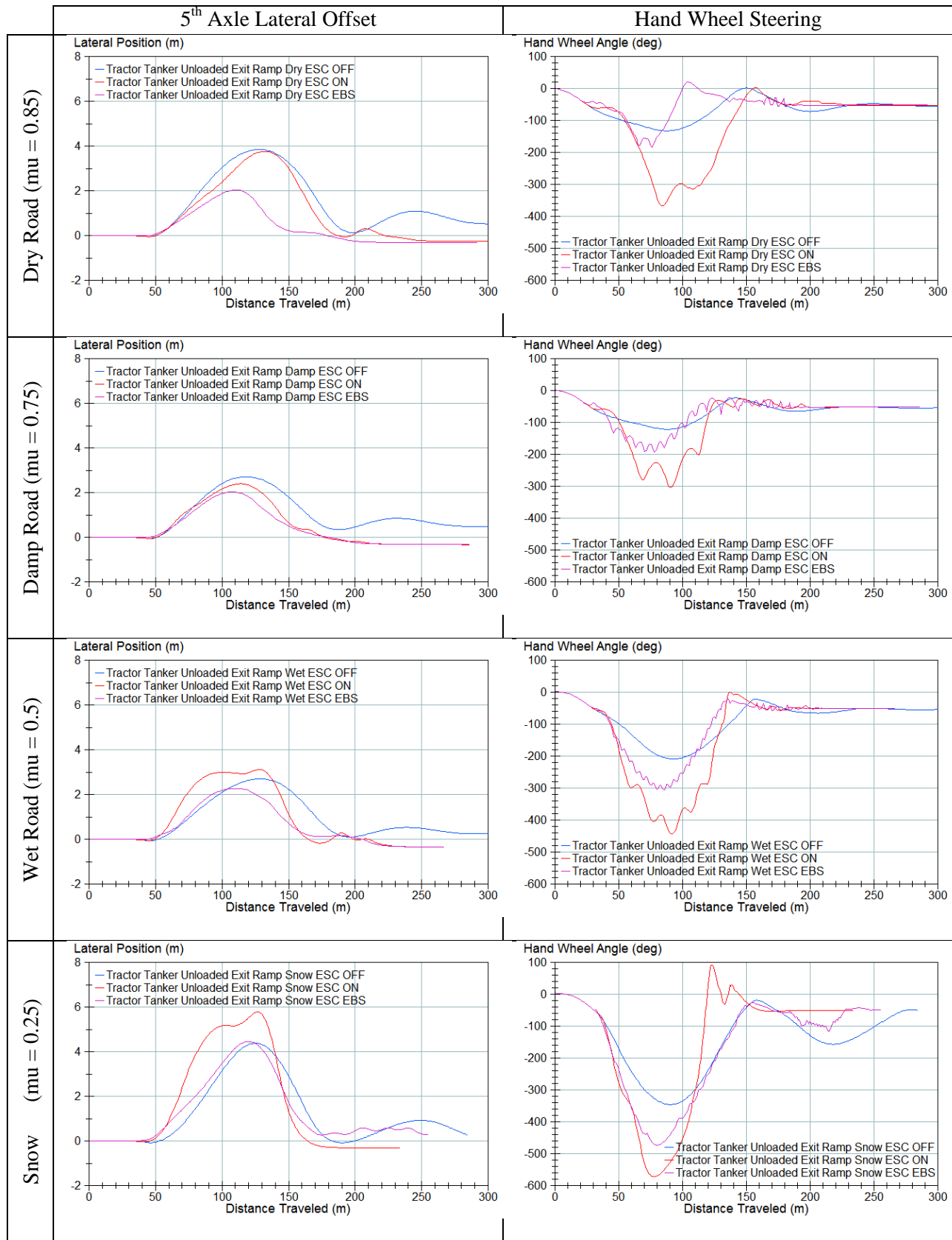


Figure 3-44. Plots. Exit ramp – unloaded vehicle – tracking error and steering demand.

Note: Only the left rear drive and left rear trailer brakes are presented for clarity. All trailer wheels see the same brake command, so showing only one trailer wheel is sufficient. Additionally the maneuver (exit ramp) primarily uses the left side drive axle for heading control (yaw reduction) and both left drive wheels see the same command. This simplification makes it easier to observe the differences among the three control cases.

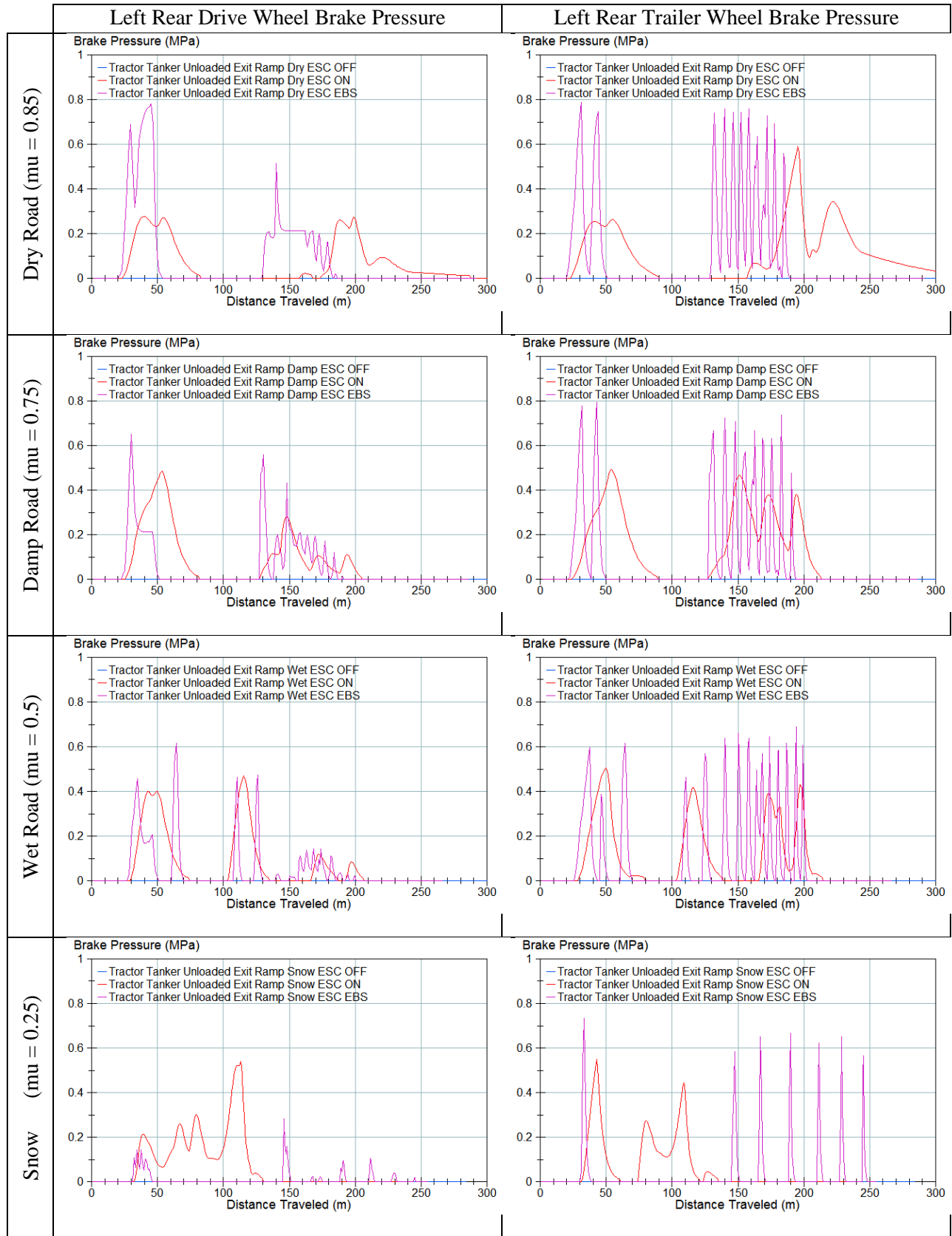


Figure 3-45. Plots. Exit ramp – unloaded vehicle – brake pressures.

This ESC system could not handle the cases with low friction. While algorithm tuning is a factor in the poor performance, the key reason for the poor performance was that traction was insufficient to slow the vehicle and maintain vehicle heading and orientation (Figure 3-46). The better performance of the ECBS brake system (fast, short pulses in Figure 3-45) resulted in lower trailer side slip and better performance, relative to pneumatic brakes, but it was still not significantly different from the base vehicle.

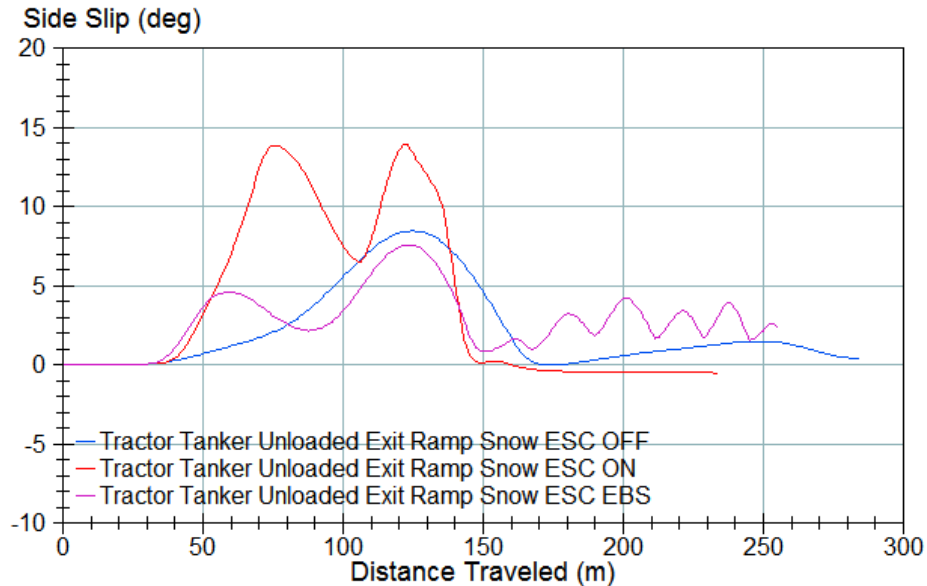


Figure 3-46. Plot. Exit ramp – unloaded vehicle – trailer side slip ($\mu = 0.25$).

3.4.5 Loaded Vehicle in a Lane Change

The loaded vehicle in a lane change maneuver (Figure 3-47) was a demanding test for the ESC system. As is typical, roll stability due to untripped rollover was a greater concern at higher road friction levels, and lateral tracking was the greater concern with less friction (Figure 3-48).

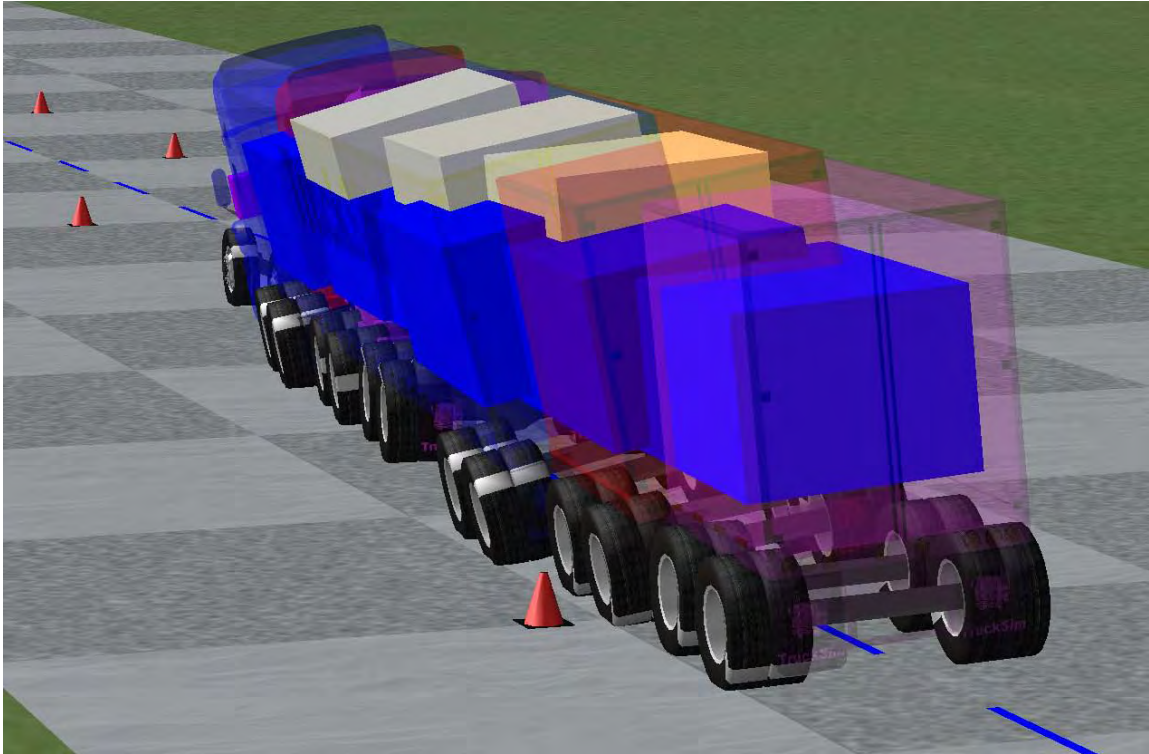


Figure 3-47. Animation still. Lane change – loaded vehicle – roll illustration ($\mu = 0.85$).

Both the pneumatic and electronic ESC systems were able to improve roll stability (1% for the pneumatic and 6% for the ECBS) as shown in Figure 3-48. The significant advantage for the ECBS ESC system comes from the fact that the ECBS system could slow the vehicle more quickly (Figure 3-49), as the brakes could be actuated more quickly. This is especially evident in the trailer brake pressures (Figure 3-50).

The ESC systems also improved offtracking of the trailer for higher μ situations as well, though this was primarily a function of the lower final speed of the vehicle.

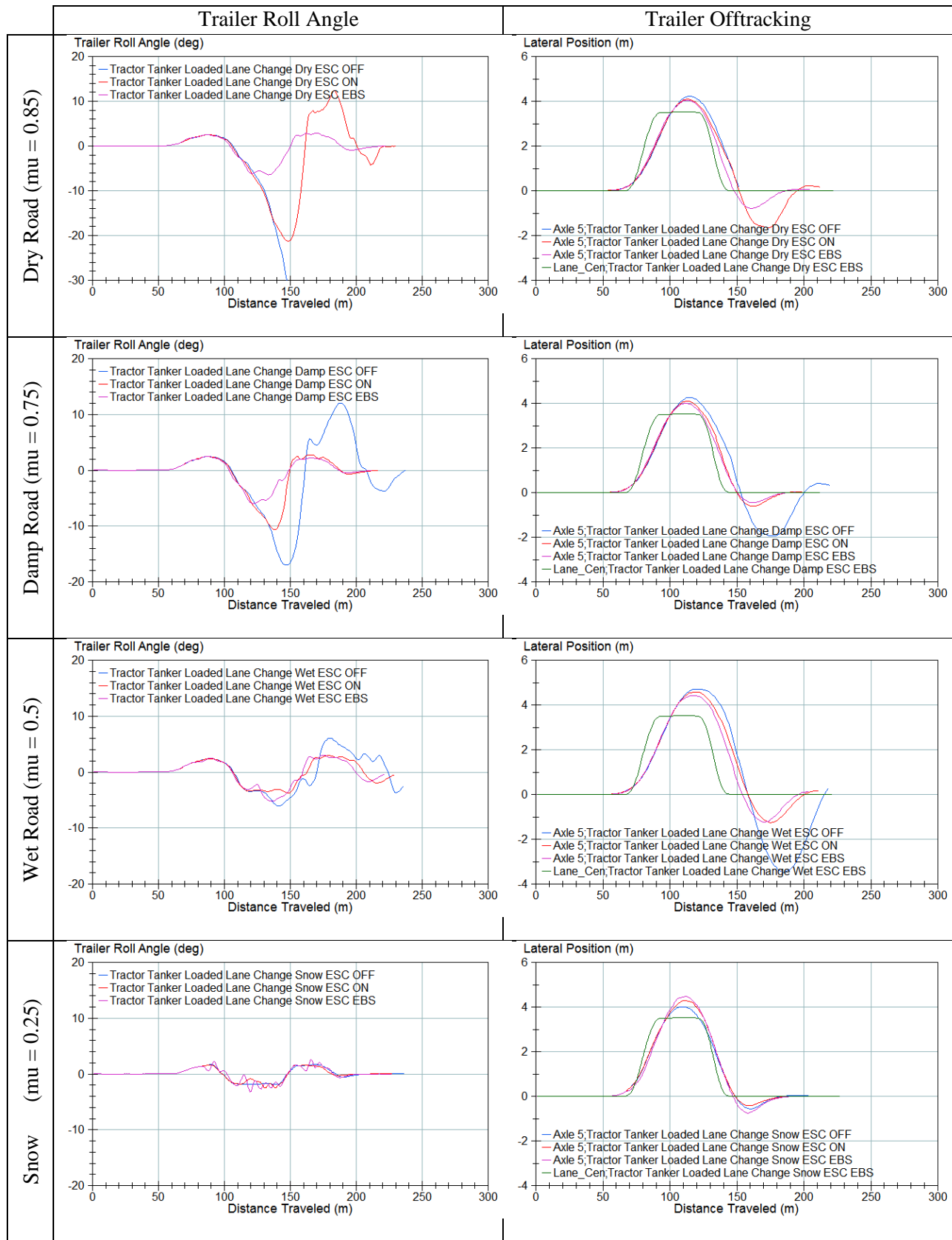


Figure 3-48. Plots. Lane change – loaded vehicle – roll and tracking errors.

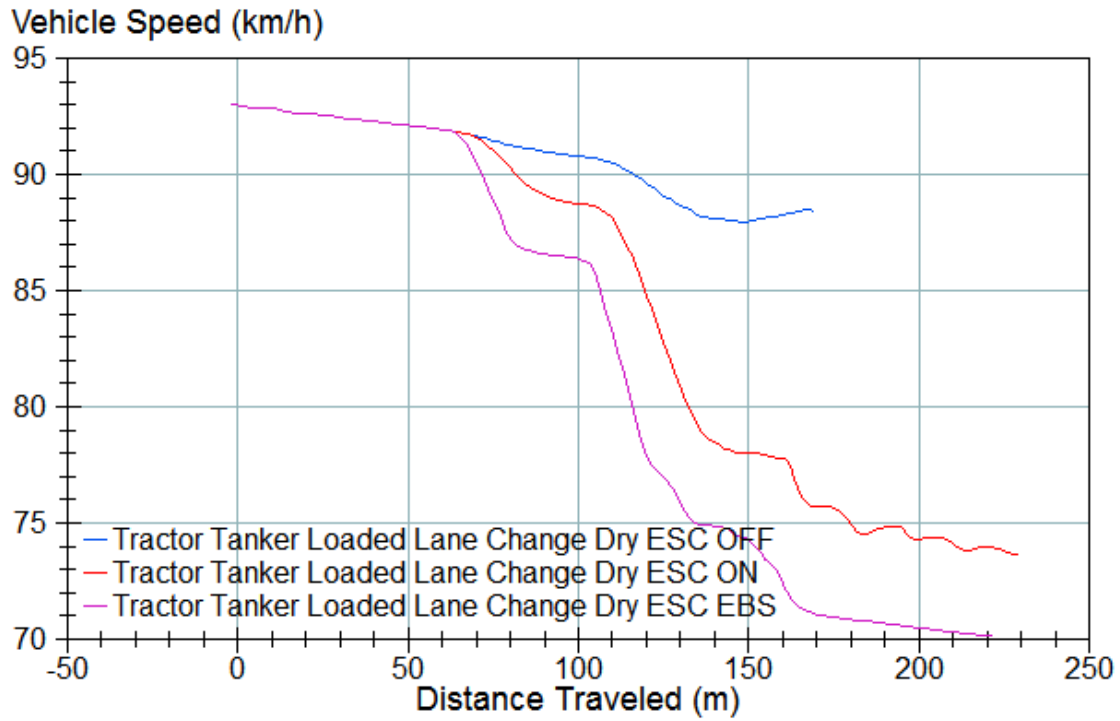


Figure 3-49. Plot. Lane change – loaded vehicle – vehicle speed ($\mu = 0.85$).

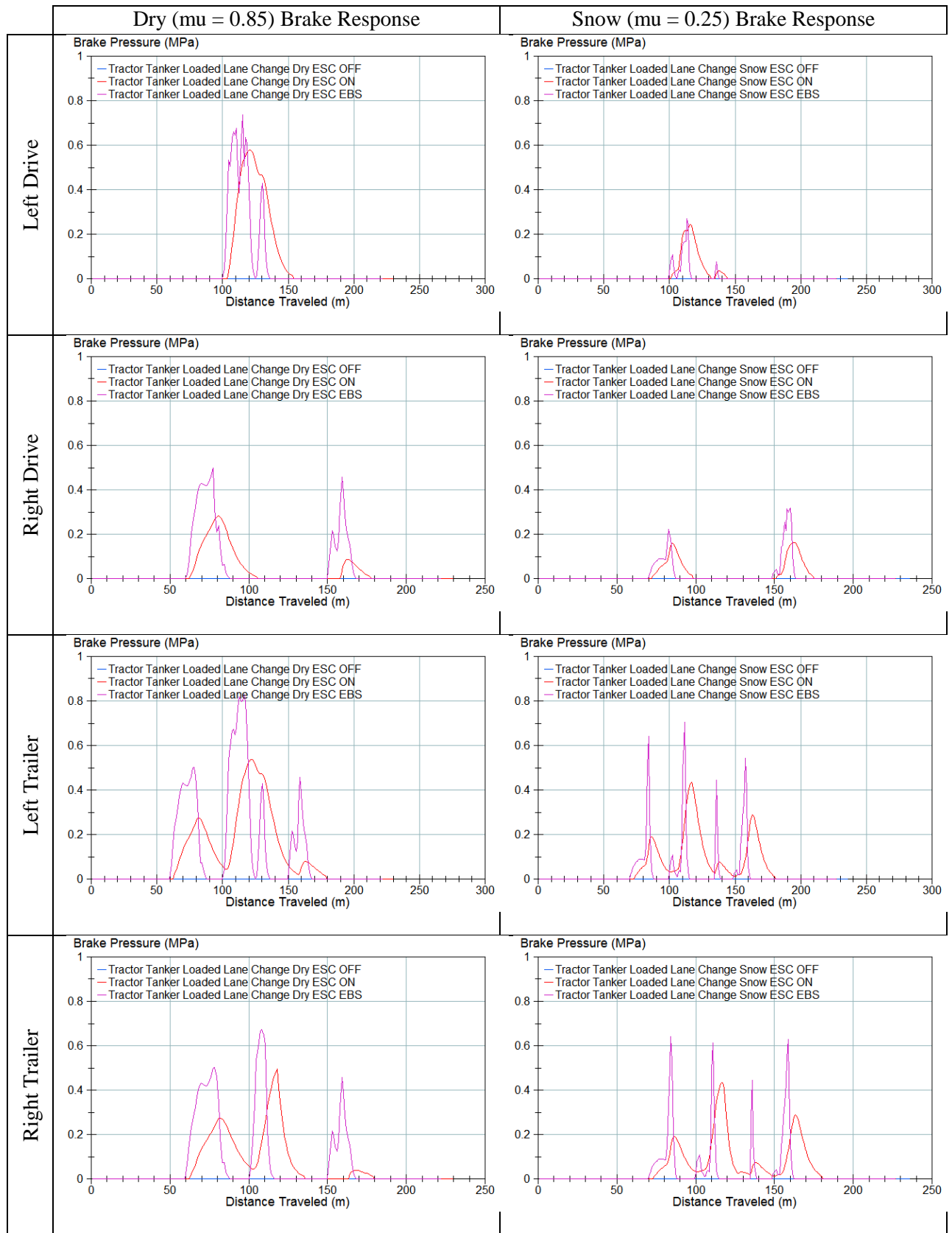


Figure 3-50. Plot. Lane change – loaded vehicle – brake pressures.

While the ESC improved vehicle performance in wet and dry conditions, the ESC systems did not appreciably improve stability in snow. The lack of traction on the 0.25 μ surface resulted in very low speeds, which produced low lateral accelerations and almost no roll, and which meant that no roll correction was needed. The low traction level also limited offtracking correction, resulting in very little value for the system in snow. This is essentially the same issue noted in the loaded exit ramp maneuver. The solution may be for the ESC system to deactivate much like ABS systems deactivate at low speed when they are counterproductive.

3.4.6 Unloaded Vehicle in a Lane Change

The final maneuver evaluated was the empty vehicle lane change (Figure 3-51). As with the previous simulation cases, the ESC algorithm performed well in dry and wet conditions (Figure 3-52). The ESC plus ECBS system also improved vehicle performance in snow ($\mu = 0.25$), albeit only slightly.

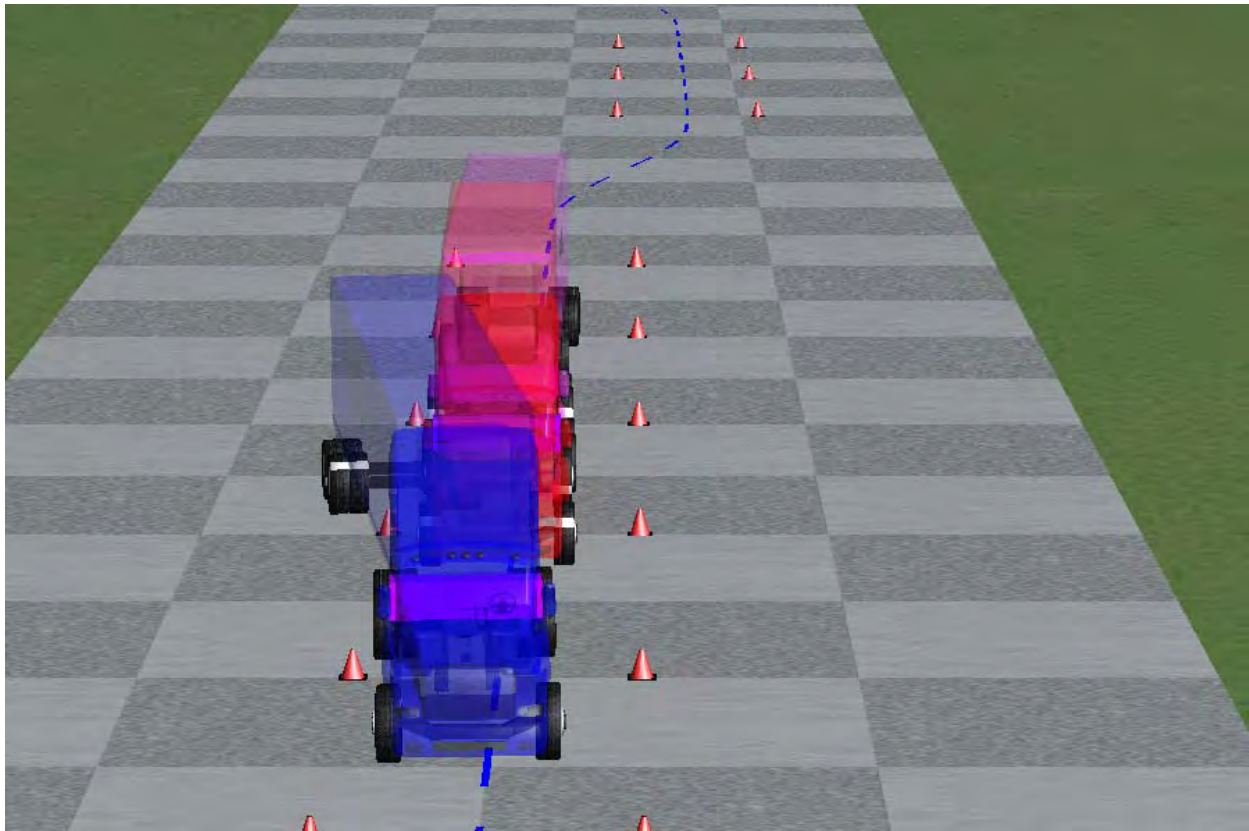


Figure 3-51. Animation still. Lane change – unloaded vehicle – yaw illustration ($\mu = 0.85$).

Figure 3-52 shows that when there is sufficient traction, both ESC systems can reduce the swing-out of the trailer. Only when the surface traction is low does the pneumatic ESC system begin to fail, as the brake pressure cannot be modulated fast enough to maintain lateral stability (Figure 3-53). In particular, note the left drive brake demand in snow. For the pneumatic ESC system, the command to activate the brakes and then release is so quick that the brake pressure never builds at the wheel, as the delays consume the entire command.

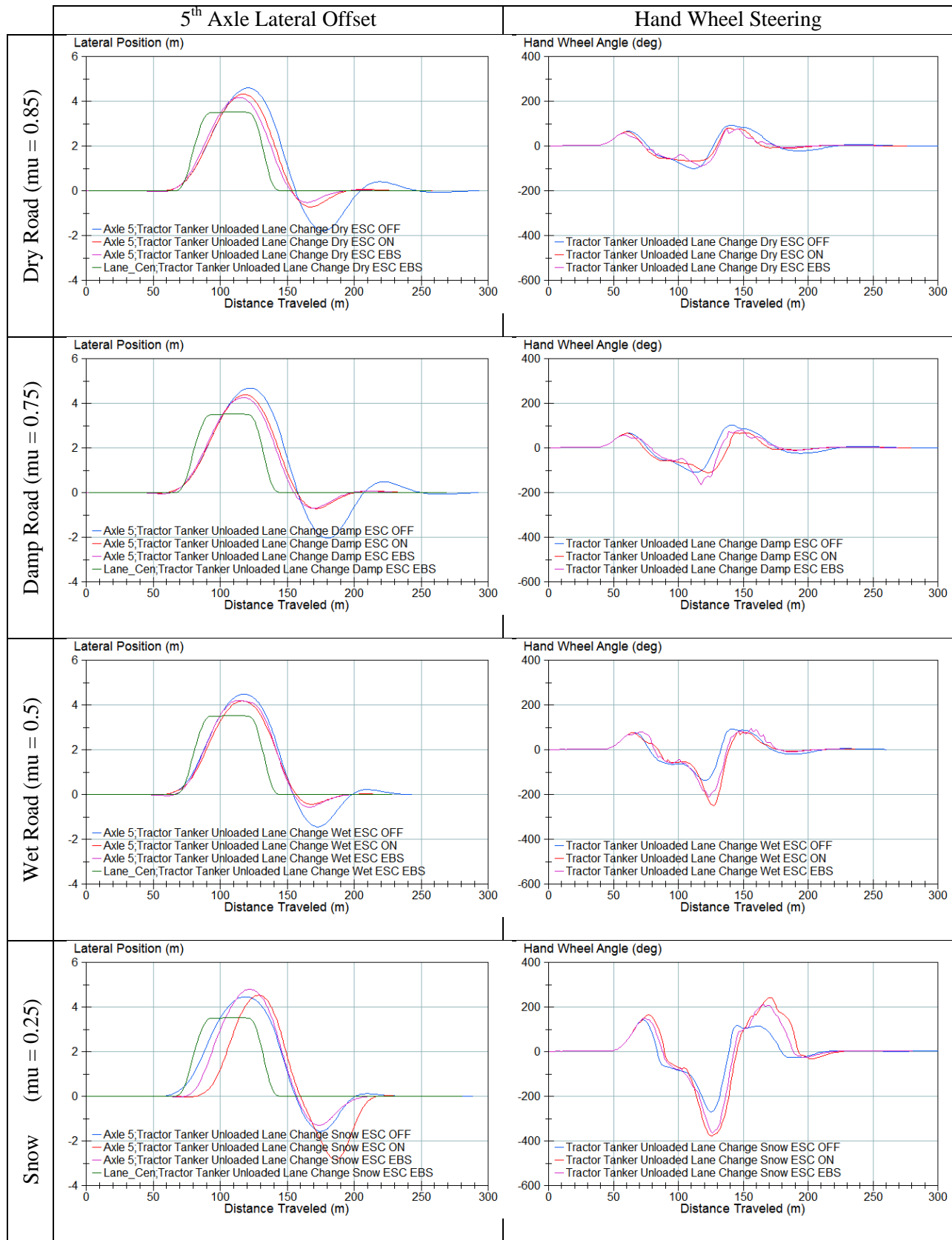


Figure 3-52. Plots. Lane change – unloaded vehicle – tracking error and steering demand.

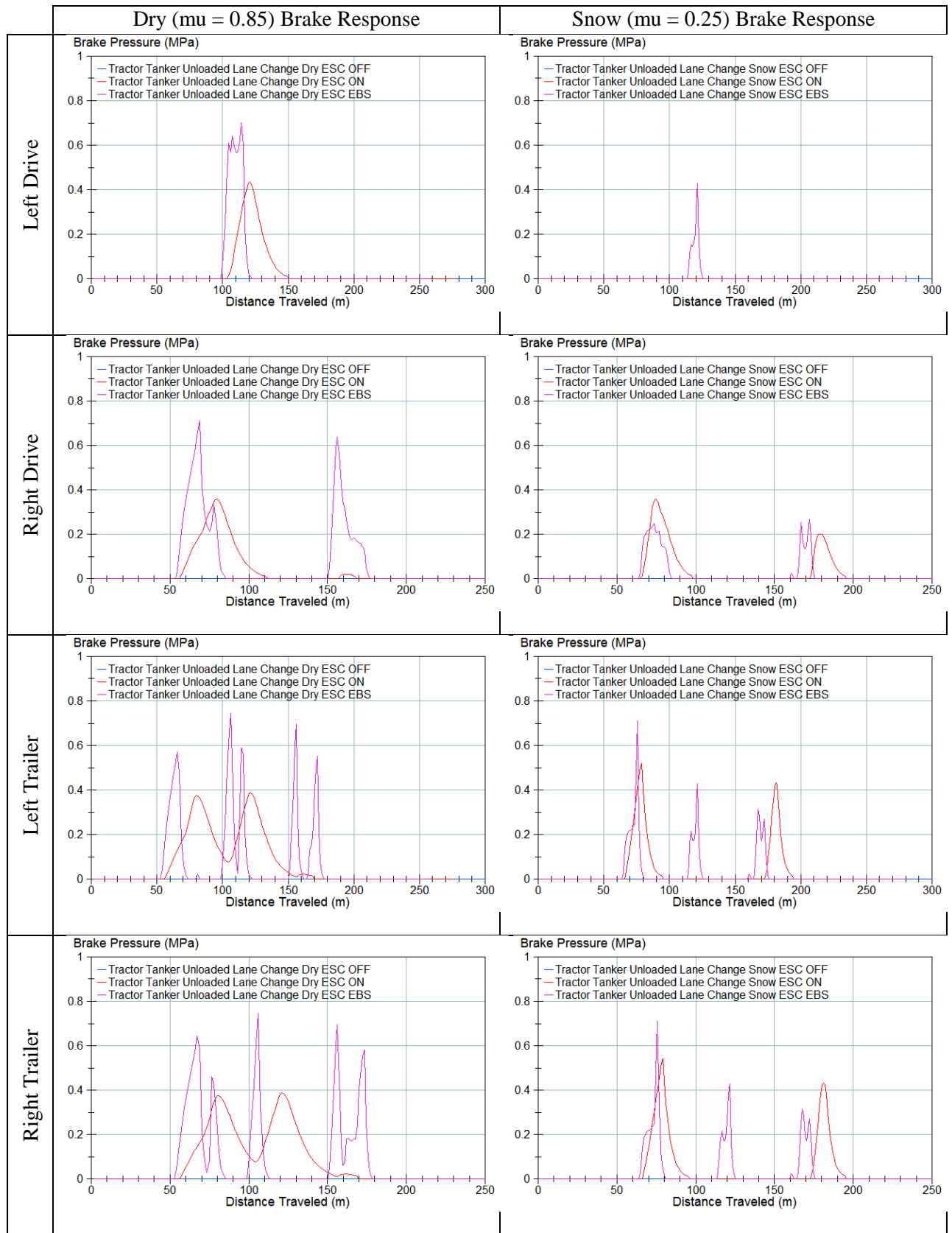


Figure 3-53. Plots. Lane change – unloaded vehicle – brake pressure.

In addition to improving the lane holding of the vehicle, the tractor and trailer side slip angles were also improved with the ESC systems, as shown in Figure 3-54. This makes the vehicle feel more secure and gives the driver more confidence in the vehicle. The only case where the side slip angles increase with ESC was for the trailer in snow, as the trailer struggled to maintain the deceleration and lateral traction balance.

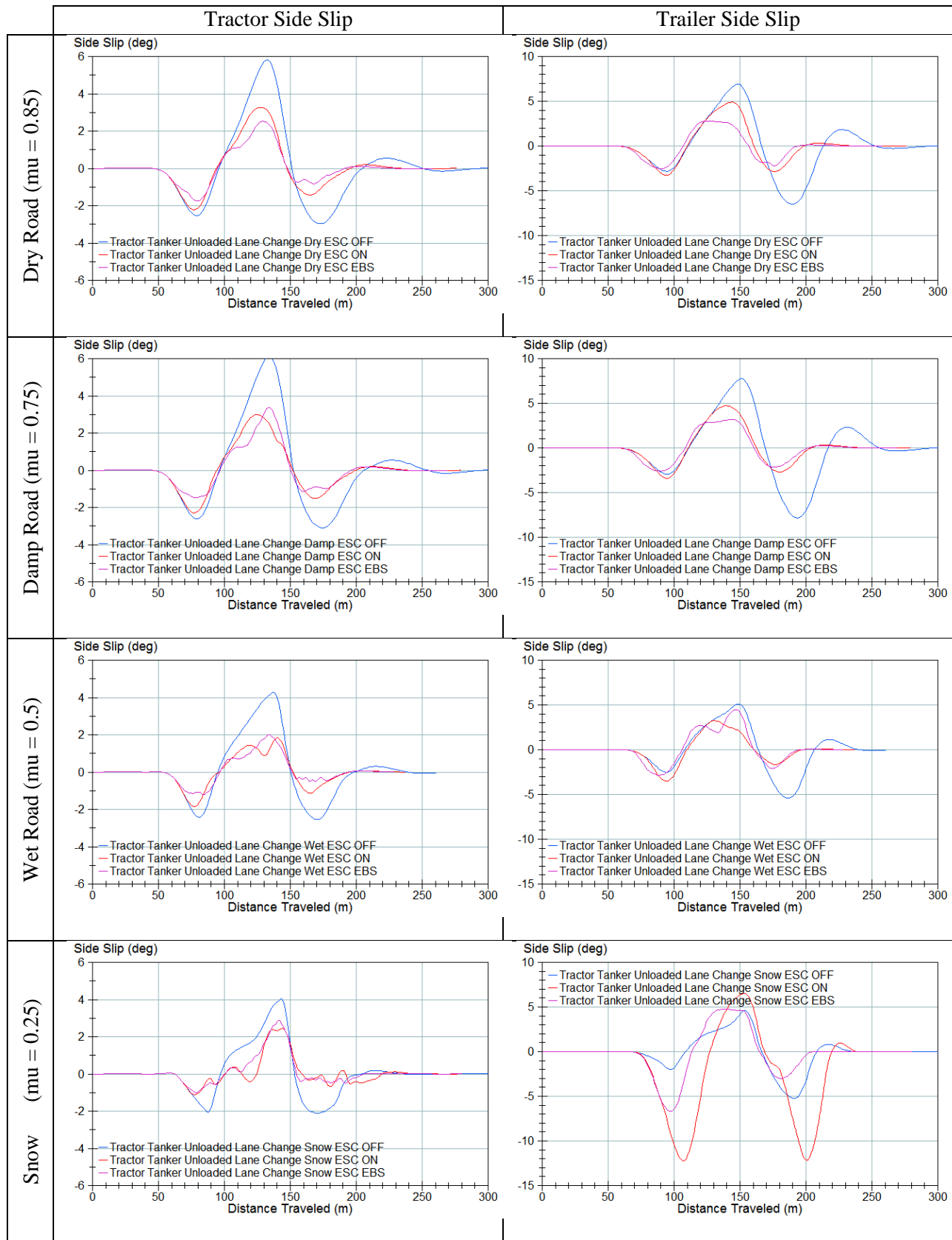


Figure 3-54. Plots. Lane change – unloaded vehicle – side slip angles.

3.5 Critical Control Issues

In many cases, it is possible to introduce instability through application of the brakes even when the goal is to improve stability. Several examples of this have been documented in the analysis above, such as increasing lateral path divergence to maintain roll stability and increasing path divergence to control jackknife and swing-out instability. The vast majority of the control tuning developed for this model was spent on managing these trade-offs. The following is a summary of the more significant issues.

3.5.1 Brake Response Time

As shown in section 3.4.4, the response of the ESC system in a low friction environment can result in a poorer system response than the conventional vehicle. The limitations of the pneumatic ESC system in low friction environments are also seen in section 3.3.4, where the ECBS system had significantly reduced stopping distances for both loaded and unloaded configurations (Table 3-1 and Table 3-2). The analysis indicates that it is simply not possible to control wheel speed precisely enough to maintain both lateral and longitudinal traction in low friction environments with the transport delays of existing pneumatic brake systems.

3.5.2 Proportioning of Drive and Trailer Brakes

As drivers often fear a jackknife or trailer swing-out accident more than a head on collision (Section 2.2.2), a priority of the ESC system was to ensure that stable intra-vehicle dynamics were maintained. To aid in maintaining tractor to trailer stability, a block was added to the controller to make sure that the drive axles were never exposed to a braking force greater than the trailers when the ESC system attempted to mitigate rollover (Figure 3-55).

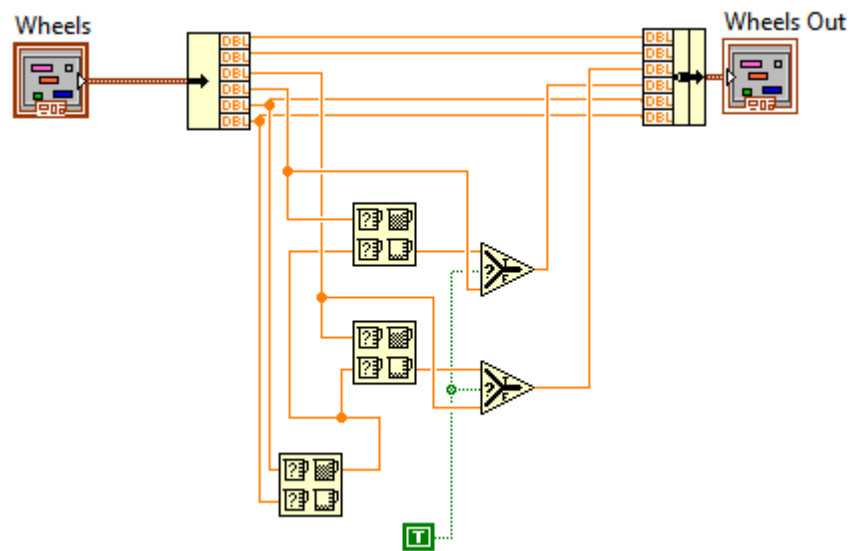


Figure 3-55. Diagram. Drive axle brake limiter.

Braking the drive axles can result in the trailer pushing the tractor. If the trailer is not aligned with the tractor, the result can be similar to an inverted pendulum where the base (tractor) is not moving forward as quickly as the pendulum (trailer) and the trailer pivots around the tractor. The method used to limit the drive brake force in this model is admittedly rather crude and has the negative effect of limiting the yaw controller's efforts to enhance tractor rotation in an understeer situation. But the simulation cases here did not require much yaw enhancement, and the method worked well enough to demonstrate the need for tractor to trailer brake balancing.

To show the consequences of not balancing the brakes, the loaded vehicle on the exit ramp was evaluated without the drive axle limiter on a wet ($\mu = 0.5$) road (Figure 3-56). The green truck, which was exposed to maximum drive axle brake pressures (Figure 3-57), experienced a large articulation angle and nearly jackknifed. Figure 3-58 shows the side slip angles of the tractor and trailer. As the tractor is the unit with the large side slips, the tractor, and not the trailer, is yawing too much. Thus the event is a jackknife event and not the trailer's failure to turn with the vehicle. For the example case presented here, the drive axle pressure was approximately double the trailer brake pressure (Figure 3-57).

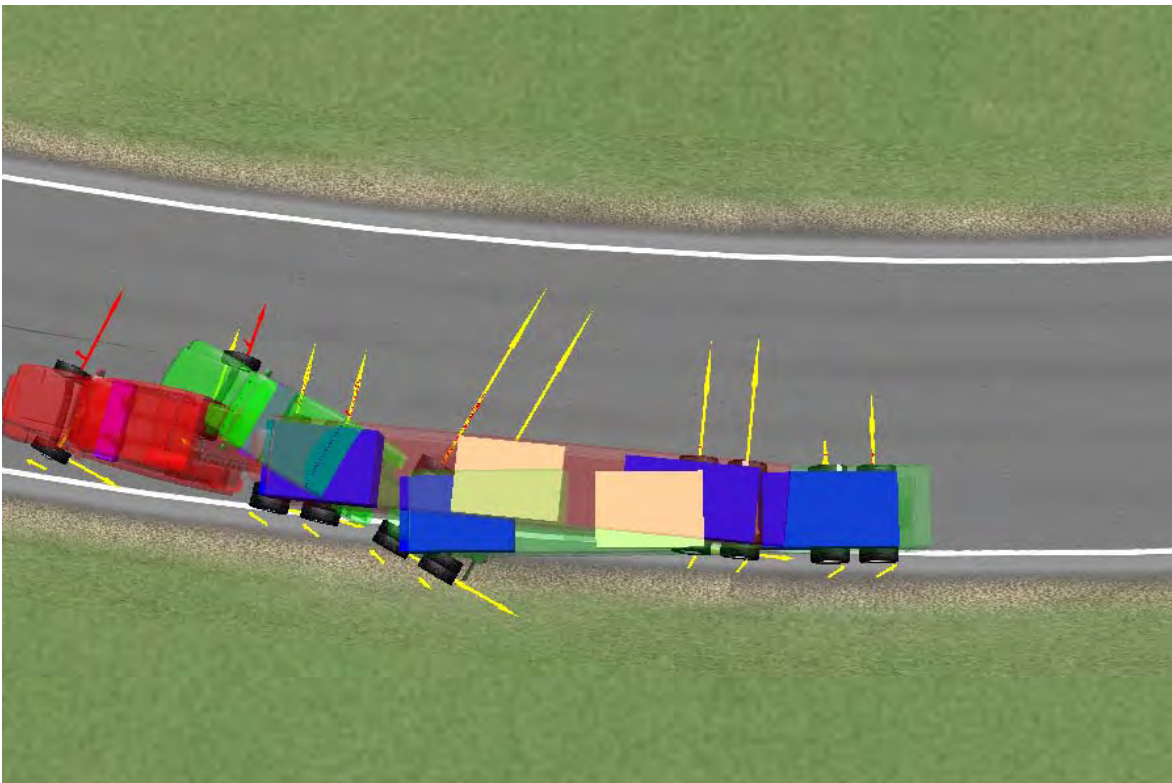


Figure 3-56. Animation Still. Jackknife at the drive axle, induced by braking.

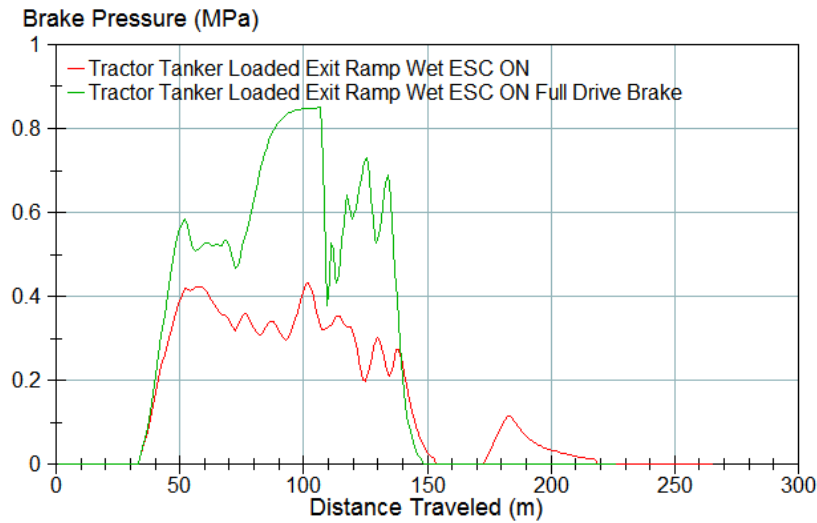


Figure 3-57. Plot. Exit ramp – loaded vehicle – drive axle brake pressure ($\mu = 0.5$).

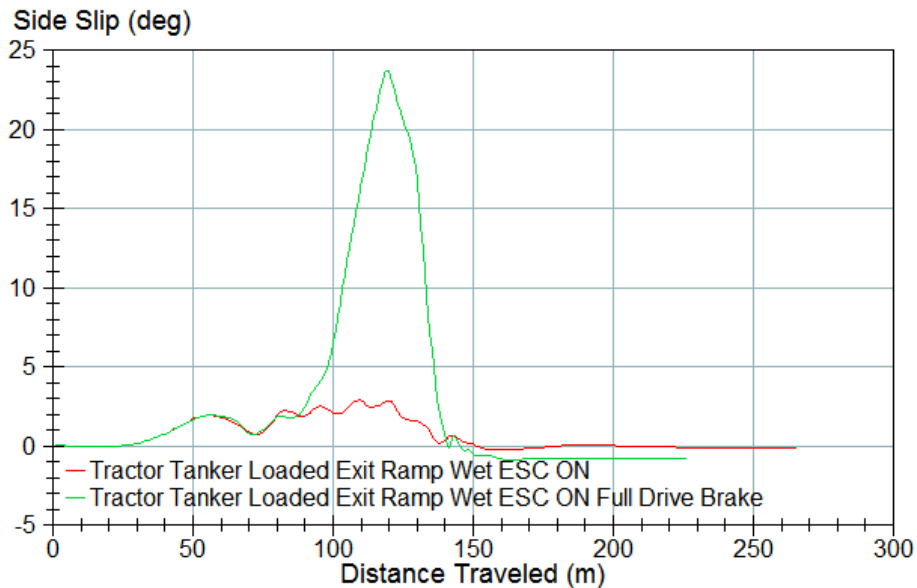


Figure 3-58. Plot. Exit ramp – loaded vehicle – tractor side slip ($\mu = 0.5$).

3.5.3 Pulsing of Trailer Brakes to Manage Swing-out

The ESC controller developed in this exercise placed roll control as the primary stability requirement. However, absolute focus on roll stability was not always the best approach and, paradoxically, could lead to some roll stability issues. To illustrate this point, a simulation was run without the stability check for brake induced vehicle yaw deviation. For the loaded exit ramp case on a wet road, the ESC system intervened quickly to slow the vehicle (Figure 3-59). But as the brake pressure increased, the wheel speeds decreased (Figure 3-60), which reduced the lateral force potential of the trailer.

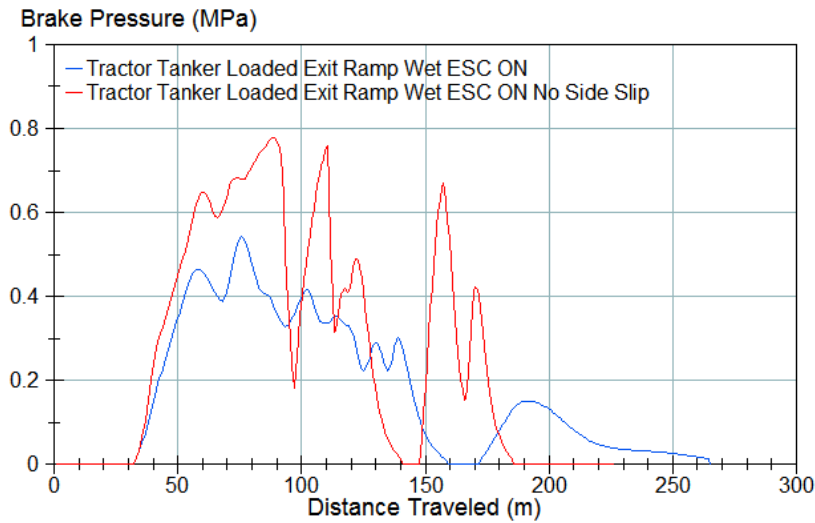


Figure 3-59. Plot. Exit ramp – loaded vehicle – trailer brake pressure – side slip control illustration ($\mu = 0.5$).

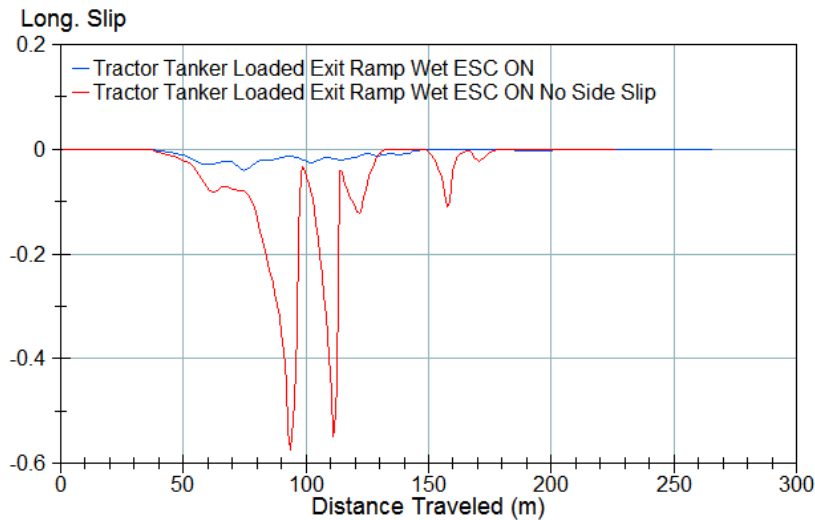


Figure 3-60. Plot. Exit ramp – loaded vehicle – trailer wheel speed – side slip control wheel speed ($\mu = 0.5$).

The reduction in lateral force produced very large side slip angles (Figure 3-61). When the brakes were released (100 meters into the maneuver), the lateral force suddenly built up, resulting in a near rollover of the trailer (Figure 3-62). Thus, while roll stability was the primary concern, there was a limit to the priority such that instability was not introduced as a consequence of overly aggressive actions to mitigate rollover.

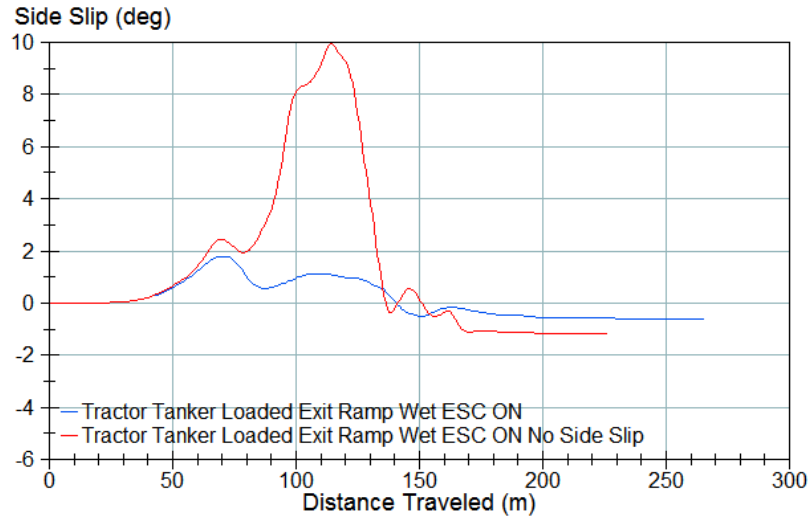


Figure 3-61. Plot. Exit ramp – loaded vehicle – trailer side slip – side slip control wheel speed ($\mu = 0.5$).

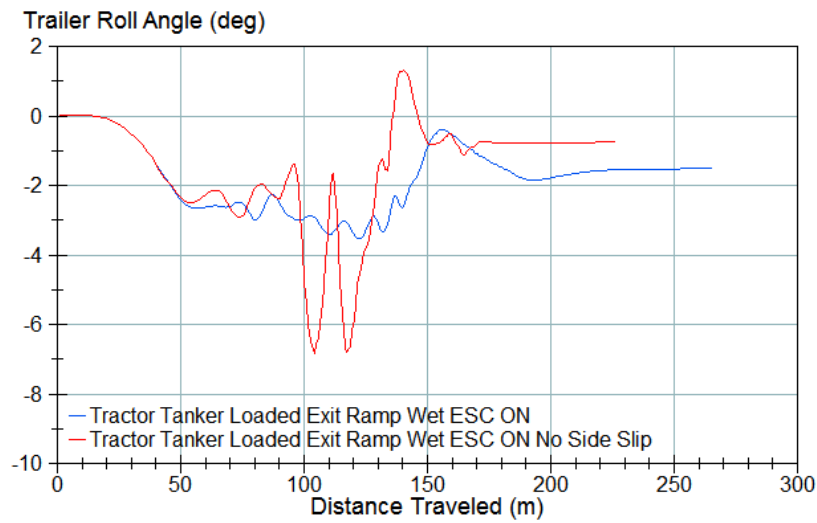


Figure 3-62. Plot. Exit ramp – loaded vehicle – trailer roll – side slip control wheel speed ($\mu = 0.5$).

3.6 Conclusions

The purpose for developing the stability controller presented here was threefold:

- Determine stability priorities between the tractor and trailer, as well as yaw vs. roll stability limitations and how the differing stability requirements for the differing units interacted
- Assess the potential benefits of ESC
- Determine what effect electronic controlled brakes might have

The results confirmed the initial assumptions on commercial vehicle stability and indicate that significant work will be needed to develop an optimal ESC system for class 8 vehicles.

3.6.1 Relative Effectiveness of Air and ECBS in Braking

The straight line stopping performance (section 3.3.4) indicated a significant advantage for the ECBS system, particularly for low friction conditions. By minimizing the brake command transport delays, the wheels could be controlled in a much tighter slip ratio range and the wheels could be braked and released much more quickly. Both of these attributes allowed the tires to operate in their peak traction region. For low friction cases, where lower brake pressures are required to lock a wheel, this was even more important, as the ESC system tried to maintain the optimal brake pressure on the wheels.

3.6.2 Tuning the Electronic Stability Controller

From the results in Section 3.4, it is clear that ESC systems can improve the dynamic performance of commercial vehicles. However, they provide only a relatively small stability margin and cannot invalidate the laws of physics. If the vehicle's inertia is greater than the restorative potential of the ESC system, the vehicle will still crash.

While an ESC system cannot prevent all crashes, it was shown that the ESC system could choose the less severe crash type based on algorithm design (jackknife is better than rollover, path divergence is better than jackknife, etc.). It was also shown that lower μ surfaces were more sensitive to controller intervention. Finally, as with the straight braking analysis, better wheel control through electronic controlled brakes improved the stability of the vehicle in all cases.

It should also be noted that the controller algorithm was not re-tuned for the ECBS model. The same stability intervention criteria and methods were used for both the pneumatic and ECBS systems. Re-tuning the ESC algorithm for the ECBS system would, in all probability, have resulted in even better performance of the ESC plus ECBS system. This was not done so that the effect of the brake change alone was more apparent.

3.6.3 Future work

The most significant limitation of the stability controller developed here was that stability modes were not evaluated simultaneously, but rather in a sequential, tiered structure. Some of the compromises, such as limiting tractor brakes to avoid a jackknife, might be eliminated if the entire vehicle's stability could be assessed as a whole.

Migrating to a controller that captures the yaw and roll stability of each unit and integrates the stability of each unit into a cohesive control strategy would be much easier with a single set of equations describing the motion of the complete vehicle. This remains as one of the key points that needs to be addressed in future work.

3.6.4 Discussion on Extension to Multi-Trailer Vehicles

The need to develop a better method to assess the entire vehicle's stability will become even more important when additional units are added. As shown here, the stability of one unit affects the stability of the other unit, and any attempts to improve stability of one unit also affect the other unit. The issues associated with unit-to-unit interaction will increase as additional units are added. At the same time, the management of the vehicle's stability becomes more important as more units are added, bringing more potential instability sources.

The recommendation for further work is to expand the model's linearized reference vehicle by defining the equations of motion to include multiple trailers and then to develop a weighting system whereby the stability of each unit is captured and weighed against the other units to determine the optimal controller response.

This Page Intentionally Left Blank.

Chapter 4 – Sensors and Protocols

The purpose of this section was to develop a hardware bench test system to implement the ESC algorithms discussed in Chapter 3, for later installation on a vehicle. The major tasks were:

- The selection of measurement sensors
- The implementation of sensor-to-controller communication
- The implementation of controller-to-controller communication.

The goal was to develop the methodology required to collect the needed vehicle state information, to transmit input information to the ESC system, and then transmit ESC output commands to the brake actuators. Additionally this effort considered the extension of the ESC strategies to LCVs. The research concluded with the development of a hardware bench test system that could validate a development controller for implementation on a vehicle for testing ESC algorithms. The hardware bench test system included sensors, controllers, and actuators. Communication protocols and hardware connections were assembled. This phase did not include the instrumentation of a complete vehicle control system but rather the development of the technologies and concepts needed to do so.

As shown in Figure 4-1, the hardware bench test system consisted of three major components. First, the development controller included computer processors, analog-to-digital input and digital-to-analog output converters, and networking hardware to implement and test control algorithms such as those developed in the previous chapter. The second major component was a stationary mockup of the air brake system on a tractor and semitrailer, consisting of the brake actuators that would affect braking control on an actual vehicle. The third major component was a set of sensors used to provide information to the development controller about the vehicle dynamic state. The purpose of the hardware bench test system was to demonstrate that the development controller could receive information about the vehicle's dynamic state from all the available sensors located anywhere on the tractor or trailer, process the information in real time, and generate the output signals to power and control the actuators affecting vehicle dynamics. Because the development controller could consist of several CPUs, and sensors could reside on several different networks on the vehicle, the integration of the ESC system is not a trivial task, and the hardware bench test system serves the role of an integration validation tool.

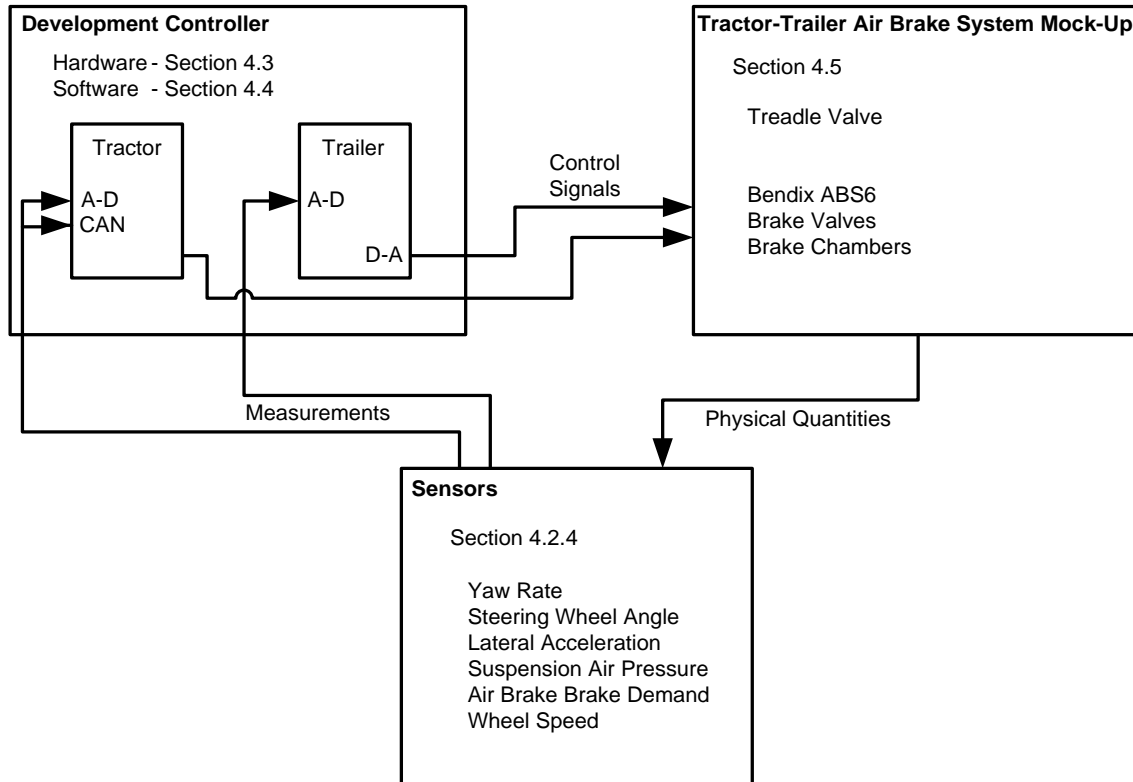


Figure 4-1. Diagram. The hardware bench test system.

4.1 Test and Demonstration Plan

The approach consisted of four steps:

- Specification and acquisition of system-under-test components, sensors and controller design, and development tools
- System-under-test and controller system assembly
- System functional test
- System performance tests.

As of this writing, the system has been assembled and the functional and performance tests are pending.

4.1.1 Braking System

ABS-6 is the name Bendix gives to its advanced brake control system. This system “provides core antilock braking, along with Bendix Smart ATC (its brand of automatic traction control) and ESP (covering understeer, oversteer, and rollover situations)” (Bendix Commercial Vehicle Systems LLC 2006).

The ABS-6 includes the electronic control unit (the Bendix ECU), air pressure sensors, an integrated yaw rate sensor and accelerometer, a steering wheel angle sensor and six wheel speed sensors (two for the front axle and four for the tandem rear axle of the tractor). Since ABS-6 controls an air brake system, it also includes the traction relay valves, the ABS modulator valves, brake chambers, and air lines that are typical of air brake installations on a commercial vehicle.

The ABS-6 system provides sensors only for the tractor, as it is a tractor-based ABS. Additional sensors were provided for the trailer to measure yaw rate, acceleration, and air reservoir pressure.

4.1.2 Sensors

The selection of sensors for the hardware bench test system was based on the vehicle configuration and required measurements implied in Section 3.2.2 and shown in Table 4-1.

Table 4-1. Sensor requirements and specifications.

Parameter	Measurement	Resolution
Steering Wheel Angle	-180 deg to + 180 deg	+/- 1 deg
Sideslip Angle	-15 deg to + 15 deg	+/- 0.3 deg
Lateral Velocity	-15 m/s to + 15 m/s	+/- 0.15 m/s
Longitudinal Velocity	0 m/s to 50 m/s	+/- 0.5 m/s
Yaw Velocity	-50 deg/s to +50 deg/s	+/- 0.5 deg/s
Roll Angle	-15 deg to + 15 deg	+/- 0.15 deg

Practical sensor selection requires the consideration of tradeoffs between performance and cost. Because information about the ESC system needs is insufficient and tradeoffs between performance and cost cannot yet be measured, the sensors selected should be considered as acceptable for performance requirements.

The hardware bench test system was implemented in conjunction with an installation of the Bendix ABS-6 ESC system. The ABS-6 system uses a proprietary ECU that is communicating with a set of sensors and actuators on the vehicle. The hardware bench test system used the sensor information from the Bendix ABS-6 system to fulfill part of the sensor requirements for this task. This methodology was a test of the ability to piggy-back onto an existing ABS system pre-installed on a tractor-semitrailer vehicle.

4.1.3 Communication Networks

A variety of sensor-to-controller communication methods were tested. Several sensors used the CAN-bus protocol to communicate with the controller, while the output of several other sensors was read directly by the controller using ADCs. For details, see Sections 4.2.5 and 4.3.1.

Two methods were used for communicating between the tractor development controller and the trailer development controller. The first was a high-speed 32-bit VME-bus-based network architecture, which NI calls “MXI,” and the second was conventional Ethernet.

The VME-bus standard is a computer bus standard that was first developed by Motorola for its popular 68000 line of microprocessors. It has since become widely used for many computer processor interface applications and has become the dominant technology for backplane development (NI Developer Zone - National Instruments 2011d).

MXI interconnects multiple devices using a flexible cabling method similar to GPIB (the IEEE-488 Standard Digital Interface for Programmable Instrumentation), but uses a hardware memory-mapped communication scheme that eliminates software overhead, providing for fast and real-time control systems where the tractor and trailer control units must be synchronized. Thus far, MXI has not been applied on production vehicles. The MXI Interface is described in detail in the discussion of networking in Section 4.5.1.

Although MXI is fast and flexible, its use implies a centralized control architecture, with one CPU controlling the entire combination vehicle, since MXI essentially makes all PXI chassis a slave to the one with the CPU. The merits of centralized control versus distributed control on a combination vehicle is a topic of research. In order to be able to investigate the performance of both options, an Ethernet network was used to allow multiple development controllers distributed across the combination vehicle.

Ethernet is the familiar computer networking technology introduced in the 1980s to manage local area networks of computers. Standardized by IEEE 802.3, Ethernet is a protocol governing how data is placed on and retrieved from a common transmission medium. Because Ethernet does not imply any hardware specification related to computer memory or the CPU, it relies on software overhead to manage data transfer in a control system application.

4.1.4 Functional Testing

Functional testing of the hardware bench test system verified that the implementation provides the required operations. The development controllers on the tractor and semitrailer needed to communicate with each other. The communication needed to be synchronous so that the performance was well determined. Data was transferred between them with a global time stamp. The development controllers need to control their respective brake systems in real time.

4.2 Vehicle System Hardware

A hardware bench test system was designed and built for the above tests. The bench test system consisted of a framework for holding the system-under-test, the development controllers, and accessories such as power supplies and electric cabling. The system-under-test is discussed below. This discussion breaks the system up according to the following technologies:

(1) Braking System, (2) Pneumatic Components, (3) Electrical Components, (4) Sensors, and (5) Networks.

4.2.1 Braking System

The braking system components used in this research were supplied by Bendix and were an example of the Bendix ABS-6 ESC system in current production on Volvo VN and VHD Series Class 8 truck tractors.

An overview of a typical braking system is shown in Figure 4-2. In this figure, the functional elements of the braking system are depicted in the approximate locations they would reside in an actual vehicle, with the front axle at the top of the figure. The brake hardware from the brake pedal (treadle valve) out to the air chamber was included in the hardware bench test system, but the actual brake mechanisms (S-cam, brake drum, and shoes) were not.

The treadle valve provides the driver's control to the front and rear traction relay valve. The controller for TCS can also control the front and rear traction relay valve. The controller for ABS can control each ABS modulator valve. The individual air chamber at each wheel is therefore controlled either by the driver through the treadle valve, or by a controller command to a traction relay valve or an ABS modulator valve. In this way, each wheel brake can be controlled independently to manage the vehicle's dynamic behavior.

The system architecture is shown in Figure 4-3. It contains traction relay valves controlling the pneumatic brake command signal to the brake air chambers on each axle. The rear tandem axle of the tractor is controlled by one traction relay valve, and the trailer axle is controlled by the front axle traction relay valve.

The treadle valve controls primary (drive axles) and secondary (steer axle and trailer) pneumatic circuits. In addition, TCS and ABS are accomplished by logical controllers that activate traction relay valves and ABS modulator valves respectively. In this way, the system consists of building blocks, where ABS can be offered as a feature separately from TCS, and TCS can be offered as a feature separately from ESC.

The wheel brakes are controlled by either a foot-operated valve or, when intervention is required to control the vehicle's dynamic behavior, by electronic control. The front axle and the rear axles are each controlled by a valve that implements a command signal from one or the other brake control source. The trailer brakes are operated via a pneumatic signal from the tractor.

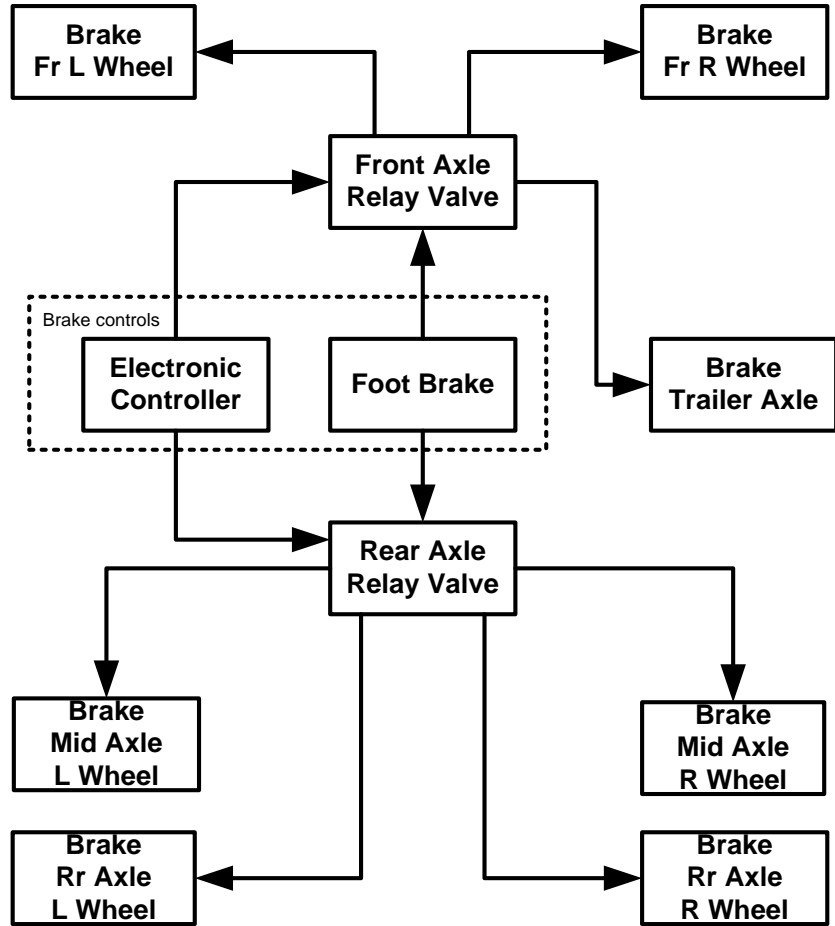


Figure 4-2. Diagram. Simplified schematic of a typical air brake system.

Figure 4-3 also shows, labeled with dashed-line boxes, the sensors used in the system. The details of these sensors, and their connectivity to the system and controls, are covered in Section 4.2.4.

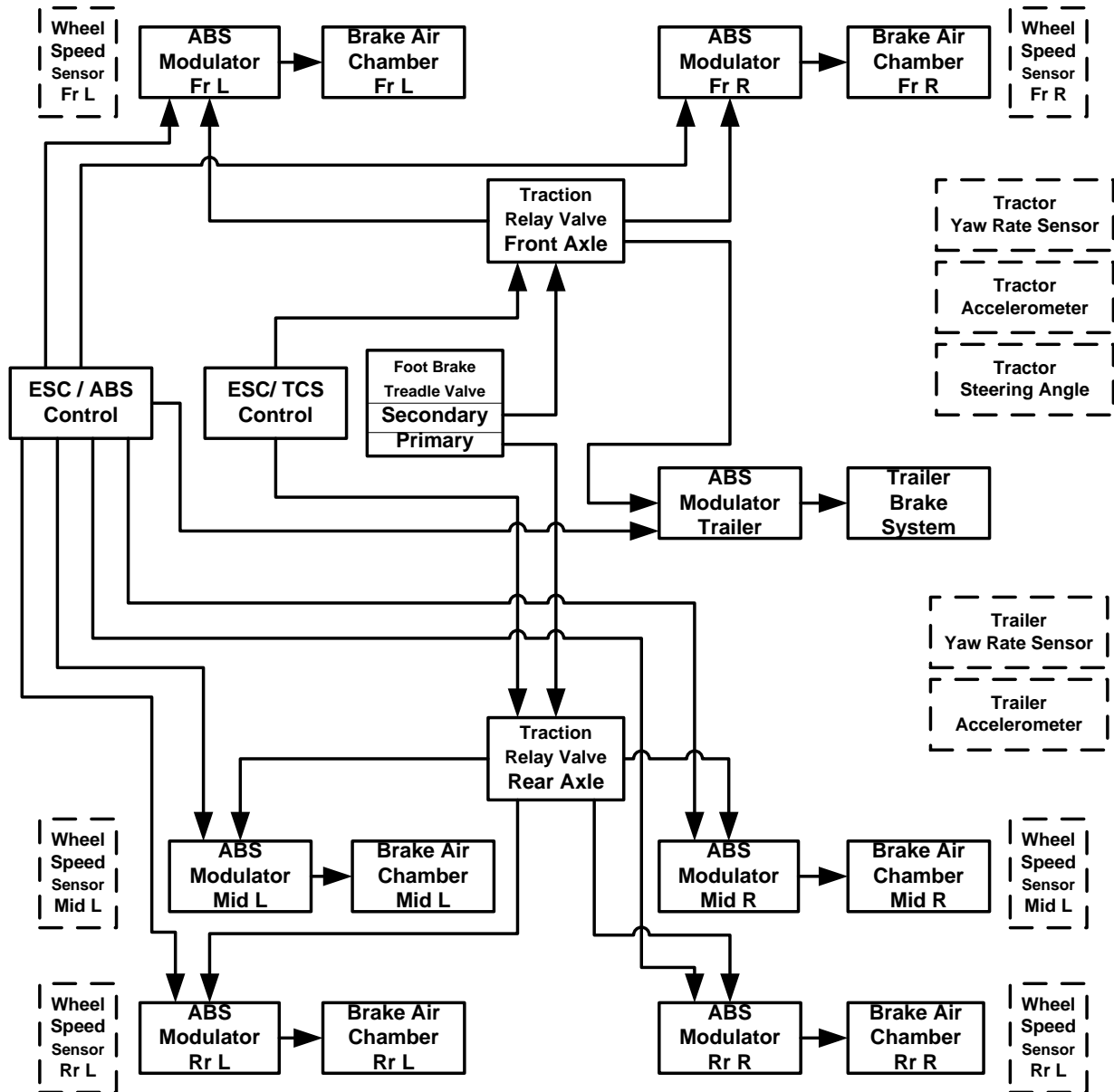


Figure 4-3. Diagram. Hardware system-under-test, brake system functional layout.

4.2.2 Pneumatic Controls

Since the system-under-test was not actually installed on a truck, the pneumatic controls of the brake system were powered by the laboratory's 0.85 MPa (120 psi) shop air. FMVSS 121 requires that the air compressors in air brake systems for buses cut in at 586 kPa (85 psi) and for trucks cut in at 689 kPa (100 psi) (NHTSA 2004), so the hardware bench test system setup air supply provides a similar pneumatic environment to an actual truck. The 0.9 m³/min (30 cfm) capability of the shop was adequate.

A layout of the pneumatic design of the brake system is shown in Figure 4-4. This figure shows the air supply, providing pressurized air to the treadle valve and each traction relay valve. This

pressurized air could then be supplied as commanded by actuating the treadle valve (foot brake) or through electric control of the traction relay valve.

The Bendix ABS-6 system includes pressure sensors to sense the state of pressure in the vehicle suspension, and also to sense the actuation of the brake by the driver. If these pressures are not present, ABS-6 may generate fault codes. In order to avoid this situation, the air pressure sensors for the Bendix ABS system were plumbed to provide the appropriate pressure signals. As there was no air suspension present in the test setup, the suspension pressure sensor was plumbed directly to the air supply.

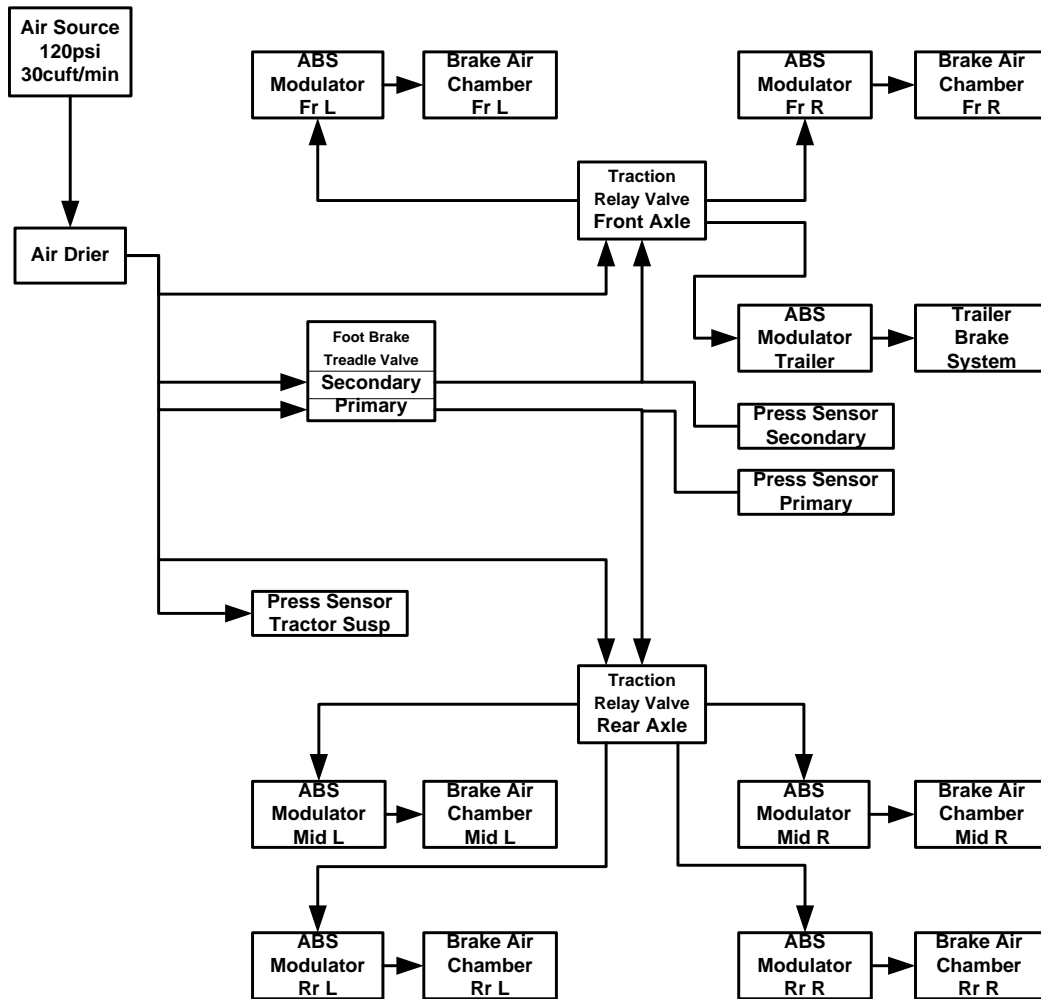


Figure 4-4. Diagram. Brake system pneumatic functional layout.

4.2.3 Electrical Components

The system-under-test was attached to a control system to implement the new stability control programs under development. This implied that the development controller would take the sensor inputs of, and generate command signals to control the actuators of, the Bendix ABS-6 system. A functional layout of the electrical controls of such an implementation is shown in Figure 4-5.

In this layout, the functionalities of the ESC development controller for ABS and TCS were separated, as the demands for brake release or brake application were addressed to each function respectively. All sensor inputs were for processing by the development controllers in both the single and dual CPU configurations.

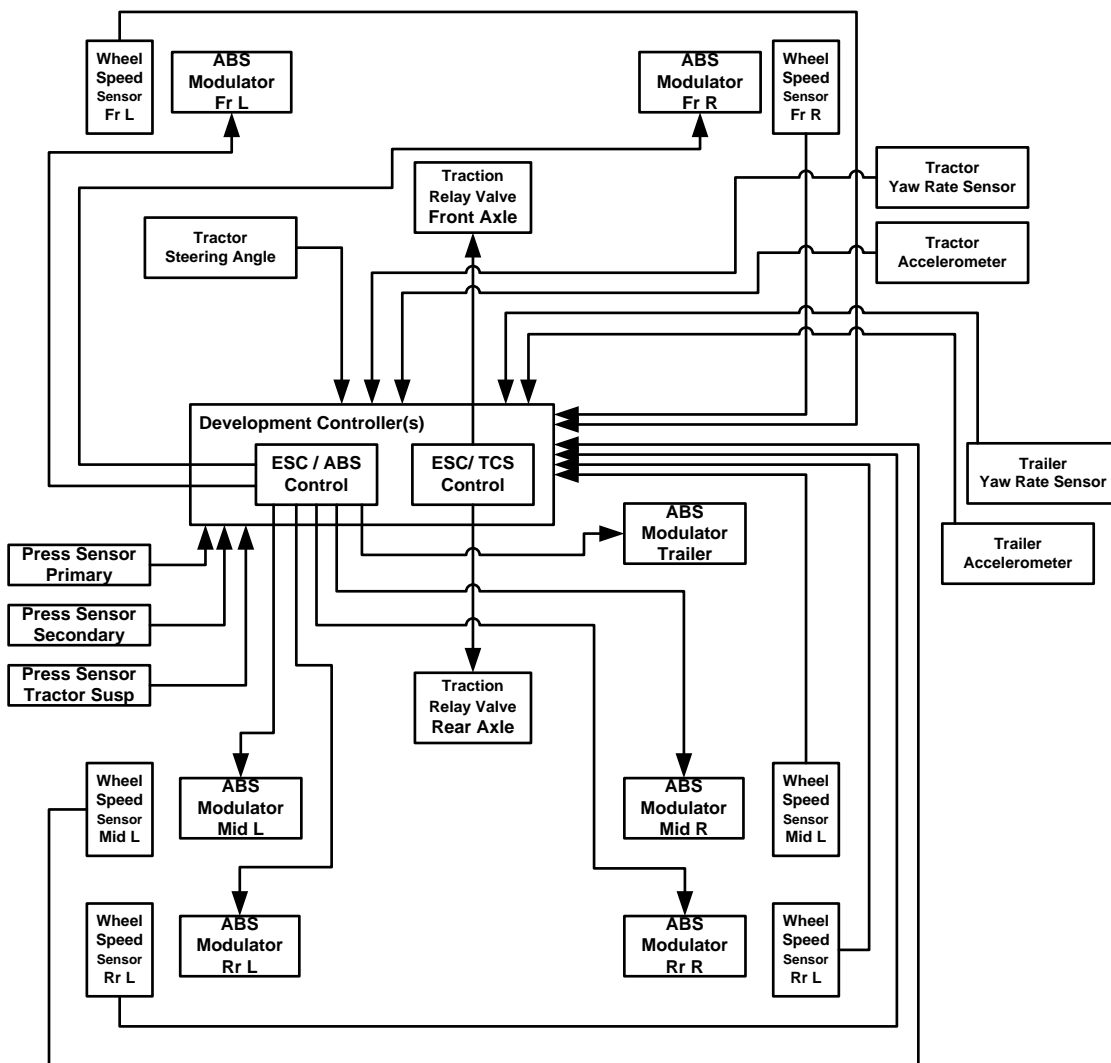


Figure 4-5. Diagram. Brake system electrical functional layout.

4.2.4 Sensors

A number of sensors are required. The purpose of the hardware bench test system was not to provide a life-like input but to provide a way to test that an input could be measured. The hardware bench test system is a tool for setting up controller hardware prior to an actual on-vehicle testing. It cannot be used in its current form to evaluate the controller algorithms because it does not account for vehicle dynamics and it does not apply realistic inputs to all sensors simultaneously.

Yaw Rate

The yaw rate sensor used for tractor measurements was the Bendix YAS-60, which also measures lateral acceleration. This sensor reported vehicle lateral acceleration and rotations about the vertical axis, using a dedicated serial communication link (CAN), also referred to as the sensor CAN, shared with the steering angle sensor, and used power and ground inputs supplied by the E-60 Bendix ECU (Bendix Commercial Vehicle Systems LLC 2005).

For the trailer yaw rate measurement, a Kistler DAG dual axis angular rate sensor was used. This angular rate sensor provided the measurement about the vertical axis and longitudinal axis, with a range of ± 150 degrees per second and a frequency response from 25 Hz down to 0 Hz (DC).

Steering Wheel (Hand Wheel) Angle

The steering wheel sensor was the Bendix SAS-60 Steering Angle Sensor. This sensor reported steering wheel position to the Bendix ABS-6 E-60 ECU using a serial communication link (CAN) shared with the yaw rate sensor. Its power and ground inputs were supplied by the E-60 ECU (Bendix Commercial Vehicle Systems LLC 2005).

Accelerometer

The lateral acceleration signal for the tractor was obtained from the Bendix YAS-60 sensor described above.

Additional acceleration measurements for the tractor and trailer each were made by a Dytran 7523A1 accelerometer. This accelerometer was a capacitive type triaxial accelerometer, providing lateral, vertical, and longitudinal acceleration measurements, with a range of ± 2 g and a frequency response down to DC.

Air Pressure

The pressure of air in the tractor suspension was measured by a ceramic capacitive Bendix pressure sensor. The sensor generated a voltage signal proportional to pressure while being supplied with power and ground by the Bendix E-60 ECU.

Additional pressure measurements for the trailer were made by an Omega PX209-300G5V. This was a solid state piezoresistive pressure transducer using a micro-machined diffused silicon diaphragm.

The Bendix ABS-6 system also provided pressure sensors for brake demand.

Wheel Speed

The wheel speed sensor used was the Bendix W-24 Wheel Speed Sensor. This sensor generated an AC signal that varied in voltage and frequency proportional to wheel speed (Bendix Commercial Vehicle Systems LLC 2005).

4.2.5 Networks

Two network architectures were developed and evaluated. In both architectures, electronics to communicate with sensors and actuators on the tractor were mounted in the backplane of one housing or chassis, and the corresponding electronics for the semitrailer was mounted in a separate chassis. The distinction between the two architectures is that one had a single CPU to control both chassis, and the other had two CPUs, one in each chassis.

The backplane in each chassis was PCI Express standard, a high-speed serial communication for attaching hardware devices to a computer. (National Instruments Products and Services 2011q). Analog data input and output to both tractor and trailer backplanes was provided for through the inclusion of data acquisition (DAQ) cards in both devices. The tractor's Bendix brake system has sensors that communicate through the tractor's CAN interface (SAE J1939), and the chassis for the tractor received data from them via the CAN. The trailer chassis did not use a CAN.

The single-CPU architecture used one development controller to manage sensing and actuation on both the tractor and the semitrailer. The high-speed data link provided by the National Instruments MXI Interface between two chassis backplanes effectively made the backplane chassis in the trailer an extension of the tractor controller. This implementation is shown in Figure 4-6. In the case of the single-CPU implementation, an Ethernet connection to the PXI chassis provided an attachment of a laptop to the CPU for servicing and data collection. The dual-CPU architecture used two development controllers with one managing the tractor's sensing and actuation and the other doing the same for the semitrailer. The two controllers were connected by a high-speed Ethernet network served by a switch, which also provided for the attachment of a laptop to the network for system servicing and data collection. This implementation is shown in Figure 4-7.

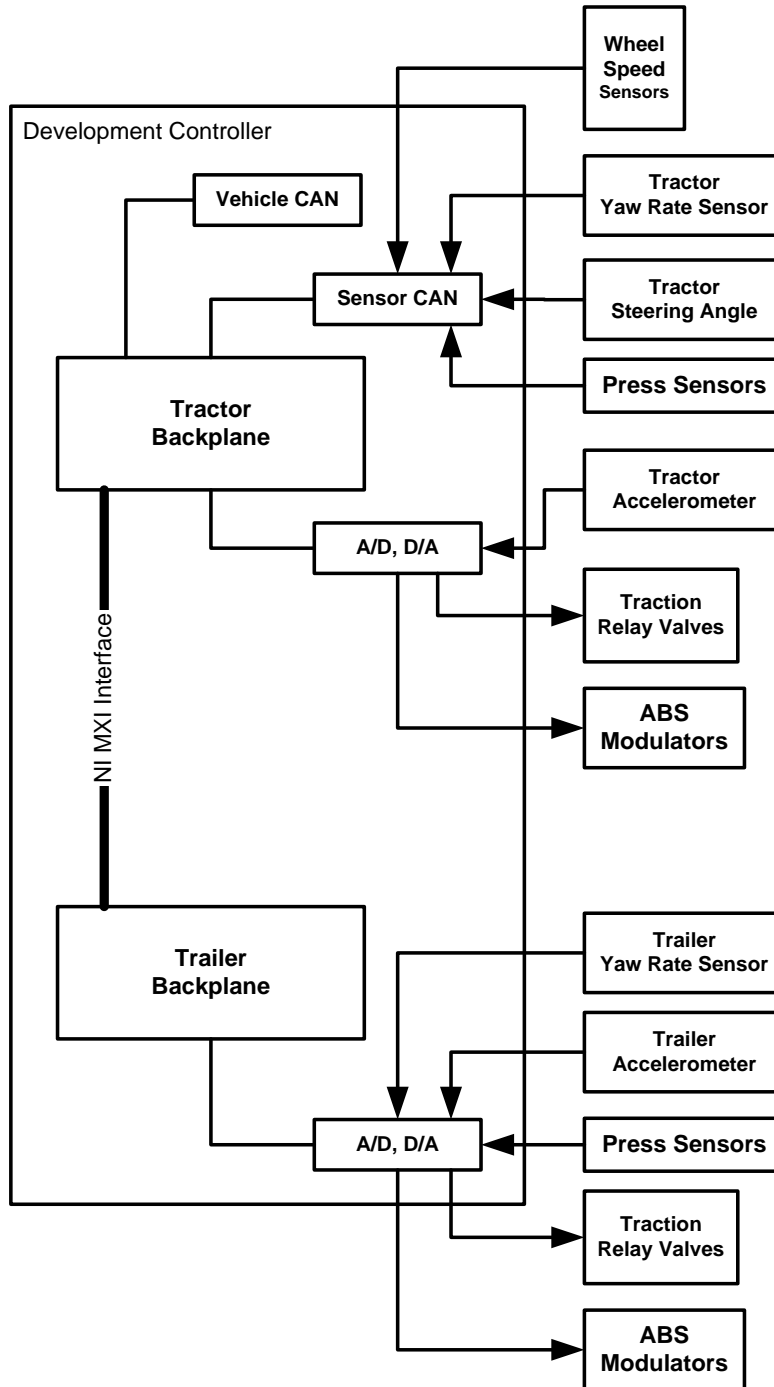


Figure 4-6. Diagram. Brake system network functional layout – single CPU controller.

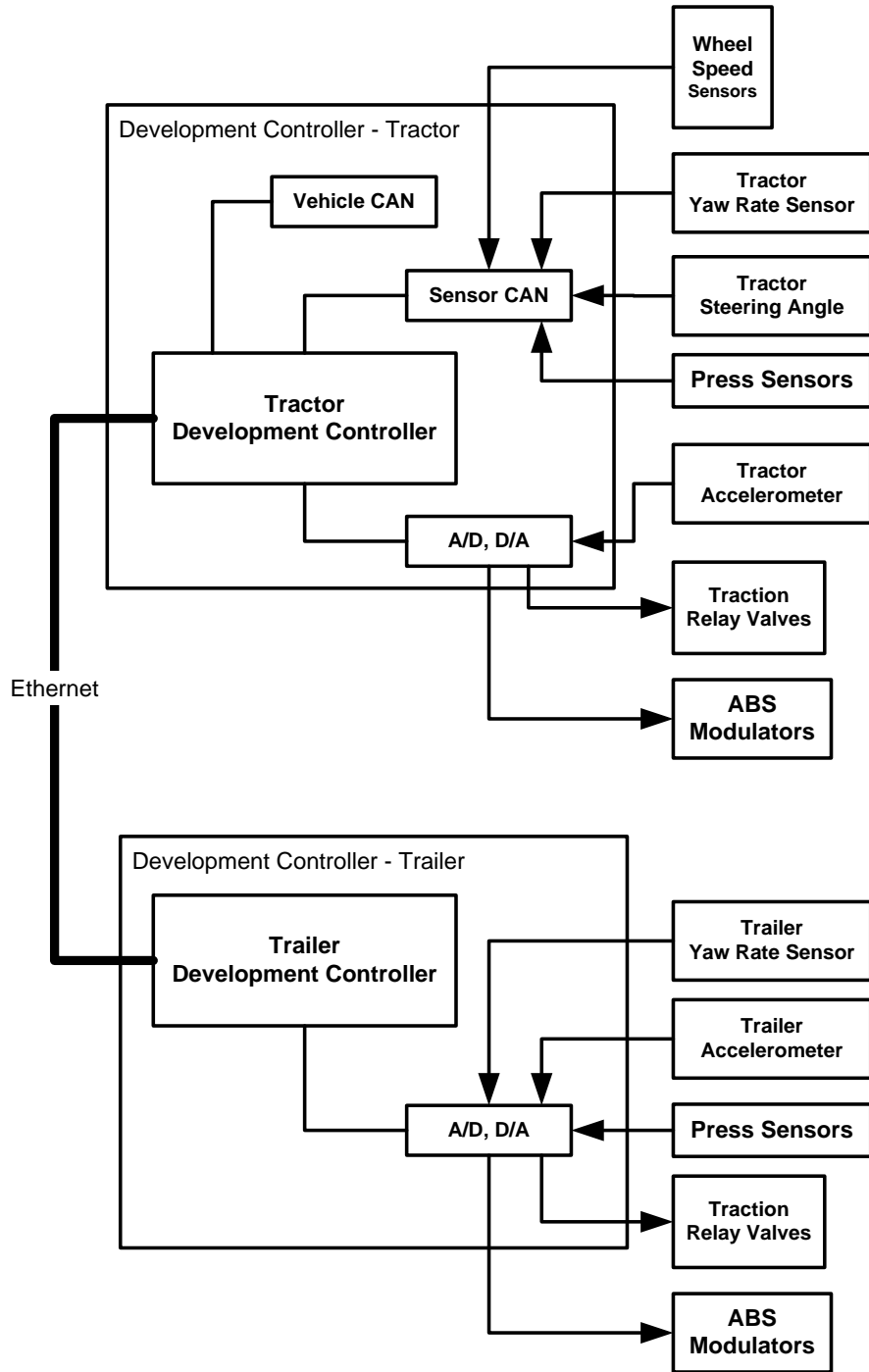


Figure 4-7. Diagram. Brake system network functional layout – dual CPU controller.

4.3 Development Controller Hardware

The development control system hardware consisted of two PCI-bus-based backplane chassis with CPU, network interface, and DAQ resources installed. The details of these devices will now be discussed.

4.3.1 Control System Configurations

The basis of the development controller was the National Instruments PXI chassis system. PXI (PCI eXtensions for Instrumentation) is a PC-based platform for measurement and automation systems. PXI combines PCI-bus features with the rugged, modular, Eurocard packaging of CompactPCI and adds specialized synchronization buses and key software features.

The PXI chassis is the backbone of the controller development system. It provides the power, cooling, and communication buses of PCI and PCI Express for the controller and its modules. XI CPUs eliminate the need for an external computer to serve as the controller, therefore providing a complete system contained within the PXI chassis. The PXI chassis includes the CPU, hard drive, Ethernet, and peripherals. Their operating system is LabVIEW[®] Real-Time.

Each device used in the development controllers will now be introduced.

PXI CPUs

Each PXI could include a CPU. Two types of PXI CPUs were available, the PXI-8187 and the PXI-8106. They are both computers with similar capability, varying only in details of core specification, processing speed, and memory.

Specifications of the PXI-8187 (National Instruments Products and Services 2011m)

- 2.5 GHz Pentium 4-M processor
- 256 MB DDR RAM standard, 1 GB
- Integrated hard drive, USB 2.0, Ethernet.

Specifications of the PXI-8106 (National Instruments Products and Services 2011l)

- 2.16 GHz Intel Core 2 Duo T7400 dual-core processor
- 512 MB (1 x 512 MB DIMM) dual-channel 667 MHz DDR2 RAM standard, 4 GB
- 10/100/1000BASE-TX (Gigabit) Ethernet, ExpressCard/34 slot, and 4 Hi-Speed USB ports
- Integrated hard drive.

These CPUs were installed on one of two backplane chassis, either the PXI-1002 (4-slot chassis) or the PXI-1042Q (8-slot chassis). (National Instruments Products and Services 2011i; National Instruments Products and Services 2011j)

Analog Input and Output

PXI data acquisition devices handled the input of sensor data that did not come through the CAN and the output of actuator commands. A PXI-6259 was used in each PXI chassis, one for the tractor and one for the trailer.

Specifications of the PXI-6259 (National Instruments Products and Services 2011k)

- Four 16-bit analog outputs (2.8 MS/s); 48 digital I/O; 32-bit counters
- Correlated DIO (32 clocked lines, 10 MHz)
- NI-DAQmx driver software and NI LabVIEW[®] SignalExpress interactive data-logging software.

To facilitate electric harness connections, the harness interface was done through NI SBC-68 connector blocks (National Instruments Products and Services 2011f).

CAN

The acquisition of data from the sensor CAN and vehicle CAN was accomplished by incorporating a CAN interface into each PXI chassis. For the tractor controller, the PXI-8513/2, a two-channel interface, was chosen, while for the trailer a single-channel PXI-8513 interface was chosen.

PXI-8513 (National Instruments Products and Services 2011n)

- 1- and 2-port XS CAN interface
- NI-XNET driver for developing frame and signal applications in LabVIEW[®]
- NI-XNET device-driven DMA engine for coupling the CAN bus to host memory to minimize message latency
- Integrated CAN databases
- Synchronization, 1 μ s timestamps for integration with NI DAQ, digitizers, switches, large systems.

Networking

MXI-bus (NI Developer Zone - National Instruments 2011c)

The network adopted for the single CPU configuration was the National Instruments MXI-bus. The MXI-bus is a powerful, high-speed communication link that interconnects devices using a flexible cabling scheme. Derived from the VME-bus (see section 4.3.3), MXI provides a high-performance way of controlling PXI systems using commercially available desktop computers

and workstations. National Instruments developed and published the MXI specification and released it as an open industry standard in 1989.

MXI-bus provides the performance of an embedded PXI computer while also providing the flexibility of general purpose PCs. MXI-bus is described as a 32-bit system bus on a cable (NI Developer Zone - National Instruments 2011c). It connects multiple devices using a hardware memory-mapped paradigm that eliminates software overhead. These devices can then directly access each other's resources through reads and writes to their address locations, so that individual devices on a MXI-bus behave as a single system with a shared address space.

The MXI-bus implementation in this research used the PXI-8364 and PXI-8361 MXI Express interface cards (National Instruments Products and Services 2011h).

The configuration of the Single CPU Controller is shown in Figure 4-8.

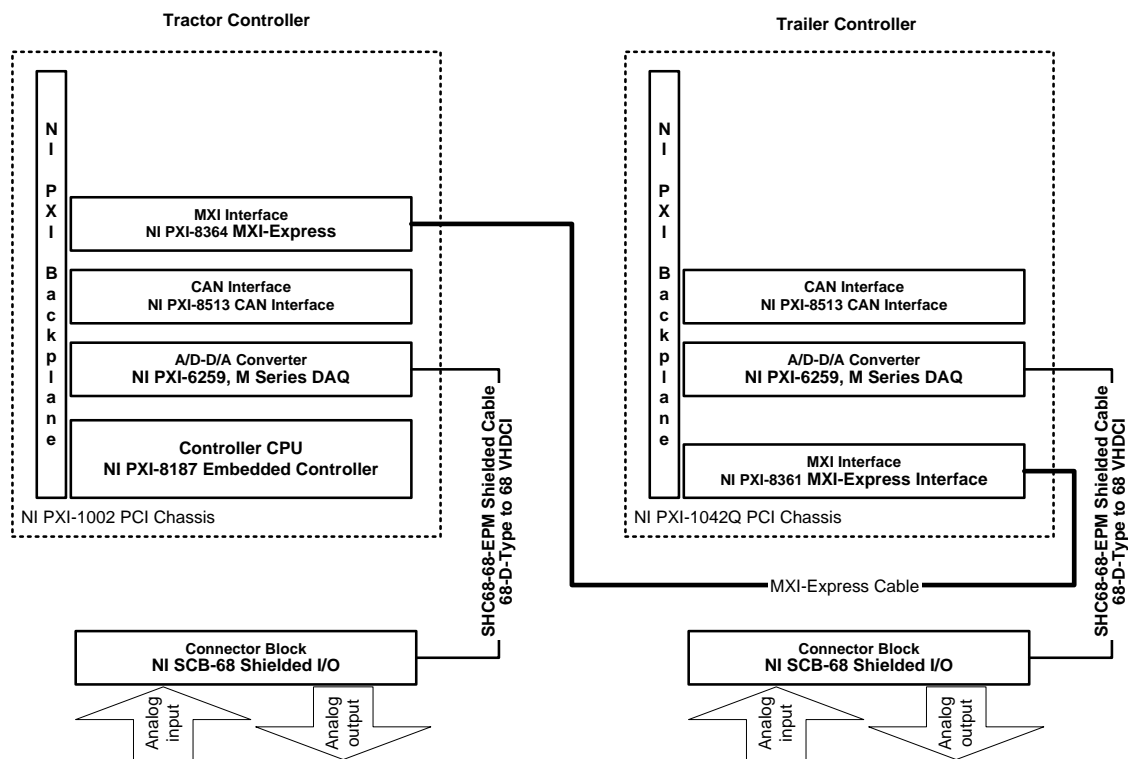


Figure 4-8. Diagram. Development controller configuration – single CPU controller.

Ethernet

The Dual CPU option was almost identical to the single CPU option with respect to the individual computer chassis features. The only difference, aside from the number of CPUs, was the type of network link between the two PXI chassis. An Ethernet network connection was used for the Dual-CPU option.

The configuration of the Dual CPU Controller is shown in Figure 4-9.

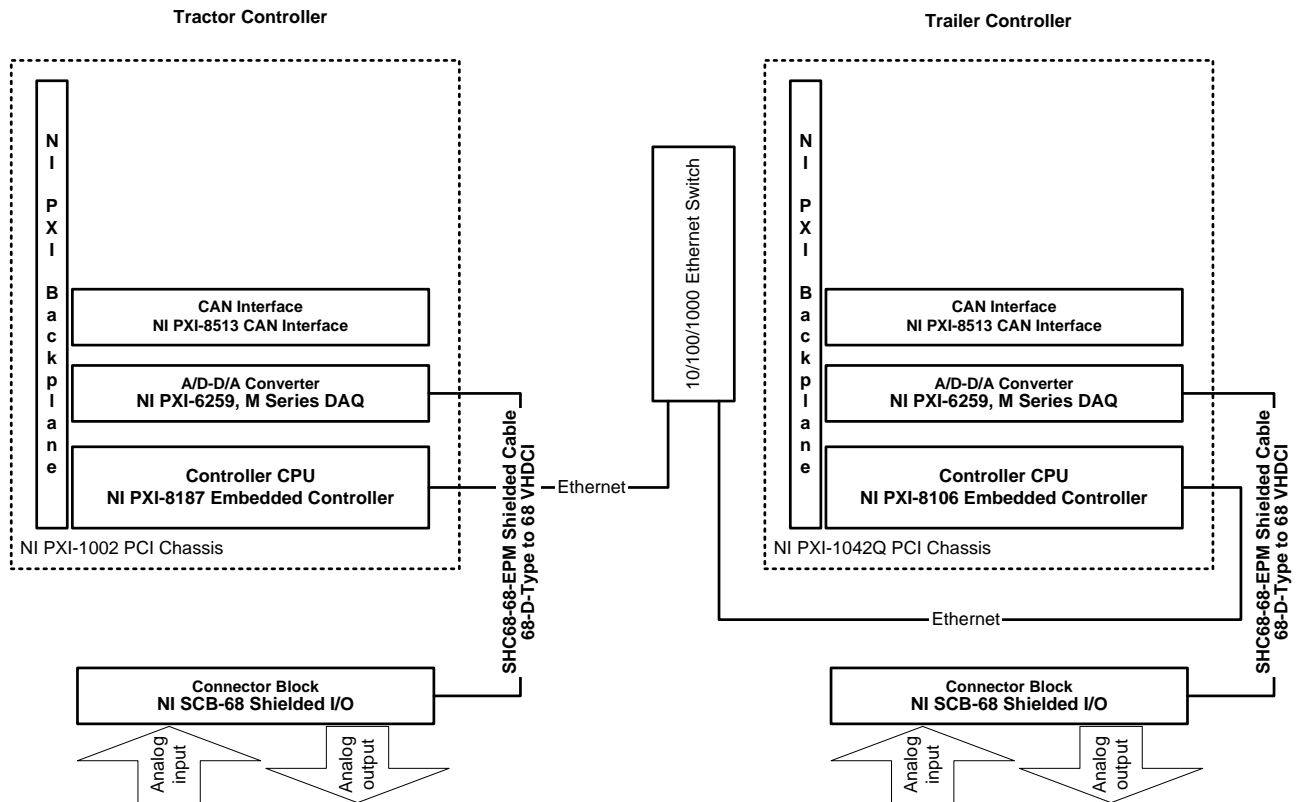


Figure 4-9. Diagram. Development controller configuration – dual CPU controller.

4.3.2 Control System Electrical Hardware

The details of the control system electrical system can be seen in Figure 4-10.

Power Supplies

The PXI Chassis used for the controllers in this project each contained their own power supply. In addition, several sensors required a supply of power, so additional power supplies were used as needed. The power requirements for the valve solenoids for the brake system air valves were unknown. The analog output of the PXI-6259 DAQ card was limited to a power of 10W, which was considered not to be enough power to control the brake solenoid. To provide a flexible power supply solution for this component, a 12V wet-cell lead acid battery was used as the power source, with switching provided by individual high-capacity relays, controlled by the DAQ card mounted in the PXI chassis. The battery was kept charged during testing by a 1A battery charger.

Volvo Electric Harnesses

To provide electrical connectivity to the Bendix ABS-6 system, an electrical harness was obtained for an example Volvo truck (Volvo truck electrical harness 21588437 Rev. P01, 21565326 Rev. P02 and 20915063 Rev. 02). This harness, including the cab and frame sub-harnesses and master fuse box, also required 12V power, and was also attached to the 12V wet-cell battery.

Dummy Loads for Bendix Controller

The ECU of the Bendix ABS-6 system contains a number of fault-detection features to provide for fault-tolerance and reliability and safety. One of these features was a check on the electrical load imposed by air valve solenoids. If these loads were different from a certain value, the Bendix ECU would limit the system functionality. To mitigate this possibility during testing, equivalent solenoid coils were obtained and connected to the Volvo truck electrical harness, so that the Bendix ABS-6 ECU would see the desired electrical load during operation. The actual valve solenoids of the system-under-test were connected to the development controllers, as implied by Figure 4-5.

CAN Interface Taps

To obtain data from the Bendix system's sensor CAN network, a tap was made into the sensor CAN at the Steering Wheel Angle sensor node.

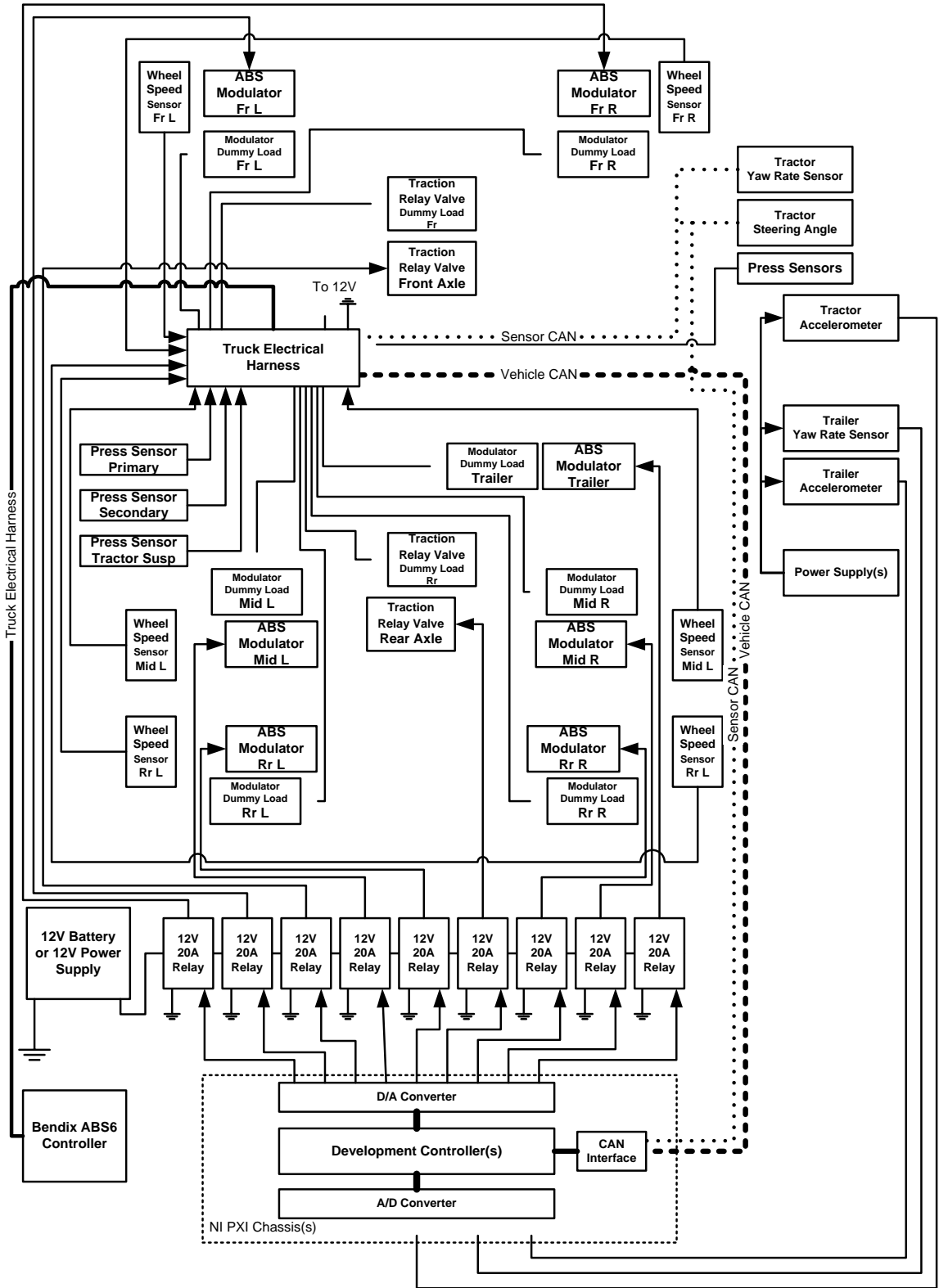


Figure 4-10. Diagram. Control system electrical schematic.

4.4 Control System Development Software

The single or dual CPUs in Section 4.3 ran software on a platform developed for the chassis. The software will be described first, followed by the measurement and data inputs.

4.4.1 Control System Software

LabVIEW[®] (Laboratory Virtual Instrumentation Engineering Workbench) is a software platform for the development of data acquisition, control systems, and data analysis applications in an industrial setting. It is a graphical programming environment using a block diagram with icons and wires.

LabVIEW[®] uses a graphical programming language called G (not to be confused with G-Code). In LabVIEW[®], execution is determined by the structure of the graphical block diagram. The wires in the block diagram propagate variables. LabVIEW[®] program execution is based on dataflow, which means that nodes in a LabVIEW[®] program execute as soon as all the data becomes available and different parts can execute in parallel.

LabVIEW[®] Real-Time was used in this research. The LabVIEW[®] Real-Time Module and RT Series hardware delivers deterministic, real-time performance for data acquisition and control systems. Using LabVIEW[®] graphical programming, LabVIEW[®] Real-Time embedded control applications using PID control can be developed on a laptop, and then downloaded and executed on an independent hardware target. LabVIEW[®] Real-Time targets include an embedded processor running LabVIEW[®] RTOS and real-time hardware drivers run with the same API calls as in LabVIEW[®] (National Instruments Products and Services 2011a).

NI-DAQmx

NI-DAQmx is National Instruments' data acquisition software driver (National Instruments Products and Services 2011g). NI-DAQmx driver software provides a single programming interface for programming analog input, analog output, digital I/O, and counters on each multifunction DAQ hardware device. NI-DAQmx controls every aspect of data acquisition, including NI signal conditioning devices, from configuration, to programming in LabVIEW[®], to low-level operating system and device control.

NI Measurement and Automation Explorer

Measurement & Automation Explorer (MAX) (National Instruments Products and Services 2011p; National Instruments 2011) is a graphical user interface used to configure instrument drivers and provide access to CAN, DAQ, PXI and other types of devices.

NI X-NET 1.3

The NI-XNET 1.3 API (National Instruments Technical Sales 2011) provides function calls in LabVIEW[®] so signals and frames can be easily sent to and from applications. The following data transfer modes were tested:

- Single-point signal input and output modes read and write the most recent values received for each signal.
- Waveform signal input and output modes use the time when the signal frame is received to resample the signal data to a waveform at a fixed sample rate. These modes were used for synchronizing XNET data with DAQmx analog/digital input channels and plotting waveforms.
- XY signal input and output modes return exact XY pairs of a signal's timestamp and its value.
- Stream input and output modes for frames read or write every frame on the network.
- Queued frame input and output modes read and write frame data from a dedicated queue per frame, used for identifying and recording CAN messages.

4.4.2 Data Sets and Parameters

Digital data came to the development controller through the CAN, as is typical on heavy duty trucks. The chassis had ADCs for data coming directly from sensors.

Receiving CAN Data

To communicate with hardware on the CAN network, XNET must understand the communication format in the actual embedded system. The embedded communication is described by a file, such as a CANdb (.dbc) file, which is called a database. The database contains many object classes, each of which describes an entity in the embedded system (National Instruments 2009, 4-8). The following object classes exist:

- Database: Each database is represented as a distinct instance in NI-XNET.
- Cluster: Each database contains one or more clusters, where the cluster represents a collection of hardware products connected over a shared cabling harness. In other words, each cluster represents a single CAN network.
- ECU: Each ECU represents a single hardware product in the embedded system. The cluster contains one or more ECUs connected over a CAN cable. It is possible for a single ECU to be contained in multiple clusters, in which case it behaves as a gateway between the clusters.

- **Frame:** Each frame represents a unique unit of data transfer over the cluster cable. The frame bits contain payload data and an identifier that specifies the data (signal) content. Only one ECU in the cluster transmits (sends) each frame, and one or more ECUs receive each frame.
- **Signal:** Each frame contains zero or more values, each of which is called a signal. Within the database, each signal specifies its name, position, length of the raw bits in the frame, and a scaling formula to convert raw bits to/from a physical unit.

The database was created and accessed through the XNET Database Editor. An example database is shown in Figure 4-11.

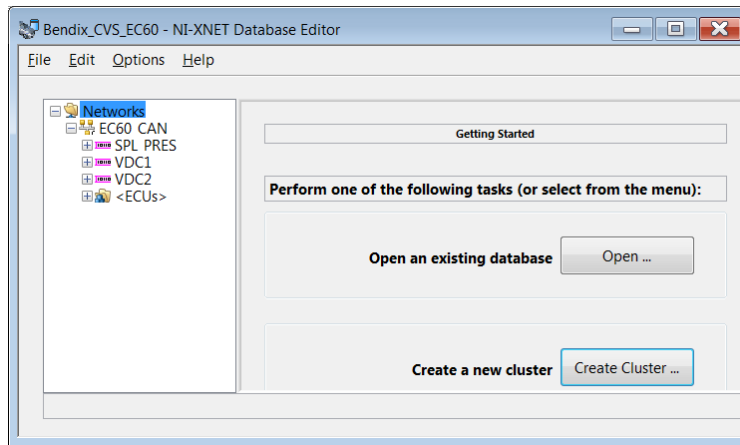


Figure 4-11. Screen shot. NI-XNET database editor.

In the database a cluster was defined for the sensor CAN network of the system-under-test. The frame properties for each data variable defined on the CAN in the system-under-test are shown in Table 4-2 and the signal properties are shown in Table 4-3. The byte order is “Little Endian.” This refers to the convention where bytes at lower addresses have lower significance (the word is stored little-end-first). See Figure 4-12 for the input screens in the XNET Database Editor. The CAN message can be parsed and scaled within the CAN session setup, to provide the engineering data output directly as needed.

Table 4-2. CAN frame properties for system-under-test.

Frame	Arbitration	Length	Transmit Time
SPL PRES	18FEAE21h	8 Byte	1 s
VDC1	18FE4F0Bh	8 Byte	0.1 s
VDC2	18F0090Bh	8 Byte	0.02 s

Table 4-3. CAN signal properties for system-under-test.

Frame	Signal	Range	Resolution	Start Bit	# of Bits	Data type	Byte Order	Units	Scale
SPL PRES	Pneumatic Supply Press			0	8	Unsigned	Little Endian		1
SPL PRES	Trailer Air Pressure			8	8	Unsigned	Little Endian		1
SPL PRES	Service Brake Air	2000 to 0	0.08 bar per bit	16	8	Unsigned	Little Endian	kPa	8
SPL PRES	Service Air Pressure	2000 to 0	0.08 bar per bit	24	8	Unsigned	Little Endian	kPa	8
VDC1	Status 1			0	8	Unsigned	Little Endian		1
VDC1	Status 2			8	8	Unsigned	Little Endian		1
VDC2	Steer Angle	-31.374 to 31.374	1/1024 rad per bit	0	16	Signed	Little Endian	rad	0.0000977
VDC2	Yaw Rate	-3.92 to 3.92	1/8192 rad per bit	24	16	Unsigned	Little Endian	Rad/s	0.000977
VDC2	Lat Accel	-15.687 to 15.687	1/2048 m/s ² per bit	40	16	Signed	Little Endian	m/s ²	0.000488
VDC2	Long Accel	-12.5 to 12.5	0.1 m/s ² per bit	56	8	Signed	Little Endian	m/s ²	0.1

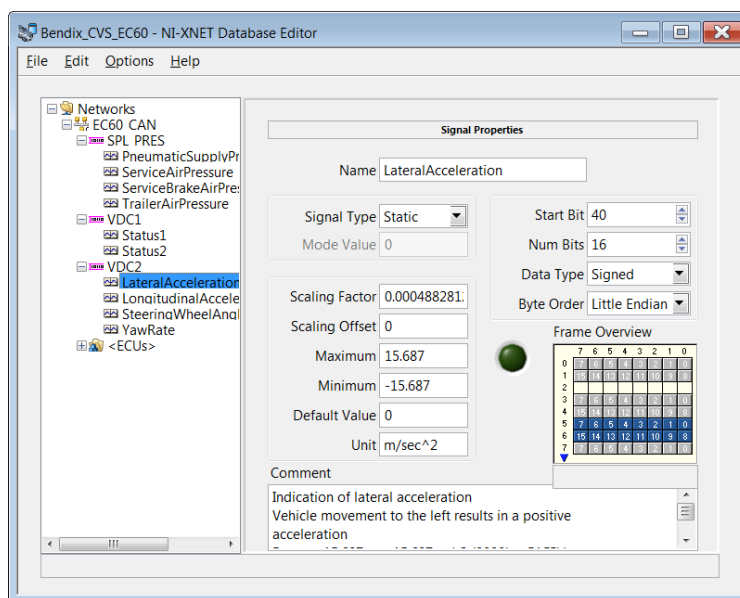


Figure 4-12. Screen shot. NI-XNET, Setting CAN signal properties.

The CAN session in the LabVIEW[®] project represents the controller code. The virtual instrument that controls the CAN session includes a setup screen where the CAN port number is selected and the desired frames are selected (see Figure 4-13).

The programmatic representation of the CAN session appears in Figure 4-14. In this view, the frame rate, CAN port termination property (XNET allows software-configurable termination), and error state properties can be set. Messages can be parsed in the program, and data time stamped according to the PXI global clock, allowing careful management of component performance if the device on the CAN also publishes a time stamp in its messages. The precise measurement of the timing of events system-wide is an important advantage of doing controller development using the PXI-based systems.

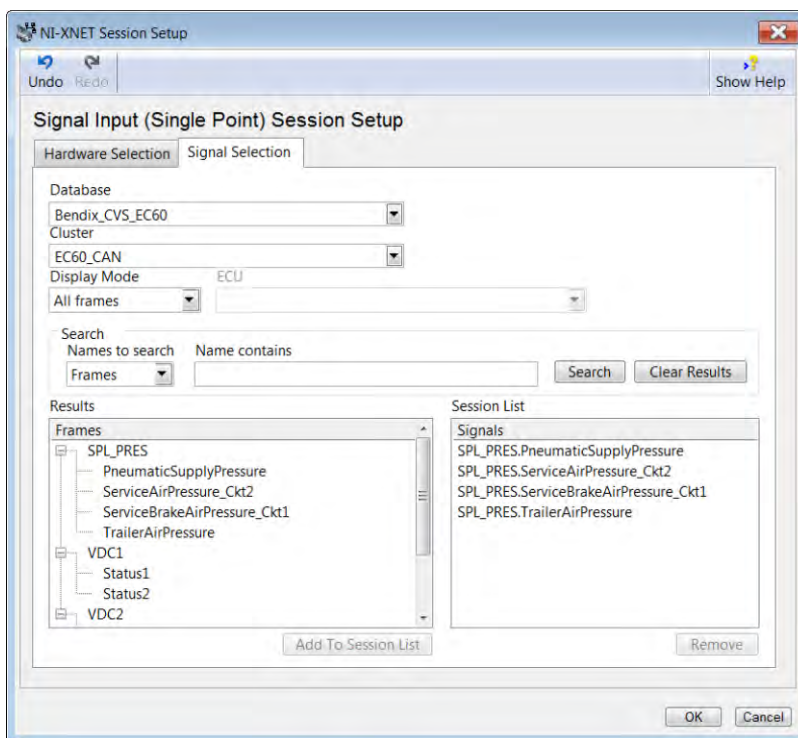


Figure 4-13. Screen shot. CAN port configuration.

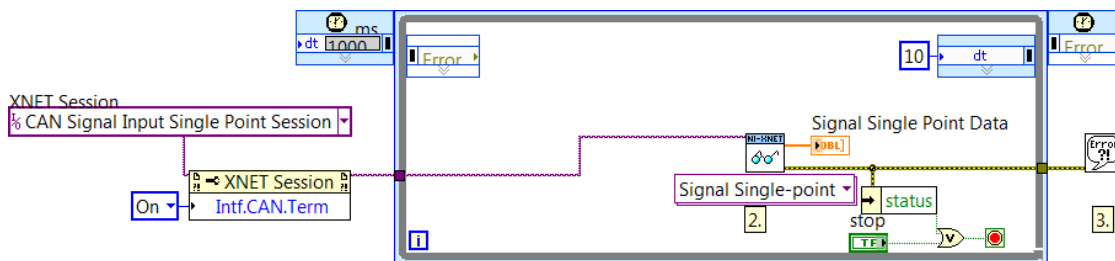


Figure 4-14. Diagram. CAN frame capture implemented in a LabVIEW[®] program.

Receiving and Transmitting Analog Signals

Data acquisition setup and management of I/O in LabVIEW[®] is facilitated by a graphical interface. LabVIEW[®] works with NI-PXI hardware to make pin assignments and signal conditioning straightforward (see Figure 4-15).

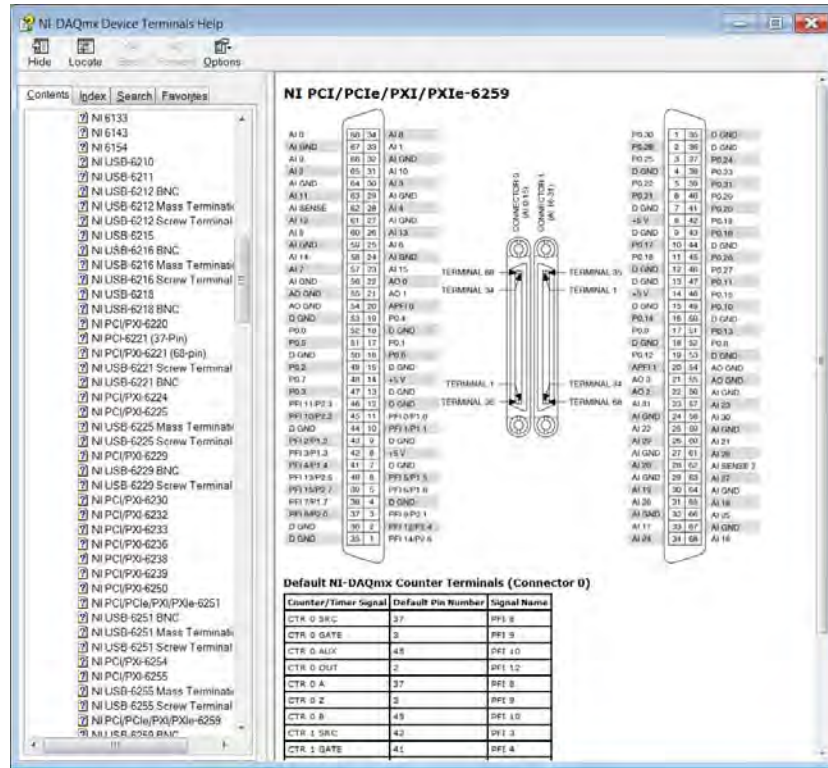


Figure 4-15. Screen shot. NI-DAQ I/O terminal assignments.

Pin assignments can be interactively confirmed (see Figure 4-16). The MAX can provide for formal calibration of the data acquisition setup (see Figure 4-17).

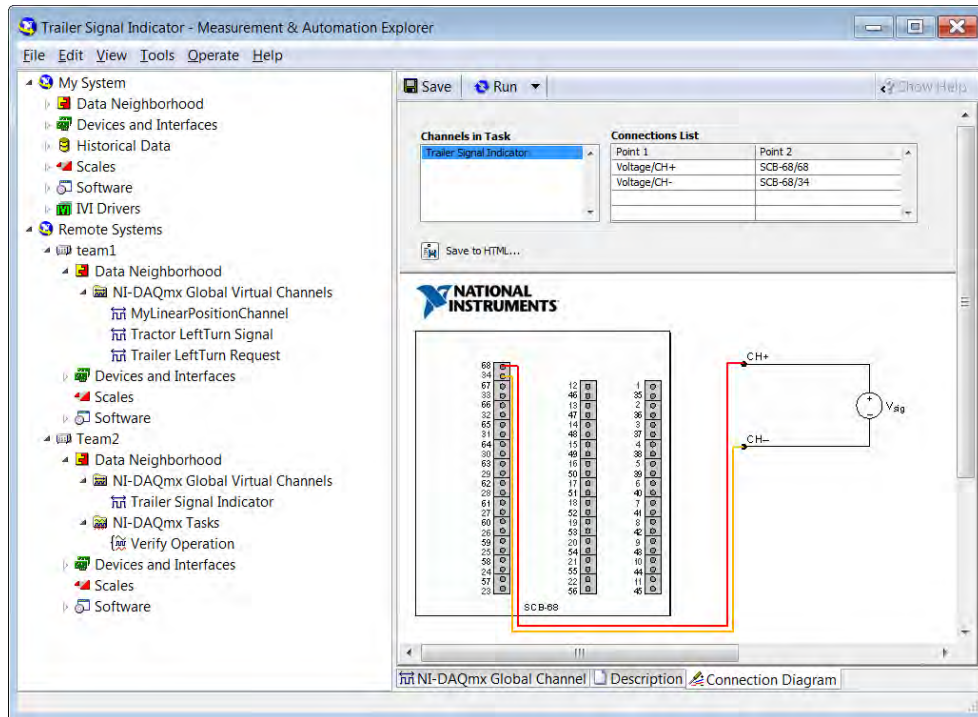


Figure 4-16. Screen shot. NI MAX connection diagram.

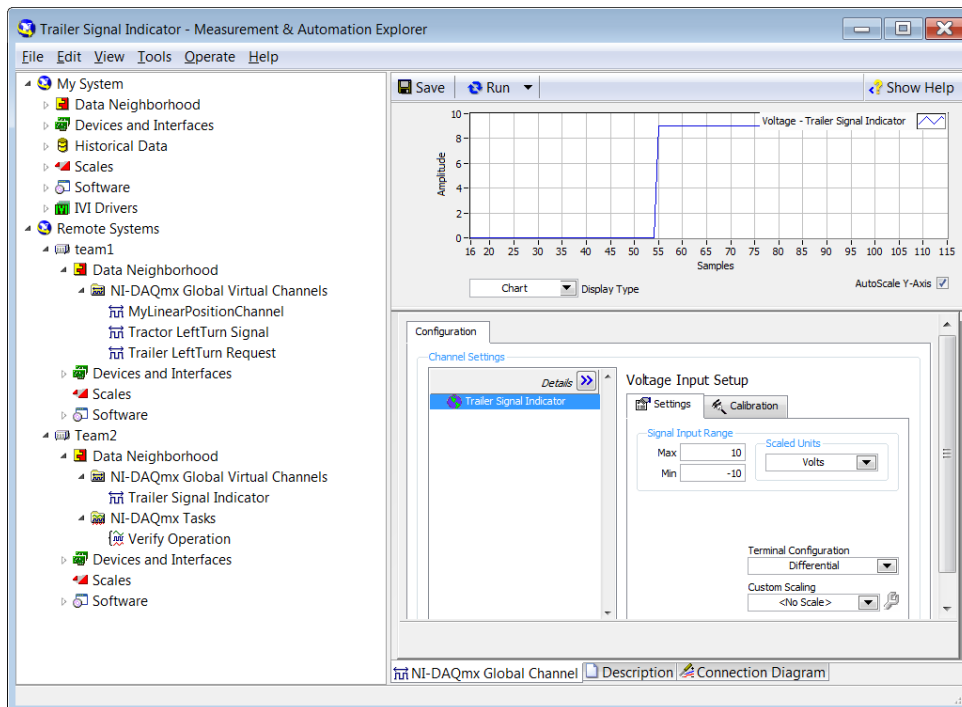


Figure 4-17. Screen shot. NI MAX data plot and calibration.

4.5 *Physical Implementation*

All the equipment described above was built in a hardware bench test system.

4.5.1 *System-Under-Test Hardware*

The system-under-test was assembled on a stainless-steel table, which served as a rigid platform for the actuators and sensors. The table also served as a workbench for the development controllers, as well as a chassis to hold the electrical harnesses for the system-under-test and the development controllers. See Figure 4-18.



Figure 4-18. Photo. Hardware bench test system.

Speed Sensor

In order to provide for a speed signal, a simple speed sensor input array was designed, using a tone wheel mounted on a bearing, which was spun by hand to provide a speed sensor signal. All the individual speed sensors were excited by a common tone wheel. A generic tone wheel was used. See Figure 4-19.



Figure 4-19. Photo. Speed sensor array around the tone ring.

Other Sensors

Since the system-under-test was not actually connected to a vehicle, no actual yaw rate could be measured. To simulate the rotation of the vehicle, the yaw rate sensor was simply turned by hand. Similarly, lateral acceleration was simulated by gravity.

Use of Air Cylinder for Brake Air Chamber

The use of actual brake air chambers to receive the air supply for braking was considered unnecessary. The requirement for this part was simply to hold air under pressure and to exhaust the air when the brakes were released. In place of actual air brake chambers, aluminum pressure cylinders, such as are commonly available on the market, were used. The ports of the air cylinders were drilled and tapped to receive a fitting such as a typical air brake cylinder would use, in order to provide the correct flow characteristics. The pressure cylinders chosen for this research had a volume of 49 cubic inches (Figure 4-20). Bendix engineers confirmed that this volume was suitable for the test purpose of this study.

Physical Layout of Components



Figure 4-20. Photo. Air cylinder, traction relay valve, ABS modulator, treadle valve.

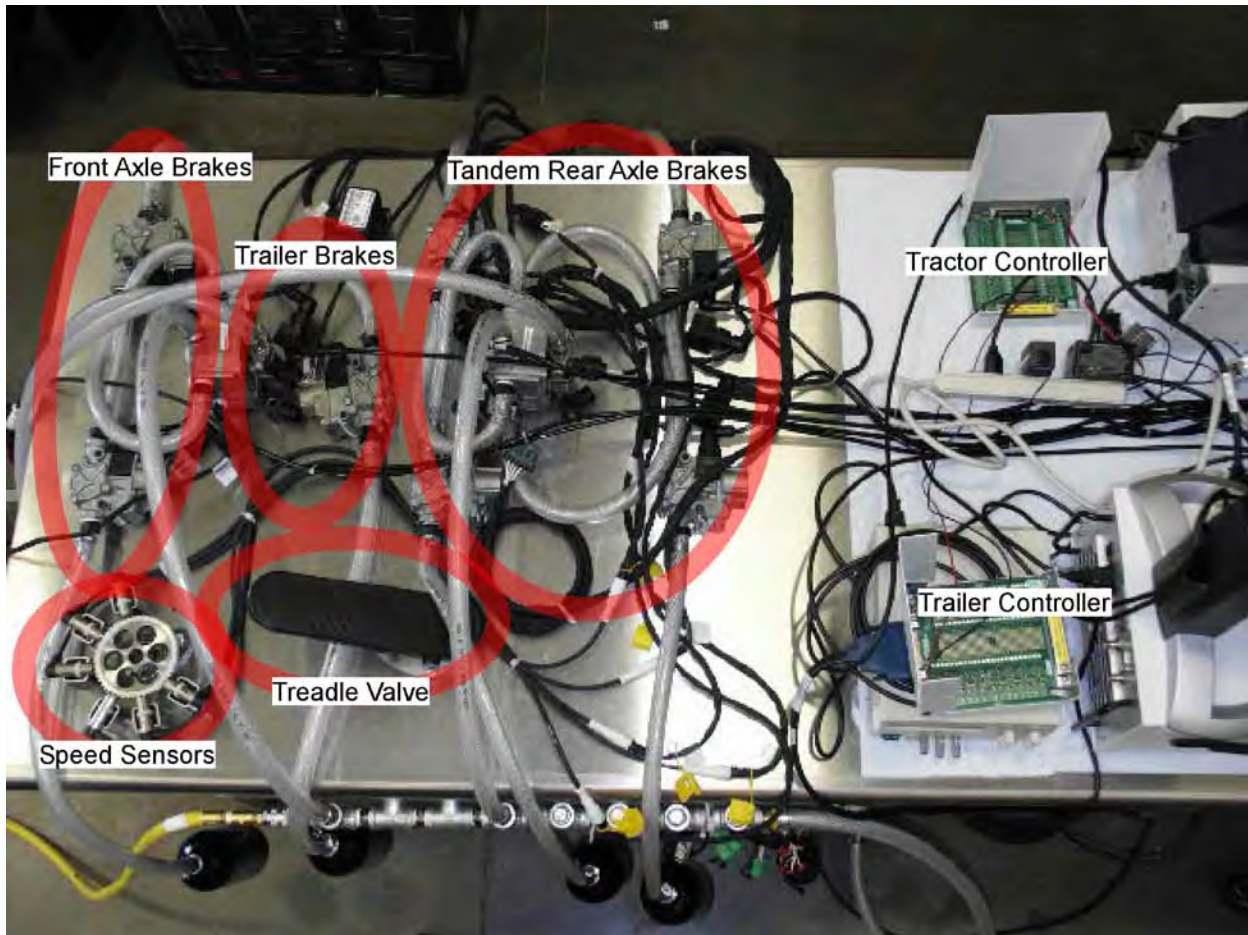


Figure 4-21. Photo. Layout of test stand assembly.

4.5.2 Controllers

The development controllers consisted of two NI PXI chassis. The tractor controller was a PXI-1002 chassis with a PXI-8187 CPU installed. In the case of the dual CPU option, the trailer controller was a PXI-1042Q chassis with a PXI-8106 CPU installed (See Figure 4-22 and Figure 4-23). In the case of the single CPU option, the PXI-8106 CPU was omitted.



Figure 4-22. Photo. Development controller for trailer (left) and tractor (right).



Figure 4-23. Photo. PXI chassis for trailer (top) and tractor (bottom).

The use of the PXI-8187 Embedded Controller limits the Ethernet bandwidth to 100 Mbps. This is far more than the rate at which measurement data needs to be transmitted between the tractor and trailer. Whether two separate controllers need to communicate more quickly as they process the data is a separate question. In case this speed is not fast enough to provide adequate bandwidth between the tractor and trailer, but a Dual CPU option is still desired, the other

network option is to use another CPU with 1Gbit/s Ethernet. For example, the PXI-8108 and PXI-8196 both provide 1Gbit Ethernet.

Other network resources available on the PXI platform include CAN, LIN (National Instruments Products and Services 2011c), FlexRay (National Instruments Products and Services 2011b), DeviceNet (National Instruments Products and Services 2011d), and GPIB (National Instruments Products and Services 2011e).

4.6 Results and Applications

The hardware bench test system was assembled and completed, and Section 4.1.4 functional testing was successfully concluded. Data was collected from both analog inputs and CAN inputs from both PXI chassis and passed to the other chassis, for both single- and dual-CPU configurations. Furthermore, signals were sent deterministically between the two PXI chassis for both configurations.

Since the development of a truck based hardware implementation of an ESC control system is predicated on the completion of functional testing of the hardware bench test system, the remaining parts of this testing will need to be completed as part of the next phase of developments. No technical barriers are foreseen to finishing this work.

4.6.1 Truck Brake Systems

The products of this research can be used in a variety of ways to test ESC system developments on heavy commercial vehicle braking systems.

For instance, the development of ECBS on trucks for the North American market is currently a topic of interest. This hardware bench test system can be used to test the implications of new braking system actuation technologies associated with electronic braking systems.

Also, in the development of new braking control systems for heavy commercial vehicles, it would be beneficial to test these developments with components from each braking system manufacturer. Differences in performance of these components could affect the overall performance of the braking system as a whole.

Future work with this test apparatus would benefit from the hardware to control a complete tandem axle on a trailer. This would include adding a solenoid-operated relay valve, four ABS modulator valves, and four wheel speed sensors.

4.6.2 Development Control System Hardware and Software

The products of this research can also be used in a variety of ways to test control system developments on heavy commercial vehicle braking systems.

For instance, the capability of various configurations of controllers, networks, data acquisition systems, and data analysis methods can be tested using this hardware bench test system.

The hardware bench test system can be used to explore bandwidth requirements for communication between vehicle unit stability-control-system controllers. Through analysis of sensor throughput and control signal requirements, the hardware system would provide a platform for developing a specification for such communication.

Various network or data acquisition devices might be evaluated in the development of a new control system. This hardware bench test system can be used to discover problems with the integration of these devices into the control system.

Another use for the system would be to determine potential communication architectures for communication between vehicle unit stability-control-system controllers.

Further, various kinds of sensors and sensor systems could be tried in the development of a new control system. This hardware bench test system can be used to verify the connectivity and performance of these sensors prior to implementation on an actual test vehicle.

Finally, various methods in fault detection and fault tolerance can be researched using this hardware bench test system, since failures can be simulated in a safe and predictable way

4.6.3 Generalizations to Longer Combination Vehicles

As noted, the need to develop a better method to assess the entire vehicle's stability will become even more important as additional trailer units are added. Because the issues of data acquisition and hardware control also become more complex, the need for a test apparatus to develop and prove the control system concept also becomes more important as additional trailer units are added. The hardware bench test system can serve as a tool for controller development for these vehicles.

Because of the modular design of the hardware bench test system, the addition of more trailers can be easily accommodated by the addition of the brake actuation hardware and sensors. The additional data acquisition requirements can be met with the PXI analog input/output cards chosen. Additional controllers can be added as nodes on an Ethernet network in the case of a multi-CPU option, or using the MXI-bus in the case of a single CPU option.

Chapter 5 – Feasibility of Intra-Vehicle Wireless Communication

Recent advances in wireless technology have enabled high data rates as well as higher reliability and security in intra-vehicle wireless communication, even in harsh commercial vehicle wireless environments. The benefits of using wireless communication for vehicle stability control are numerous. While many challenging problems exist because of the harsh wireless conditions in intra-vehicle networks, the research results in this section show that these problems may be overcome with the appropriate wireless networking techniques. In particular, potential problems, such as channel fading, packet collisions, occlusion, congestion, and interferences, can be overcome using a combination of techniques, including rate adaptation, dynamic channel hopping, multi-hop routing, and efficient broadcast.

5.1 Benefits of Wireless Electronic Stability Control

There are many benefits in utilizing intra-vehicle wireless communication to support a vehicle stability control system where the sensor and actuator control data is transmitted wirelessly between the tractor and trailers. First, trailers and tractors may be interchanged easily without the need to plug in the connectors for the sensor and actuator signal cable. (This is especially important when one trailer in a combination is equipped and another is not.) The signals will be dynamically transmitted through the wireless channels at a high data rate and reliability. Second, the wireless channel enables transmission of different type of signals typically sent through different types of cables, such as the CAN data bus, serial cable, and Ethernet. Commercial vehicle drivers need not deal with the different types of connectors. Third, wireless transmission can enable the different types of signals to be integrated into a single standard for wireless sensor data and actuator transmission. This will simplify the development of new sensors and actuators, which may eliminate the need to deal with different types of sensor and actuator data bus protocols.

5.2 Challenging Problems of Intra-Vehicle Wireless Communication

Intra-vehicle wireless communication presents many challenging problems due to the harsh wireless conditions in which intra-vehicle networks operate where wireless transmission may deteriorate due to many reasons, including channel fading, collisions, occlusion, congestion, and interference.

As wireless technologies proliferate in many applications for wireless access by mobile/portable devices, the increasing amount of wireless traffic leads to poor channel quality. Channels can deteriorate due to any of six main reasons:

1. Signal fading caused by signal propagation loss between two associated stations and effects of multi-paths
2. Collision caused by simultaneous transmissions from different stations

3. Interference from nearby unrelated signals or jammers
4. Congestion in the network that may cause packet loss
5. Occlusion due to objects that obstruct radio propagation
6. Antenna placement and orientation as well as vehicle movement, that may cause deterioration in wireless reception.

Since these causes cannot be eliminated due to the unstable nature of the wireless medium, appropriate adaptive protocols must be used to address each of these sources of wireless channel degradation more accurately.

To improve the performance of wireless vehicle networks, the main characteristics of outdoor wireless transmission environments as well as the effects of mobility must be understood.

First, the signal propagation delay increases in outdoor wireless networks due to larger transmission distance compared to indoor wireless networks, which in turn may affect the performance of the MAC protocol. Second, the outdoor wireless environment has increased delay spread that causes inter-symbol interference. Third, Doppler effects due to mobility may require sophisticated channel estimation.

Capabilities for dynamic reconfiguration of the system will be required to handle the situation where some trailers in a multi-trailer combination are equipped with ESC (wireless or not) and other trailers are not. As trailers are being interchanged, the trailers will communicate with the tractor ESC controller regarding their positions and sensor capabilities. Trailers not equipped with ESC will not communicate with the tractor controller. After the interchange is complete, the tractor controller will know the final configuration of the trailers, and the sensor data received will be associated correctly with each ESC-equipped trailer. The ESC system will then use the correct sensor data from the respective trailers to control the tractor-trailer behavior.

5.3 Summary of Wireless Communication Protocols

Wireless vehicle networks may be built using different wireless protocols, such as IEEE 802.11a/b/g/n, dedicated short-range communication (DSRC) (IEEE 802.11p), WiMAX, ZigBee, etc. To select the best wireless protocol for intra-vehicle wireless networks, performance and usability studies were performed to compare these wireless protocols, particularly in the commercial vehicle environments. Some of these studies were based on qualitative analyses, while others were based on performance measurements of the actual wireless transmission using performance tools, such as a product named “Iperf.”

5.3.1 IEEE 802.11a/b/g/n (Wi-Fi)

The IEEE 802.11 standard consists of a family of protocols. In this particular category, a group of related protocols are commercially available, i.e., IEEE 802.11a/b/g/n protocols, which are

generally known as Wi-Fi networks. Versions a, b, and g are prior versions; the current version, IEEE 802.11n, is the highest performing. There are many benefits in using IEEE 802.11n because of its many advanced features, including multiple-input, multiple-output (MIMO), spatial multiplexing, MCS (Modulation and Coding Scheme), STBC (Space-Time Block Code), channel bonding, and frame aggregation. These features enable IEEE 802.11n to transmit at a rate of more than 100 Mbps (with two antennas) with reasonably low packet loss rate. This is the main reason that IEEE 802.11n was selected over the other protocols for the prototype intra-vehicle wireless network for supporting ESC.

IEEE 802.11n operates in two ISM bands, either in the 83.5 MHz bandwidth of the 2.4GHz band or at the 125 MHz bandwidth of the 5.8 GHz band. The bit rate of the wireless link depends on the size of the spectrum. However, the bit rate limitation can be overcome using MIMO antenna technology, which uses several antennas to create multiple streams of data. Depending on the number of antennas, IEEE 802.11n can achieve a bit rate of up to 300 Mbps, when configured with three antennas. The transmission range of IEEE 802.11n in ideal conditions is about 53.3 meters or 175 feet (in the 2.4 GHz frequency block), longer than a turnpike double with two 14.6-meter (48-foot) trailers (Ervin et al. 1984).

However, in vehicle wireless networking environments, there are some pitfalls in the use of IEEE 802.11n (as well as the other wireless protocols described below), which could affect the performance and reliability of intra-vehicular wireless communication. The performance could degrade due to the harsh operating environment, including mobility, congestion, collision, interference, jamming, vibration, and antenna polarization mismatch. This research work shows how performance may be improved using techniques for overcoming some of these problems. Although the study used IEEE 802.11n, the techniques may also be extended to other protocols, e.g., DSRC.

5.3.2 DSRC (IEEE 802.11p)

The main advantage of using DSRC is that it uses the 5.9 GHz band that is specially allocated for vehicle networks, whereas IEEE 802.11n is used for a very wide range of wireless applications. However, the main disadvantage is that it does not include many of the advanced features of IEEE 802.11n, and thus gives lower performance and reliability.

The U.S. Federal Communications Commission (FCC) allocated the 75 MHz bandwidth of the 5.9 GHz band for vehicle-to-vehicle and vehicle-to-infrastructure wireless communication in 1999 (Cheng et al. 2007). The commission then established the service and license rules for DSRC service, which operates on the 5.850 to 5.925 GHz band for public safety and private applications in vehicular networks. In 2001, ASTM International selected IEEE 802.11a as the underlying radio technology of DSRC's physical layer (ASTM 2003). In 2004, the IEEE started the work on the 802.11p amendment and wireless access in vehicular environments (WAVE) standards based on the ASTM standard. The transmission range of DSRC is about 1000m.

DSRC supports both safety and commercial non-safety applications by providing separate channels. The 75 MHz licensed spectrum is divided into 7 different channels with 10 MHz channel bandwidth each. Both safety and non-safety applications can co-exist through a periodic Time Division Multiplexing (TDM) scheme. TDM in the application level is achieved using time synchronization between the communicating units, e.g., using Universal Coordinated Time, as proposed in the IEEE communication standards in development for the DSRC band.

5.3.3 WiMAX

WiMAX is designed for wireless metropolitan-area networks. It provides a service range of up to 31 miles (50 km), shared data rates of up to 70Mbps, and a peak data rate of up to 268Mbps. The WiMAX standard IEEE 802.16a supports non-line-of-sight transmission in the range between the 2GHz and the 22GHz bands. IEEE 802.16e-2005 supports mobility, but has a peak downstream data rate of 12Mbps and an upstream data rate of 2Mbps to 5Mbps. Its range is less than 50 km. WiMAX operates on both the unlicensed frequencies of the 2.4GHz and 5.8GHz bands and the licensed frequencies of the 2.5GHz and 3.5GHz bands. For industrial purposes, the licensed spectrum is used. Mainly because of the licensed frequencies and the low throughput, WiMAX is not considered for wireless vehicle communication.

5.3.4 Other Wireless Communication Protocols

There are other low-powered wireless protocols, such as ZigBee (IEEE 802.15.4) and Bluetooth (IEEE 802.15.1). These wireless protocols are designed for wireless personal area networks (WPANs) with smaller coverage area and lower power consumption. ZigBee operates at the frequency spectrum of 902 to 928 MHz and 2.4 GHz, whereas Bluetooth operates at 2.4 GHz. The transmission range of ZigBee is 100 meters, while that of Bluetooth is only 10 meters. On the other hand, the data rate of ZigBee is only 20 to 250 kbps, while that of Bluetooth is 1 Mbps. Because of their low data rates and transmission range, these protocols are not considered for vehicle networks.

5.4 Improving Reliability and Throughput in Wireless Vehicle Networks

Although IEEE 802.11n provides high throughput and reliability, the actual transmission could degrade due to many problems in the harsh operating environments of commercial vehicle wireless networks. Different techniques must be developed to improve the performance by overcoming these problems that include mobility, congestion, collision, interference, channel fading, jamming, vibration, and antenna polarization mismatch.

The goal was to focus on techniques that will give high throughput and reliability in spite of the presence of collision, channel fading, interference, and congestion. Wireless transmission degradation is often caused by a combination of these factors. Since different techniques are used to overcome different forms of degradation, it is important to detect accurately the real cause of the wireless degradation. Small probe packets are used to distinguish the three main types of wireless degradation: collision, channel fading, and interference. If the cause of

degradation is interference, then the secure and robust framework that uses dynamic channel selection can be used. If the cause is collision, then the appropriate collision avoidance protocols, such as RTS (Request to Send) and CTS (Clear to Send), can be used. If the cause is channel fading, then the Fast Recovery Rate Adaptation can be used. If the cause of degradation is due to severe channel fading, then a multi-hop routing protocol can be used to avoid packet loss. Congestion in emergency broadcast scenarios can be avoided using an efficient broadcast algorithm that combines aggregation with coding techniques. The methods for overcoming wireless degradation are summarized in Table 5-1.

Table 5-1. Selection of methods for overcoming wireless channel degradation.

Causes of Wireless Channel Degradation	Collision	Channel Fading	Interference	Severe Channel Fading	Broadcast Congestion
Methods for Overcoming Wireless Problems	Collision Avoidance Protocol	Rate Adaptation Algorithms	Dynamic Channel Selection	Multi-Hop Routing	Efficient Broadcast with Aggregation

5.4.1 Secure and Robust Framework for Wireless Intra-Vehicle Networks

The core integrated vehicle network and framework is designed to manage the wireless channels in the wireless intra-vehicle network. It monitors channel quality and interference to provide high-throughput communications, network authentication, emergency message propagation, and multi-hop packet forwarding. It uses a cluster-based network architecture that dynamically creates clusters. A cluster head node (CN) in each cluster serves as a dynamic channel hopping coordinator for its cluster members so that different channels are allocated to different communication links to avoid potential co-channel interference. The network cluster provides secure wireless networking using IEEE 802.11i, as implemented in Wi-Fi Protected Access (WPA). The IEEE 802.11i standard provides security mechanisms for Robust Security Network, including 4-way handshake and group key handshake. WPA implements the majority of the IEEE 802.11i standard, including the Temporal Key Integrity Protocol, which supports encryption and message integrity checks to prevent replay attacks. The network cluster supports network authentication and encryption that are useful for ensuring that the wireless intra-vehicle network of one tractor trailer will not affect that of another in a nearby or adjoining highway lane.

In this secure and robust framework, dynamic channel hopping can be used for overcoming jamming and interference. The system first accurately determines if interference (and not fading) is the actual cause of transmission degradation, in which case the dynamic channel hopping algorithm will select a new channel with the least interfering signals and thus avoid the interference (which may be caused by external sources). The dynamic channel hopping

algorithm is similar to the dynamic frequency selection (DFS) algorithm. In this framework, when wireless nodes need to communicate, the Master node that has interference detection capabilities will select the best channel. If interference is detected, the system selects another channel with the least interference.

5.4.2 Fast Recovery Transmission Rate Adaptation Method

The second method for improving throughput and reliability is using a Fast Recovery Rate Adaptation (FRRA) algorithm. This uses small probe packets to accurately determine whether the cause of poor transmission throughput is fading or interference. If the cause is fading, then the transmission rate is reduced in order to improve the delivery ratio, i.e., reduce packet error rate, thus improving the vehicular network robustness and throughput. Since wireless conditions may change frequently, this algorithm provides fast recovery when the dominant problem changes from fading to interference, in which case the algorithm will switch to methods for avoiding interference and maintaining high transmission rate. The effect of FRRA rapid reaction to the changing wireless conditions will allow FRRA to improve the throughput and reliability of intra-vehicle wireless networks.

5.4.3 Reliable and High-Connectivity Multi-hop Communication Protocol

The third method for improving throughput and reliability is to use multi-hop wireless transmission. This method is used when the system determines that wireless transmission over a single link results in a severe fading problem, possibly due to distance or reduced transmission power. Severe fading problems may also occur when there is radio occlusion, such as from the trailer to the tractor, or occlusion between vehicles. When severe channel fading occurs, rate adaptation methods will not help. In this case, reliable multi-hop forwarding through intermediate nodes on the trailer and truck will ensure reliable transmission between these nodes. (Each node represents a device that is equipped with wireless transceiver, antenna, processor, and storage.) The routing algorithm selects the multi-hop path that provides the best transmission quality and network connectivity for forwarding packets. The network connectivity information will first be modeled based upon statistical network density data, and then will be updated after real-time density information is collected. Because in the multi-hop scheme, the distance between nodes in each hop is relatively short, the transmission reliability is relatively high. Hence reliable transmission of sensor and actuator data can be achieved using multiple short but reliable wireless links.

5.4.4 Efficient Broadcast Protocol

Broadcast packets such as emergency messages may cause congestion in wireless channels. In order to improve performance in these highly congested wireless conditions, a more efficient broadcast protocol is required to reduce congestion and improve throughput. To demonstrate the feasibility of a more efficient broadcast protocol, the Auburn University vehicle wireless network team developed an efficient broadcast protocol that aggregates broadcast packets at

intermediate nodes and then re-broadcasts them to others. The hierarchical aggregation of observations was used in dissemination-based, distributed traffic information systems. Instead of carrying specific values, the aggregates in this study contain a probabilistic approximation. This scheme can overcome two central problems of existing aggregation schemes for vehicular networks. First, when multiple aggregates of observations for the same area are available, it is possible to combine them into an aggregate containing all information from the original aggregates. Second, any observation or aggregate can be included into higher level aggregates, regardless of whether it has already been previously added. Using this efficient broadcast protocol, the number of packets in the wireless networks can be reduced, thus improving the throughput and reliability.

5.5 Implementation of Wireless Intra-Vehicle Networks

The implementation of wireless intra-vehicle networks requires an understanding of how throughput and latency requirements of the vehicle ESC system can be satisfied by the actual performance of the wireless hardware, network protocols, and software. Throughput is measured by the number of bits actually transmitted per second. Latency is the time from which a message is transmitted to the time it is received, which includes the time spent in the network protocols and operating systems.

5.5.1 Requirements for Wireless Communication in Vehicle Electronic Stability Control

To implement wireless intra-vehicle networks, the minimum raw data rates for transmission of sensor and actuator control data in a wireless vehicle ESC system must be computed. Since the minimum data rate does not consider packet loss, higher data rates would be necessary to handle retransmissions due to packet loss. By estimating the packet loss and minimum data rate, the actual data rate that is required can be derived.

The wireless communication link between the trailer controller and the tractor controller supports transmission of sensor data from the trailer to the tractor and control data in the reverse direction. Each sensor data packet contains all the desired vehicle parameters, whereby the total minimum sensor data packet size is 30 bytes. Each sensor data packet contains the following sensor information:

- Trailer Ax, Ay, and Az (3 bytes)
- Trailer Angular Rate (yaw, roll, pitch) (3 bytes)
- Trailer Angle (yaw, roll, pitch) (5 bytes)
- Trailer Position (Latitude, Longitude) (16 bytes)
- Two Trailer Wheel Speeds (2 bytes)
- Air Suspension Load (2 bytes).

Since side slip can be calculated from the yaw rate, lateral acceleration, and GPS data, this sensor data includes all the state and vehicle parameters that are required for ESC as described in Section 3.2.2. The total number of bytes of sensor data in each packet is 31. Assuming that the sensor and control data is transmitted through TCP (Transmission Control Protocol) for reliability, then the additional header sizes for TCP, internet protocol (IP), and IEEE 802.11n are 20 bytes, 20 bytes, and 34 bytes, respectively. Hence, the total number of bytes in each sensor data packet is $31+20+20+34$ bytes, i.e., 105 bytes or 105×8 bits.

Since the update rate of the sensor data is 100 Hz, the minimum required bandwidth for the wireless sensor data transmission is $105 \times 8 \times 100$ bits/sec, i.e., 84 kbps. This bandwidth required for ESC is well below the 24 Mbps transmission rate of IEEE 802.11g, even with a high packet drop rate. This rate is comparable to the typical baud rate of OBD systems, 100 kbps. From experience with transmission over distances of 30 to 50 meters, the packet drop rate is below 10%. Assuming that a retransmission is sufficient to retransmit dropped packets, then the actual sensor rate is 84×1.1 kbps, i.e., 92.4 kbps. Although the drop rate could be higher in the harsh tractor-trailer environment, the required transmission should still be supported. Tests of the wireless transmission in the actual triple tractor-trailer environment showed packet loss rates of less than 10% and transmission throughput of about 40 Mbps. Other road and weather conditions may cause weak transmission and disconnections due to interference, collisions, non-line of sight problems (occlusion), and channel fading. Attenuation from heavy rain will likely cause a drop in the transmission throughput, although experiments to measure throughput degradation due to rain have not been conducted. In future work, more tests will be performed in poor weather conditions to determine how much the throughput will drop due to the effects such as splash and accumulated snow on the wireless transmission.

The packet size of the control data is 2 bytes. Each control packet contains the following control data: Left Side Brakes (1 byte) and Right Side Brakes (1 byte). When added to the additional header for TCP (20 bytes), IP (20 bytes), and IEEE 802.11n (34 bytes), then the total packet size of the control data packet is $2+20+20+34$ bytes, i.e., 76 bytes or 76×8 bits. With the update rate of 100 Hz for control data, then the total minimum bandwidth required is $76 \times 8 \times 100$ bps = 60.8 kbps. Again, assuming packet drop rate of 10% and that only one retransmission is required for each dropped packet, then the actual control data rate is 66.9 kbps. Thus the total required bandwidth for both the sensor and control data is 158.4 kbps. This is again well below the 40 Mbps transmission rate of IEEE 802.11n.

The total delay for transmitting each sensor signal or data packet should include transmission time, propagation, and processing delay. From field measurements, the total delay for each packet transmission is typically 1 or 2 milliseconds. The transmission delay is very small, i.e., less than 0.03 milliseconds, based on the packet size of 832 bits for all the vehicle sensor parameters as listed above, and the transmission rate of 40 Mbps.

The above delay is based on a packet drop rate of less than 10% for the distance of 30 to 50 meters as in field measurements. However, if the transmission channel is weak, higher drop rates and retransmissions will result and will increase the latency to possibly 10 milliseconds for each packet transmission.

5.5.2 Wireless Hardware Configuration of Wireless Vehicle Electronic Stability Control

The configuration of the wireless hardware for implementing a wireless vehicle ESC system consisted of a Mini-ITX (Model NM10-A-E), manufactured by ZOTAC, with Intel Atom D510 1.66GHz Dual-core CPU and 4GB memory. In the current experiments, two IEEE 802.11n wireless cards were tested: Ubiquiti SR71-E (Atheros AR9280 chipset) and Intel Centrino N6200. Both of them support most functions provided by the IEEE 802.11n standard. The storage on the platform was a solid state disk 50GB hard drive.

Since cost efficiency is paramount in intra-vehicle communications, standard commercial omnidirectional antennas were used in the experiment: D-Link 7dBi omni-directional antenna (ANT24-0700). Most commercial IEEE 802.11n radios are designed for indoor use and are limited to 100mW, which is smaller than the outdoor radios (1W). On the other hand, transmitting at high power outputs will result in very low data rates due to delay spread, which is the time delay in which reflected radio signals arrive after the direct signal has arrived at the receiver. Since delay spread will cause interference with other signals, a lower data rate is required to avoid interference. Hence, very few high-power IEEE 802.11n radios are available for outdoor environments. Most wireless IEEE 802.11n radios transmit using low-gain vertical omni-directional dipole antennas such as the D-Link 7dBi selected for this study.

5.5.3 Networking Protocols for Transmission of Sensor and Actuator Control Data

For wireless transmission of the sensor data and the actuator control data between the tractor controller and the trailer sensor hub, several networking protocols and software applications are required, including TCP, IP, IEEE 802.11n MAC, CAN data bus, USB, and serial data bus. Since a variety of sensor types may be used, different types of sensor communication protocols may be used. For instance, u-blox brand GPS uses USB, Novatel GPS uses serial bus, Oxford RT uses User Datagram Protocol (UDP), and string potentiometers analog-to-digital (A/D) converters use the CAN data bus. To transmit data from these sensors to the different sensor communication protocols over the wireless channels, there are two extreme design approaches: either collect all the sensor and control data into packets using a special software and transmit the packets or simply tunnel the sensor and control data over the wireless channels using ssh (secure shell). In the current experiments, the simpler tunnel approach was used, so that the sensor data that was sent through the CAN data bus was received over the ssh connection as CAN data at the other end of the wireless tunnel. Since ssh is connection-oriented and implemented using TCP, packet transmissions over the ssh were reliable, i.e., any packet that was dropped was automatically retransmitted by TCP up to seven retransmissions.

In some sensors, such as Oxford RT, sensor data is transmitted over UDP packets. In this case, the UDP packets needed to be forwarded through different subnets, such as the sensor hub subnet, the wireless subnet, and the controller subnet. By using IP routing, UDP packets were automatically routed from the sensor hub to the controller at the tractor.

TCP and UDP packets were transmitted over IP and IEEE 802.11n MAC protocols. In order to improve the performance of these transmissions, it is important to improve the performance of the wireless IEEE 802.11n MAC layer where most of the performance degradation was expected to occur. The implementation of three main methods for improving performance at the IEEE 802.11n MAC layer is described below.

5.5.4 Implementation of Fast Recovery Rate Adaptation Method

The Fast Recovery Rate Adaptation Algorithm was implemented in the “ath9k” driver for IEEE 802.11n executing first on the Fedora14 Linux Operating System and later revised for Fedora15 with compatible wireless version 2.6.38.2-2. The implementation contains codes for measuring and analyzing performance of the protocol.

One of the main issues encountered in IEEE 802.11n wireless transmission is a tendency for a large number of frame errors, which can be corrected using retransmissions through the proper automatic request response protocol. However, setting the right retransmission limit becomes important. At first, the retransmission limit, i.e., multi-rate retry (MRR), was set to only 4. This means that FRRA abandons a frame that it fails to transmit four consecutive times. In this case, when the MRR was set at 4, experience shows that the protocol will drop many frames. However, when the MRR was set at 20 (r0:8 r1:4 r2:4 r3:4), then the number of dropped frames was very much reduced. The MRR notation of (r0:8 r1:4 r2:4 r3:4) means that when a frame transmission fails, the protocol will retry transmission first at rate r0 for another seven times and if those fail, it will then retry transmission at a lower rate of r1 for four times. If those fail, it will retry transmission at a lower rate r2 for four times and if those fail, it will retry transmission at a lower rate of r3 for another four times. If all those fail, then the frame will be dropped; otherwise the frame is transmitted successfully. This MRR setting was the same as used in the ath9k rate adaptation and in Minstrel.

5.5.5 Implementation of Multi-Hop Communication Protocol

The multi-hop protocol is implemented at the application layer using UDP socket programming libraries. Since it is implemented at the application layer, the communication time is slightly longer than if it were implemented at the network layer (Figure 5-1). However, network layer implementation is more complex and kernel debugging is more time consuming. This application layer implementation could be re-implemented at the network layer in the actual software distribution, where efficiency is important.

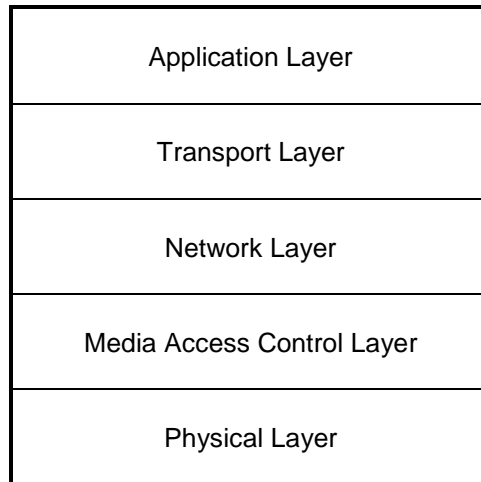


Figure 5-1. Diagram. Network architecture.

The implementation of the multi-hop protocol execution was tested on four Mini-ITXs (Model NM10-A-E), manufactured by ZOTAC, with Intel Atom D510 1.66GHz Dual-core CPU and 4GB memory. In the multi-hop experiments, Ubiquiti SR71-E (Atheros AR9280 chipset) IEEE 802.11n wireless cards were tested. The wireless cards were configured in ad hoc mode for the multi-hop protocol. For the purpose of the current tests, the multi-hop protocol application used static routing based on a configuration file.

For the purpose of measuring performance in terms of throughput, packet loss rate, and latency, codes were implemented for collecting the necessary measurement data, e.g., number of packets and timestamps. To ensure that the timing of the four mini-ITXs is consistent, they were time synchronized with each other using NTPd (Network Time Protocol daemon). The timestamps were placed right before sending and right after receiving packets.

5.5.6 Implementation of Efficient Broadcast Protocol

To study the performance improvement of the implementation of the efficient broadcast protocol, many wireless nodes were necessary. Since it was difficult to conduct these tests on the limited number of wireless nodes available, this test was conducted using the ns-2 network simulation tool. Using ns-2 simulation, the performance improvement of efficient broadcast over traditional broadcast can be studied when there are several hundred wireless nodes. When there are large numbers of broadcasting wireless stations, the performance can be reduced drastically. Efficient broadcast can alleviate this problem by reducing the number of packets being broadcast. The implementation of the efficient broadcast protocol on ns-2 can be easily re-implemented in the actual wireless devices when the need arises. The ns-2 network simulation tool is a discrete event simulator that is commonly used for simulation of routing protocols, particularly in ad-hoc networking research, and supports many popular network protocols. It offers simulation results for both wired and wireless networks.

5.6 Experimental Results and Analysis of Wireless Intra-Vehicle Networks

Experiments were conducted to study the reliability and performance of wireless networks for intra-vehicle networking under different wireless conditions and network configurations. Their performance and reliability were measured in terms of throughput and packet loss rate. Based on analysis of these results, methods were developed for overcoming these wireless networking problems, including a rate adaptation algorithm, multi-hop routing, and efficient broadcast with aggregation. The performance and reliability of these methods were measured and evaluated to show improvements.

5.6.1 Experimental Setups for Studying Performance of Wireless Intra-vehicle Communication

Three main experimental setups were used for studying the performance of wireless intra-vehicle communication using IEEE 802.11n:

1. Auburn University National Center for Asphalt Technology (NCAT) test track with a tractor and triple trailer combination (Figure 5-2)
2. Minivan on the I-85 highway
3. Static outdoor test environment beside Shelby Center at Auburn University.

To compare performance and reliability, the experiments were conducted using wireless devices and network protocols based on a combination of different parameters as follows:

- IEEE 802.11n wireless cards used were either Ubiquiti SR71-E or Intel Centrino N620
- The frequencies tested were 2.4 GHz and 5.8 GHz
- The rate adaptation algorithms studied were FRRA, ath9k, Minstrel, and fixed rate
- Either one stream or two stream transmission was used
- Three different antenna orientations were used.

The software used for measuring the performance of IEEE 802.11n transmission throughput and reliability was Iperf. The results of network throughput and data packet loss evaluations were collected for the different experimental setups to study the impact of each configuration and condition on IEEE 802.11n performance and reliability. The performance of a wireless intra-vehicle network can be affected by the surrounding conditions, interferences, and network congestion level. Variations of the performance results provided by Iperf provide a better understanding of the effect of different channel conditions and insights into how performance of IEEE 802.11n can be improved for intra-vehicle networks. To establish a baseline for all measurements and eliminate effects of variation of channel conditions, the network throughput was measured at 5 ft range with an unobstructed line of sight before each experiment. When there was no variation in throughput and data loss results, different experiments were initiated.

To study the effect of antenna polarization mismatch on wireless intra-vehicle networks, experiments were performed with wireless transmission using a triple tractor-trailer running on the NCAT test track at Auburn University. Figure 5-2 shows the tractor and triple trailer and the

NCAT test track used in the experiments. The wireless transmission tested was between the third trailer and the tractor, with a distance of about 30.5 meters (100 feet). Figure 5-3 shows how the wireless controllers (Mini-ITXs) and the antennas are attached to the third trailer and were used in the experiment. In the figure, the wireless device shown is attached to the third trailer and a similar wireless device is attached to the tractor. The tractor-trailer moved at a speed of about 48 km/hr (30 mph).



Figure 5-2. Photo. NCAT test track at Auburn University.

Each wireless controller was attached with two D-Link 7dBi antennas and connected to a ublox LEA EVK-6T GPS. The triple tractor trailer was then driven around the NCAT track for about 15 minutes in each of two experiments. In the first experiment, the GPS data that was collected at the third trailer was recorded and transmitted wirelessly through IEEE 802.11n to the controller at the tractor. In the second experiment, as the triple tractor-trailer was driven around the NCAT track for 15 minutes, the wireless controllers ran Iperf tests with gradually increasing transmission rate (bandwidth). The results of these tests are discussed in Section 5.6.2 below.



Figure 5-3. Photo. Wireless controller and antennas attached to the third trailer.

To study the effect of Spatial Multiplexing Malfunction (SMM) on network reliability, the experimental setup for wireless intra-vehicle road tests used a mid-sized vehicle that was equipped with two IEEE 802.11n test platforms, with two antennas on each platform. One platform with two transmitting antennas was mounted on the rear right. Another platform with two receiving antennas was mounted on the front-right side of the vehicle. One static test and two road tests were performed. The static test was conducted with the mid-sized vehicle parked behind the Shelby Center Building at Auburn University. The road tests were conducted on the I-85 highway from Auburn, Alabama, to Columbus, Georgia, with the mid-sized vehicle moving at speeds of up to 104.6 km/hr (65 mph). The first road test involved one bent antenna to test the SMM case. In the second road test, all antennas worked well as a normal case for comparison with the SMM performance.

To study the effect of STBC and the number of streams on network performance, three different configurations of bent antennas were investigated, as shown in Figure 5-4. STBC is a technique used in IEEE 802.11n for reducing data loss by transmitting multiple copies of the same data across several antennas to improve the reliability of data transfer since various received versions of the data can be exploited. For STBC to function properly, the number of streams used in IEEE 802.11n networks should be carefully chosen, because one malfunctioning stream will significantly reduce the network performance. Each configuration had one pair of antennas aligned properly but not the other pair. For each of these configurations, three road tests were conducted: 1) double stream operation without STBC, 2) double stream operation with STBC, and 3) single stream operation with STBC. The network setup consisted of two test platforms (with two antennas each) placed on the right side of the vehicle about 15.2 meters (50 ft) apart from each other.

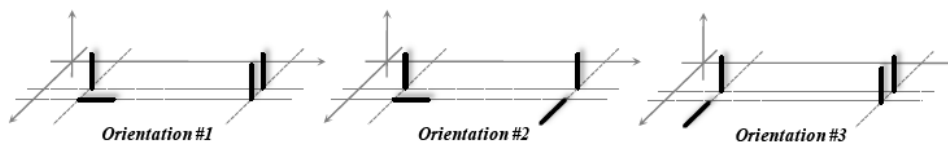


Figure 5-4. Diagram. Three antenna alignment configurations for STBC and streams tests.

To study the effect of different antenna alignment on network performance, experiments were performed with three different alignment configurations as shown in Figure 5-5. These antenna alignments were designed to overcome the problems of Antenna Polarization Mismatch and SMM in wireless intra-vehicle networks. In these experiments, the antenna alignment that was needed to maximize wireless network throughput was investigated. These antenna alignment tests used two test platforms (with two antennas in each platform), separated by a distance of 15.2 meters (50 ft) from each other. The road tests were also conducted on the I-85 highway from Auburn, Alabama, to Columbus, Georgia, with the vehicle moving at speeds of up to 104.6 km/h (65 mph).

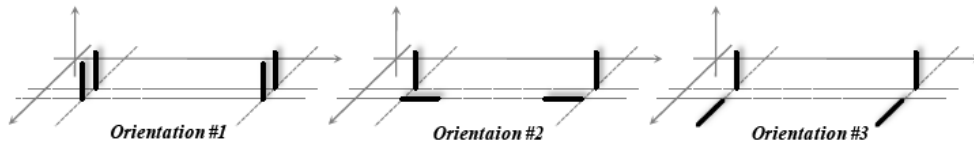


Figure 5-5. Diagram. Three antenna alignment configurations for optimal antenna alignment tests.

Two sets of tests, stationary and mobile, were conducted to measure the performance of FRRA, ath9k, and Fixed-Rate (fixed at 117 Mbps) algorithms. The ath9k protocol used its own rate adaptation algorithm. The distance between the sending and receiving antennas was fixed at 3 meters (10ft). Test bandwidths ranged from 31Mbps to 99Mbps at 3Mbps intervals. The loss rate was averaged throughout all the experiments.

To study the performance and reliability of multi-hop packet forwarding, tests were performed using the ad hoc network that had been set up with four wireless mini-ITXs with IEEE 802.11n radios. The mini-ITXs were synchronized and the information on the number of packets transmitted per time period and the packet loss was collected, whereby the throughput and packet loss metrics were calculated. In the first experiment, the objective was to show how throughput will decrease as the number of hops increase due to sharing of the wireless channel. Throughput was measured for one hop over 10 meters (33 feet), two hops over 20.1 meters (66 feet), and three hops over 30.5 meters (100 feet). In the second experiment, the intent was to show that throughput will decrease as the distance increases. Throughput performance was compared for 1 hop over distances of 10, 20.1, and 30.5 meters (6, 33, and 100 feet). In the third experiment, the purpose was to show that over the same distance of 100 feet, the throughput performance and reliability of one hop transmission is low, whereas the reliability of three hop transmission over 30.5 meters (100 feet) is stable.

5.6.2 Results of Antenna Polarization Mismatch in Wireless Intra-vehicle Communication

Antenna polarization mismatch occurs when the two antennas are not parallel to each other. Data transmission is reliable between transmitting and receiving antennas when both antennas have the same spatial orientation, i.e., have the same polarization. Otherwise, the power of wireless signal propagation between the two antennas will be reduced, causing the signal to noise ratio (SNR) at the receiving antenna to be reduced. Hence the data delivery ratio is reduced. Since mobile vehicular networks cannot guarantee the same (and constant) polarization between two antennas on two moving vehicles, antenna polarization mismatch will always occur, causing a reduction in the packet delivery ratio and throughput.

In the experiment to transmit GPS information wirelessly from the third trailer to the tractor, the results showed that the GPS data was transmitted correctly with no loss and at a rate of approximately 4kbps to 6kbps (due to the slow rate in which the GPS generated the data). This performance is possible even in the presence of antenna polarization mismatch.

Experiments were performed to measure the maximum throughput and packet loss in mobile wireless intra-vehicle networks in the presence of polarization mismatch. When the truck was stationary at the garage, and the test bandwidth was increased to 100 Mbps, the actual throughput kept increasing linearly to 100 Mbps (Figure 5-6). In a separate experiment, Figure 5-7 shows that when the truck was moving around the track, the actual throughput increased linearly as the test bandwidth is increased to 45 Mbps. (Test bandwidth is the maximum transmission rate that was set for the wireless protocol to transmit.) However, when the test bandwidth was increased further from 45 Mbps to 100 Mbps, the actual throughput fluctuated between 40 Mbps and 60 Mbps (Figure 5-7). This degradation in network performance occurred in both the straight and curved portions of the NCAT test track. This is an interesting result. When the tractor-trailer was stationary, the throughput could be increased to 100 Mbps. However, when the tractor-trailer was moving, the maximum throughput was limited to 40 Mbps by the significant packet loss due to antenna polarization mismatch. The main reason for this appears to be that when the tractor is moving, the movements and vibration of the third trailer relative to the tractor may have caused the two stream transmission of IEEE 802.11n to fail due to antenna polarization mismatch, because only one stream is possible. This leads to the limit of 40 Mbps throughput. The packet loss also increased to about 10% at 50 Mbps transmission rate when the truck was moving, compared to only 3% packet loss when the truck was stationary.

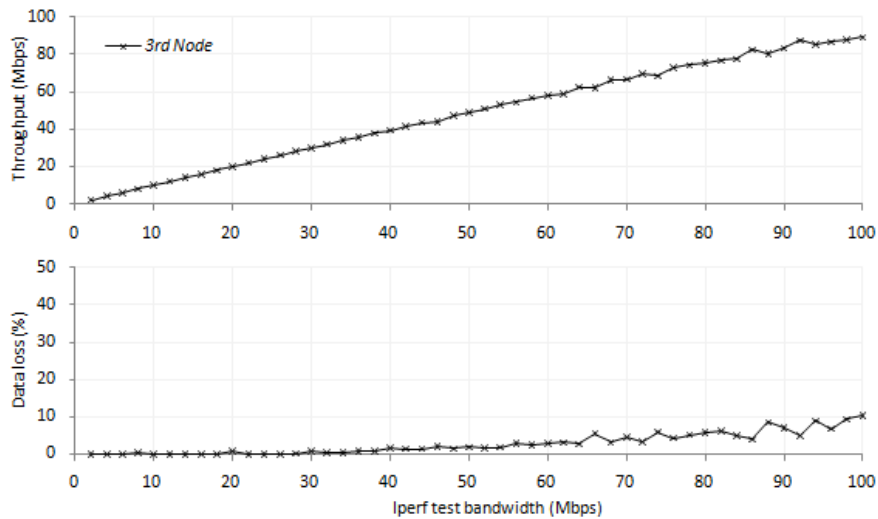


Figure 5-6. Plot. Results of wireless intra-vehicle networks with tractor-trailer stationary in NCAT garage.

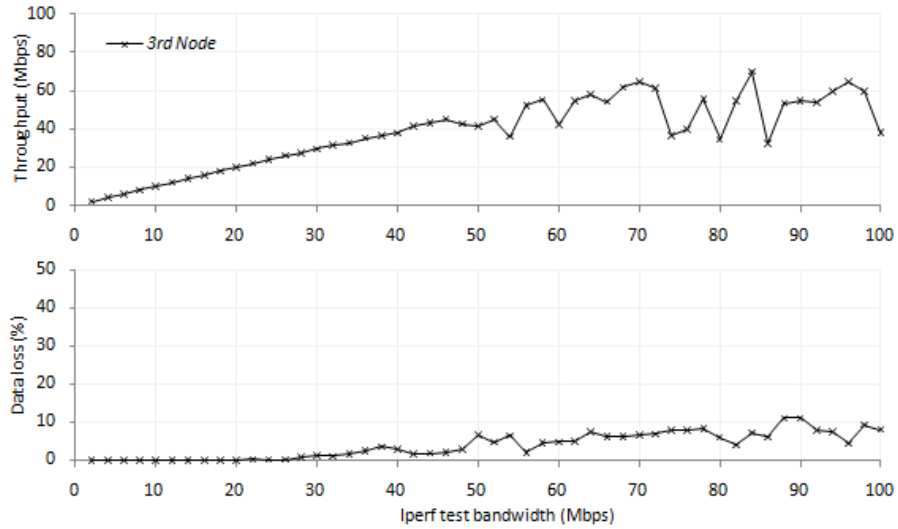


Figure 5-7. Plot. Results of wireless intra-vehicle networks with tractor-trailer running at NCAT test track.

5.6.3 Results of Spatial Multiplexing Malfunction (SMM)

Spatial multiplexing uses simultaneous transmission from independent and separately encoded data signals (or streams) through each of the multiple transmit antennas to improve throughput performance. However, spatial multiplexing will malfunction when there is a failure of some of these data streams, possibly due to problems with the transmit antennas. Since spatial multiplexing is used extensively in IEEE 802.11n to improve performance, a malfunctioning of this feature can drastically reduce the network performances.

The results of intra-vehicle road tests, shown in Figure 5-8, demonstrate some interesting phenomena. During the road tests, one of the transmitting antennas was bent by the strong winds. When that occurred, the data rates of the transmitter dropped from 130Mbps (MCS index 15) to 65Mbps (MCS index 7), the throughput oscillated drastically, and higher data loss was observed. (MCS index is the number that identifies the Modulation and Coding Scheme used to achieve the transmission rate.) This shows that spatial multiplexing does not work well with malfunctioning antennas, so the rate adaptation algorithm in IEEE 802.11n has to select a lower data rate (MCS index 7 to 0) for the single spatial stream. Therefore, the study shows that the rate adaptation algorithm in the IEEE 802.11n platforms tested does not work well in the SMM situation. That means that a new rate adaptation algorithm is needed for IEEE 802.11n to deal with the SMM issue.

The results in Figure 5-8 also show that in both the static test and road test, when the antennas were aligned properly, good network performance could be achieved in terms of high throughput, low data loss, and stable transmission data rate. Therefore, spatial multiplexing in IEEE 802.11n requires properly aligned antennas, which is not possible in typical wireless vehicle networks. Furthermore, weather changes and unstable power supplies in vehicle networks may cause asymmetrical antenna performance, leading to further degradation in

throughput and network reliability. For a wireless network supporting an ESC system to be reliable, it must be improved using advanced techniques such as those investigated in this research.

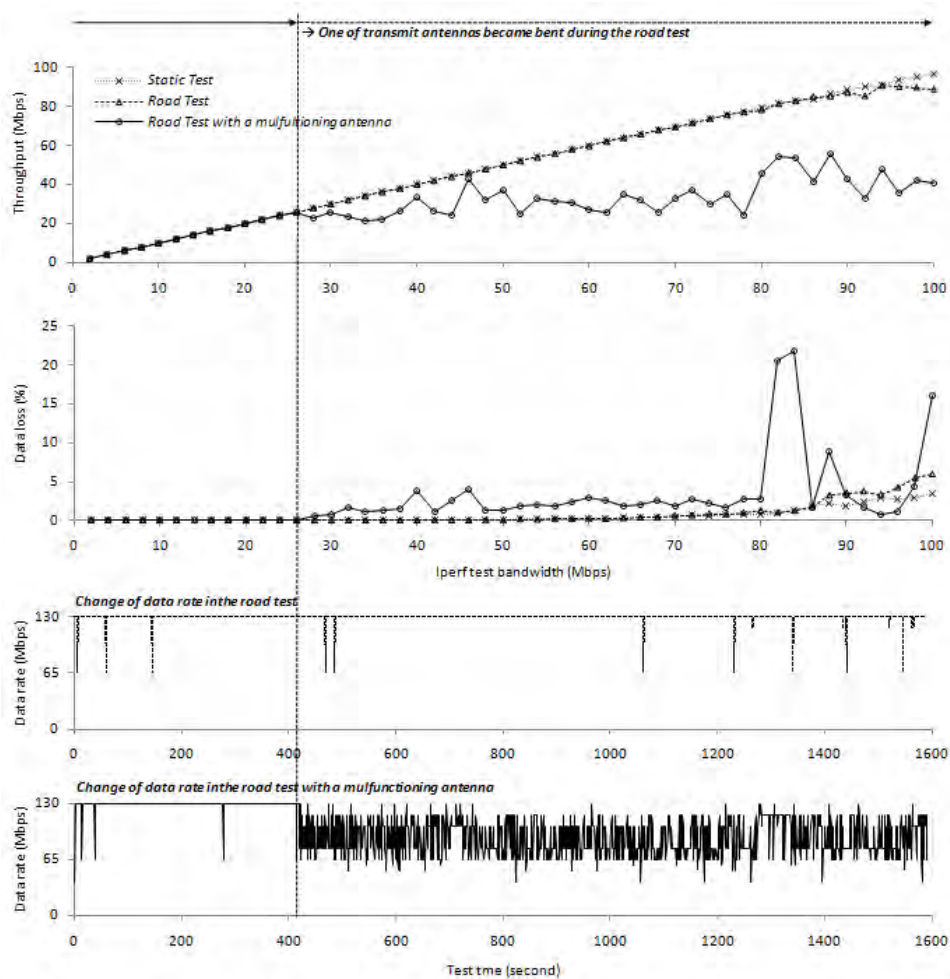


Figure 5-8. Plot. Results of throughput and packet loss with spatial multiplexing malfunction.

5.6.4 Results of Space-Time Block Code (STBC) and the Number of Streams

Figure 5-9 shows road test results of throughput, packet loss, and data rates for Orientation #1. Results for other orientations, which are similar, are omitted for brevity. The figure depicts the throughput, data loss, and changes of data rate for three scenarios: double stream operation without STBC, double stream operation with STBC, and single stream operation with STBC. The double stream operation without STBC did not work well because of the SMM issue as described above. Similar network performance can be found for the double stream operation with STBC due to the bent antenna. Interestingly, the single stream operation gives the best network throughput results.

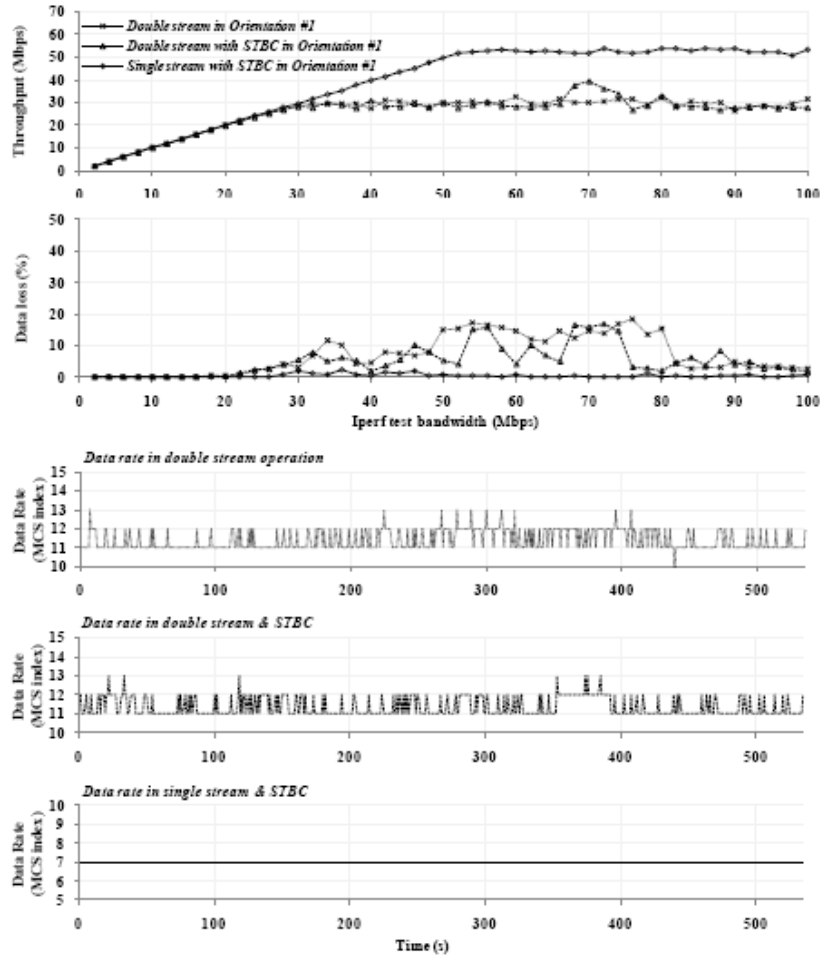


Figure 5-9. Plot. Results of tests on effects of STBC and number of streams.

The results in Figure 5-9 also show that the rate adaptation mechanism provided by IEEE 802.11n did not work properly in the present experiments. This is because even though single stream operation can effectively solve the problem caused by poor antenna alignment, the current rate adaptation algorithm of IEEE 802.11n is not aware of this antenna alignment problem. Instead it assumes that the problem is due to channel fading and tries to correct the problem using an ineffective technique of reducing the data rates. In fact, IEEE 802.11n tries data rates from MCS index 13 to 11 for the double stream operations. Figure 5-9 shows a very high frequency of data rate changes in the double stream with the STBC case compared to pure double stream without STBC. However, the data rate of single stream with STBC did not change at all and remained constant at MCS index 7, because this stream used the pair of antennas that were properly aligned. This is the main reason that the single stream gave the highest throughput performance compared to both of the two-stream cases.

Hence, single stream operation provides more reliable networks with improperly aligned antennas. Also, the optional STBC function of IEEE 802.11n helps in improving the network stability even for the string stream transmission. These test results show that performance of

wireless intra-vehicle networks will be improved for ESC if single stream with STBC is used in the IEEE 802.11n network.

5.6.5 Results of Optimal Antenna Alignments

Previous experimental results have provided better insights into the problems of Antenna Polarization Mismatch and SMM in wireless intra-vehicle networks. Based on these new insights, methods to overcome these problems were investigated through further experiments to investigate the antenna alignment needed to maximize wireless network throughput. The difference between optimal antenna alignment and avoiding polarization mismatch is that when the truck is moving, then polarization mismatch cannot be avoided; hence the maximum throughput can be obtained only using Orientation #3 in Figure 5-3. Although it is very difficult to implement antennas that are perfectly aligned all the time in real vehicle networks, it is still important to understand the optimal antenna alignment that gives the best network performance, which can take advantage of spatial multiplexing and rate adaptation algorithms.

Outdoor antenna alignments are more important than indoor antennas because in indoor environments, IEEE 802.11n may use multi-path signal reflections from building walls. On the other hand, in a typical (outdoor) vehicular network on the roads or highways, there are usually insufficient multi-path signals.

From the experiment results shown in Figure 5-10, the antenna configuration of Orientation #3 gave the antenna alignment that provided the maximum network throughput. In this configuration, there was one pair of vertical antennas and another pair of horizontal antennas, described as follows.

The main technique used by IEEE 802.11n to achieve a high throughput is spatial multiplexing, which allows data to be split and transmitted via independent data streams from different antennas. The best antenna alignments would be those that are most effective in achieving maximal spatial multiplexing in IEEE 802.11n. Three antenna configurations were designed to achieve this, as shown in Figure 5-4. The results in Figure 5-10 show the best antenna configuration. Orientation #1 uses parallel alignment of all antennas, which is considered the basic setting for WiFi antennas. Orientations #2 and #3 are better antenna alignments that are expected to provide the optimal alignment, since they cover both vertical and horizontal orientations.

The test results in Figure 5-10 show the throughput, data loss, and changes of data rate for each of the three examples discussed above. Orientation #1, the basic IEEE 802.11n antenna alignment, does not work well because it covers only one antenna polarization. Interestingly, Orientation #3 gives the best network performance in terms of higher throughput, lower data loss, and stable data rate during the test. This configuration effectively uses orthogonal spatial streams to deliver data, so signals on both vertical and horizontal polarizations are well covered. Although the antenna alignment in Orientation #2 is similar to Orientation #3, its performance is

worse than Orientation #3 because the signals on the horizontal polarization are weaker in that orientation.

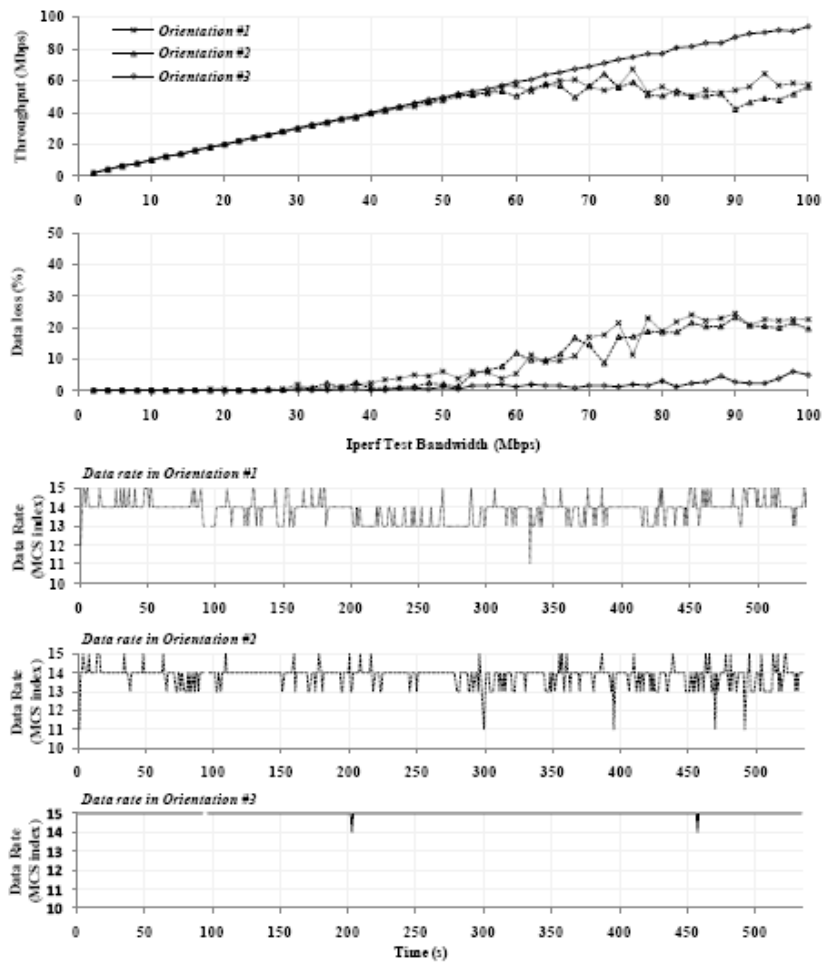


Figure 5-10. Plot. Results of tests on optimal antenna alignments.

These experimental results show that antenna-polarization diversity is critical for supporting spatial multiplexing more effectively and thus results in higher data rates and greater reliability compared to a system with only one single polarization. Therefore, IEEE 802.11n technology should consider the antenna polarization effect to fully utilize its functionality and maximize its performance and reliability for wireless intra-vehicular networks.

5.6.6 Results of Throughput Performance of Fast Recovery Rate Adaptation (FRR) Algorithm

The results of stationary tests with the FRR algorithm in Figure 5-11 show that FRR gives a slightly better performance and lower loss rate than ath9k and fixed rate (117Mbps). FRR performs slightly better for all test bandwidths from 31 to 99 Mbps. FRR particularly performs better than the ath9k rate adaptation algorithm for test bandwidths from 85 Mbps to 99 Mbps.

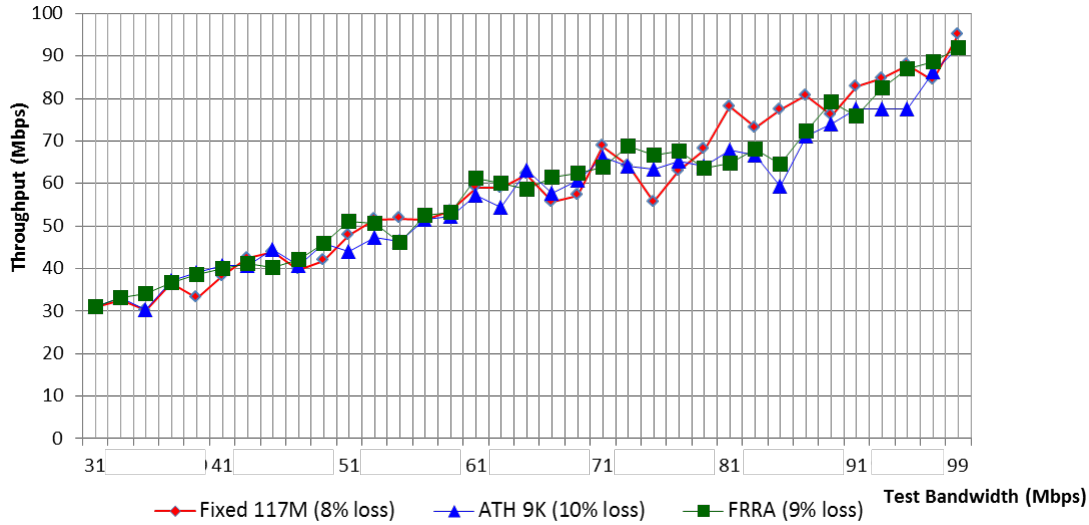


Figure 5-11. Plot. Results of stationary tests of fixed rate, ath9k, and FRRA algorithms.

The results of mobile tests (at 20 mph) with the FRRA algorithm in Figure 5-12 show that FRRA still gives a slightly better performance and lower loss rate than ath9k and fixed rate (117Mbps) for test bandwidths from 31 to 81 Mbps. However, from 85 Mbps to 91 Mbps, FRRA performs worse than the other protocols. This can be attributed to the behavior of FRRA, which responds too aggressively to channel quality variation, adversely affecting the throughput. In future work, methods for further improving FRRA by using more advanced techniques will be investigated, particularly for addressing the problems of spatial multiplexing that were discussed previously. Future work will include more tests on FRRA to demonstrate that since FRRA can distinguish between collisions and channel fading, it will better handle large variations in the actual vehicle networking environments that may cause excessive collisions and channel fading.

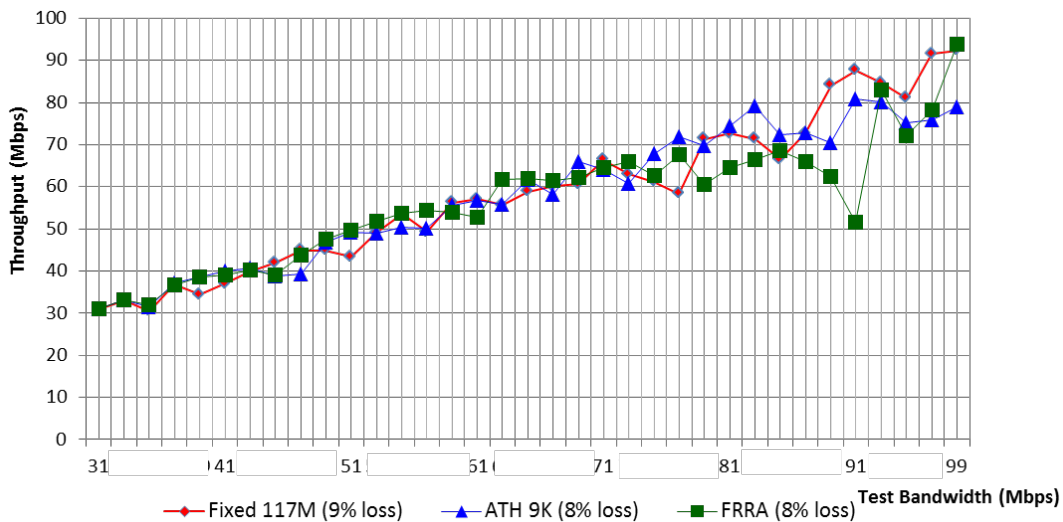


Figure 5-12. Plot. Results of mobile tests of fixed rate, ath9k, and FRRA algorithms.

5.6.7 Results of Performance of Multi-Hop Wireless Protocol

The results of the throughput tests of multi-hop packet forwarding are shown in Figure 5-13, where the maximum throughput of 1 hop over 10 meters (33 feet) distance is 14 Mbps, that of 2 hops over 20.1 meters (66 feet) is 7 Mbps, and that of 3 hops over 30.5 meters (100 feet) is 5 Mbps. In the 3 hop test, this result shows that the bandwidth is shared among the three links equally, whereby the maximum throughput of 14 Mbps for the 1 hop transmission is split into three wireless channels, each with 5 Mbps. The packet loss rate is 0 in these tests. In 3 hop forwarding, the packet loss can be reduced since the distance in each hop is considerably shorter than the distance covered by a single hop. In supporting ESC applications, the reliability provided by transmission over the shorter distance in each hop will ensure that the important sensor and actuator control information is transmitted reliably, i.e., with very low loss rate.

To show the reduction in performance over longer distances, the test results in Figure 5-14 show that as the distance of one hop increases from 1.8 meters to 30.5 meters (6 feet to 100 feet), the throughput performance drops from 15 Mbps to 11 Mbps. This shows that as the distance between the hops increases, packet loss will increase and throughput will decrease. Hence for long-distance transmission, it is more reliable to transmit the packet over multiple numbers of hops, each covering a shorter distance.

Regarding throughput degradation for 1 hop over a large distance, the test results in Figure 5-15 show that for 1 hop over 30.5 meters (100 feet), the throughput is reduced to 11 Mbps (instead of 14 Mbps over 10 meters, or 33 feet distance), whereas the throughput for 3 hops over 30.5 meters (100 feet) remains the same at 5 Mbps.

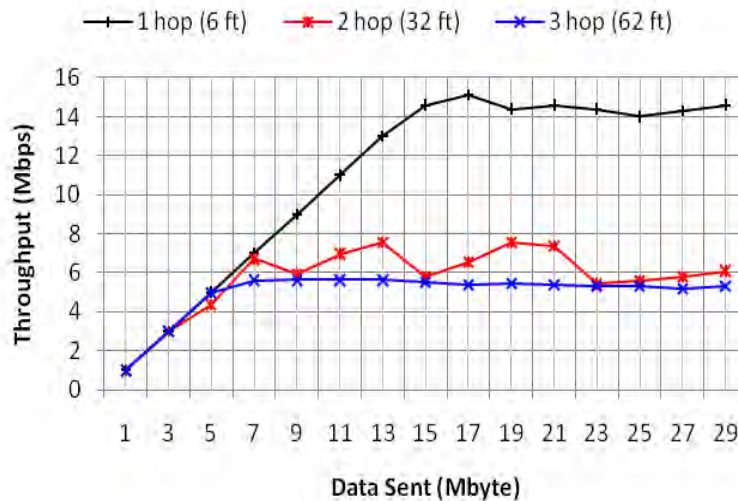


Figure 5-13. Plot. Results of throughput tests of multi-hop packet forwarding.

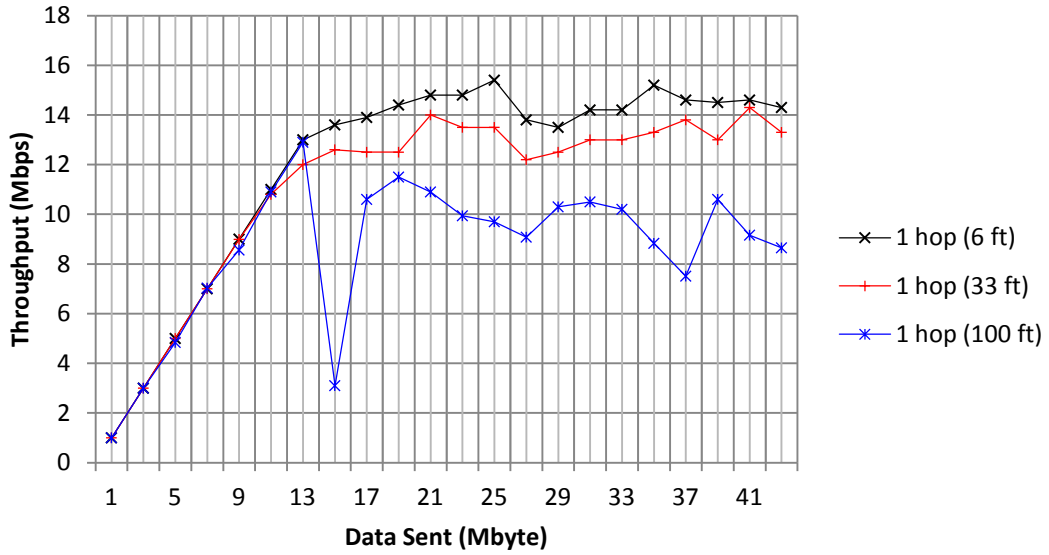


Figure 5-14. Plot. Results of throughput tests for different distances in each hop.

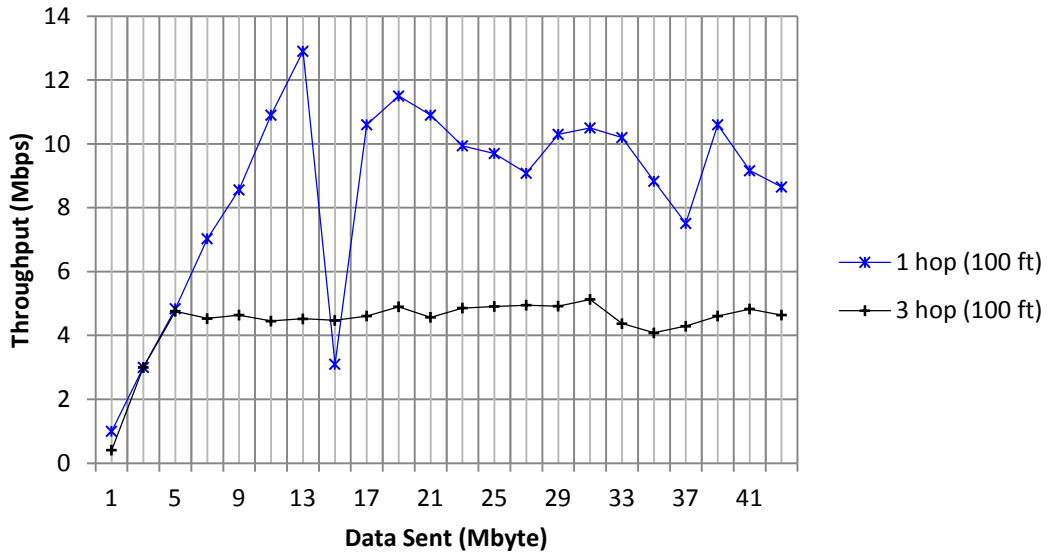


Figure 5-15. Plot. Results of throughput tests for different number of hops over the same distances.

The results of the multi-hop experiment are summarized in Table 5-2. The majority of the values were obtained from the experiments and some values were obtained by interpolation.

Table 5-2. Maximum throughput rate achieved at different distances in the multi-hop experiments.

Number of Hops	Distance			
	2 m (6 ft)	10 m (33 ft)	20.1 m (66 ft)	30.5 m (100 ft)
1	15 Mbps	14 Mbps	13 Mbps	12 Mbps
2	9 Mbps	8 Mbps	7 Mbps	6 Mbps
3	6 Mbps	5 Mbps	5 Mbps	5 Mbps

Similar antenna installations were on all three trailers in a separate test (Lim & Bevly, 2011). Throughput performance was degraded only slightly when all three trailers were transmitting to the tractor at the same time. As the test bandwidth increased to 8 Mbps, the throughput increased linearly to 8 Mbps and then leveled at 8 Mbps. The antennae and controllers on Trailers 1 and 2 can be used to forward data packets between Trailer 3 and the tractor. In this particular configuration, the maximum throughput drops down to about 4 Mbps. The main reason for this drop in throughput is that when the intermediate trailers are forwarding packets, the additional transmissions cause higher interferences or contentions for bandwidth. This configuration should aid reliable transmission when severe weather conditions impair direct transmission between the third trailer and the tractor.

5.6.8 Results of Performance of Efficient Broadcast Protocol

The performance and reliability of the efficient broadcast protocol is measured by its throughput, and delivery ratio. Figure 5-16 shows the comparison of throughput between traditional broadcast and efficient broadcast with aggregation. Intuitively, throughput is proportional to the number of nodes; however, in traditional broadcast, the increased number of nodes may interrupt transmissions due to the flooded data packets. Therefore, in traditional broadcast, throughput significantly degrades as the number of nodes increase. On the other hand, efficient broadcast with aggregation does not increase the number of packets and hence throughput actually increases as the number of nodes increase.

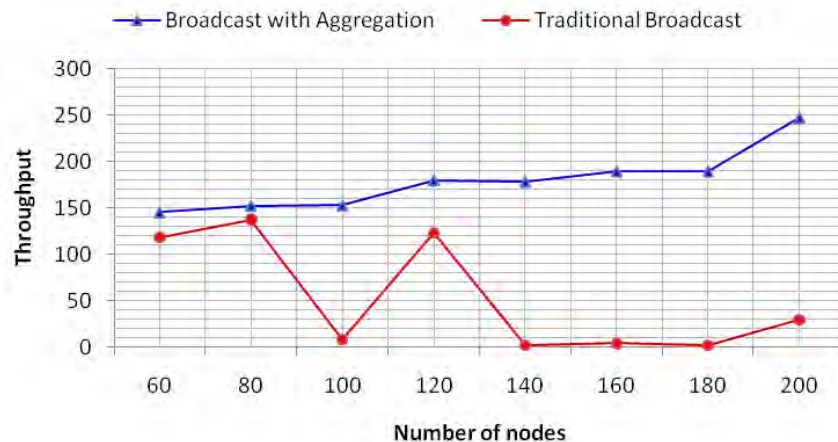


Figure 5-16. Plot. Throughput for broadcast with aggregation and traditional broadcast.

Delivery ratio is defined as the number of packets received at the destination divided by the number of packets transmitted. As can be seen in Figure 5-17, traditional broadcast shows a very unstable rate as the number of nodes changes, whereas in the case of efficient broadcast with aggregation, the delivery ratio remains constant as the number of nodes increases.

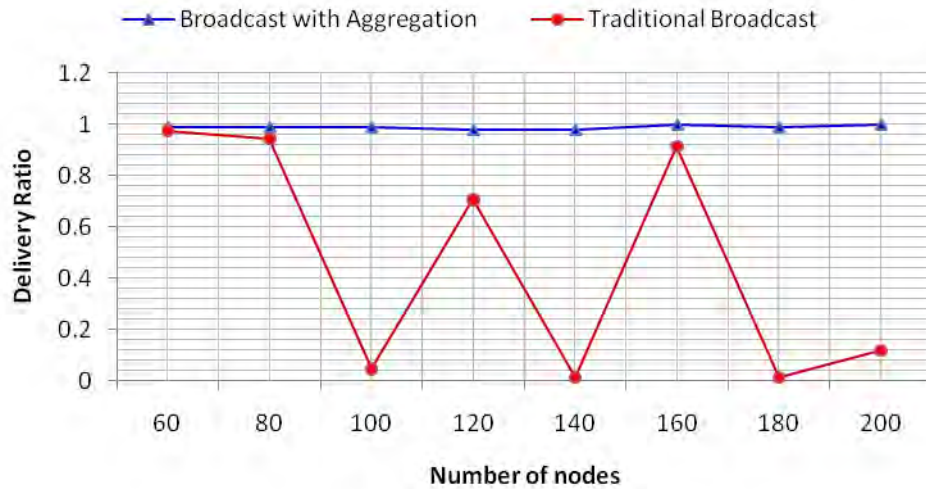


Figure 5-17. Plot. Delivery ratio for efficient broadcast with aggregation and traditional broadcast.

5.7 Conclusions

The main result of these studies on the feasibility of intra-vehicle wireless networks shows that it is feasible to build wireless networks that will satisfy the communication requirements of ESC systems for commercial tractor trailer combinations.

5.7.1 Satisfying the Requirements for Intra-Vehicle Wireless Communication

Experimental results with IEEE 802.11n wireless transmission show that a minimum of 20 Mbps throughput can be achieved even in the presence of wireless transmission problems, such as polarization mismatch and SMM. Test results also show that packet loss rate is limited to no more than 10%. Also, the total throughput requirement of ESC applications, for both the sensor and control data, is 158.4 kbps, even after taking into account a 10% packet loss rate. This shows that IEEE 802.11n links can be used to satisfy the communication requirements of intra-vehicle wireless networks for supporting ESC applications.

With further improvements in the IEEE 802.11n MAC protocols, such as using more advanced rate adaptation protocols, multi-hop packet forwarding, and efficient broadcasting, the throughput performance and reliability of wireless links can be further improved to ensure that intra-vehicle wireless networks support ESC systems at a higher level of confidence.

5.7.2 Selection of Wireless Communication Protocols

IEEE 802.11n is selected for implementing intra-vehicle wireless networks because of the various performance enhancing techniques used in this protocol, which provide the highest throughput (up to 300Mbps), such as MIMO, spatial multiplexing, MCS, STBC, and channel bonding. Their performance in the outdoor vehicle networking environment has been investigated, showing that the performance in terms of throughput and packet loss rate is adequate for supporting ESC even in the presence of wireless transmission problems that were studied, such as polarization mismatch and spatial multiplexing malfunction.

In comparison, the throughput of DSRC radios, such as Kapsch DSRC radios, is only about 3 Mbps. Because IEEE 802.11n provides significantly higher throughput than DSRC radio, it is appropriate to use it for implementing intra-vehicle wireless networks. Despite this, since DSRC is designated for vehicle-to-vehicle and vehicle-to-infrastructure communication, there is a need for DSRC to be used for inter-vehicle communication. However, it is feasible to maintain two vehicle wireless networks: IEEE 802.11n for intra-vehicle communication and DSRC for inter-vehicle and vehicle-infrastructure communications.

5.7.3 Future Work

Although the present experimental studies and requirement analysis show that IEEE 802.11n can satisfy the requirements for wireless ESC systems, the actual implementation of wireless networking for ESC in tractor-trailer environments needs further investigation. The wireless system will be designed for ESC, and actual performance results will be measured and analyzed. The actual performance results can be compared to this design analysis and the outcome could be used to enhance the design and implementation in order to improve performance further.

Failure detection, recovery from failure, fault-tolerant mechanisms, and fail safe operations are all important aspects of any deployed safety system. For example, the various ESC units must fail to a safe condition in the event that the networks fail so that the vehicle is no worse than current vehicles, which do not communicate. These questions need to be investigated more thoroughly. The report has touched on this only superficially. More investigation is needed on how to detect failure, what recovery mechanisms are needed (e.g., whether and how to shut down the system), and what fault-tolerant methods can be used (e.g., whether redundant communication links or controllers will prevent failures).

This Page Intentionally Left Blank.

Chapter 6 – Conclusions and Recommendations

This project comprised three separate but complementary tasks to improve the stability of heavy duty combination motor vehicles. An algorithm to apply existing principles of ESC to an entire vehicle was developed and demonstrated in simulations. A hardware bench test system for observing the practical behavior of physical components has been assembled and demonstrated. Finally, a robust method of wireless communication between the tractor and multiple semitrailers was demonstrated on a tractor in combination with three semitrailers.

All three of these efforts can be taken forward and integrated to lead to the next generation of ESC for heavy duty trucks.

6.1 Stability Control Algorithm

An algorithm for improving the stability of a tractor semitrailer combination vehicle has been developed and demonstrated in simulations. The algorithm accounts for both roll and yaw instabilities, and it acts in a way that can manage a developing instability in one mode without diminishing the stability of other modes. Time-domain simulations have shown its effectiveness in transient and steady-state maneuvers. The algorithm works on a range of surface frictions, though some maneuvers on extremely slippery surfaces are only minimally improved.

Though the stability algorithm was implemented in a simulation, its inputs were limited to quantities that can be measured in an actual vehicle. This established the bandwidth needed to implement the measurement and control system, providing guidance to the subsequent tasks.

The algorithm uses a tiered approach—it calculates the stability margin for the tractor and trailers and for roll and yaw in sequence. The simulations have shown this approach to be effective, but a more robust approach is possible. If a single, integrated set of the equations of motion for the entire vehicle were developed, then the stability could be expressed in state space. That is, the stability threshold could be expressed in a compact mathematical formula rather than as a sequence of tests. This would allow the control interventions to be optimized, automatically balancing any conflicting needs.

6.2 Hardware Bench Test System Demonstration

The hardware bench test system for a complete tractor-semitrailer brake system and control unit was built and exercised. The system has the flexibility to implement different architectures within the controller. The sensing and decision-making processors can be a single, centralized unit, or they can be a pair on the tractor and semitrailer.

Functional and performance test protocols for the equipment have been written, and the next step is to execute those tests. The equipment is available to serve its purpose in future research, experimenting with the performance of different sensors and actuators, control algorithms, and electronics architectures.

6.3 *Wireless Intra-Vehicle Communication*

Wi-Fi has been demonstrated on a three-semitrailer combination unit in motion. A throughput rate in excess of what is necessary for the control algorithms presented in Chapter 3 has been experimentally confirmed. The throughput rate is limited only by the wireless equipment itself when the vehicle is stationary. Nearly 100 Mbps was achieved. Vibration of the vehicle in motion limited the reliable throughput rate to 40 Mbps.

Work should continue to reduce the cost and improve the reliability of intra-vehicle communication. Dedicated hardware could be made to cost less money when manufactured in quantities and to use less power. Research in algorithms and protocols has proven the reliability needed for a system that supports safety functions.

Chapter 7 – References

- Abraham, S., Meylan, A., and Nanda, S. 2005. 802.11n MAC design and system performance. In: IEEE International Conference on Communications, 2005, vol 5, pp 2957–2961.
- Aga, M., and Okada A. 2003. Analysis of Vehicle Stability Control Effectiveness from Accident Data. Vol. JSAE Paper No. 541. Yokohama Japan: JSAE.
- Andersky, F., and Conklin, R. 2008. Road map for the future. Making the case for full-stability. Bendix Commercial Vehicle Systems LLC, http://www.bendix.com/media/documents/products_1/BW2719-Road_Map_for_the_Future.pdf.
- Anderson, R., and Bevly, D.M. 2010. Using GPS with a model-based estimator to estimate critical vehicle states. *Vehicle System Dynamics* 48 (12): 1413-38.
- Antonov, S., Fehn, A., and Kugi, A. 2008. A new flatness-based control of lateral vehicle dynamics. 46 (9): 780-801.
- Arant, M. 2010. Assessing the effect of chassis torsional stiffness on the accuracy of heavy vehicle understeer and rollover modeling. Masters, Clemson University.
- Arant, M., Pape, D., Nelson, S., Franzese, O., Knee, H.E., Hathaway, R., Keil, M., LaClair, T., Kapseong, R., and Upul, A. 2009. U19: Heavy truck rollover characterization (phase-B) final report. National Transportation Research Center Incorporated, DTRT06G-0043, <http://tris.trb.org/view.aspx?id=908531>.
- ASTM International. 2003. Standard Specification for Telecommunications and Information Exchange Between Roadside and Vehicle Systems – 5 GHz Band Dedicated Short Range Communications (DSRC) Medium Access Control (MAC) and Physical Layer (PHY) Specifications; ASTM E2213-03.
- Balasubramanian, A., Mahajan, R., Venkataramani, A., Levine, B.N., Zahorjan, J. 2008. Interactive wifi connectivity for moving vehicles. In: Proceedings of the ACM SIGCOMM 2008 Conference on Data Communication, 2008, pp 427–438.
- Barickman, F., et al. 2009. NHTSA’s Class 8 Truck-Tractor Stability Control Test Track Effectiveness. Vol. Paper Number 09-0552. Transportation Research Board.
- Bayan, F.P., Cornetto, A.D., Dunn, A.L., and Sauer, E. 2009. Brake timing measurements for a tractor-semitrailer under emergency braking. Society of Automotive Engineers International 2009-01-2918.
- Bedner, E., Fulk, D., and Hac, A. 2007. Exploring the trade-off of handling stability and responsiveness with advanced control systems. Society of Automotive Engineers International 2007-01-0812.
- Bendix Commercial Vehicle Systems LLC. 2004a. The Air Brake Handbook.

- Bendix Commercial Vehicle Systems LLC. 2004b. Service Data: Bendix M-32 and M-32QR AntiLock Modulators. Vol. SD-13-4870. Bendix Commercial Vehicle Systems LLC;.
- Bendix Commercial Vehicle Systems LLC. 2004c. Service Data: Bendix WS-24 AntiLock Wheel Speed Sensor. Vol. SD-13-4860. Bendix Commercial Vehicle Systems LLC;.
- Bendix Commercial Vehicle Systems LLC. 2005. Brochure: Bendix EC-60 ABS / ATC / ESP Controllers (Advanced Models). Available from http://www.bendix.com/media/documents/products_1/absstability/truckstractors/134869.pdf.
- Bendix Commercial Vehicle Systems LLC. 2006. Brochure: Bendix ABS-6 Advanced with ESP Stability System. Available from http://www.bendix.com/media/documents/products_1/absstability/truckstractors/BW2472_ABS6.pdf.
- Bendix Commercial Vehicle Systems LLC. 2007. Brochure: Bendix E-6 & E-10 Dual Brake Valves.
- Bendix Commercial Vehicle Systems LLC. 2008a. Brochure: Bendix Actuation Products - Wheel End.
- Bendix Commercial Vehicle Systems LLC. 2008b. Brochure: Bendix ATR-6 and ATR-3 Antilock Traction Relay Valves.
- Bendix Spicer Foundation Brake LLC. 2011a. Brochure: Bendix Air Disc Brakes. Available from <http://www.foundationbrakes.com/media/documents/airdiscbrakes/overviewbrochure.pdf>.
- Bendix Spicer Foundation Brake LLC. 2011b. The Compelling Case For Air Disc Brakes in Heavy Trucks. Elyria, OH 44035: Bendix Spicer Foundation Brake LLC.
- Bendix Spicer Foundation Brake LLC. 2011c. Bendix Continues Ongoing Commitment to the Improvement of Highway Safety. [database online]. [cited July 02 2011]. Available from http://www.bendix.com/media/documents/products_1/Safety_Position_Paper_FINAL2.pdf.
- Best, M. C., Gordon, T., and Dixon, P.J. 2000. An extended adaptive kalman filter for real-time state estimation of vehicle handling dynamics. *Vehicle System Dynamics* 34 (1): 57-75.
- Brazeau, M. 2011. The Electro-Motive Story. in General Motors Heritage Center [database online]. [cited July 02 2011]. Available from http://history.gmheritagecenter.com/wiki/index.php/The_Electro-Motive_Story.
- Brothers, E. 2009. FMVSS 121 brake option review. in *Fleet Equipment Magazine* [database online]. [cited July 02 2011]. Available from http://www.fleetequipmentmag.com/Item/68426/fmvss_121_brake_option_review.aspx.

- Brown, T., Schwarz, C., Moeckli, J. and Marshall, D. 2009. Heavy Truck ESC Effectiveness Study Using NADS. DOT HS 811 233, U.S. Department of Transportation National Highway Traffic Safety Administration.
- Bychkovsky, V., Hull, B., Miu, A., Balakrishnan, H., Madden, S. 2006. A measurement study of vehicular internet access using in situ Wi-Fi networks. In: Proceedings of the 12th Annual International Conference on Mobile Computing and Networking, pp 50–61.
- Chan, B. 2010. Evaluation of Full and Partial Stability Systems on Tractor Semi Trailer Using Hardware-in-the-Loop Simulation. Vol. 2010-01-1902. SAE.
- Cheli, F., Sabbioni, E., Pesce, M., and Melzi, S. 2007. A methodology for vehicle sideslip angle identification: comparison with experimental data. *Vehicle System Dynamics* 45(6): 549-563.
- Chen, B.C., and Peng, H. 1999. Rollover warning of articulated vehicles based on a time-to-rollover metric. ASME International Congress and Exposition, Knoxville, TN.
- Chen, L., and Shieh, Y.A. 2011. Jackknife prevention for articulated vehicles using model reference adaptive control. Proceedings of the Institution of Mechanical Engineers, Part D: Journal of Automobile Engineering 225(1): 28-42.
- Cheng, C., and Cebon, D. 2011. Parameter and state estimation for articulated heavy vehicles. *Vehicle System Dynamics* 49(1): 399-418.
- Cheng, L., Henty, B.E., Stancil, D.D., Bai, F., and Mudalige, P. 2007 Mobile Vehicle-to-Vehicle Narrow-Band Channel Measurement and Characterization of the 5.9 GHz Dedicated Short Range Communication (DSRC) Frequency Band. In: *IEEE Journal on Selected Areas in Communications* 25(8): 1501–1516.
- Choi, S., and Cho, D.W. 2001. Design of nonlinear sliding mode controller with pulse width modulation for vehicular slip ratio control. *Vehicle System Dynamics* 36 (1): 57-72.
- Cisco Systems. 2011. Ethernet Technologies. Available from http://docwiki.cisco.com/wiki/Ethernet_Technologies.
- CVSA. 2011. Operation Air Brake/Brake Safety Week. Website of Commercial Vehicle Safety Alliance. Available from http://www.cvsa.org/programs/op_airbrake.php.
- Daily, R., and Bevly, D.M. 2004. The use of GPS for vehicle stability control systems. *Industrial Electronics, IEEE Transactions* 51(2): 270-277. ISSN 0278-0046.
- Dang, J. 2004. Preliminary Results Analyzing the Effectiveness of Electronic Stability Control Systems. Vol. DOT HS 809 790. National Highway Traffic Safety Administration.
- Davis, L. 2011. Automotive Buses. Available from http://www.interfacebus.com/Design_Connector_Automotive.html#h.

- Dominguez, M.A., Marino, P., Poza, F., and Otero, S. 2007. Communication Networks for Vehicular Electronic Devices. EUROCON, 2007. The International Conference on Computer as a Tool Issue Date: 9-12 Sept. 2007 On page(s): 1061 - 1067.
- Du, H., and Zhang, N. 2008. Robust stability control of vehicle rollover subject to actuator time delay. Proceedings of the Institution of Mechanical Engineers.Part I: Journal of Systems and Control Engineering 222 (3): 163-74, <http://dx.doi.org/10.1243/09596518JSCE471>.
- Dunn, A.L. 2003. Jackknife stability of articulated tractor semitrailer vehicles with high-output brakes and jackknife detection on low coefficient surfaces. Doctor of Philosophy, Ohio State University.
- ECE R13. 2008. Agreement concerning the adoption of uniform technical prescriptions for wheeled vehicles, equipment and parts which can be fitted and/or be used on wheeled vehicles and the conditions for reciprocal recognition of approvals granted on the basis of these prescriptions. E/ECE/324; E/ECE/TRANS/505; Rev.1/Add.12/Rev.6. Regulation 13. Uniform provisions concerning the approval of vehicles of categories M, N and O with regard to braking. United Nations Economic Commission for Europe. Available at <http://live.unece.org/fileadmin/DAM/trans/main/wp29/wp29regs/r013r6e.pdf>.
- El-Gindy, M. 1995. An Overview of Performance Measures for Heavy Commercial Vehicles in North America. International Journal of Vehicle Design, vol. 16.
- Electro-Motive Diesel. 2011. About Electro-Motive Diesel. in Electro-Motive Diesel Inc. [database online]. [cited Jul 02 2011]. Available from http://www.emdiesels.com/emdweb/company/company_index.jsp.
- Eriksson, J., Balakrishnan, H., and Madden, S. 2008. Cabernet: Vehicular content delivery using WiFi. In: Proceedings of the 14th ACM International Conference on Mobile Computing and Networking, 2008, pp 199–210.
- Ervin, R.D., Fancher, P.S., and Gillespie, T. 1984. An Overview of the Dynamic Performance Properties of Long Truck Combinations. UMTRI-84-26, University of Michigan (UMTRI).
- Etschberger, K. 2001. Controller Area Network: Basics, Protocols, Chips and Applications. IXXAT Press.
- FMCSA. 2011. Commercial Vehicle Information Systems and Networks (CVISN). Federal Motor Carrier Safety Administration, U.S. Department of Transportation. Available from <http://www.fmcsa.dot.gov/facts-research/cvisn/>.
- Federal Railroad Safety Appliances Act. 1893. An Act to Promote the Safety of Employees and Travelers upon Railroads by Compelling Common Carriers Engaged in Interstate Commerce to Equip Their Cars with Automatic Couplers and Continuous Brakes and Their Locomotives with Driving-wheel Brakes, and for Other Purposes. U.S. Congress, Act of Mar. 2, 1893, 27 Stat. 531, 45 U.S.C. § 2 (1988 ed.), recodified, as amended, 49 U. S. C. A.§20302 (Supp. 1995).

- Fiehe, S., Riihijärvi, J., and Mähönen, P. 2010, Experimental study on performance of IEEE 802.11n and impact of interferers on the 2.4 GHz ISM band. In: Proceedings of the 6th International Wireless Communications and Mobile Computing Conference, 2010, pp 47–51.
- Freightliner LLC. 2007. Electronically Controlled Braking Systems (ECBS) Intelligent Vehicle Initiative Field Operational Test. Vol. DTFH61-02-X-00096. U.S. Department of Transportation Federal Highway Administration.
- Gao, X., Yu, Z., Neubeck, J., and Wiedemann, J. 2010. Sideslip angle estimation based on input-output linearisation with tire-road friction adaptation. *Vehicle System Dynamics* 48 (2): 217-34.
- Ghoneim, Y.A., Lin, W.C., Sidlosky, D.M., Chen, H.H., Chin, Y.K., and Tedrake, M.J. 2000. Integrated chassis control system to enhance vehicle stability. *International Journal of Vehicle Design* 23 (1): 124-44.
- Gonzalez, O. 2009. Hall Effect Sensors and Magnetoresistive Sensors. Available from http://sandoval-gonzalez.com/5_hall.pdf.
- Goodarzi, A., Ghajar, M., Baghestani, A., and Esmailzadeh, E. 2009. Integrated Yaw and Roll Moments Control for Articulated Vehicles. *Society of Automotive Engineers International* 2009-01-2874.
- Grego, P.W. 2002. Commercial vehicle anti-lock braking systems, Trucking Law Committee, <http://www.postschell.com/docs/publications/88.pdf>.
- Haldex Commercial Vehicle Systems. 2011. Haldex ModulX Air Disc Brake. Available from <http://www.haldex.com/en/north-america/media/pressreleases--news/news/CVS/HALDEX-ModulX-AIR-DISC-BRAKE/?menu=7106>.
- Hamamatsu Photonics Japan. 2011. Steering Wheel Angle Sensor. Available from http://jp.hamamatsu.com/products/sensor-ssd/pd218/pd238/index_en.html.
- Hedlund, J., and Blower, D. 2011. Large Truck Crash Causation Study. Federal Motor Carrier Safety Administration. U.S. Department of Transportation.
- Holdgreve, R. 1999. Window to the Past - Early trucks, buses and campers. in Delphos Historical Society, Delphos Herald Newspaper [database online]. [cited July 02 2011].
- Honeywell International. 2011. Bendix History. [cited July 02 2011]. Available from <http://www.bendixbrakes.com/company/>.
- Huh, K., Lim, S., Jung, J., et al. 2007. Vehicle Mass Estimator for Adaptive Roll Stability Control. *Society of Automotive Engineers International*, 2007-01-0820.
- ISO. 1992. ISO 11898 - Road Vehicles - Interchange of digital information - Controller Area Network (CAN) for high-speed communication. International Organization for Standardization (ISO).

- ISO. 1994. ISO 11519-2 - Road Vehicles - Low Speed serial data communication - Part 2: Low-speed Controller Area Network (CAN). International Organization for Standardization (ISO).
- Jarupan, B., and Ekici, E. 2011 A survey of cross-layer design for VANETs. *Ad Hoc Networks* 9(5):966–983.
- Jerbi, M., Marlier, P., and Senouci, S. 2007. Experimental assessment of V2V and I2V communications. In: *IEEE International Conference on Mobile Ad Hoc and Sensor Systems*, 2007, pp 1–6.
- Kamnik, R., Boettiger, F., and Hunt, K. 2003. Roll dynamics and lateral load transfer estimation in articulated heavy freight vehicles. *Proceedings of the Institution of Mechanical Engineers, Part D: Journal of Automobile Engineering* 217 (11): 985-97, <http://dx.doi.org/10.1243/095440703770383884>.
- Kharrazi, S., and Thomson, R. 2008a. Analysis of Heavy Truck Accidents with Regard to Yaw and Roll Instability—Using LTCCS Database. *Heavy Vehicle Transport Technology*, Paris, France.
- Kharrazi, S., and Thomson, R. 2008b. Study of heavy truck accidents with focus on manoeuvres causing loss of control. *International Journal of Vehicle Safety* 3(1): 32-44.
- Kienhöfer, F.W., Miller, J.I., and Cebon, D. 2008. Design concept for an alternative heavy vehicle ABS system. *Vehicle System Dynamics* 46 (1): 571-83.
- Kim, J. 2010. Effect of vehicle model on the estimation of lateral vehicle dynamics. *International Journal of Automotive Technology* 11(3): 331-337.
- Knee, H.E., Capps, G., Franzese, O., Pollock, P., Coleman, D., Janajreh, I., Haas, S., Frey, N., Law, E.H., Johnson, E., Petrolino, J., and Rice, D. 2005. Heavy truck rollover characterization: New-generation single tires vs. standard duals. 2005 International Truck & Bus Safety & Security Symposium, Alexandria, Virginia.
- Ko, Y.E., and Lee, J.M. 2002. Estimation of the stability region of a vehicle in plane motion using a topological approach. *International Journal of Vehicle Design* 30 (3): 181-92, <http://dx.doi.org/10.1504/IJVD.2002.002032>.
- LaClair, T., Knee, H.E., Franzese, O., et al. 2010. U24 Heavy Truck Rollover (Phase C). DTRT06G-0043. National Transportation Research Center Incorporated. Available at http://www.ntrci.org/library/U24_Heavy_Truck_Rollover_Phase_C_FINAL_1288900197.pdf.
- Liebemann, E.K., et al. 2003. Safety and Performance Enhancement: The Bosch Electronic Stability Control (ESP). Vol. SAE 2004-21-0060. SAE.
- Liebemann, E.K., Schuh, J., Meder, K., and Nenninger, G. 2004. Safety and performance enhancement: The bosch electronic stability control (ESP). *Society of Automotive Engineers International* 2004-21-0060.

- Lim, A., and Bevly, D. 2011. U29: Commercial Vehicle Secure Networks For Safety and Mobility Applications, Final Report to National Transportation Research Center, Inc., U.S. Department of Transportation, Research and Innovative Technology Administration, Grant #DTRT-06-G-0043.
- Limroth, J. 2009a. Real-time vehicle parameter estimation and adaptive stability control. Doctorate., Clemson University, <http://etd.lib.clemson.edu/documents/1263410198/>.
- Limroth, J. 2009b. Real-Time Vehicle Parameter Estimation and Equivalent Moment Electronic Stability Control. Clemson University (unpublished).
- Limroth, J., Kurfess, T. and Law, E.H. 2009. U13: Co-Simulation of Heavy Truck Tire Dynamics and Electronic Stability Control Systems (Phase A). National Transportation Research Center, Inc. University Transportation Center, Knoxville, TN.
- Ma, W.H., and Peng, H. 1999. Worst-Case Vehicle Evaluation Methodology - Examples on Truck Rollover/Jackknifing and Active Yaw Control Systems. *Vehicle System Dynamics* 32(4): 389-408.
- MacAdam, C.C. 1982. A Computer-Based Study of the Yaw/Roll Stability of Heavy Trucks Characterized by High Centers of Gravity. SAE Technical Paper Series 821260.
- MacAdam, C.C., Hagan, M., Fancher, P.S., et al. 2000. Rearward amplification suppression (RAMS). UMTRI-2000-47, Contract Number: DTFH61-96-C-00038, University of Michigan Transportation Research Institute.
- Mack Trucks LLC. 2011. History of Mack Trucks. in Mack Trucks LLC [database online]. [cited July 02 2011]. Available from <http://www.macktrucks.com/default.aspx?pageid=254>.
- Mahajan, R., Zahorjan, J., and Zill, B. 2007. Understanding wifi-based connectivity from moving vehicles. In: *Proceedings of the 7th ACM SIGCOMM Conference on Internet Measurement, 2007*, pp 321–326.
- Manning, W.J., and Crolla, D.A. 2007. A review of yaw rate and sideslip controllers for passenger vehicles. *Transactions of the Institute of Measurement and Control* 29(2): 117-135.
- Master-Car Builders Association. 1887. Report of the Proceedings of the 21st Annual Convention of the Master-Car Builders Association. Minneapolis MN ed. Nos. 49 & 51 Park Place, New York, NY: Martin B. Brown.
- Mechanical Simulation Corporation. 2009a. CarSim. Vol. 7.01. Mechanical Simulation Corporation, 912 N Main St, Ann Arbor, MI.
- Mechanical Simulation Corporation. 2009b. TruckSim. Vol. 8. Mechanical Simulation Corporation, 912 N Main St, Ann Arbor, MI.
- Medvedev, I., Bjerke, B., Walton, R., Ketchum, J., Wallace, M., and Howard, S. 2006. A comparison of MIMO receiver structures for 802.11n WLAN - performance and complexity.

In: IEEE 17th International Symposium on Personal, Indoor and Mobile Radio Communications, 2006, pp 1–5.

- Mercedes Benz UK. 2011. Trucks Revolutionise Transport - First Truck Produced by Gottlieb Daimler. in Mercedes Benz UK Ltd. [database online]. [cited July 02 2011]. Available from http://www2.mercedes-benz.co.uk/content/unitedkingdom/mpc/mpc_unitedkingdom_website/en/home_mpc/truck/home/aboutus/mercedes-benz_truck0/the_first_truck.html.
- Meritor WABCO. 2011. Press Release: Meritor WABCO Air Disc Brake Technology Offers Alternative Solutions to Meet Stopping Distance Regulation Changes. Available from [http://www.meritorwabco.com/\(S\(ougl1y1yubtlivmmggdbz3zyw\)\)/PressReleaseDetail.aspx?news_id=33&AspxAutoDetectCookieSupport=1](http://www.meritorwabco.com/(S(ougl1y1yubtlivmmggdbz3zyw))/PressReleaseDetail.aspx?news_id=33&AspxAutoDetectCookieSupport=1).
- Murphy, R.W., Limpert, R., and Segel, L. 1971. Bus, truck, tractor/trailer braking system performance. Vol 1 of 2: Research Findings. Vol. Con- FH-11-7290. Ann Arbor MI: University of Michigan Transportation Research Institute.
- Nantais, N. 2006. Active Brake Proportioning and its Effects on Safety and Performance. Master of Applied Science, University of Windsor, Windsor, Ontario, Canada.
- National Instruments. 2009. NI-XNET Hardware and Software Manual.
- National Instruments. 2011. What Is Measurement & Automation Explorer (MAX)? Available from <http://digital.ni.com/public.nsf/allkb/71544521BDE34FFB86256FCF005F4FB6>.
- National Instruments Products and Services. 2011a. LabVIEW Real Time. Available from <http://sine.ni.com/nips/cds/view/p/lang/en/nid/2381>.
- National Instruments Products and Services. 2011b. NI PCI-8517/2. Available from <http://sine.ni.com/nips/cds/view/p/lang/en/nid/207325>.
- National Instruments Products and Services. 2011c. NI PXI-8516. Available from <http://sine.ni.com/nips/cds/view/p/lang/en/nid/208356>.
- National Instruments Products and Services. 2011d. NI PXI-8532. Available from <http://sine.ni.com/nips/cds/view/p/lang/en/nid/207763>.
- National Instruments Products and Services. 2011e. NI PXI-GPIB. Available from <http://sine.ni.com/nips/cds/view/p/lang/en/nid/1588>.
- National Instruments Products and Services. 2011f. NI SCB-68. Available from <http://sine.ni.com/nips/cds/print/p/lang/en/nid/1180>.
- National Instruments Products and Services. 2011g. NI-DAQmx. Available from <http://www.ni.com/dataacquisition/nidaqmx.htm>.

- National Instruments Products and Services. 2011h. PCI Control of PXI via MXI-Express. Available from <http://sine.ni.com/ds/app/doc/p/id/ds-308/lang/en>.
- National Instruments Products and Services. 2011i. PXI-1002. Available from <http://www.ni.com/pdf/products/us/2pxic25-29.pdf>.
- National Instruments Products and Services. 2011j. PXI-1042Q. Available from <http://sine.ni.com/nips/cds/print/p/lang/en/nid/13909>.
- National Instruments Products and Services. 2011k. PXI-6259. Available from <http://sine.ni.com/nips/cds/print/p/lang/en/nid/14129>.
- National Instruments Products and Services. 2011l. PXI-8106. Available from <http://sine.ni.com/nips/cds/print/p/lang/en/nid/203442>.
- National Instruments Products and Services. 2011m. PXI-8187. Available from <http://sine.ni.com/nips/cds/print/p/lang/en/nid/13972>.
- National Instruments Products and Services. 2011n. PXI-8513. Available from <http://sine.ni.com/nips/cds/view/p/lang/en/nid/207322>.
- National Instruments Products and Services. 2011o. What is LabVIEW? Available from <http://www.ni.com/labview/whatis/>.
- National Instruments Products and Services. 2011p. What is NI-MAX? Available from <http://digital.ni.com/public.nsf/allkb/1C60EDAB0E3AAA5F86256D24006BFA68>.
- National Instruments Products and Services. 2011q. What is PXI? Available from <http://sine.ni.com/np/app/main/p/ap/global/lang/en/pg/1/sn/n24:PXI-FSLASH-CompactPCI/fmid/3>.
- National Instruments Technical Sales. 2011. High-Performance NI-XNET Interfaces for CAN, LIN and FlexRay NI PCI-851x, NI PXI-851x, NI 986x. Available from <http://sine.ni.com/ds/app/doc/p/id/ds-97/lang/en>.
- NHTSA. 2004. Title 49 CHAPTER V PART 571.121 of Federal Motor Vehicle Safety Standards. in National Highway Traffic Safety Administration [database online]. [cited July 19 2011]. Available from http://edocket.access.gpo.gov/cfr_2004/octqtr/pdf/49cfr571.121.pdf.
- NHTSA. 2009. Federal Motor Vehicle Safety Standards; air brake systems. NHTSA–2009-0083 49 CFR Part 571, (RIN: 2127-AJ37).
- NHTSA. 2010. Federal Motor Carrier Safety Administration standard no. 121; air brake systems. Chapter V—National Highway Traffic Safety Administration, U.S. Department of Transportation. Part 571—Federal Motor Vehicle Safety Standards. Vol. 571.121.

- NHTSA. 2011. NHTSA vehicle safety and fuel economy rulemaking and research priority plan 2011-2013. National Highway Traffic Safety Administration.
- NHTSA/DOT. 2004. NHTSA Traffic Safety Facts 2004 Data: Large Trucks. in National Highway Traffic Safety Administration [database online]. [cited Jul 02 2011]. Available from <http://www-nrd.nhtsa.dot.gov/Pubs/809907.pdf>.
- NI Developer Zone - National Instruments. 2011a. Is LabVIEW a general purpose programming language? Available from <http://zone.ni.com/devzone/cda/tut/p/id/5313>.
- NI Developer Zone - National Instruments. 2011b. Piezoresistive Accelerometer. Available from <http://zone.ni.com/devzone/cda/ph/p/id/183>.
- NI Developer Zone - National Instruments. 2011c. Short Tutorial on VXI. Available from <http://zone.ni.com/devzone/cda/tut/p/id/2899>.
- NI Developer Zone - National Instruments. 2011d. VME and PXI Platforms: A Comparison. [cited July 19 2011]. Available from <http://zone.ni.com/devzone/cda/tut/p/id/5712>.
- Palkovics, L., and Fries, A. 2001. Intelligent electronic systems in commercial vehicles for enhanced traffic safety. *Vehicle System Dynamics* 35 (4-5) (05): 227-89, <http://dx.doi.org/10.1076/vesd.35.4.227.2044>.
- Pape, D., Arant, M., Hall, D., Nelson, S., Petrolino, J., Franzese, O., Knee, H.E., et al. 2008. U02: Heavy truck rollover characterization (phase-A) final report. National Transportation Research Center Incorporated, DTRT06G-0043.
- Pape, D., Arant, M., Brock, W., Broshears, E., Chitwood, C., Colbert, J., Hathaway, R., Keil, M., LaClair, T., Patterson, J., Petrolino, J., Pittro, C., Spezia, A., and Wafer, D. 2011. U32: Vehicle Stability and Dynamics Longer Combination Vehicles, Final Report to National Transportation Research Center, Inc., U.S. Department of Transportation, Research and Innovative Technology Administration, Grant #DTRT-06-G-0043.
- Park, J.I., Yoon, J.Y., Kim, D.S., and Yi, K. 2008. Roll state estimator for rollover mitigation control. *Proceedings of the Institution of Mechanical Engineers, Part D: Journal of Automobile Engineering* 222(8): 1289-1311.
- Paul, T., and Ogunfunmi, T. 2008. Wireless LAN comes of age: Understanding the IEEE 802.11n amendment. *IEEE Circuits and Systems Magazine* 8(1): 28-54.
- Paul, T., and Ogunfunmi, T. 2009. Evolution, insights and challenges of the PHY layer for the emerging IEEE 802.11n amendment. *IEEE Communications Surveys Tutorials* 11(4):131-150.
- Paul, U., Crepaldi, R., Lee, J., Lee, S.J., and Etkin, R. 2011. Characterizing WiFi link performance in open outdoor networks. In: *IEEE Communications Society on Sensor and Ad Hoc Communications and Networks*, 2011, To appear.

- PCB Electronics. 2004. Capacitive Accelerometers. Available from http://www.pcb.com/Linked_Documents/Vibration/Cap_Accels_0704.pdf.
- PCB Electronics. 2011. Function of Piezoelectric Accelerometers. Available from http://www.pcb.com/techsupport/tech_accel.php.
- Racelogic. 2009. Noiseless Measurements: Integrating Inertial Sensors with GPS. Available from http://www.insidegnss.com/special/elib/VBOX_3i_and_IMU_Integration_Article.pdf.
- Racelogic. 2010. Racelogic VBox: GPS + Inertial Integration. Available from http://www.racelogic.co.uk/_downloads/vbox/Application_Notes/IMU_Integration_Flyer.pdf
- Robert Bosch GmbH. 1991. CAN Specification Version 2.0. Robert Bosch GmbH.
- Rodengen, J. 1999. George Westinghouse and the Air Brake. In *The History of American Standard*. Write Stuff Enterprises.
- Sampson, D.J.M. 2000. Active roll control of articulated heavy vehicles. Doctor of Philosophy, University of Cambridge.
- Sampson, D.J.M., and Cebon, D. 1998. An investigation of roll control system design for articulated heavy vehicles. *Proceedings of the International Symposium on Advanced Vehicle Control Proc. 4th Int. Symp. AVEC '98*.
- Seiff, H. 1994. Heavy Truck Brake Adjustment-Problems And Solutions. *Proceedings of Fourth International Symposium on Heavy Vehicle Weights and Dimensions, June 25-29, 1995*.
- South Carolina Department of Transportation. 2011. Air Brake Drum Drawing, South Carolina Commercial Driver's License Manual.
- Stallings, W. 2004. IEEE 802.11: Wireless LANs from a to n. *IT Professional* 6(5):32–37.
- Stapleton, D. 1997. *The Encyclopedia of Cleveland History: Automotive Industry*. in Case Western Reserve University [database online]. [cited July 02 2011]. Available from <http://ech.cwru.edu/ech-cgi/article.pl?id=AI3>.
- Stein, J.H. 1989. Defective equipment and tractor-trailer crash involvement. *Accident Analysis & Prevention*, Volume 21, Issue 5, October 1989, Pages 469-481 21, no. 5:469.
- Synnstvedt, P. 1895. *Evolution of the Air-Brake: A Brief But Comprehensive History of the Modern Railroad Brake*. 256 Broadway, New York NY: Locomotive Engineering.
- Tekin, G., and Unlusoy, Y.S. 2010. Design and simulation of an integrated active yaw control system for road vehicles. *International Journal of Vehicle Design* 52: 5-19.
- Tianjun, Z., Changfu, Z., Zheng, H., Tian, C., and Zheng, H. 2007. Yaw/Roll stability modeling and control of HeavyTractor-SemiTrailer. *Society of Automotive Engineers International* 2007-01-3574.

- Tianjun, Z., and Liyong, J. 2009. Dynamic modeling and roll control of heavy tractor-semitrailer. Paper presented at 2009 Pacific-Asia Conference on Circuits, Communications and Systems (PACCS 2009), <http://dx.doi.org/10.1109/PACCS.2009.44>.
- Tin Leung, K., James, F.W., Purdy, D., and Dunoyer, A. 2011. A review of ground vehicle dynamic state estimations utilising GPS/INS. *Vehicle System Dynamics* 49 (1): 29-58.
- Tseng, H.E., et al. 1999. The Development of Vehicle Stability Control at Ford. *IEEE/ASME Transactions on Mechatronics*, vol. 4, no. 3, September 1999.
- Wabtec Corporation. 2008. Westinghouse Air Brake Company History. Available from <http://www.wabtec.com/corp/history.asp>.
- Wang, C.Y., and Wei, H.Y. 2009. IEEE 802.11n MAC enhancement and performance evaluation. *Mobile Networks and Applications* 14(6):760-771.
- Wang, J., and Hsieh, M.F. 2009. Vehicle yaw-inertia- and mass-independent adaptive steering control. *Proceedings of the Institution of Mechanical Engineers, Part D (Journal of Automobile Engineering)* 223: 1101-1108.
- Watson Industries Inc. 2010. Angular Rate Sensor Owner's Manual. Available from http://www.watson-gyro.com/files/rate_gyro_ARS-C132-1A_manual.pdf.
- Westinghouse, G. 1869. Improvement in Steam-Power Brake Devices.
- Westinghouse, G. 1872a. Improvement in Steam Air Brakes.
- Westinghouse, G. 1872b. Improvement in Steam Power Air Brakes and Signals.
- Winkler, C., et al. 1976. Predicting the braking performance of trucks and tractor-trailers. Phase III technical report. Vol. UM-HSRI-76-26-1. University of Michigan Transportation Research Institute.
- Winkler, C.B., and Ervin, R.D. 2006. Turning of Single and Multi-Unit Trucks. University of Michigan.
- Woodrooffe, J., et al. 2009a. Analysis of Potential Benefits of Larger Trucks for U.S. Businesses Operating Private Fleets. Ann Arbor MI: University of Michigan Transportation Research Institute.
- Woodrooffe, J., et al. 2009b. Safety Benefits of Stability Control Systems for Tractor-Semitrailers. Vol. DTNH22-06-H-00058. NHTSA.
- Woodrooffe, J., Blower, D., and Green, P. 2010. Analysis of Stability Control Systems for Tractor-Semitrailers. Heavy Vehicle Transport Technology, 11th Heavy Vehicle Transport Technology Symposium, Melbourne, Australia.

- Wurster, U., Ortlechner, M., and Schick, B. 2010. First ECE 13/11 homologation of electronic stability control (ESC) by vehicle dynamics simulation – challenges, innovations and benefits. International Symposium on Advanced Vehicle Control. Loughborough, UK.
- Xiao, Y. 2005. IEEE 802.11n: Enhancements for higher throughput in wireless LANs. *IEEE Wireless Communications* 12(6):82–91.
- Yanakiev, D., Eyre, J., and Kanellakopoulos, I. 1997. Longitudinal Control of Heavy Vehicles with Air Brake Actuation Delays. Proceedings of the American Control Conference, Albuquerque, New Mexico June 1997.
- Yoon, J., Cho, W., Yi, K., and Koo, B. 2009. Vehicle stability control scheme for rollover prevention and Maneuverability/Lateral stability improvement. Society of Automotive Engineers International 2009-01-0826.
- Yoon, J., Kim, D., and Yi, K. 2007. Design of a rollover index-based vehicle stability control scheme. *Vehicle System Dynamics* 45(5): 459-475.
- Yoon, J., Yim, S., Cho, W., Koo, B., and Yi, K. 2010. Design of an unified chassis controller for rollover prevention, manoeuvrability and lateral stability. *Vehicle System Dynamics* 48 (11): 1247-68.
- Yu, H., Güvenç, L., and Özgüner, Ü. 2008. Heavy duty vehicle rollover detection and active roll control. *Vehicle System Dynamics* 46 (6): 451-70.
- Zhou, S., Guo, L., and Zhang, S. 2008. Vehicle yaw stability control and its integration with roll stability control. Chinese Control and Decision Conference.

This Page Intentionally Left Blank.